NAZARBAYEV UNIVERSITY

ENG 400 - CAPSTONE PROJECT II

DESIGN OF A 12-STORY HIGH-RISE OFFICE BUILDING IN LOS ANGELES, CALIFORNIA, USA.

GROUP 1

Student names and ID

Alibi Seitkaliyev	202018187
Amirmagruf Amantay	202060345
Tangguli Zhubanysh	201939626
Bekbarys Aidaraliyev	201917515
Aruzhan Gabit	202083276
Malika Sissenova	202025936

Date of submission: 26 April, 2025

This page was intentionally left blank.

DECLARATION

We hereby declare that this report entitled “Design of 12 storey office building in Los Angeles, California, USA” is the result of our own project work except for quotations and citations, which have been duly acknowledged. We also declare that it has not been previously or concurrently submitted for any other degree at Nazarbayev University.

Alibi Seitkaliyev 

Amirmagruf Amantay 

Tangguli Zhubanysh 

Bekbarys Aidaraliyev 

Aruzhan Gabit 

Malika Sissenova 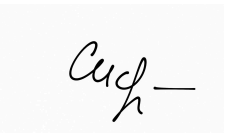

Date of submission: 25 April, 2025

ACKNOWLEDGEMENTS

We want to express our sincere gratitude to our professors Mert Guney, Dichuan Zhang, Chang-Seon Shon, Alfrendo Satyanaga, Sung-Woo Moon, Abid Nadeem, Ferhat Karaca, Jong Kim, and other Civil and Environmental Engineering Department faculty members for their guidance and support in carrying out this capstone project.

ABSTRACT

This paper proposes designing and constructing a 12-story office building at 940 N Sycamore Avenue in Los Angeles, California.

The architectural design of the building aligns with the list of building codes, namely International Building Code (IBC), California Building Code (CBC), Los Angeles Municipal Code (LAMC), and California Building Standards Code (CBSC).

The structural part aligns with the American Society of Civil Engineers (ASCE) guidelines. SAP 2000 software was used for the structural analysis of the building. Reinforced concrete is chosen as the main construction material due to its accessibility and cost-effectiveness.

After preparing the soil profile of the site, Mat and Pile foundations were designed. We choose a group pile foundation due to its ability to support high loads. Moreover, calculations showed that settlement of a group of piles is significantly lower than settlement of mat foundation.

Keywords: office building, Los Angeles, architectural design, structural design, materials, geotechnical analysis.

Table of Contents

Introduction **17**
1.1 Problem Statement 18
1.2 Ethics and Professional Responsibilities 18
Adherence to Academic Integrity 18
Ethical Data Collection and Usage 19
Professional Collaboration and Contributions 19
Environmental and Societal Impact Awareness 19
Presentation of the Report 19
Commitment to Continuous Learning 20
2. Architectural Design **21**
2.1 Overview of the building 21
2.2 Site Selection 22
2.3 Site Analysis 23
2.4 Design Concept 27
2.5 Design Codes 28
2.6 Geometry Design and Site Layout 29
2.7 Architectural Calculations 39
2.8 Leadership in Energy and Environmental Design (LEED) 50
2.9 Life Cycle 55
3. Structural Design **57**
3.1 Material Selection 57
3.1.1 Non-structural materials selection 58
3.1.1.1. Floor finishing 58
3.1.1.2. Interior and exterior wall structures 60
3.1.1.3. Roof parapets 61
3.1.1.4. Roof drainage system 61
3.2 Development of an analytical model 62
3.3. Analysis of the Gravity Load Resisting System (GLRS) 65
3.3.1. Calculation of Dead, Live and Snow Loads. 65
3.3.1.1. Dead Load Analysis 65
3.2.1.2. Live Load Analysis 69
3.2.1.3. Snow Load Analysis 73
3.2.2. Member Size Estimation 73
3.2.2.1 Structural layout 73
3.2.2.2. Estimation of Size Dimensions of Columns 77
3.2.3. Assigning Forces to SAP2000 80
3.2.3.1. Assigning forces to selected 2D frame 80
3.2.3.2. Assigning forces to 3D frame 87

3.3. Analysis and Design of Lateral Force Resisting System (LFRS) 93
3.3.1 Calculation of Seismic Loads 93
3.3.1.1. Calculation of seismic loads including the Torsional effects 99
3.3.2. Calculation of Wind Loads 102
3.3.2.1. Wind Loads with Torsional Effect 102
3.3.3. Assigning Forces to SAP2000 111
3.3.3.1. Assigning forces to selected 2D frame 111
3.3.3.2. Assigning forces to 3D frame 113
3.4 Lateral Drift Analysis 117
3.4.1 Wind Drift Calculations 117
3.4.2 Seismic Drift Calculations 119
3.4.3. Comparison of lateral drifts for hand, 2D and 3D SAP2000 Calculations 120
3.4.4 Amplified inter-story seismic drift 122
3.4.5 Stability analysis 123
3.4.6 Irregularities check 125
3.4.7 Internal Forces Calculations 126
3.4.8 Comparison Internal force results for 2D, 3D and Hand calculations under Dead load 128
3.4.9 Internal forces verifications under Wind load 131
3.5 Structural Design 135
3.5.1 Structural member design using SAP2000 135
3.5.1.1 Major Beams 135
3.5.1.2 Columns 136
3.5.1.3 Two-way slab 137
3.5.2 Hand Calculations for structural member design. 138
3.5.2.1 Major Beams 138
3.5.2.2 Columns 141
3.5.2.3 Two-way slab 145
3.5.2.4 Joint design 147
3.5.2.5 Reinforcement detailing 149
3.5.2.6 Development length 150
3.5.2.7 Special seismic provisions for reinforcement detailing 152
3.5.2.8 Structural serviceability design 153
4. Geotechnical Design 155
4.1. Site Description 155
4.1.1. Soil Profile 155
4.1.2. Seismic Analysis 158
4.1.3. Water Level 160
4.1.4. Liquefaction Potential Index Calculations. 160
4.2. Site Response Analysis 165

4.3. Foundation design 168
4.3.1. Shallow foundation 168
4.3.2. Mat foundation 169
4.3.3. Pile foundation design 175
4.3.3.1. Single pile design 175
4.3.3.2. Group of piles 186
4.3.4. Settlement 189
4.3.4.1. Elastic Settlement 189
4.3.4.2. Consolidation settlement of group piles 191
4.3.5. Lateral Earth Pressure 193
4.4. Retaining wall design 194
Check for sliding along the base 197
4.5. Software analysis of bearing capacities 199
4.5.1. Axial Bearing Capacity 199
4.5.2. Lateral bearing capacity of pile foundation 202
4.6. Reinforcement design of a Pile Cap. 207
4.6.1. Pile cap 207
4.6.2. Single pile 211
4.8. Sheet pile design 213
4.8.1. Hand calculations 213
4.8.2. Numerical analysis on PLAXIS 215
4.9. Software analysis of pile foundation under loading 217
4.10. Construction procedure 218
5. Construction Management 221
5.1. Charter 221
5.2. Feasibility study 223
5.3. Cost/benefit estimation 224
5.4. Work breakdown structure 234
5.5. Scheduling 235
5.6. Risk management 239
5.7. Quality management 242
5.8. Procurement planning/ Stakeholder analysis 245
5.9. Construction safety 249
Table 5.6. Phased Project-Specific Accident Prevention Plan. 249
5.10. Construction site planning 251
6. Environmental engineering 253
6.1. Introduction 253
6.2 Site Analysis 253
6.2.1 Existing Drainage System 254
6.2.2 Slope Analysis 255
6.3 Grading and Drainage Design 256

6.3.1 Slope Arrow Analysis 256
6.3.2 Grading Plan 256
6.3.3 Cut and Fill Analysis 257
6.4 Drainage Plan 258
6.4.1 Proposed Drainage System 258
6.5 Stormwater Quantity Estimation 260
6.5.1 The Rational Method 260
6.5.2 Area Classification 261
6.5.3 Rainfall Intensity 261
6.5.4.Time of Concentration (Tc) 262
6.6 Drainage Design 264
6.6.1 Manning's Equation 264
6.6.2 Final Cross-Sectional Views of Drainage Channels 265
7. Conclusion 268
8. References 269
9. Appendix 275
9.1 Appendix A 275
9.2 Appendix B 280
9.3 Appendix C 291
9.4 Appendix D 297
9.5 Appendix E 309

List of Tables

Table 1.1. Project disciplines.
Table 2.1. Life cycle costs
Table 2.2. Service life
Table 3.1. Comparison between reinforced concrete and steel structures
Table 3.2. Concrete properties
Table 3.3. Reinforcing steel properties
Table 3.4. Reinforcing steel properties
Table 3.5. Dead load calculations of the first floor.
Table 3.6. Dead load calculations of the typical floor of the office.
Table 3.7. Dead load calculation of the roof
Table 3.8. Calculation of the weight of interior wall on the typical floor per span (7 meters)
Table 3.9. Calculation of the weight of exterior wall on the typical floor per span (7 meters)
Table 3.10. Floor live load reduction.
Table 3.11. Roof live load reduction.
Table 3.12. Final results of volume calculations.
Table 3.13. Loads applied to columns and tributary areas.
Table 3.14. Dimensions of columns
Table 3.15. Calculations of the Effective seismic weight.
Table 3.16. Lateral seismic force at each floor.
Table 3.17. Direct forces and torsion for both axes with forces on each frame.
Table 3.18. Calculation of seismic loads on each frame for the first floor.
Table 3.19. Constants depending on exposure categories.
Table 3.20. Height effect constants depending on the exposure category of the site.
Table 3.21. Results of Kz calculations.
Table 3.22. Case 1 calculations results.
Table 3.23. Case 2 calculation results.
Table 3.24. Calculation of wind loads on each frame for the first floor.
Table 3.25. Case 3 calculation results.
Table 3.26. Case 4 calculation results.
Table 3.27. The hand calculations results of internal forces under wind load
Table 3.28. Summary of exterior slab design
Table 3.29. Summary of interior slab design
Table 3.30. Final selected bars for major beams
Figure 3.31. Interior slab panel reinforcement bars.
Table 3.32. Exterior slab panel reinforcement bars.
Table 3.33. Final selected bars for columns.
Table. 3.34. Lap slices for columns values
Table 4.1. Full soil profile
Table 4.2. Modulus of elasticity of sandy soils
Table 4.3. CSR calculation results.
Table 4.4. CRR calculation results.
Table 4.5. LPI calculation results.
Table 4.6. Values for calculation of soil pressure
Table 4.7. Soil pressure below the mat for each column
Table 4.8. Point Bearing Capacity calculations for piles in Clay layers.
Table 4.9. Calculation results for the skin friction of piles in the Clay layers.

Table 4.10. q' estimation.
Table 4.11. Q_p estimation results for piles in Sand.
Table 4.12. Calculation of the frictional resistance in Sand using the general formula.
Table 4.13. Calculation of Q_s in Sand using the method of Coyle and Castello.
Table 4.14. Results of the calculation of skin resistance in Sand using SPT-N values.
Table 4.15. Total frictional resistance at different depths.
Table 4.16. Calculation results of the negative skin friction.
Table 4.17. Group pile design parameters.
Table 4.18. Bearing capacities of the pile groups and exerted column loads.
Table 4.19. Elastic settlement of group piles.
Table 4.20. Active earth pressure calculations.
Table 4.21. Calculation of moments of forces resisting overturning about C
Table 4.22. Comparison of settlement and bearing capacities.
Table 4.23. Calculations of lateral loads
Table 4.24. Constant modulus of subgrade reaction and subgrade modulus at depth values
Table 4.25. Lateral load bearing capacity and lateral load values
Table 4.26. Pile deflection values and coefficients
Table 4.27. Reinforcement configuration for groups of piles.
Table 4.28. Pile Reinforcement Design for each pile group.
Table 5.1. Building cost estimation from RSMeans.
Table 5.2. Total Cost Calculation for the project.
Table 5.3. Risk Assessment.
Table 5.4. Vendor list for construction materials.
Table 5.5. Stakeholder matrix.
Table 5.6. Phased Project-Specific Accident Prevention Plan.
Table 6.1. Calculation of each area time of concentration and runoff quantity.
Table 6.2. Calculation of each pipe sizes.
Table 9.1 Frame Stiffness Calculations.
Table 9.2. Seismic forces calculations including the torsional effect (Floor 2).
Table 9.3. Seismic forces calculations including the torsional effect (Floor 3).
Table 9.4. Seismic forces calculations including the torsional effect (Floor 4).
Table 9.5. Seismic forces calculations including the torsional effect (Floor 5).
Table 9.6. Seismic forces calculations including the torsional effect (Floor 6).
Table 9.7. Seismic forces calculations including the torsional effect (Floor 7).
Table 9.8. Seismic forces calculations including the torsional effect (Floor 8).
Table 9.9. Seismic forces calculations including the torsional effect (Floor 9).
Table 9.10. Seismic forces calculations including the torsional effect (Floor 10).
Table 9.11. Seismic forces calculations including the torsional effect (Floor 11).
Table 9.12. Seismic forces calculations including the torsional effect (Floor 12).
Table 9.13. Seismic forces calculations including the torsional effect (Floor 13 - Roof).
Table 9.14. Calculation of wind forces on each frame including the torsional effect for Case 2 (Floor 2).
Table 9.15. Calculation of wind forces on each frame including the torsional effect for Case 2 (Floor 3).
Table 9.16. Calculation of wind forces on each frame including the torsional effect for Case 2 (Floor 4).
Table 9.17. Calculation of wind forces on each frame including the torsional effect for Case 2 (Floor 5).

Table 9.18. Calculation of wind forces on each frame including the torsional effect for Case 2 (Floor 6).
Table 9.19. Calculation of wind forces on each frame including the torsional effect for Case 2 (Floor 7).
Table 9.20. Calculation of wind forces on each frame including the torsional effect for Case 2 (Floor 8).
Table 9.21. Calculation of wind forces on each frame including the torsional effect for Case 2 (Floor 9).
Table 9.22. Calculation of wind forces on each frame including the torsional effect for Case 2 (Floor 10).
Table 9.23. Calculation of wind forces on each frame including the torsional effect for Case 2 (Floor 11).
Table 9.24. Calculation of wind forces on each frame including the torsional effect for Case 2 (Floor 12).
Table 9.25. Calculation of wind forces on each frame including the torsional effect for Case 2 (Floor 13 - Roof).
Table 9.26. Calculation of wind forces on each frame including the torsional effect for Case 4 (Floor 2).
Table 9.27. Calculation of wind forces on each frame including the torsional effect for Case 4 (Floor 3).
Table 9.28. Calculation of wind forces on each frame including the torsional effect for Case 4 (Floor 4).
Table 9.29. Calculation of wind forces on each frame including the torsional effect for Case 4 (Floor 5).
Table 9.30. Calculation of wind forces on each frame including the torsional effect for Case 4 (Floor 6).
Table 9.31. Calculation of wind forces on each frame including the torsional effect for Case 4 (Floor 7).
Table 9.32. Calculation of wind forces on each frame including the torsional effect for Case 4 (Floor 8).
Table 9.33. Calculation of wind forces on each frame including the torsional effect for Case 4 (Floor 9).
Table 9.34. Calculation of wind forces on each frame including the torsional effect for Case 4 (Floor 10).
Table 9.35. Calculation of wind forces on each frame including the torsional effect for Case 4 (Floor 11).
Table 9.36. Calculation of wind forces on each frame including the torsional effect for Case 4 (Floor 12).
Table 9.37. Calculation of wind forces on each frame including the torsional effect for Case 4 (Floor 13 - Roof).

List of Figures

Figure 2.1 3D view of the office building.
Figure 2.2 Top view of the construction site (Google Maps).
Figure 2.3 Wind directions of the construction site.
Figure 2.4 Axis analysis of the site location.
Figure 2.5 Bus stops and bicycle lines near the building area.
Figure 2.6 Top view of the construction site.
Figure 2.7 Main features of our office building.
Figure 2.8 Evolution of the building.
Figure 2.9 Top view of the site of construction.
Figure 2.10 Floor plan of the first floor of the office.
Figure 2.11 Floor plan of the second floor of the office.
Figure 2.12 Floor plan of the typical floor (3-12 floors).
Figure 2.13 Front view of the office building.
Figure 2.14 Side view of the office building.
Figure 2.15 Interior view of the office building.
Figure 2.16 Underground parking traffic flow.
Figure 2.17 Floor plan of the underground parking.
Figure 2.18 Section cut view.
Figure 2.19 Section cut view.
Figure 2.20 Site layout traffic flow.
Figure 2.21 Parking Layout of the site.
Figure 2.22 Parking space size.
Figure 2.23 3D View of the Staircases.
Figure 2.24 First Floor Staircase dimensions.
Figure 2.25 Typical Floor Staircase dimensions.
Figure 2.26 Elevator doors dimensions.
Figure 2.27 Emergency exit path for the first floor.
Figure 2.28 Emergency exit path for the second floor.
Figure 2.29 Emergency exit path for the typical floors.
Figure 2.30 LEED Integrative Process
Figure 2.31 LEED Location and Transportation.
Figure 2.32 LEED Sustainable Sites.
Figure 2.33 LEED Water Efficiency.
Figure 2.34 LEED Energy and Atmosphere.
Figure 2.35 LEED Materials and Resources.
Figure 2.36 LEED Indoor Environmental Quality.
Figure 2.37 LEED Innovation.
Figure 2.38 LEED Regional Priority.
Figure 2.39 LEED Final Points.
Figure 2.40 Life cycle costs of the project.
Figure 3.1 The typical floor slab structure.
Figure 3.2 Exterior wall structure.
Figure 3.3 Interior wall structure.
Figure 3.4 Scupper at parapet wall (Copper Development Association, n.d.)
Figure 3.5 Geometry of the office building in SAP2000
Figure 3.6 Structural layout of the building.
Figure 3.7. The chosen frame for assigning lateral forces.
Figure 3.8. SAP2000 Material Properties: (a) Concrete, (b) Rebar.

Figure 3.9. SAP2000: Column section properties.
Figure 3.10. SAP2000: Major beam section properties.
Figure 3.11 SAP2000 Frame property/stiffness modification factors: (a) Column, (b) Beam.
Figure 3.12 SAP2000 Joint Restraints: Fixed support.
Figure 3.13 SAP2000: Diaphragm Constraint.
Figure 3.14. Assigned dead loads on 2D frames in SAP2000.
Figure 3.15. Assigned live loads on 2D frames in SAP2000.
Figure 3.16. Assigned roof live loads on 2D frame in SAP2000.
Figure 3.17 SAP2000: Slab Section.
Figure 3.18 SAP2000: Slab property modifiers.
Figure 3.19 SAP2000: Dead area loads applied on 3D Model.
Figure 3.20 SAP2000: Dead frame loads applied on 3D Model.
Figure 3.21 SAP2000: Live area loads applied on 3D Model.
Figure 3.22 SAP2000: Live frame loads applied on 3D Model.
Figure 3.23 SAP2000: Roof live area loads applied on 3D Model ($L_r = 0.96\,kPa$)
Figure 3.24 Mass and Stiffness centers.
Figure 3.25 Design wind load cases.
Figure 3.26. SAP2000: Assigned lateral forces for Case 1 wind loads on 2D frame.
Figure 3.27. SAP2000: Assigned lateral forces for seismic loads on 2D frames.
Figure 3.28. Assigned gravity loads and lateral forces load patterns in SAP2000.
Figure 3.29. SAP2000: Assigned lateral forces for Case 1 wind loads on 3D frame.
Figure 3.30. SAP2000: Assigned lateral forces for seismic loads on 3D frames.
Figure 3.31. Internal forces for Frame A under Wind load condition
Figure 3.32. Internal forces for Frame A under Seismic load condition
Figure 3.33 Inter-story seismic drift with limit checks.
Figure 3.34 SAP2000: Moment and shear force diagram for dead load.
Figure 3.35 SAP2000: Moment and shear force diagram for live load.
Figure 3.36 SAP2000: Moment and shear force diagram for wind load.
Figure 3.37 SAP2000: Moment and shear force diagram for seismic load.
Figure 3.38 Load arrangement.
Figure 3.39 Approximate analysis method load arrangement.
Figure 3.40 Internal forces for Frame A under dead load conditions: Axial force.
Figure 3.41 Internal forces for Frame A under dead load conditions: Shear force.
Figure 3.42. Internal forces for Frame A under dead load conditions: Moment diagram.
Figure 3.43 Internal forces for Frame A under wind load conditions: Axial force.
Figure 3.44 Internal forces for Frame A under wind load conditions: Shear force.
Figure 3.45 Internal forces for Frame A under wind load conditions: Moment diagram.
Figure 3.46 The structural design check in SAP2000 software.
Figure 3.47 Major beam design values of the 2nd floor beam from SAP2000.
Figure 3.48 Column values taken from SAP2000 software.
Figure 3.49 Slenderness ratio check chart
Figure 3.50 Beam-column joint free body diagram.
Figure 4.1. USGS Seismic Hazard map.
Figure 4.2. Shear-Wave Velocity Graph.
Figure 4.3. Boundary conditions.
Figure 4.4. Configuration of Phase_1.
Figure 4.5. Accelerogram of Landers Earthquake.
Figure 4.6. Soil deformation.
Figure 4.7. Acceleration along the x-axis.

Figure 4.8. PSA.
Figure 4.9. Fast Fourier transformation.
Figure 4.10. The separation of raft foundation into strips.
Figure 4.11. Pile layout.
Figure 4.12. Approximate dimensions for cantilever wall.
Figure 4.13. Retaining wall design.
Figure 4.14. Soil profile in GEO5.
Figure 4.15. Bearing capacity check in GEO5.
Figure 4.16. Settlement analysis in GEO5.
Figure 4.17. Displacement of corner piles in PLAXIS 3D under axial load.
Figure 4.18. Ultimate lateral resistance versus yield moment for long piles in sandy soil.
Figure 4.19. Brom's solution for calculation of pile head deflection.
Figure 4.20. Pile group for corner column.
Figure 4.21. Pile group for interior column.
Figure 4.22. Pile group for exterior column.
Figure 4.23. Cross section of a Pile Cap.
Figure 4.24. Reinforcement of a single pile in Geo5.
Figure 4.25. PZ section.
Figure 4.26. Bending moment and shear force.
Figure 4.27. Results of check for bending and shear.
Figure 4.28. Slope stability verification.
Figure 4.29. Pile layout in PLAXIS 3D.
Figure 4.30. Phases of the construction.
Figure 4.31. Total displacement of the foundation in PLAXIS 3D.
Figure 5.1. WBS of a 12-storey Office Building.
Figure 5.2. Schedule of the Project (November 2024 - December 2025).
Figure 5.3. Schedule of the Project (December 2025 - January 2027).
Figure 5.4. Schedule of the Project (January 2027 - June 2027).
Figure 5.5. Schedule of the Project (June 2027 - November 2027).
Figure 5.6 Construction Quality Checklist.
Figure 5.7. Quality metrics.
Figure 5.8.Construction site planning.
Figure 6.1. Topographic map of Project Area.
Figure 6.2. Los Angeles County Storm drain system.
Figure 6.3. Slope analysis of the site.
Figure 6.4 Slope arrow analysis of the site.
Figure 6.5 Grading of the site with elevations and slopes.
Figure 6.6 Cut and fill analysis of the site.
Figure 6.7 Preliminary grading and drainage plan of the site.
Figure 6.8. Design of tubes to the city storm drain system.
Figure 6.9. Division to small areas.
Figure 6.10. Front View.
Figure 6.11. Side View.
Figure 6.12. Final Drainage plan
Figure 9.1. SAP2000: Assigned lateral forces for Case 2 wind loads on 2D frame.
Figure 9.2. SAP2000: Assigned lateral forces for Case 3 wind loads on 2D frame.
Figure 9.3. SAP2000: Assigned lateral forces for Case 4 wind loads on 2D frame.
Figure 9.4. SAP2000: Assigned lateral forces for Case 2 wind loads on 3D frame.
Figure 9.5. SAP2000: Assigned lateral forces for Case 3 wind loads on 3D frame.
Figure 9.6. SAP2000: Assigned lateral forces for Case 4 wind loads on 3D frame.

Figure 9.7. Critical moment of the beam on the first floor.
Figure 9.8. Critical moment of the beam on the second floor.
Figure 9.9. Critical moment of the beam on the third floor.
Figure 9.10. Critical moment of the beam on the fourth floor.
Figure 9.11. Critical moment of the beam on the fifth floor.
Figure 9.12. Critical moment of the beam on the sixth floor.
Figure 9.13. Critical moment of the beam on the seventh floor.
Figure 9.14. Critical moment of the beam on the eighth floor.
Figure 9.15. Critical moment of the beam on the ninth floor.
Figure 9.16. Critical moment of the beam on the tenth floor.
Figure 9.17. Critical moment of the beam on the eleventh floor.
Figure 9.18. Critical moment of the beam on the twelfth floor.
Figure 9.19. Hand calculation of internal forces under wind load - Part 1.
Figure 9.20. Hand calculation of internal forces under wind load - Part 2.
Figure 9.21. Hand calculation of internal forces under wind load - Part 3.
Figure 9.22. Hand calculation of internal forces under wind load - Part 4.

Introduction

This project presents the design of a 12-story high rise office building. The report shows the results of an extensive literature review, the design assumptions and the detailed calculations for the proposed structure. This project includes the calculations for the architectural, structural, geotechnical parts, and also environmental and construction management details related to the building design are presented. This high-rise office building will be located at 940 N Sycamore Avenue in Los Angeles, California 90038, USA.

Table 1.1 shows the aspects that this project covers including architectural, structural, geotechnical, environmental and construction management parts.

Table 1.1. Project disciplines.

Part	Weight Distribution	Responsible person for this part
Architectural and Structural	40%	Alibi Seitkaliyev Amirmagruf Amantay
Geotechnical	35%	Malika Sissenova Aruzhan Gabit
Environmental	15%	Tangguli Zhubanysh
Construction Management	10%	Bekbarys Aidarliyev

For the architectural part, the International Building Code (IBC), California Building Code (CBC), Los Angeles Municipal Code (LAMC), and California Building Standards Code (CBSC) were used. Moreover, the LEED (Leadership in Energy and Environmental Design) concepts are also applied in this project work.

In the case of the structural part, American Society of Civil Engineers (ASCE) guidelines were followed. By calculating the dead, live, roof, snow, wind and seismic loads, the building's structural analysis will be performed.

The geotechnical part will analyze various foundation types and find the most appropriate for this 12-story office building. The environmental part includes the design of the stormwater collection system. For the construction management aspect, a feasibility study, cost estimation, scheduling, risk assessment, and project scope were developed.

The primary objectives of this project are:

- To conduct a thorough study to assess the feasibility of the planned development
- To create architectural and structural designs in compliance with building codes
- To analyze geotechnical data in order to design both foundation and basement
- To develop a design of the stormwater collection system
- To establish a construction management plan for the building
- To adhere to LEED standards for the sustainability of the building

1.1 Problem Statement

In response to Los Angeles' challenges of space utilization and economic diversification, our office building design promotes flexibility and modularity, optimizing urban space and supporting economic growth. By enhancing work-life balance through integrated wellness facilities and proximity to urban amenities, we aim to improve employee satisfaction and productivity in this densely populated city.

1.2 Ethics and Professional Responsibilities

In preparing this capstone project report, we adhered to the highest standards of ethics and professionalism to ensure that our work meets academic, professional, and societal expectations. The ethical considerations outlined below address the methodology, data handling, collaboration, and presentation of our findings, ensuring that the report reflects integrity, transparency, and accountability.

Adherence to Academic Integrity

All content in this report is original, with proper citations for any external sources or references used. We ensured that all data, codes, and calculations are our own or are appropriately credited to their original authors. Data, calculations, and

design choices were presented truthfully, without manipulation or omission of relevant details to skew results in favor of specific conclusions.

Ethical Data Collection and Usage

All technical calculations and analyses were conducted following recognized engineering codes, including the California Building Standards Code (CBSC), Los Angeles Municipal Code (LAMC), and American Society of Civil Engineers (ASCE) standards. We included detailed methodologies for structural, environmental, and safety calculations, ensuring that our results can be independently verified. While preparing this report, we respected proprietary or sensitive data by using publicly available resources and tools where required.

Professional Collaboration and Contributions

The report is a collective effort, with equitable contributions from all team members. Each individual's input is valued and acknowledged. When needed, we sought guidance from faculty and industry professionals, ensuring our work reflects real-world practices and expert insights. Differences of opinion during the preparation of this report were resolved through open dialogue and reliance on factual evidence or standards.

Environmental and Societal Impact Awareness

Recognizing the environmental implications of our project, we emphasized the use of sustainable materials and energy-efficient designs. Our design choices consider the safety, comfort, and accessibility of future occupants and the broader community in Los Angeles.

Presentation of the Report

The report is structured and written to be understandable to diverse stakeholders, including academics, professionals, and non-technical readers. Technical details are explained in a manner that balances depth with accessibility. All analyses, comparisons, and conclusions are presented without bias, relying solely on objective evaluation criteria. Graphs, figures, and renderings included in this report are created specifically for this project or properly credited. No misleading visuals have been used.

Commitment to Continuous Learning

Throughout the preparation of this report, we adhered to the professional responsibilities expected of engineers. This included not only compliance with technical and ethical standards but also the willingness to reflect, learn, and adapt our approach to achieve a report that exemplifies professionalism and integrity.

2. Architectural Design

2.1 Overview of the building

The building is a 12-story high rise commercial office designed to accommodate various business needs, located at 940 N Sycamore Avenue in Los Angeles, California, USA. The first floor of the building will contain a restaurant and open lobby spaces. The typical floors of the office will be arranged with different types of conference rooms, personnel's offices, storage rooms and break areas. In accordance with International Building Codes, the occupancy classification is Business occupancy, with special emphasis on safety and resilience against earthquakes which is a common setting for this particular region (NFSA, 2024). The following Figure 2.1 shows the rendered 3D view of the building.

Figure 2.1 3D view of the office building.

2.2 Site Selection

As it was mentioned, the site is located at 940 N Sycamore Avenue, Los Angeles, California. The top view of the construction site is given in Figure 2.2.

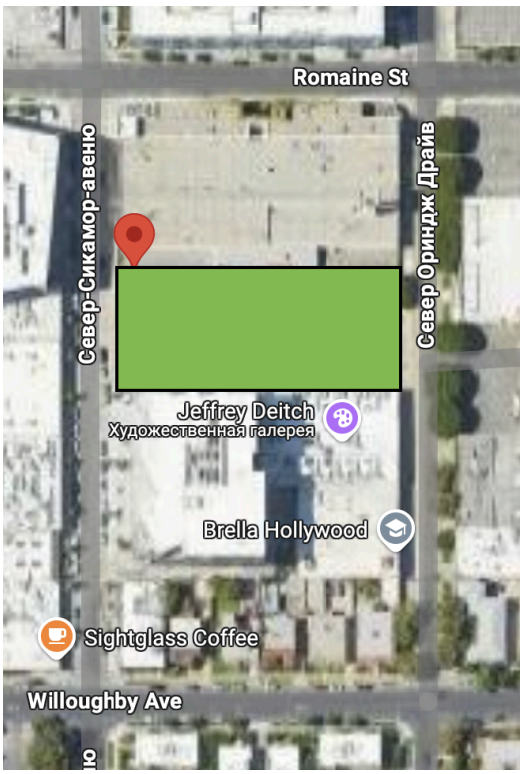

Figure 2.2 Top view of the construction site (Google Maps).

The site is located within the fast-growing neighborhood of Hollywood in Los Angeles, recognized for its mix of ultra-luxury retail, residential, and commercial projects. The area has had incredible development in the last decade, continuing to meet demands for real estate and entertainment. This site is located within a seismically active region of Southern California, which has experienced two significant earthquakes in recent years: the M6.7 Northridge earthquake in 1994 and the M6 Whittier Narrows earthquake in 1987.

Seismic Design: The site falls into seismic design Category D, requiring reinforcement in structural solutions for moderate to high seismic activity. Los Angeles is located within a seismic risk zone, so building designs must comply with strict earthquake resistance standards, enabling structures to withstand a magnitude earthquake based on a return period of 2475 years.

Wind: The prevailing wind direction is from the south-southwest, with an average wind speed of 34 m/s, which affects both ventilation and cooling strategies for the building.

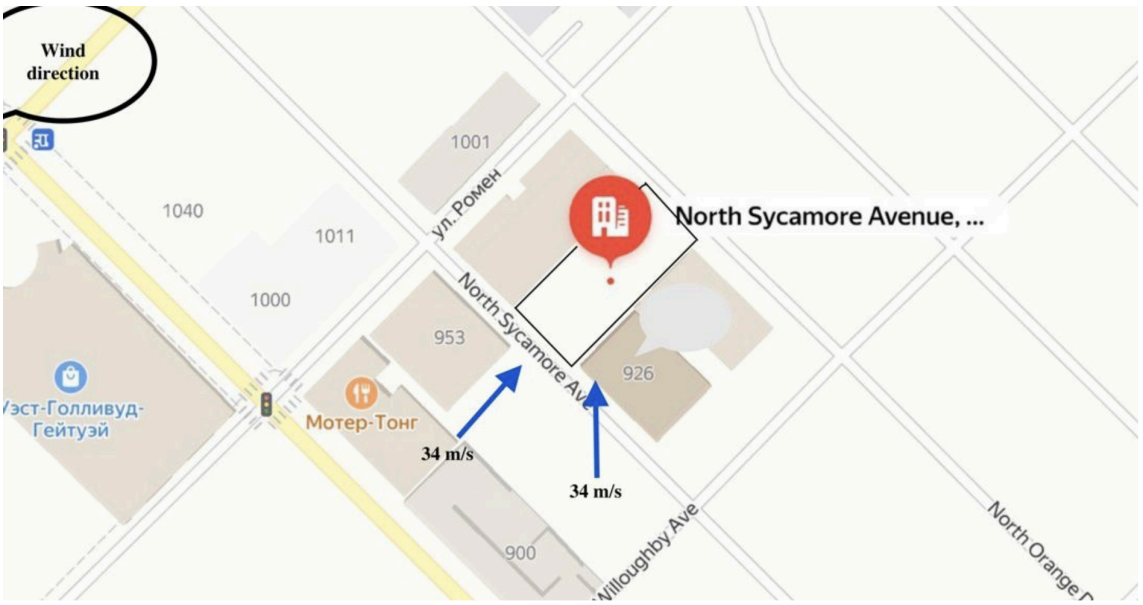

Figure 2.3 Wind directions of the construction site.

Urban Density: Sycamore Avenue is part of a heavily developing area with numerous high-rise offices, luxury shops, and service industry locations. There's a growing trend of overcrowding, driving the need for vertical development.

2.3 Site Analysis

2.3a Historical Background: Over the last century, the area surrounding 940 N Sycamore Avenue has evolved significantly. Once an industrial zone, it has now become a commercial and cultural hub. Just a few blocks away is Hollywood, the heart of the entertainment industry in Los Angeles. This particular site has hosted small-scale commercial developments and auto-related businesses due to its proximity to Sunset Boulevard. The area has primarily been zoned for commercial use, but mixed-use developments have become increasingly popular as Los Angeles expands vertically. Historical geotechnical investigations show the area was once occupied by light industrial buildings. Recent construction projects reflect ongoing gentrification, transforming the district into a creative and business-oriented area.

2.3b Orientation: The site enjoys a strategic location with easy access to major thoroughfares like Sunset Boulevard and La Brea Avenue, while benefiting from a

quieter, slightly removed position in the heart of Sycamore Avenue. Due to its urban context, there is minimal overshadowing from neighboring buildings for mid-rise developments, allowing ample daylight access from multiple directions.

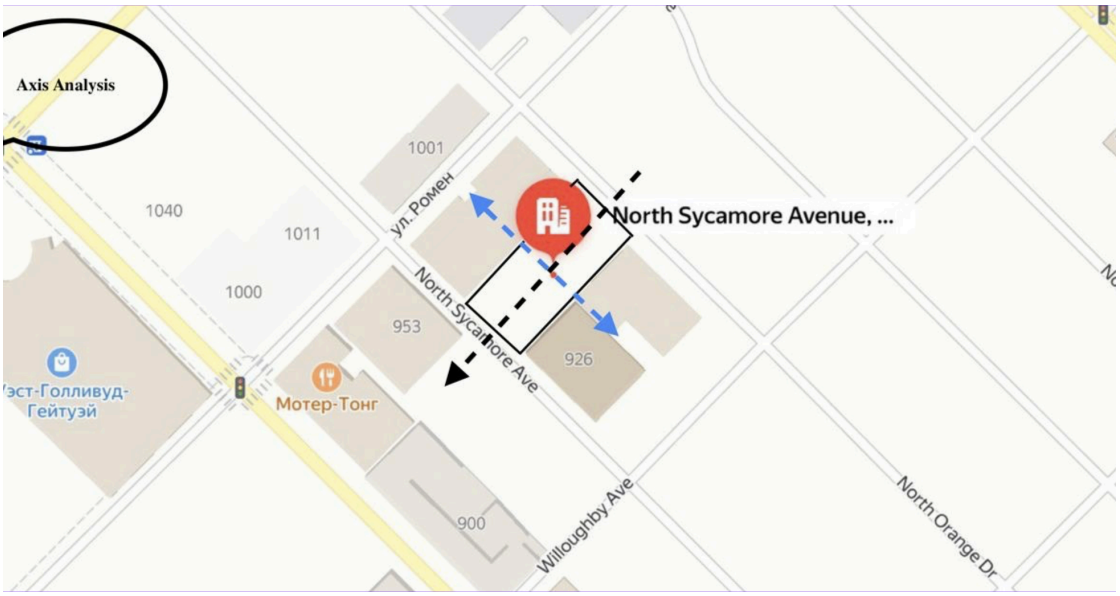

Figure 2.4 Axis analysis of the site location.

2.3c Cool Breeze Access: Proximity to the Pacific Ocean and the open layout of nearby streets provide 940 N Sycamore Avenue with consistent coastal breezes. Prevailing winds from the south-southwest offer excellent opportunities for natural ventilation, especially during hot summer months. Incorporating passive ventilation systems, such as large operable windows, rooftop vents, and strategic orientation, can reduce reliance on mechanical cooling. Wind speeds in the area average 33 m/s over a 50-year return period, and the site benefits from mild weather year-round, making natural cooling opportunities effective.

2.3d Solar Access: Using solar analysis tools like Suncalc.org and architectural software like Revit, the solar trajectory for the site was calculated. The site enjoys approximately 12 hours and 41 minutes of sunlight daily, with a shadow length of about 2.81 meters during peak solar exposure. The building should capitalize on southern and eastern exposures to maximize daylight and energy efficiency. South-facing windows will benefit from consistent light, while solar shading devices like louvers should be incorporated to reduce direct solar heat gain during peak hours. Energy-efficient materials and glazing, such as electrochromic or low-E glass, will enhance thermal

comfort and allow for large window designs that connect indoor spaces to outdoor views.

2.3e Site-Specific Variables and Climate-Responsive Design:

- **Temperature:** The Mediterranean climate features warm, dry summers and mild winters. Summer highs average 39°C, while winter lows can drop to 2.7°C. Thermal mass materials, shading devices, and natural ventilation will help minimize overheating while maintaining comfort in cooler months.
- **Humidity:** With an average relative humidity of 62%, moisture management strategies, such as vapor barriers, are important, especially for basement or underground parking structures.
- **Traffic and Noise:** Sycamore Avenue is exposed to moderate vehicular traffic, particularly during rush hours. Sound insulation measures, such as double or triple-glazed windows and sound-absorbing materials, will enhance acoustic performance and make office spaces more comfortable.
- **Transportation Access:** The site benefits from proximity to public transportation systems, including multiple bus lines and the Hollywood/Highland Metro Station, which is a short walk away. It also offers easy access to major highways such as US-101, facilitating commuting by car.

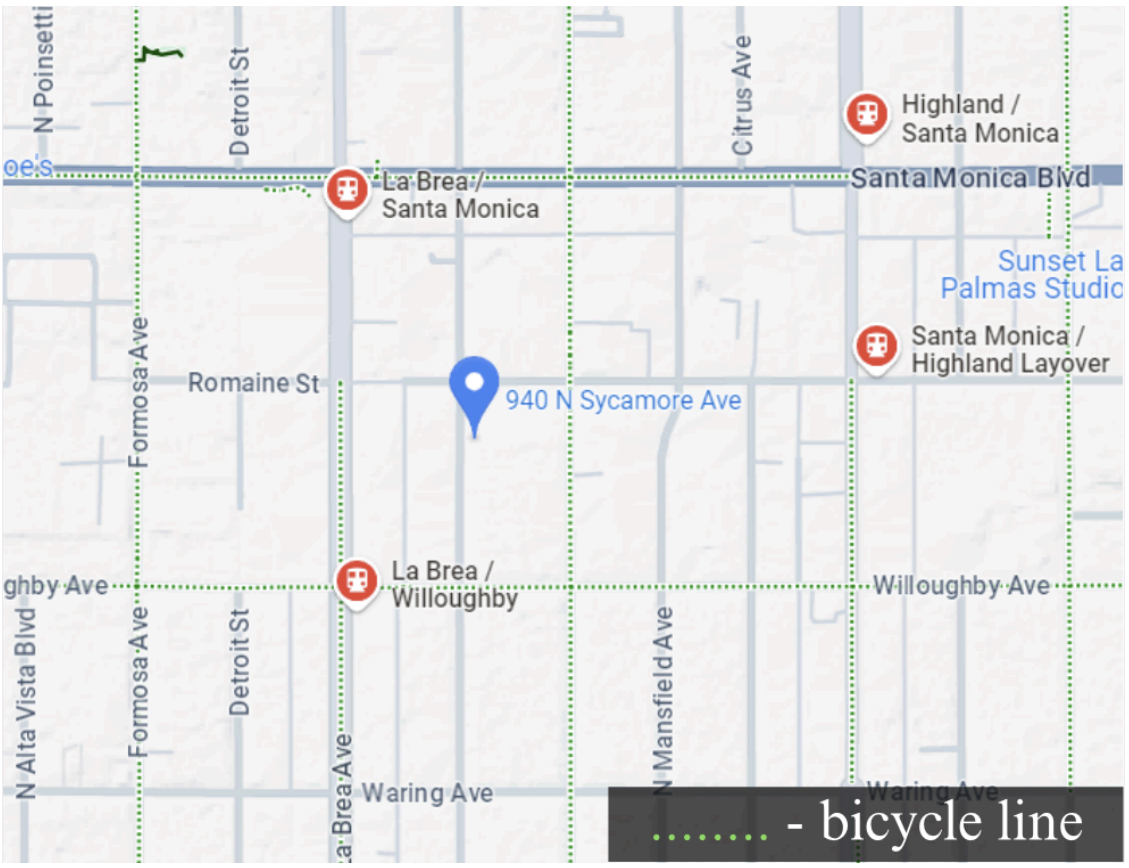

Figure 2.5 Bus stops and bicycle lines near the building area.

2.3f Views: The site offers excellent views of the Los Angeles urban landscape, particularly towards downtown LA and the nearby Hollywood Hills. Rooftop amenities or upper-level office spaces could take advantage of these views, enhancing the appeal of the building to potential tenants.

2.3g Site Survey (Overshadowing by Nearby Buildings): A survey of the area shows the site is surrounded by mid-rise buildings, typically 3 to 8 stories high. The relatively low scale of surrounding structures ensures minimal overshadowing for a 12-story building. The distance between neighboring properties allows for adequate natural light penetration throughout the year, enabling the design to maximize the use of windows and skylights.

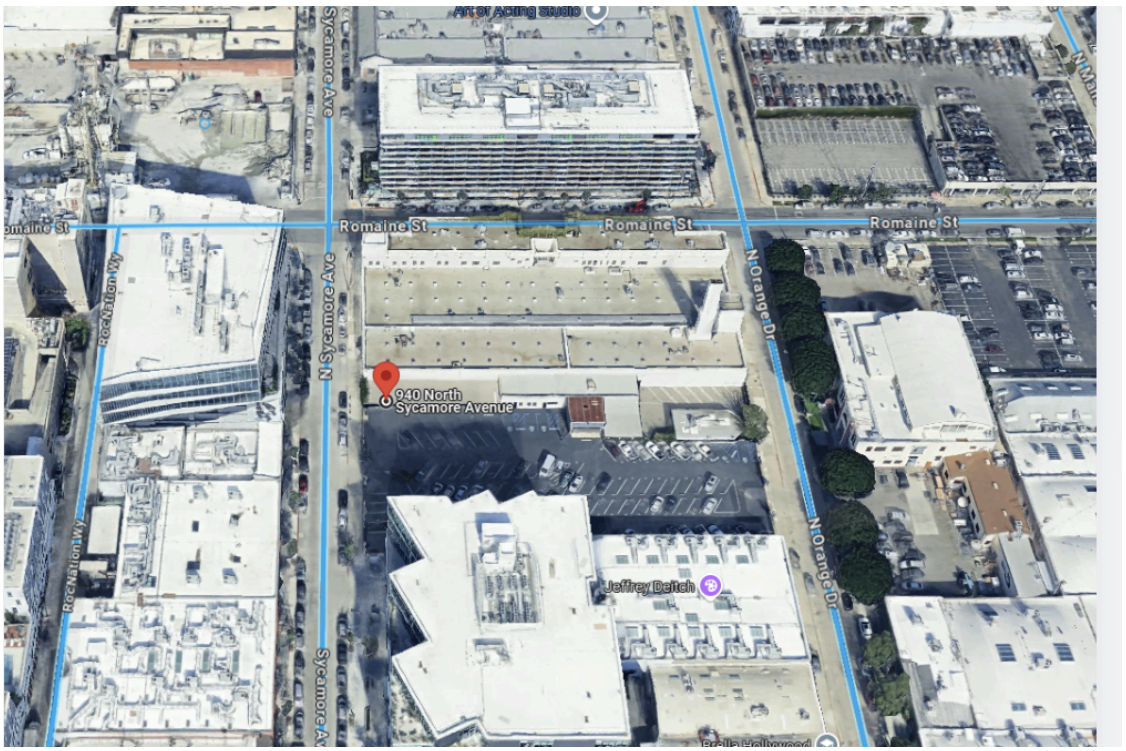

Figure 2.6 Top view of the construction site.

2.4 Design Concept

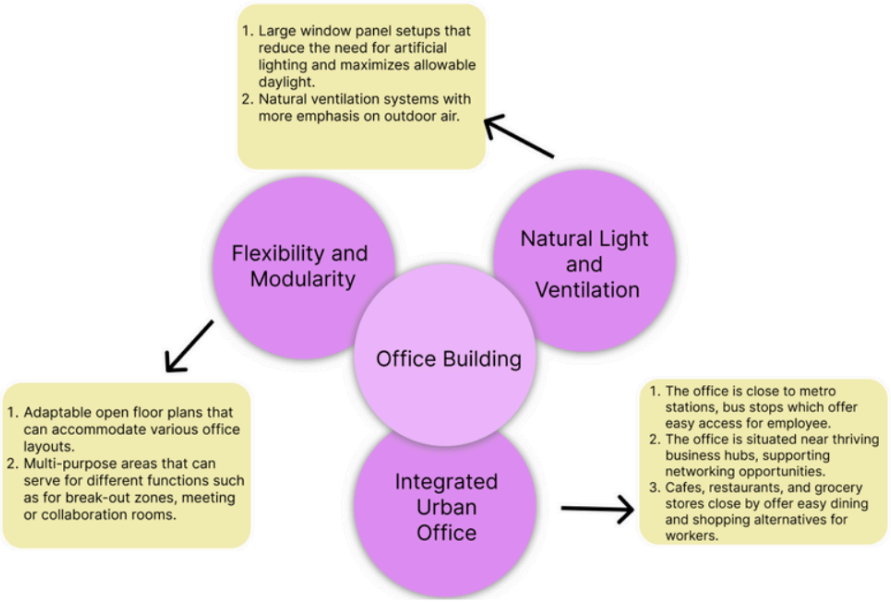

Figure 2.7 Main features of our office building.

This Figure 2.7 above shows the main features of our office building. As you can see, we highlighted 3 major advantages of our construction project.

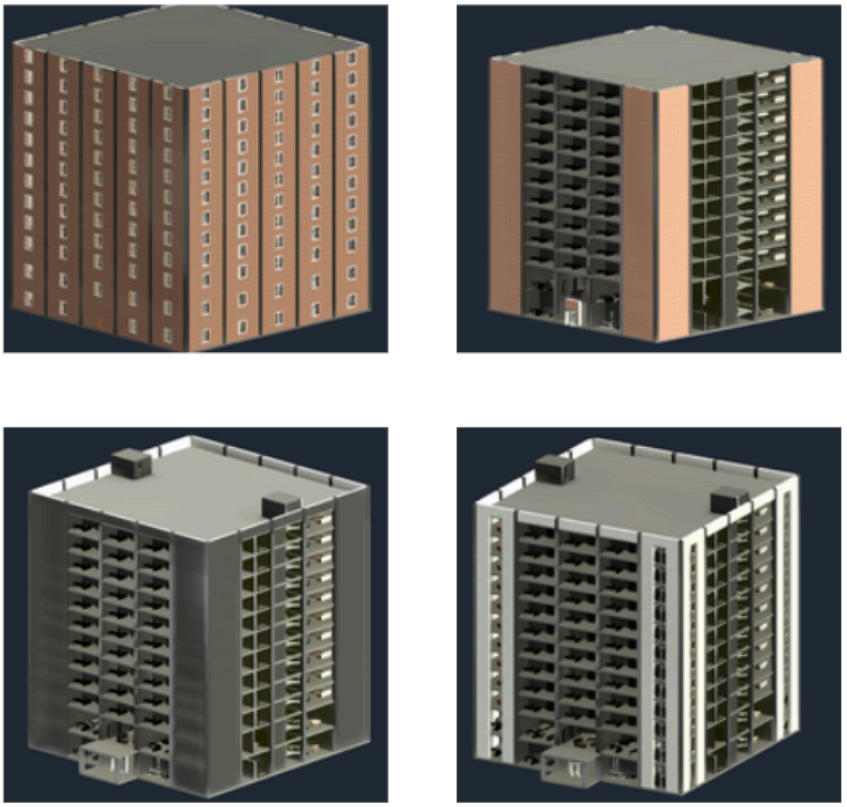

Figure 2.8 Evolution of the building.

From Figure 2.8, it can be clearly seen that compared with the first design of the building there are a lot of differences between the first and last building. It became more aesthetically pleasing, convenient, and also obtained some features that were not in the first design.

2.5 Design Codes

California Building Standards Code (CBSC) , also known as Title 24 of the California Code of Regulations, is the primary set of codes used in the design and construction of buildings in California.

The Los Angeles Municipal Code (LAMC) contains local amendments and additional regulations applicable within the City of Los Angeles.

American Society of Civil Engineers (ASCE) 7 – This standard specifies the minimum design loads for buildings, including wind and seismic loads. LA uses ASCE 7-16

International Building Code (IBC) - The International Building Code is a set of regulations ensuring public safety, health, and welfare in building construction and occupancy.

California Building Code (CBC) - The CBC is California's building code, derived from the International Building Code (IBC) and customized with amendments to meet the state's specific environmental, seismic, and safety needs.

2.6 Geometry Design and Site Layout

The office's square shape was chosen for its practical and efficient design. Its symmetrical structure evenly spreads out the weight and resists twisting forces during earthquakes, making it more stable and reliable in areas prone to seismic activity. The building's exterior will feature a modern look with wide glass panels that not only add to its visual appearance but also allow plenty of natural light inside.

Regarding the dimensions of the office, since it is a square shaped building, all sides are 35 meters long. Overall floor area is $1225\ m^2$. 1st floor, 2nd floor and 3rd floor plans differ offering a greater space utilization and functional zoning in the office. All layouts including the site plan, 1st, 2nd and typical floors, and also basement and roof layouts are shown in Figures 2.9-2.19.

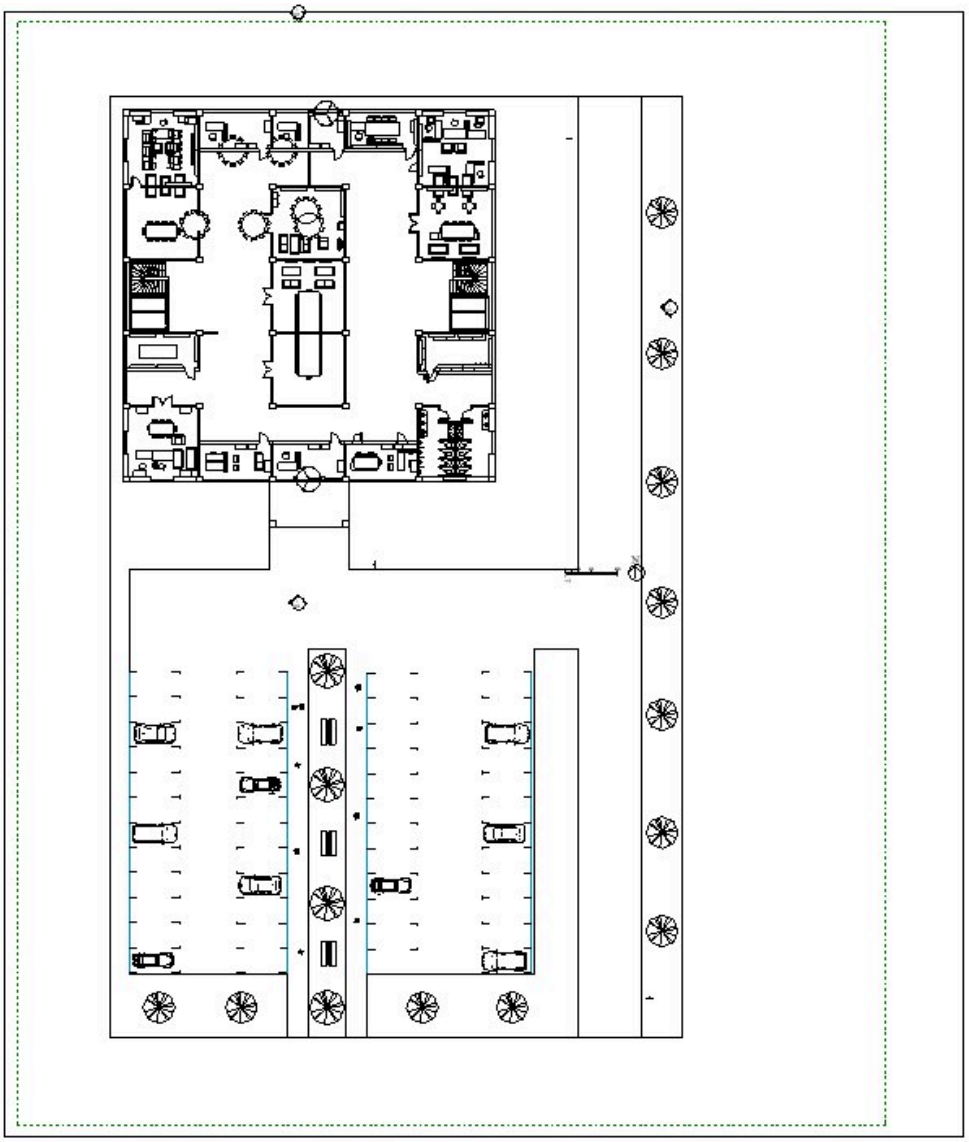

Figure 2.9 Top view of the site of construction.

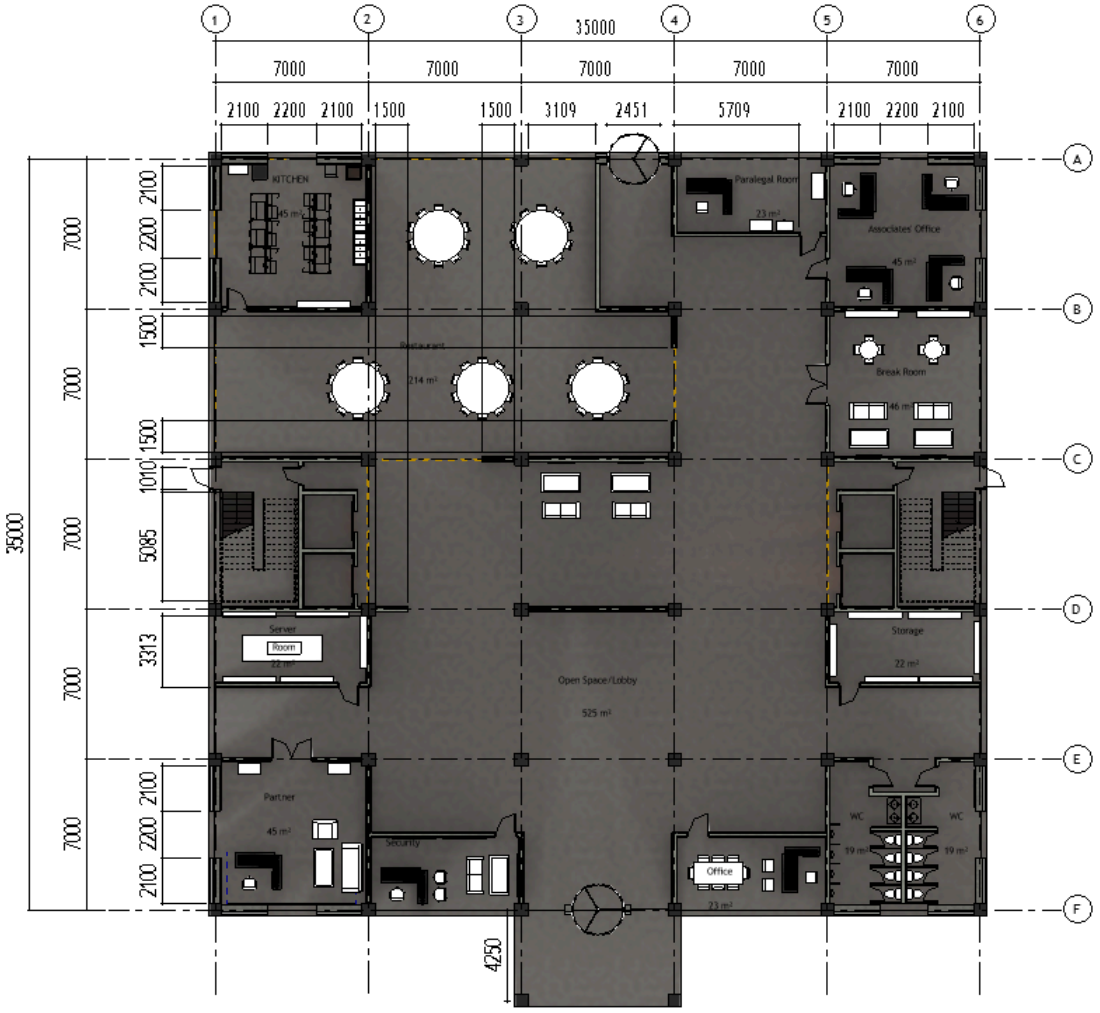

Figure 2.10 Floor plan of the first floor of the office.

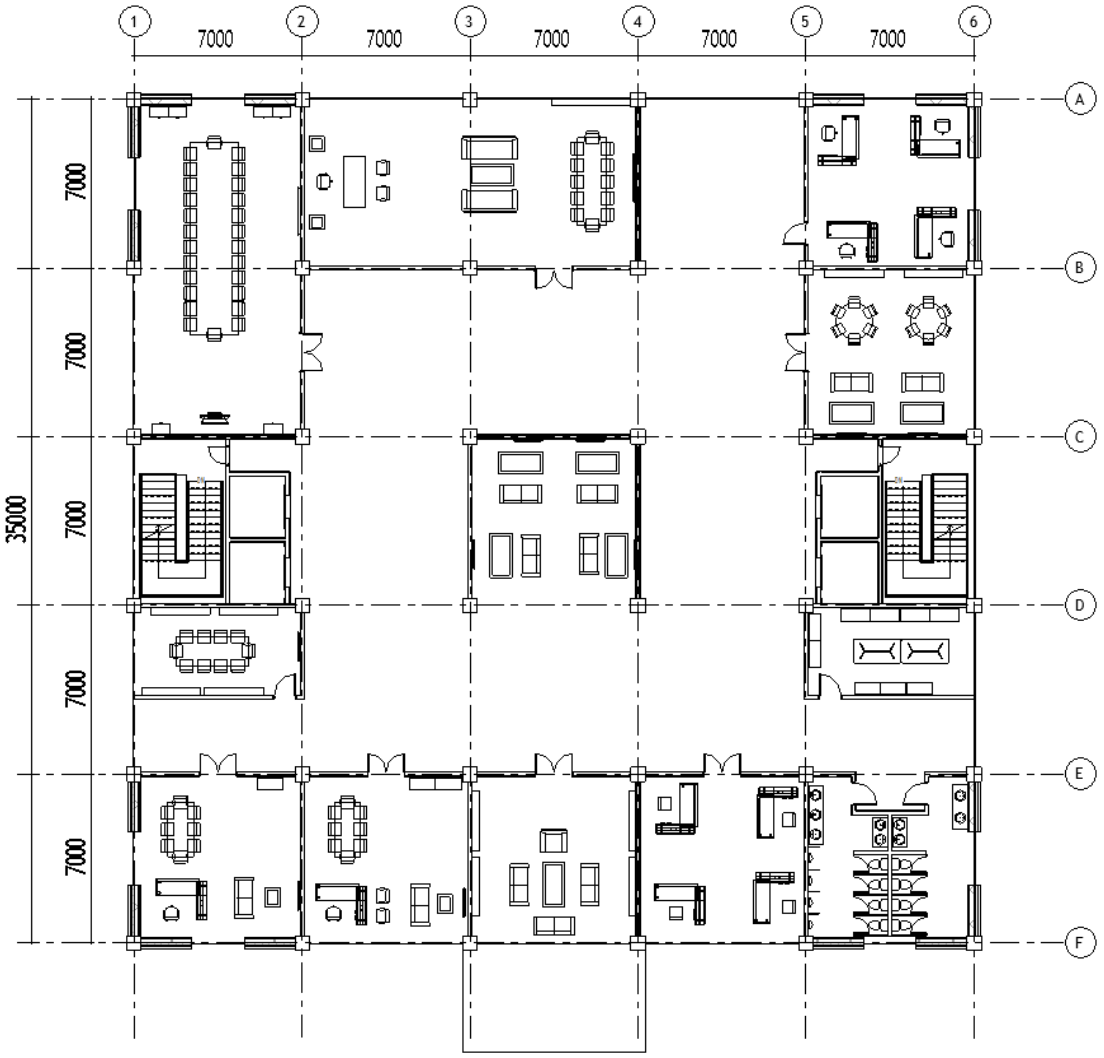

Figure 2.11 Floor plan of the second floor of the office.

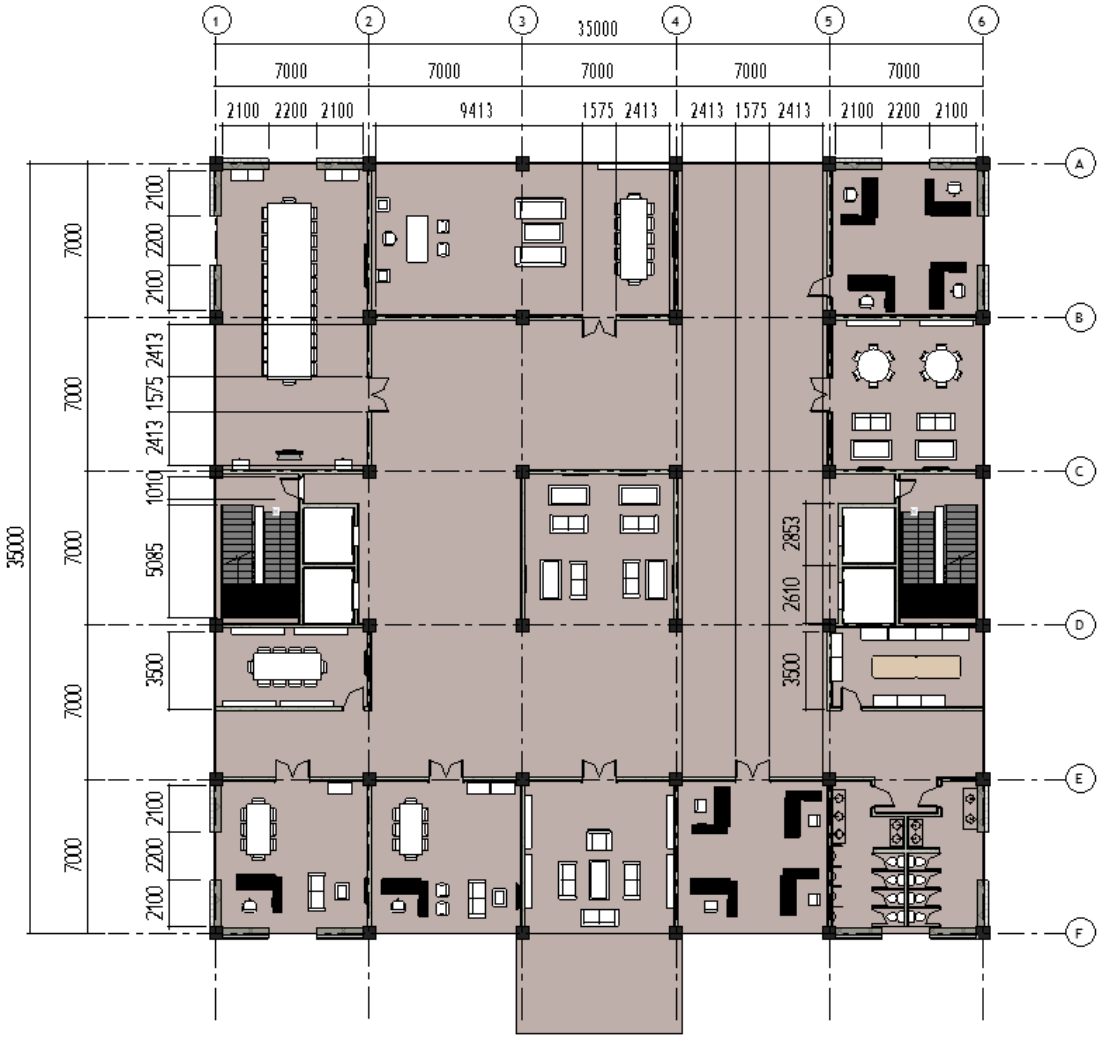

Figure 2.12 Floor plan of the typical floor (3-12 floors).

Figure 2.13 Front view of the office building.

Figure 2.14 Side view of the office building.

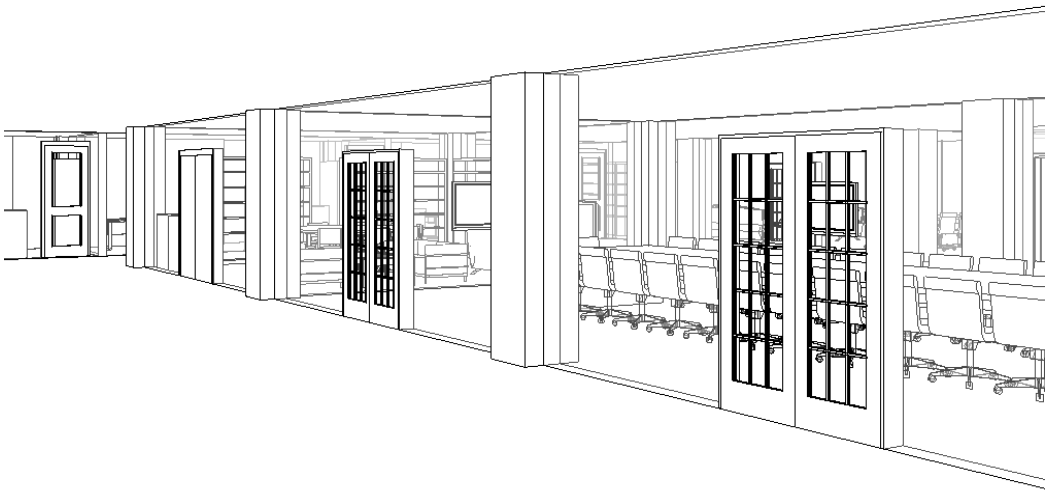

Figure 2.15 Interior view of the office building.

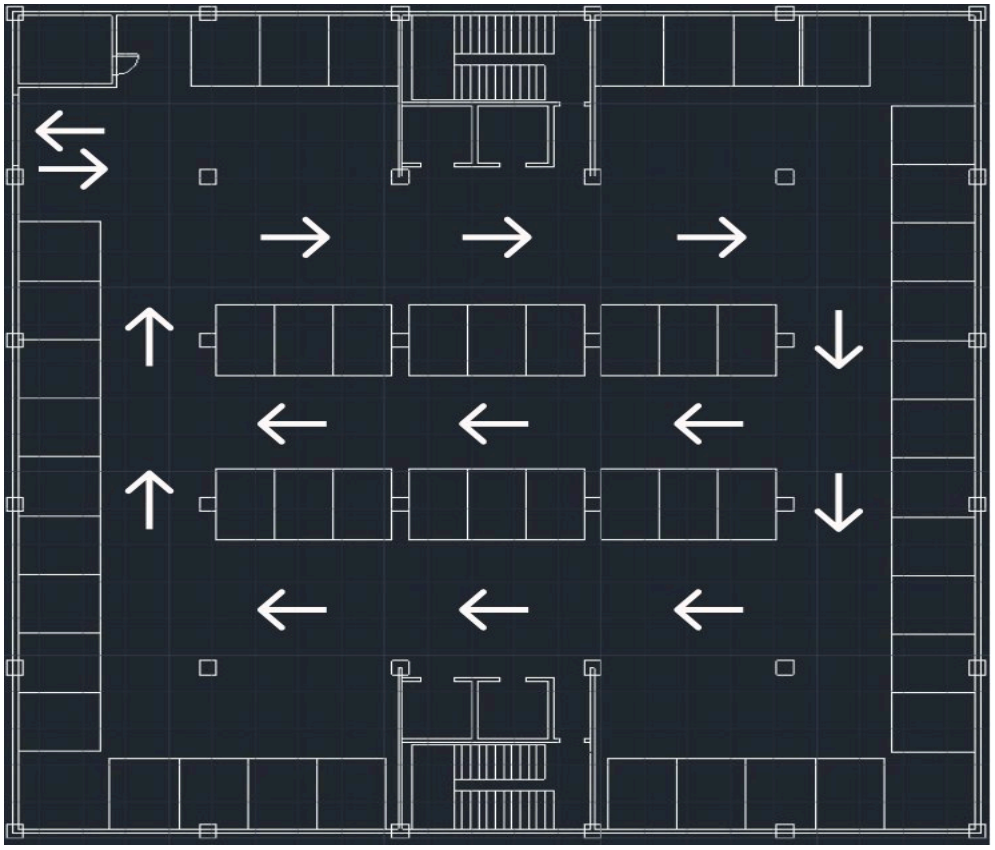

Figure 2.16 Underground parking traffic flow.

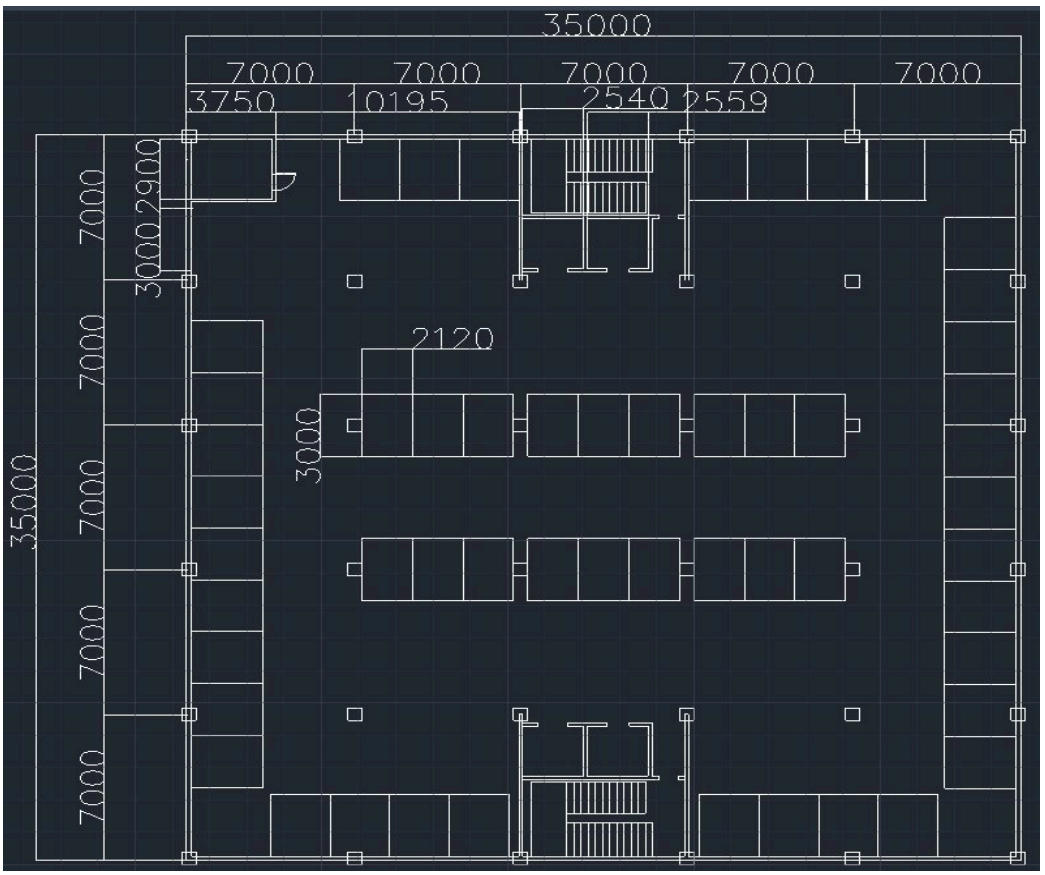

Figure 2.17 Floor plan of the underground parking.

The floor plan of the underground parking that is located in the basement of the office is given in Figure 2.17. All dimensions of the parking spaces are presented in figures. Also, the traffic flow for the parking is shown in Figure 2.16.

Figure 2.18 Section cut view.

Figure 2.19 Section cut view.

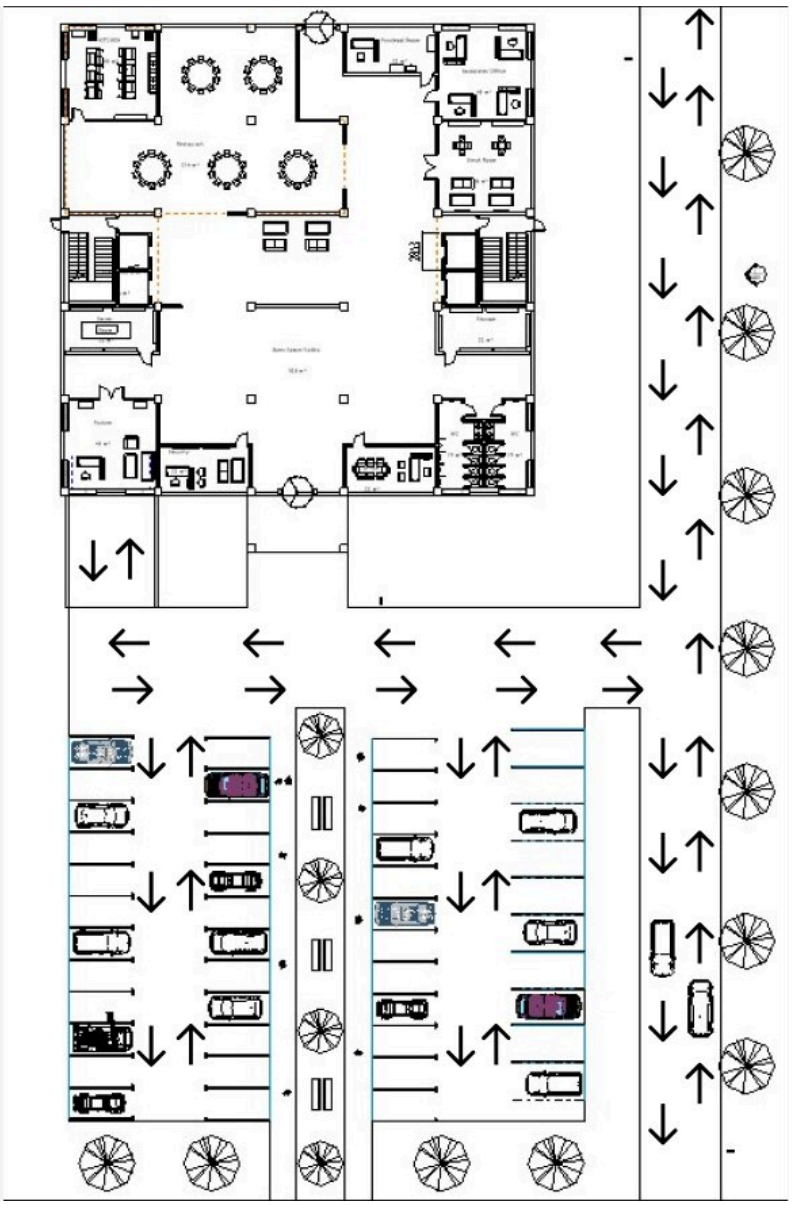

Figure 2.20 Site layout traffic flow.

Figure 2.21 Parking Layout of the site.

2.7 Architectural Calculations

Calculation of the parking space size

According to the Los Angeles Municipal Code (LAMC) Section 12.21 c, it is mentioned that there should be at least one parking space for each 500 square feet of an office building. In our case, offices' floor dimensions are 35 x 35 meters which gives us an area of 1225 square meters. Thus the LAMC requires at least 26 parking spaces for our office building. From Figure 2.6.13, Top view of the site, we can see that our exterior parking has 48 parking spaces and in the underground parking there are 53 parking spaces available. This gives us a total of 101 parking spaces overall that meets the requirements of Los Angeles Municipal Code.

According to the California Building Code (CBC) Parking Code Regulations, in Chapter 11B there are some technical requirements mentioned regarding the parking spaces. In 11B-502.2 Vehicle spaces, it is stated that the length of the parking space should be 216 inches (5486 mm) long minimum. While the width shall be 108 inches (2743 mm) minimum. These are for cars only. It also depends on the type of the vehicle. For our parking lots, they are 5500 mm long and 2800 mm wide.

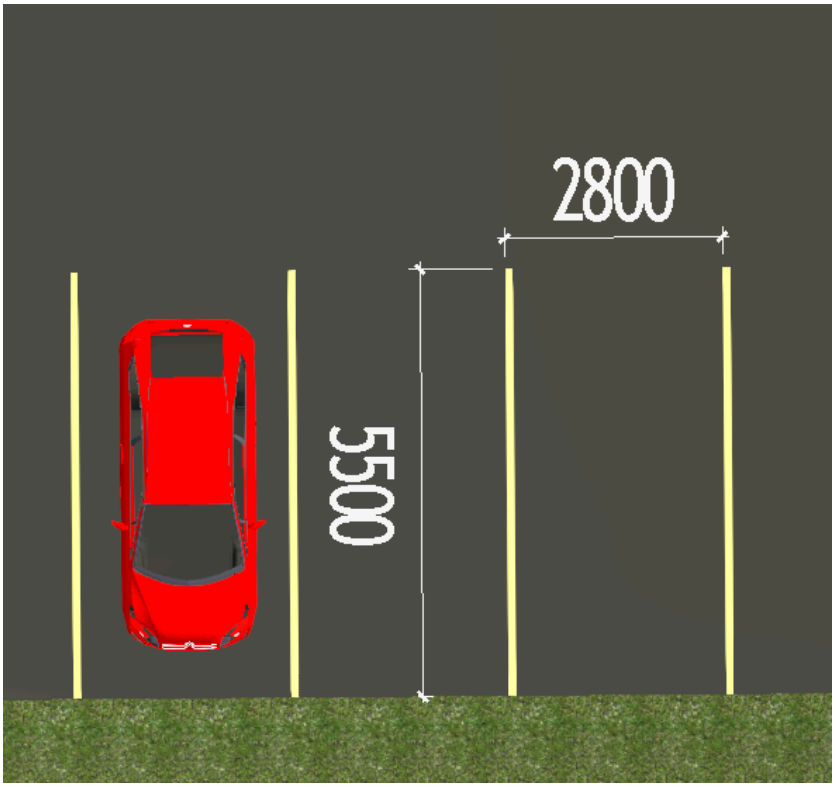

Figure 2.22 Parking space size.

Calculation of the staircases

According to California Building Code (CBC) Section 1011.5.2 of the Los Angeles County Building Code, the rise of the staircase steps should be between 4 and 7 inches. Additionally, the run size has to be 11 inches, not less than this value. Furthermore, all the threads should be uniform in size and shape. The minimum stair width is 36 (914 mm) inches based on California Building Code (CBC) Section 1011.2. According to the California Building Code (CBC) Section 10146, the height of the handrails has to be between 34-38 inches (864-965 mm). At least two staircases needed for the occupant load of 500 for the office building, which meets our requirements.

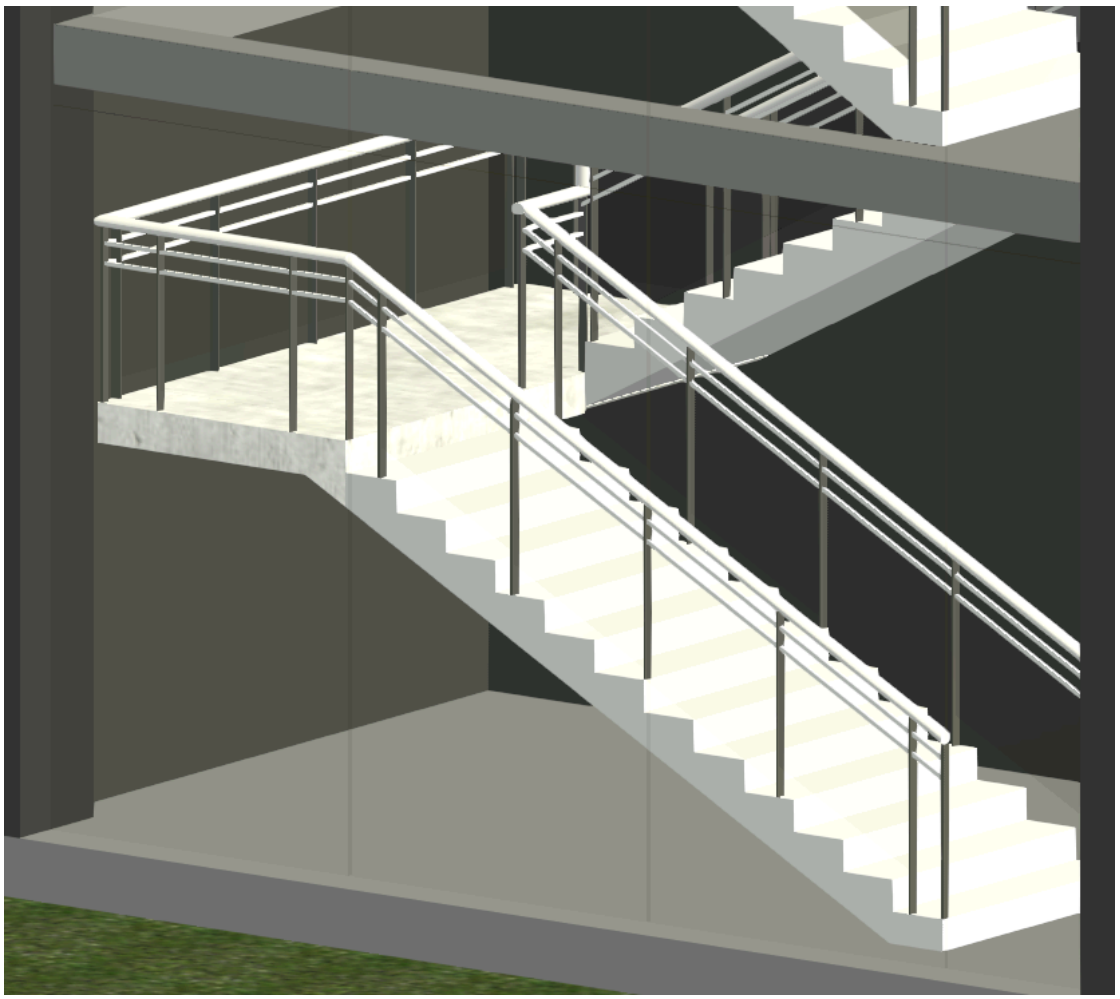

Figure 2.23 3D View of the Staircases.

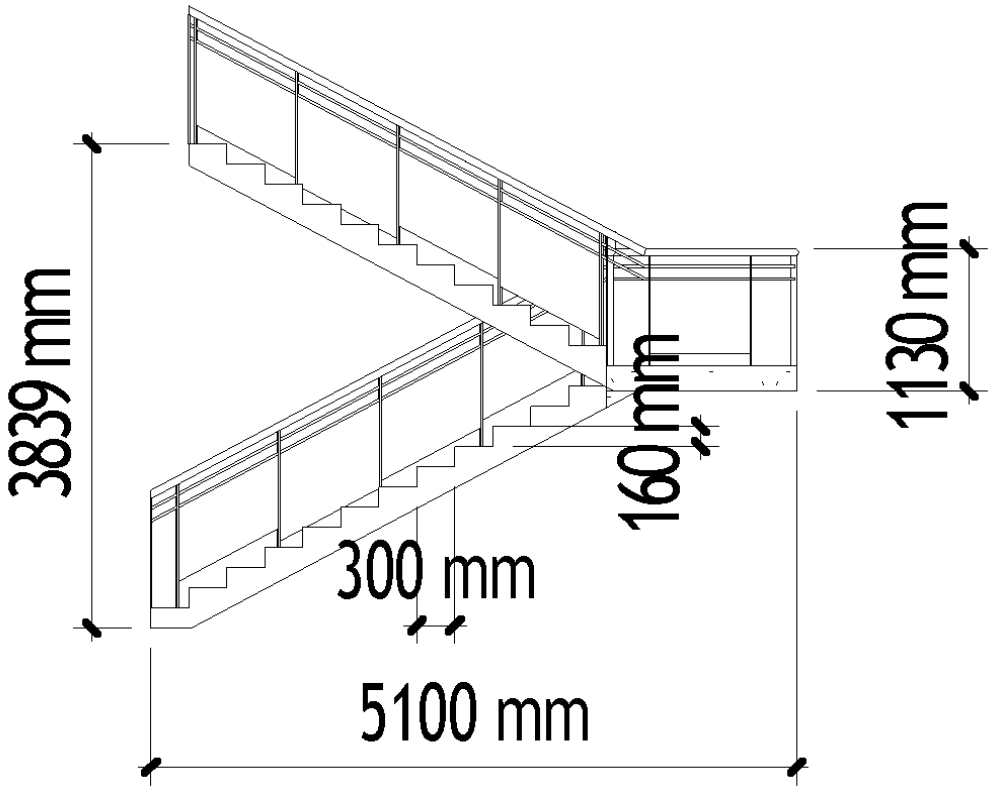

Figure 2.24 First Floor Staircase dimensions.

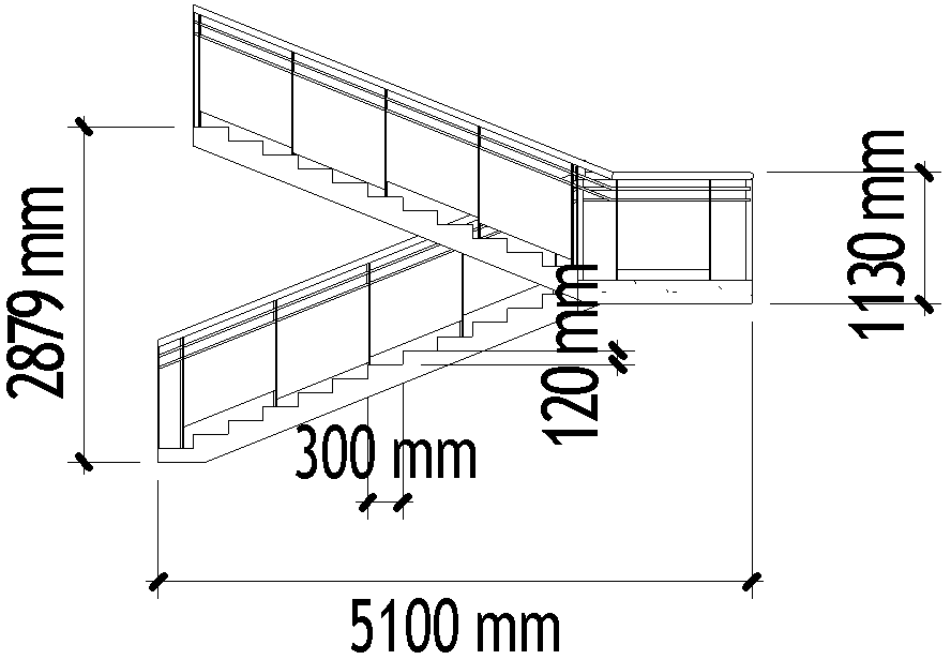

Figure 2.25 Typical Floor Staircase dimensions.

Calculation of the occupancy of the building

Number of doors and dimensions for each room based on their occupancy and function of the room.

Occupancy load is the maximum number of people that are allowed in certain spaces/rooms, and it is calculated based on the room's function and gross area. In order to determine the number of exits required for each type of the office rooms following categories have to be considered. They are a conference room, individual office rooms, server room, storage, open lobby spaces and restaurant. According to NFPA 101 Life Safety Code, occupant load factor should not be less than one occupant per 15 square feet ($1.4\ m^2$) of the gross area of the room.

Conference Room ($94 m^2$):

$$Occupancy\ Load = \frac{98\ m^2}{1.4\ m^2/person} = 70\ people$$

For the conference rooms in typical floors the number of required exits needs to be at least 2 since the occupant load is more than 50 people and distance between the exits has to be more than 1219 mm according to the International Building Code (IBC) Section 1010.1.7, which meets our requirements.

Open Lobby Space ($631\ m^2$):

$$Occupancy\ Load = \frac{631\ m^2}{14\ m^2/person} = 45.07 \simeq 46\ people$$

According to NFPA 101 Life Safety Code for the open lobby space in typical floor occupant load factor is $150\ ft^2/per\ person$ ($14\ m^2$), which gives a total occupant load of 46 people.

Storage Room ($23\ m^2$):

$$Occupancy\ Load = \frac{23\ m^2}{27.9\ m^2/person} = 0.82 \simeq 1\ person$$

Server Room ($23\ m^2$):

$$Occupancy\ Load = \frac{23\ m^2}{27.9\ m^2/person} = 0.82 \simeq 1\ person$$

Break Room ($46\ m^2$):

$$Occupancy\ Load = \frac{46\ m^2}{2.8\ m^2/person} = 16.4 \simeq 17\ person$$

For the small break room according to the NFPA 101 Life Safety Code occupancy load factor is equal to $30\ ft^2/per\ person$ ($2.8\ m^2/per\ person$) which gives a total occupant load of 17 people. All the rooms except for the conference room require only 1 exit door. During architectural design of the office building, all of these requirements were met.

Managing Partner's Room ($93\ m^2$):

$$Occupancy\ Load\ = \frac{93\ m^2}{9.3\ m^2/person} = 10\ person$$

Senior Partner's Room ($93\ m^2$):

$$Occupancy\ Load\ = \frac{93\ m^2}{9.3\ m^2/person} = 10\ person$$

Junior Partner's Room ($45\ m^2$):

$$Occupancy\ Load\ = \frac{45\ m^2}{9.3\ m^2/person} = 4.84\ \simeq\ 5\ person$$

Associate's Office Room ($23\ m^2$):

$$Occupancy\ Load\ = \frac{23\ m^2}{9.3\ m^2/person} = 2.47\ \simeq\ 3\ person$$

In each typical floor there are 6 similar office rooms for the Associate personnel. In total these 6 rooms gives a total occupant load of $3\ \times\ 6\ =\ 18\ person$.

According to NFPA 101 Life Safety Code the occupant load factor for the personal office's rooms was chosen as $100\ ft^2/per\ person$ ($9.3\ m^2/per\ person$). For all of these office rooms 1 exit is sufficient.

WC ($39\ m^2$):

$$Occupancy\ Load\ = \frac{39\ m^2}{4.6\ m^2/person} = 8.48\ \simeq\ 9\ people$$

For each typical floor the total occupant load is 187 people.

According to the International Building Code (IBC) Section 1010.1.1, minimum clear opening door width should be larger than 32 inches (813 mm), the minimum clear height for doors must be 80 inches (2032 mm) and the maximum door leaf width has to be 48 inches (1219 mm). Furthermore, door width based on the occupancy should be

considered, 0.2 inches per occupant in non-sprinklered or 0.15 inches per occupant in sprinkled system. For the rooms with occupant load of more than 50, door swing must be in the direction of the egress. All of these crucial moments were fully considered during the architectural phase of our project.

Calculation of the corridor width based on the function of the building

According to the International Building Code (IBC) Section 1020.3 Table 1020.3, the minimum corridor width for the occupancy load of less than 50 should be at least 36 inches (914 mm), and for any regular facility is at least 44 inches (1118 mm). Typical floors of our project have a corridor width of 7 meters, which meets International Building Code (IBC) requirements.

Numbers of stairs and elevators based on the occupancy and function of the building

According to the IBC 2024, number of exits or access to exits per story depends on the occupant load of the story. In our case, for the typical floor as we calculated there is an occupancy of 187 people. From Table 1006.3 of IBC, for this occupancy load factor there should be at least 2 exits from the story. Looking at the floor plan of the typical floor, we can clearly see that we have 2 emergency stairs and 4 elevators.

Window areas for each room

To determine the required dimensions for windows using IBC, we had to refer to Chapter 1031 which is about Emergency Escape and Rescue Openings (EERO). From this chapter, we know that there should be a minimum of 24 inches (610 mm) of net clear opening height and 20 inches (508 mm) of net clear opening width for windows in rooms. In our case, we have huge glasses serving as both window and wall that meet the requirements.

Natural light requirements

In section 1204 of IBC, it is written about lighting. It says that the minimum net glazed area shall not be less than 8% of the floor area of the room being considered. As mentioned above, with glass wall systems natural light level is sufficient.

Shaft

Six shafts will be present in the structure which includes four elevator shafts and two stair shafts. The building will have shafts placed in symmetrical distribution across both its blocks. The emergency fire stairs will be located at the building edges before residents access the remaining two stair shafts for their use. The construction of all shafts will use concrete as the building material and the elevator shafts will receive a two-hour fire-resistant treatment according to IBC guidelines (International Code Council, 2021).

Elevator dimensions

According to the IBC Section 3002, for buildings with stories more than 4 there should be at least one elevator. Also, the elevator car shall be of such a size to accommodate an ambulance stretcher with dimensions of 24 inches (610 mm) by 84 inches (2134 mm). Furthermore, California Building Code (CBC) Section 11B-207.4.1 specifies that elevator door widths should be at least 42 inches (1066.8 mm). Elevators that we installed in our office meet this requirement.

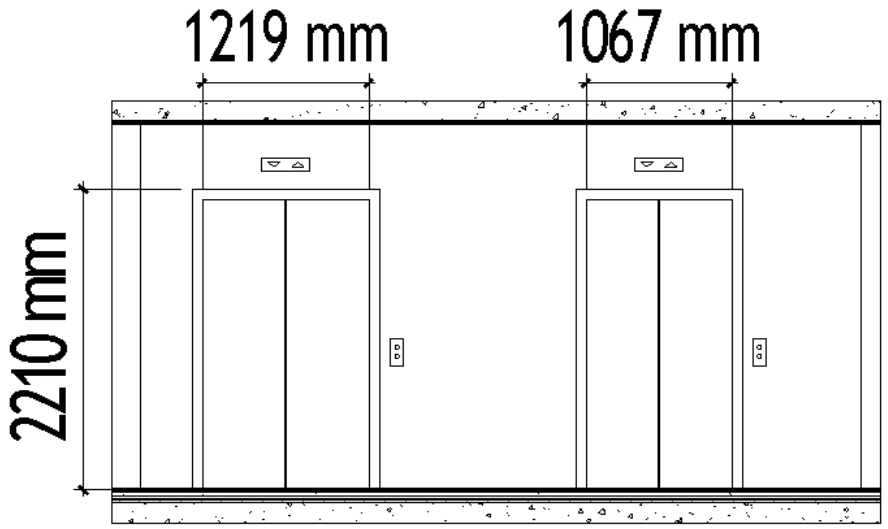

Figure 2.26 Elevator doors dimensions.

Clear height of each story

According to the International Building Code Section 1207, the minimum clear height for most occupied rooms is 8 feet (2.4 meters). Overall, the typical clear height range for Office Building of Occupancy type B is about 9 to 12 feet (2.7 to 3.6 meters)

per floor. However, 10 feet (3 meters) is a common clear height between each story, which is the same case in our design.

Calculation of the emergency evacuation path

According to the International Building Code Section 1017.2, it is mentioned that the exit access travel distance for occupancy classification of group B (Business) has to be 200 feet (60.96 meters) for without automatic sprinkler system and 300 feet (91.44 meters) for a building with automatic sprinkler system. For the first floor we considered two different evacuation routes from the farthest corner of the building.

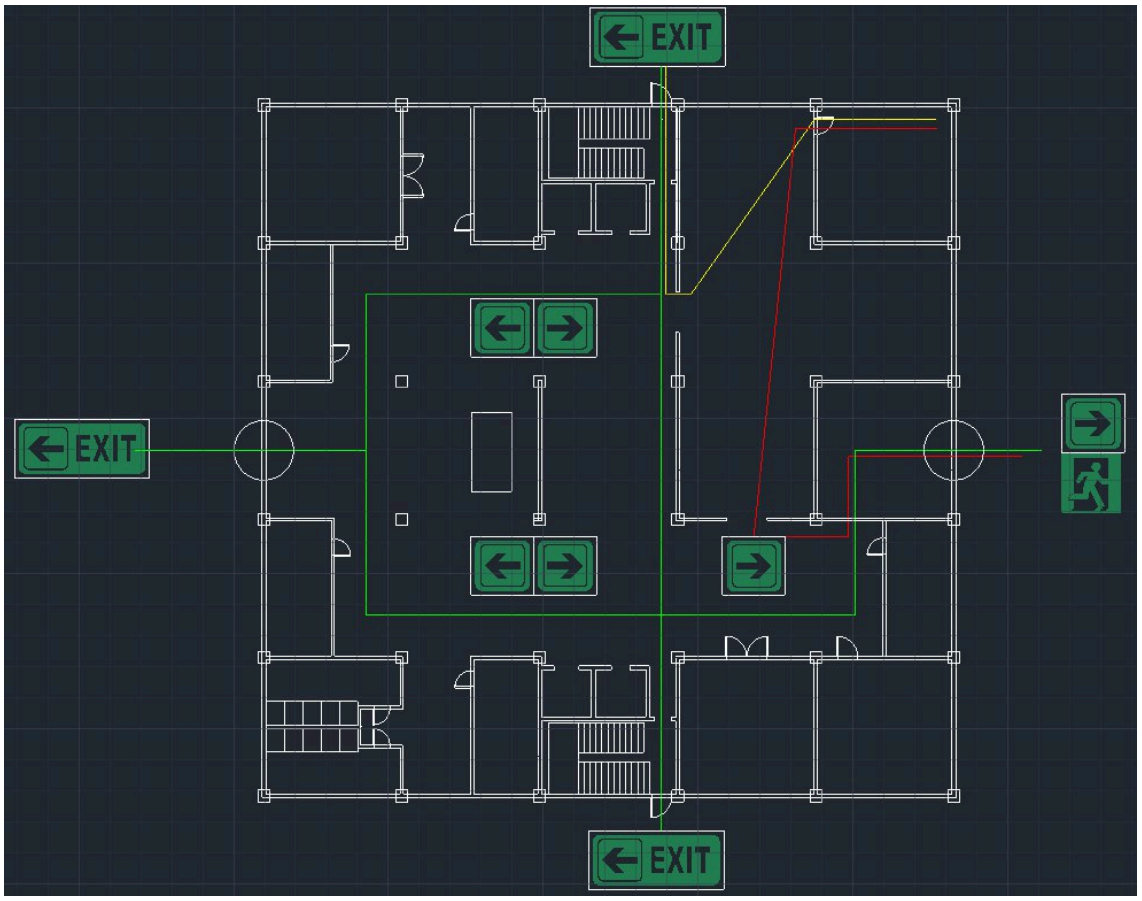

Figure 2.27 Emergency exit path for the first floor.

As you can see from the figure above, for the first floor we have 4 exit doors and the yellow line indicates the first route to the closest evacuation exit door. The travel distance for the corresponding path was calculated to be 27.81 meters. Also, the red line displays the second critical evacuation path from the farthest top right corner of the office building to the second closest evacuation exit door. Overall, the distance

traveled for this exact case was determined to be 41.99 meters. In both cases, traveled emergency evacuation distances were smaller than the distance which was established by the International Building Code for a building without sprinkler system, 60.96 meters.

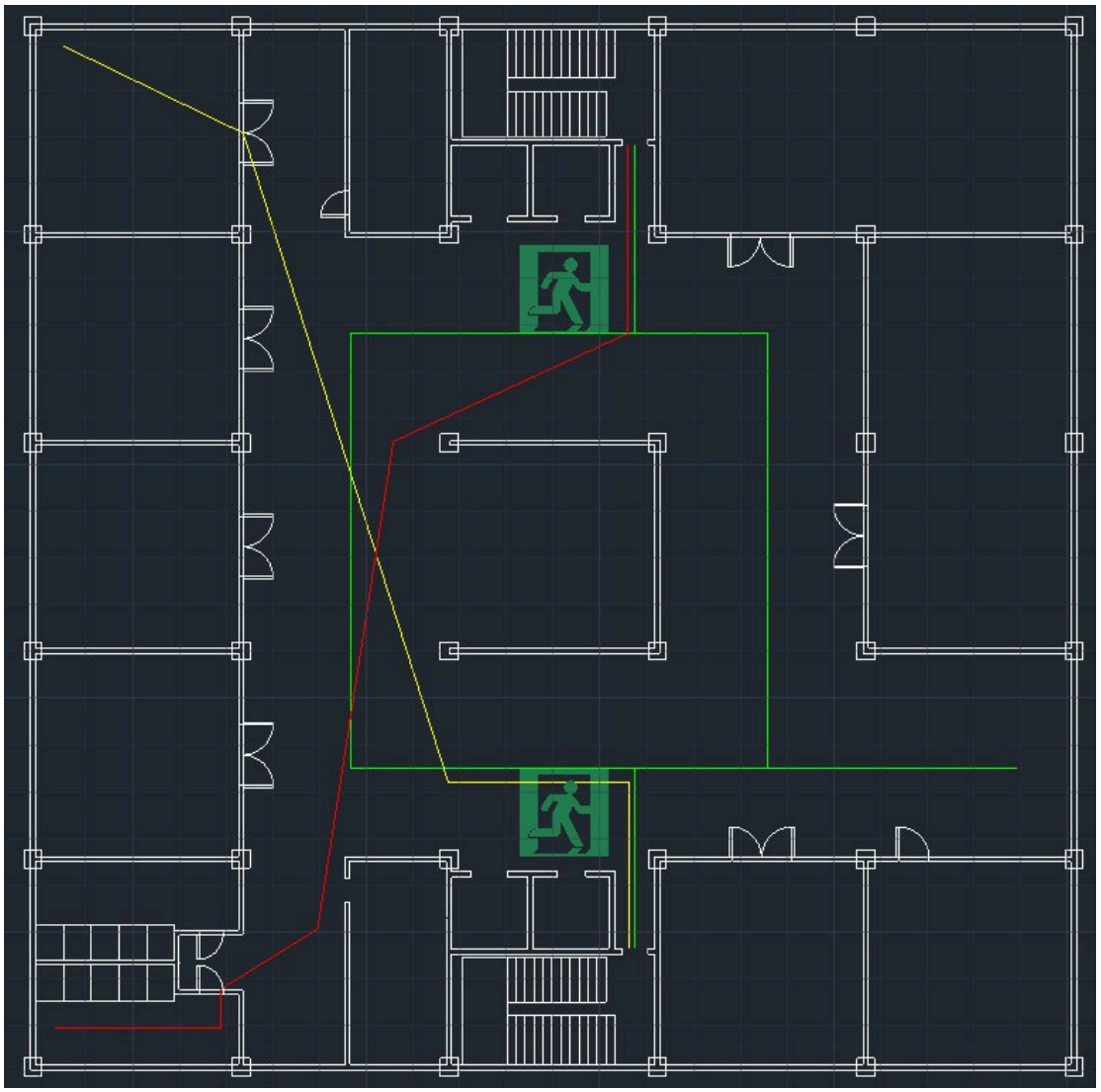

Figure 2.28 Emergency exit path for the second floor.

From the figure above, for the second floor there are 2 staircases and we considered two extreme cases of evacuation routes. The first yellow line displays the first path from farthest top left corner to the farthest second evacuation exit stairs. The travel distance for this path was calculated to be 41.05 meters. Next, the red line shows the second critical evacuation path from the farthest bottom left corner of the office building to the second farthest evacuation exit stairs on the top. Overall, the distance traveled for this exact case was determined to be 42.06 meters. In both situations,

traveled emergency evacuation distances were smaller than the distance which was established by the International Building Code for a building without sprinkler system (60.96 meters).

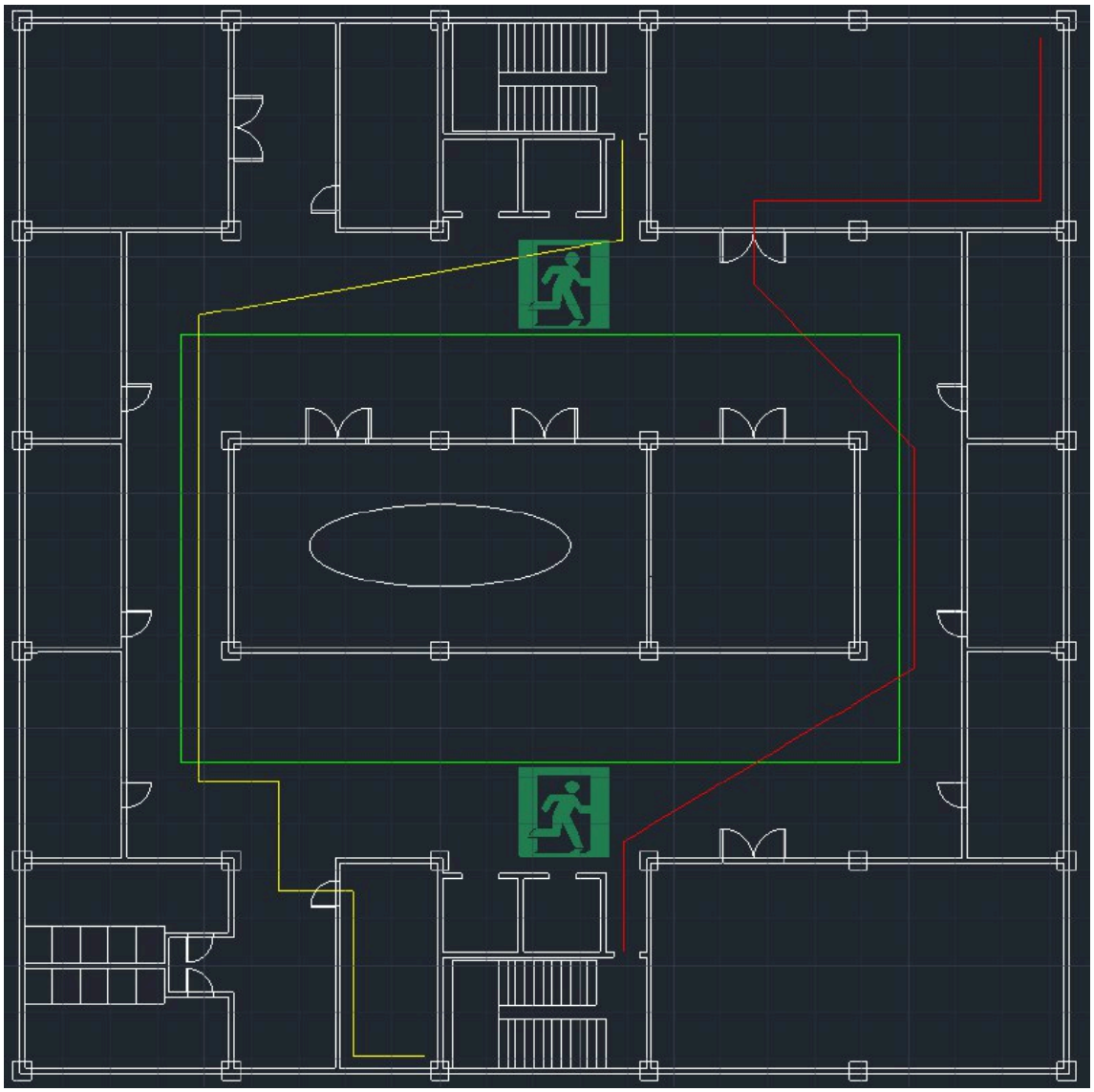

Figure 2.29 Emergency exit path for the typical floors.

For the typical floors we found two extreme cases of emergency evacuation routes from different farthest rooms to the farthest staircases. The travel distance of the red line was calculated to be 47.45 meters. The travel distance for the second yellow line was 47.00 meters. It can be stated that our office building meets International Building Code's emergency evacuation exit access travel distance standards.

2.8 Leadership in Energy and Environmental Design (LEED)

LEED (Leadership in Energy and Environmental Design) - is the world's leading green building rating system, offering a framework for creating healthy, efficient, cost-effective buildings with environmental, social, and governance benefits. LEED is a well-known symbol of sustainability, supported by people and organizations working to improve the industry (U.S. Green Building Council).

To be eligible for evaluation, the project must meet the Minimum Program Requirements. LEED certification ensures that the project meets specific standards for health, durability, and environmental sustainability. The certification levels include Certified (40-49 points), Silver (50-59 points), Gold (60-79 points), and Platinum (80+ points). Since 2004, California state regulations have required LEED certification for certain projects.

The first step in completing the LEED analysis is to choose the correct building type. There are different categories, but for our office building the category of new construction was selected. Then there are 9 different LEED categories presented.

To start with, Integrative Process is the first of 9. This category encourages early collaboration between the team projects such as engineers, architects, and other experts. This is usually done before the beginning of the project. Our office building earns 1 point out of 1 in this category since there was an early planning and collaboration.

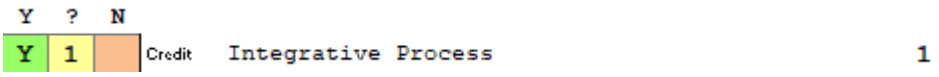

Figure 2.30 LEED Integrative Process

The Location and Transportation category is all about choosing a smart place to build. It focuses on reducing harm to the environment, making it easier for people to walk or bike, and cutting down on car pollution. It encourages projects that connect well to the city, protect nature, and support healthier, greener lifestyles. For this category, 1 point was lost from the "High Priority Site and Equitable Development" category, since the chosen site is not in a designated brownfield or priority zone, so we

do not get that point. But since the project encourages accessibility, walkability, and green transportation, it supports equitable development. So we're giving it 1 out of 2 points. Also, for the "Reduced Parking Footprint" we do not get a point at all, since we have both underground and outside parkings and we are surrounded by other parking spots. The LEED for Neighborhood Development Location category was not filled, since our location is not suitable.

0	11	0	Location and Transportation		16
		N	Credit	LEED for Neighborhood Development Location	16
Y	1		Credit	Sensitive Land Protection	1
	1		Credit	High Priority Site and Equitable Development	2
	3		Credit	Surrounding Density and Diverse Uses	5
	4		Credit	Access to Quality Transit	5
Y	1		Credit	Bicycle Facilities	1
		N	Credit	Reduced Parking Footprint	1
	1		Credit	Electric Vehicles	1

Figure 2.31 LEED Location and Transportation.

Sustainable Sites is all about taking care of the land where you build. It focuses on protecting nature, keeping rainwater from causing problems, and making outdoor spaces more enjoyable and eco-friendly. The idea is to work with the environment, not harm it. We earned 6 out of 9 points. We did a site assessment and provided open space, getting full points there. For rainwater management and heat island reduction, we took some steps but didn't go all out, so we got partial points. We also reduced light pollution with basic lighting controls, keeping it practical for the office project.

0	7	0	Sustainable Sites		10
Y			Prereq	Construction Activity Pollution Prevention	Required
Y	1		Credit	Site Assessment	1
	1		Credit	Protect or Restore Habitat	2
Y	1		Credit	Open Space	1
	2		Credit	Rainwater Management	3
	1		Credit	Heat Island Reduction	2
Y	1		Credit	Light Pollution Reduction	1

Figure 2.32 LEED Sustainable Sites.

Next, Water Efficiency is all about using water. It focuses on reducing indoor and outdoor water use, using efficient fixtures, and possibly reusing water to cut down on waste. For Water Efficiency, we earned 7 out of 11 points. We made efforts to reduce

outdoor water use with practical solutions, earning some points there. For indoor water use, we focused on water-efficient fixtures but didn't push for the highest standards. We also installed water metering and made a few adjustments for process water use, but there's still room for improvement.

0	8	0	**Water Efficiency**		11
Y			Prereq	Outdoor Water Use Reduction	Required
Y			Prereq	Indoor Water Use Reduction	Required
Y			Prereq	Building-Level Water Metering	Required
	1		Credit	Outdoor Water Use Reduction	2
	4		Credit	Indoor Water Use Reduction	6
Y	2		Credit	Optimize Process Water Use	2
Y	1		Credit	Water Metering	1

Figure 2.33 LEED Water Efficiency.

Energy and Atmosphere is all about using energy responsibly. It focuses on improving energy performance, using cleaner energy sources, commissioning systems to run efficiently, and reducing greenhouse gas emissions throughout the building's operation. Here we earned 22 out of 33 points. We worked on improving energy performance and commissioning, scoring well in those areas, but didn't go all the way to the maximum. We also installed energy metering and used refrigerants that have less environmental impact. We made some headway with renewable energy, but there's still room to improve. Overall, the approach is realistic and fits the goals for the office project.

0	22	0	**Energy and Atmosphere**		33
Y			Prereq	Fundamental Commissioning and Verification	Required
Y			Prereq	Minimum Energy Performance	Required
Y			Prereq	Building-Level Energy Metering	Required
Y			Prereq	Fundamental Refrigerant Management	Required
	4		Credit	Enhanced Commissioning	6
	13		Credit	Optimize Energy Performance	18
Y	1		Credit	Advanced Energy Metering	1
	1		Credit	Grid Harmonization	2
	2		Credit	Renewable Energy	5
Y	1		Credit	Enhanced Refrigerant Management	1

Figure 2.34 LEED Energy and Atmosphere.

Materials and Resources is about using sustainable, recycled, and local materials to reduce waste and environmental impact. It encourages efficient resource use and

recycling to make the building more eco-friendly. Our score is 9 out of 13 points. We focused on reducing the building's life-cycle impact and used environmentally transparent materials, scoring well in those areas. While we made sustainable choices in sourcing and waste management, there's still room for improvement. Overall, the approach is practical and fits the office project's goals.

0	9	0	Materials and Resources		13
Y			Prereq	Storage and Collection of Recyclables	Required
	4		Credit	Building Life-Cycle Impact Reduction	5
Y	2		Credit	Environmental Product Declarations	2
	1		Credit	Sourcing of Raw Materials	2
	1		Credit	Material Ingredients	2
	1		Credit	Construction and Demolition Waste Managem	2

Figure 2.35 LEED Materials and Resources.

Indoor Environmental Quality is about making the indoor space healthy and comfortable. It focuses on improving air quality, lighting, temperature, and noise levels to create a pleasant environment that supports well-being and productivity. In this category, we scored 13 out of 16 points. We excelled in areas like daylight, thermal comfort, and air quality assessment. While we did well with lighting and acoustics, a few areas, like low-emitting materials and air quality strategies, could be further enhanced for even better performance.

0	13	0	Indoor Environmental Quality		16
Y			Prereq	Minimum Indoor Air Quality Performance	Required
Y			Prereq	Environmental Tobacco Smoke Control	Required
	1		Credit	Enhanced Indoor Air Quality Strategies	2
	2		Credit	Low-Emitting Materials	3
	1		Credit	Construction Indoor Air Quality Managemen	1
	1		Credit	Indoor Air Quality Assessment	2
Y	1		Credit	Thermal Comfort	1
Y	2		Credit	Interior Lighting	2
Y	3		Credit	Daylight	3
Y	1		Credit	Quality Views	1
Y	1		Credit	Acoustic Performance	1

Figure 2.36 LEED Indoor Environmental Quality.

Innovation rewards creative, sustainable strategies that go beyond LEED requirements, offering unique solutions that improve environmental performance or

address specific challenges in the project. For Innovation, we earned 3 out of 6 points, losing a few points in the process.

0	3	0	**Innovation**		6
	3		Credit	Innovation	5
		N	Credit	LEED Accredited Professional	1

Figure 2.37 LEED Innovation.

Regional Priority rewards projects that tackle local environmental issues, focusing on regional challenges and sustainability goals. For this category, we earned 2 out of 4 points by focusing on energy efficiency. This includes using natural light and energy-efficient lighting, along with staff-driven initiatives to reduce energy use.

0	2	0	**Regional Priority**		4
Y	1		Credit	Regional Priority: Energy efficiency	1
Y	1		Credit	Regional Priority: Staff initiatives	1
			Credit	Regional Priority: Specific Credit	1
			Credit	Regional Priority: Specific Credit	1

Figure 2.38 LEED Regional Priority.

0	76	0	**TOTALS**	Possible Points: 110

Certified: 40 to 49 points,
Silver: 50 to 59 points,
Gold: 60 to 79 points,
Platinum: 80 to 110

Figure 2.39 LEED Final Points.

As we can see from Figure 2.39, 76 was the total mark for our project. This is a good result resulting in a Gold certification level.

2.9 Life Cycle

Concrete Mixture

The concrete mixtures were designed using Life365 online tool, with different mixture designs to address specific durability requirements. Special attention was given to corrosion resistance and earthquake performance, as these factors are critical for long-term structural integrity. The mix designs followed established best practices for creating durable concrete that can withstand challenging conditions:

1. Base case: w/cm ratio 0.42, Class F fly ash 0%, slag 0%, silica fume 0%, Rebar: Black steel, Rebar % volume of concrete: 1.2%
2. Alternative 1: w/cm ratio 0.38, Class F fly ash 20%, slag 25%, silica fume 0%, Rebar: Black steel, Rebar % volume of concrete: 1.2%
3. Alternative 2: w/cm ratio 0.38, Class F fly ash 0%, slag 30%, silica fume 8%, Rebar: Black steel, Rebar % volume of concrete: 1.2%, Barrier: Sealer
4. Alternative 3: w/cm ratio 0.38, Class F fly ash 15%, slag 30%, silica fume 0%, Rebar: Epoxy-coated steel, Rebar % volume of concrete: 1.2%

Life Cycle Cost

Based on the software, the life cycle cost of the project was calculated. In the software, costs for products and services were provided, and it can be seen below in the list. Overall, the software calculated the total cost.

1. Concrete - 76.46 $/cub.yd.
2. Black Steel - 0.45 $/lb
3. Epoxy Coated Steel - 0.60 $/lb
4. Stainless Steel - 2.99 $/lb
5. Membrane - 3.07 $/sq.ft.
6. Sealer - 0.65 $/sq.ft.
7. Inhibitor - 5.68 $/gal
8. Repair - 37.16 $/sq.ft.

Additionally, in the calculation of the total cost of the project's life cycle, the specific region of Los Angeles and its temperature cycle by each month was taken into consideration. The temperature was varying throughout the whole year, giving the lowest value in January - 56.8 F, and the highest temperature in August - 70.5 F.

The total life cycle cost for the project with different concrete mixtures is displayed in the following Table 2.1.

Table 2.1. Life cycle costs

Name	Construction Cost	Barrier Cost	Repair Cost	Life Cycle Cost
Base case	$47,137	$0	$174,594	$221,731
Alternative 1	$47,137	$0	$0	$47,137
Alternative 2	$47,137	$0	$0	$47,137
Alternative 3	$47,137	$0	$0	$47,137

Service Life

According to the Life Cycle Cost (LCC) report analysis, all the alternative mixtures turned out to be significantly more cost-effective than the base case, which lacks any durability-enhancing materials or measure, which in turn means that the alternative options will have a exactly same service life.

Table 2.2. Service life

Type	Base case	Alternative 1	Alternative 2	Alternative 3
Service Life	44.75	81	81	81

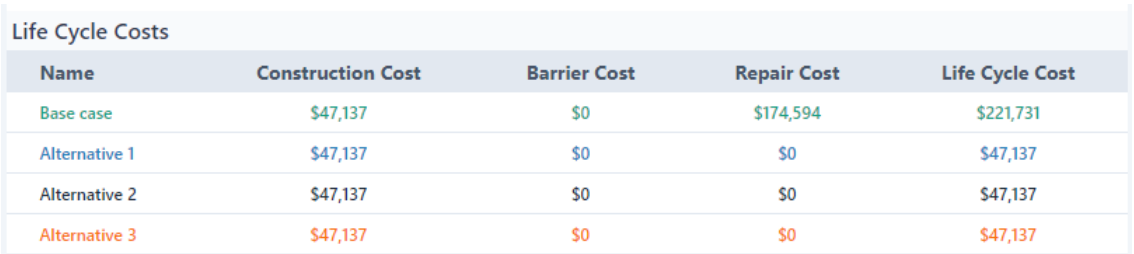
Life Cycle Costs

Name	Construction Cost	Barrier Cost	Repair Cost	Life Cycle Cost
Base case	$47,137	$0	$174,594	$221,731
Alternative 1	$47,137	$0	$0	$47,137
Alternative 2	$47,137	$0	$0	$47,137
Alternative 3	$47,137	$0	$0	$47,137

Figure 2.40 Life cycle costs of the project.

Corrosion Prevention

Since corrosion is not of significant relevance in our Los Angeles office structure, the concrete design favors long-term strength and durability over the use of additional protective components. The low water-to-cement ratio (around 0.38–0.42) forms the foundation of the mix in order to deliver high strength and low permeability. Supplementary cementitious materials—fly ash (0–20%), silica fume (0–8%), and slag (0–30%)—are incorporated to improve durability with enhanced resistance to sulfate attack, porosity reduction, and lesser risk of alkali-silica reactions.

Corrosion inhibitors and surface treatments are unnecessary because of the moderate exposure conditions. The concrete mix so obtained is effective and durable, maintaining an expected service life of over 75 years.

3. Structural Design

3.1 Material Selection

As we are constructing a high rise building wood and masonry cannot be considered as a structural material due to their major disadvantages. Wood is not a cost effective material, non-durable, has limited structural strength and susceptible to fire (M. E. Akiner et al., 2022). In the case of masonry, it was not chosen because of the poor seismic resistance and high self weight which requires more labor force than other structural elements (Admane and Murnal, 2017). The main choice was between reinforced concrete and steel frames. Thus, the comparison between these two materials was performed and given in Table 3.1. (Thapa et. al., 2020).

Table 3.1. Comparison between reinforced concrete and steel structures

Criteria	Reinforced Concrete	Steel Structure
Tensile strength	Lower	Higher
Compressive strength	Very high	High (lower than RC)
Material and Maintenance Cost	Lower	Higher

Labor cost	Higher	Lower
Labor force	Lower skilled labor	Higher skilled labor
Fire resistance	Higher	Lower fire resistance without treatment
Durability	Susceptible to cracking, but durable with maintenance	Durable with proper anti-corrosion treatment
Seismic resistance	Lower	Higher due to flexibility
Design flexibility	Flexible: cast-in-place concrete	Needs to be manufactured in factories

While steel structures provide higher tensile strength and greater resistance to wind and seismic forces, reinforced concrete was ultimately chosen as the structural material for our project. This decision is primarily based on the fact that reinforced concrete is more economical in the long run, offering better fire resistance, durability and flexibility. With modern design innovations, reinforced concrete can efficiently meet the requirements of contemporary high-rise constructions.

3.1.1 Non-structural materials selection

3.1.1.1. Floor finishing

For the floor finishing, various materials were chosen for different floor slabs. In other words, slabs for the first floor, typical floor and the roof differ since materials chosen for each case are not the same.

The structure of the first floor slab looks like following:

- 10 mm of ceramic tile on 13-mm of mortar bed as a cover
- 40 mm of lightweight concrete fill for the leveling
- 4 mm of bituminous, gravel covered as a waterproofing layer
- 20 mm of polystyrene foam for the insulation purposes

- 200 mm of structural slab from reinforced concrete
- Mechanical duct allowance for the ceiling
- 13 mm of gypsum board also for the ceiling

This all resulted in a 300 mm thick slab for the first floor.

The structure of the typical floor slab:

- 22 mm of hardwood as a cover
- 40 mm of cinder concrete screed for leveling purposes
- 10 mm of single ply sheet as a waterproofing layer
- 15 mm of rigid insulation
- 200 mm of reinforced concrete
- Mechanical duct allowance for the ceiling
- 13 mm of gypsum board for the ceiling

Typical floor slab's thickness is also 300 mm.

The structure of roof slab:

- 7 mm of three-ply ready roofing cover
- 75 mm of polystyrene foam for insulation
- 5 mm of bituminous, gravel covered as a waterproofing layer
- 50 mm of lightweight concrete fill
- 200 mm of reinforced concrete
- 13 mm of gypsum board

For the roof slab, the thickness is 350 mm.

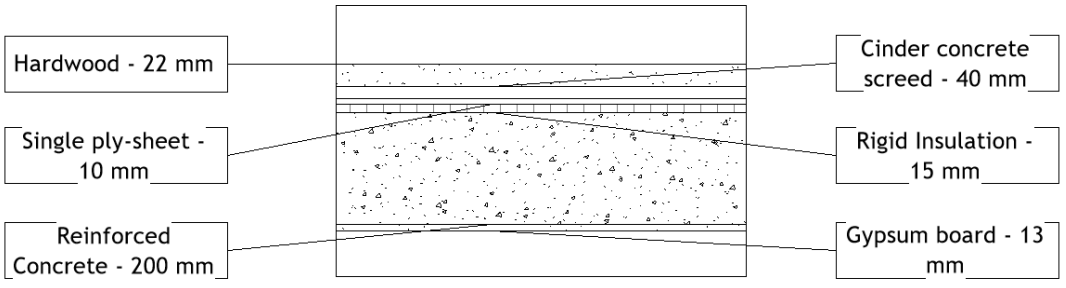

Figure 3.1 The typical floor slab structure.

3.1.1.2. Interior and exterior wall structures

It is evident that the structures of exterior and interior walls differ and the former is thicker than the latter. As a main structure for both of these walls autoclaved aerated concrete was chosen. According to Kalpana and Mohith, this type of concrete offers several advantages over the traditional one, including higher strength-to-weight ratio, effective sound insulation due to the air voids in its structure (Kalpana and Mohith, 2020). Covering, insulation and finishing layers for both types of walls will be presented below in Tables 3.5-3.7. The structure's section cut views are presented in Figures 3.1-3.3.

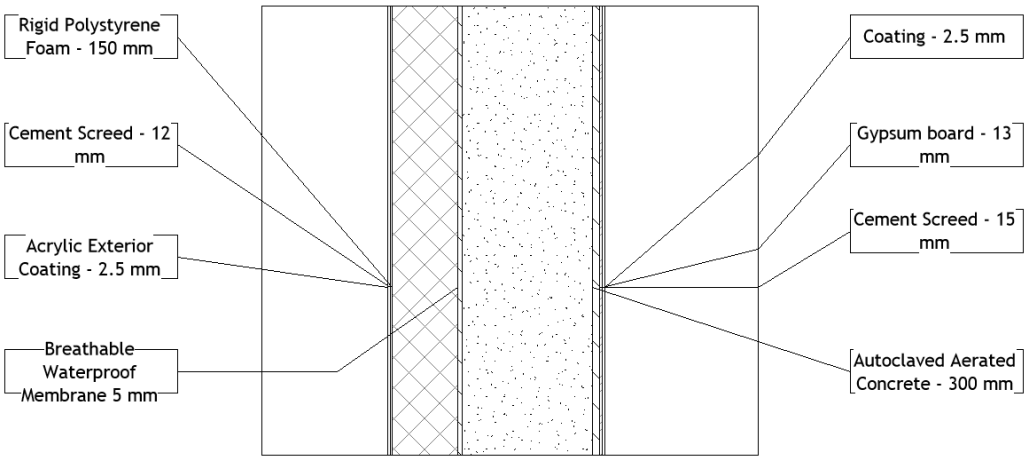

Figure 3.2 Exterior wall structure.

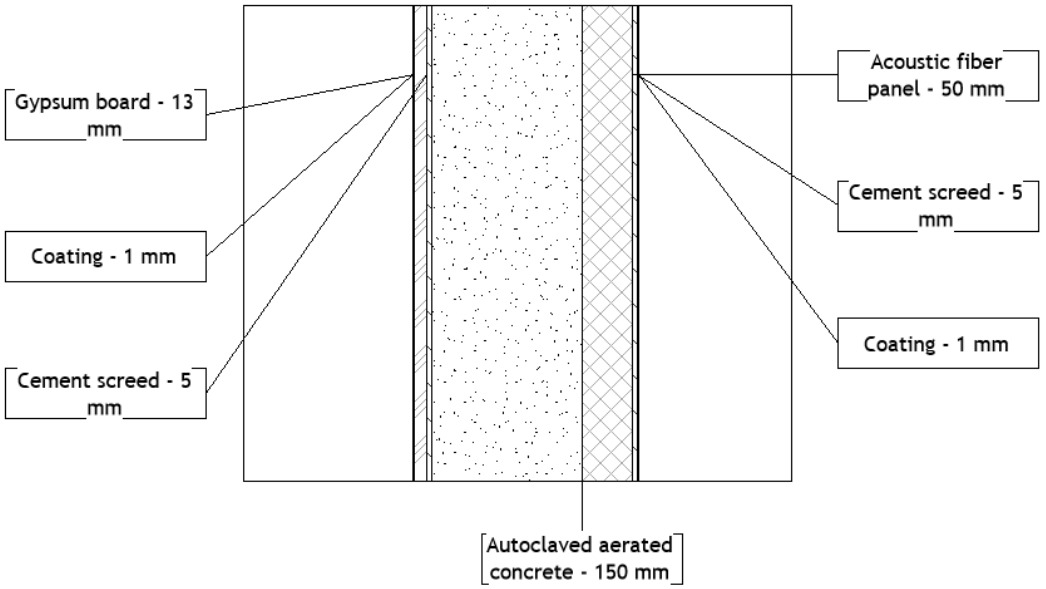

Figure 3.3 Interior wall structure.

3.1.1.3. Roof parapets

As specified by the International Building Code (2024), roof parapets must have a minimum height of 762 mm (30 inches). Consequently, a height of 1200 mm was selected for the parapet design to exceed this minimum requirement. The roof parapets structure is the same as the exterior wall to keep it aesthetically pleasing.

3.1.1.4. Roof drainage system

The scupper system built into the parapet wall with its conductor head and flange-sealed connections serves as our building's roof drainage system to guarantee waterproofing performance. The scupper receives soldered connection to the conductor head before the installation of copper flashing and counterflashing transforms it into a watertight protective edge. A cleat together with a gravel stop support water drainage from the roof.

The project team selected this detail because it provided extended durability and easy upkeep together with strong leak prevention capabilities which were imperative for an earthquake-prone building in the storm-prone Los Angeles climate.

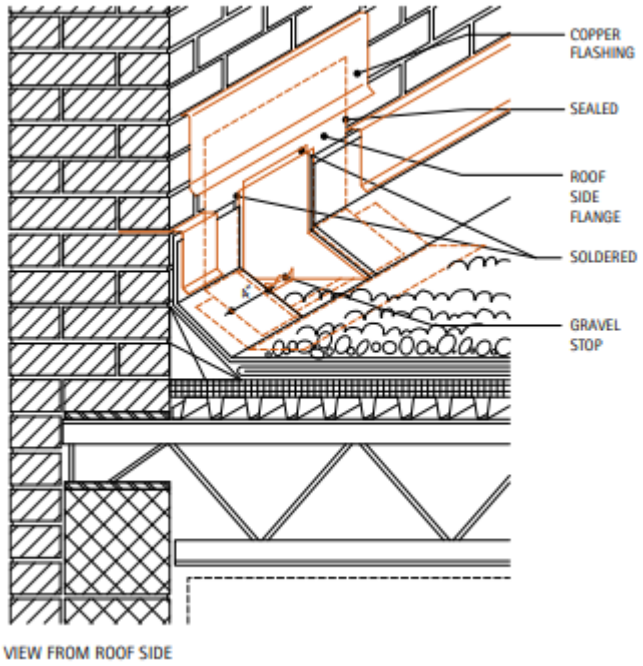

Figure 3.4 Scupper at parapet wall (Copper Development Association, n.d.)

The design complies with IBC 2021 Section 1503.4.2 requirements because the overflow scuppers possess a 4-inch (102 mm) opening position and elevated maximum height of 4 inches above the roof (International Code Council, 2021).

3.2 Development of an analytical model

This section explains how to develop an analytical model through SAP2000 software usage. All details regarding materials, geometry and boundary conditions of buildings with sections and element properties are explained in the upcoming subsections.

Model Geometry

The SAP2000 software served to develop the building model through its integration of beams and slabs and columns that functioned either as frames or shells. The software assigned frames and shells to different beam and column entities. The building geometry which was developed in SAP2000 can be seen in the following Figure 3.2.1.

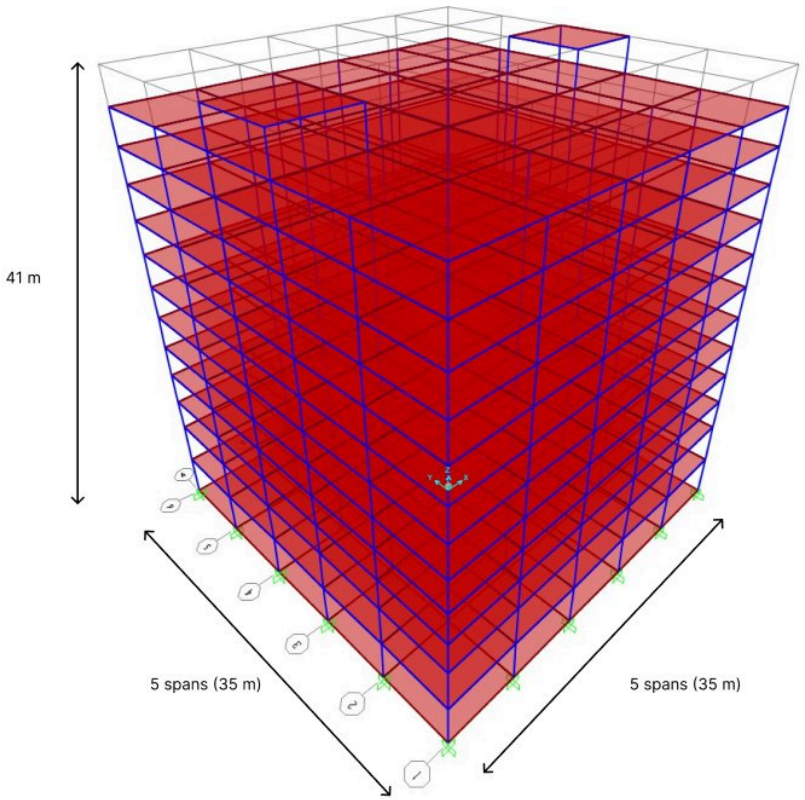

Figure 3.5 Geometry of the office building in SAP2000

Materials

Reinforced concrete was utilized as the main structural material for the office building.

Concrete

Table 3.2. presents material properties of concrete within the constructed building.

Table 3.2. Concrete properties

Component	$f_c'\ (MPa)$	$\rho\ (kN/m^3)$	$E_c\ (MPa)$	ν	$G_c\ (MPa)$
Beam	40	25	29725	0.2	12386
Column					
Slab					

Structure elements received C40 grade concrete due to its widespread use in heavy construction (Base Concrete, 2023). The equation used to determine the Young's

modulus of elasticity E_c featured as follows:

$$E_c = 4700\sqrt{f_c} \quad [1]$$

The Poisson ratio for concrete exists between 0.15 and 0.25 so researchers agreed to utilize 0.2 as the value for C40 grade concrete. The formula enabled the calculation of shear modulus G_s after inputting the following data:

$$G_c = \frac{E_c}{2\times(1+\nu)} \quad [2]$$

Reinforcing steel

Table 3.3 presents material properties of reinforcing steel within the constructed building.

Table 3.3. Reinforcing steel properties

$E\ (MPa)$	ρ (kN/m^3)	ν	$f_y\ (MPa)$
200000	76.97	0.3	420

Sections

Table 3.4 presents the cracking moment of inertia factors of structural members of the constructed building.

Table 3.4. Reinforcing steel properties

Component	Cracking moment of inertia factors
Beams	0.35
Slabs	0.7
Columns	0.25
Stairs	0.25

Elements and connections

The floor slabs in SAP2000 received modeling through shell elements under a 1000 mm x 1000 mm mesh size or smaller. A fine meshing choice was made to capture realistic stress distribution patterns and structural behavior of the building across all loading situations. The modeling process utilized frame elements for beams and

columns to create precise mathematical representations of their axial as well as their shear and bending responses. Rigid connections were implemented between beams and columns at the moment-resisting frame to achieve both full moment transfer and structural continuity needed for lateral load resistance.

Boundary conditions

The foundations of basement columns received fixed support to stop any movement or rotation from occurring. The construction points connecting the basement with the first floor received restrictions on vertical and horizontal motions but allowed rotations for lateral force management.

3.3. Analysis of the Gravity Load Resisting System (GLRS)

3.3.1. Calculation of Dead, Live and Snow Loads.

3.3.1.1. Dead Load Analysis

For the dead load analysis, all calculations were done according to chapter 3 of ASCE 7 (American Society of Civil Engineers). For the calculation of dead load from the first floor, typical floor and roof slabs, their structures were analyzed. Results are in Tables 3.2-3.4. For the design of structural members, critical loads were chosen.

Table 3.5. Dead load calculations of the first floor.

Component	Material type	Thickness, mm	Load, kN/m2
Cover	Ceramic tile	10	0.77
	Mortar bed	13	
Leveling	Lightweight concrete fill	40	0.015
Water-proofing	Bituminous, gravel covered	4	0.26
Insulation	Polystyrene foam	20	0.0004
Structural Slab	Reinforced concrete	200	23.6

Ceiling	Mechanical duct allowance		0.19
	Gypsum board	13	0.008
Total		300	6.6444

Table 3.6. Dead load calculations of the typical floor of the office.

Component	Material type	Thickness, mm	Load, kN/m2
Cover	Hardwood	22	0.19
Leveling	Cinder concrete screed	40	0.017
Water-proofing	Single ply sheet	10	0.03
Insulation	Rigid insulation	15	0.04
Structural Slab	Reinforced concrete	200	23.6
Ceiling	Mechanical duct allowance		0.19
	Gypsum board	13	0.008
Total		300	5.954

Table 3.7. Dead load calculation of the roof

Component	Material type	Thickness, mm	Load, kN/m2
Cover	Three-ply ready roofing	7	0.05
Leveling	Lightweight concrete fill	50	0.015
Water-proofing	Bituminous, smooth surface	5	0.07
Insulation	Polystyrene foam	75	0.0004

Structural Slab	Reinforced concrete	200	23.6
Ceiling	Mechanical duct allowance		0.19
	Gypsum board	13	0.008
Total		350	5.914

Following that, the dead load from partition and exterior walls and also roof parapets were calculated. In the case of partition walls, there was an assumption that their weight is uniformly distributed over the floor area. Whilst, the load of exterior walls and parapets fall on edge beams. In the case of the roof parapets, it was suggested to use the exterior wall structure for both safety and aesthetic reasons. The only difference is their height which is 1200 mm. Other results of all calculations are given in Tables 3.8-3.9.

Table 3.8. Calculation of the weight of interior wall on the typical floor per span (7 meters)

	Material type	Thickness, mm	Height, mm	Span, mm	Volume, m3	Density, kg/m3	Weight, kg
Cement plaster	Cement Screed	5	3000	7000	0.105	2,407.32	252.77
Insulation	Acoustic fiber panel	50	3000	7000	1.05	64.00	67.20
Autoclaved aerated concrete	Autoclaved aerated concrete	150	3000	7000	3.15	580.00	1827.00
Cement plaster	Cement Screed	5	3000	7000	0.105	2,407.32	252.77
Exterior side	Gypsum board	13	3000	7000	0.273	668.00	182.36
Finish layer	Coating	2	3000	7000	0.042	1,250.00	52.50
Total		220			4.62		2382.00

Table 3.9. Calculation of the weight of exterior wall on the typical floor per span (7 meters)

Component	Material type	Thickness, mm	Height, mm	Span, mm	Volume, m3	Density, kg/m3	Weight, kg
Exterior finish	Acrylic exterior coating	5	3000	4200	0.063	1250	78.75
Cement plaster leveling	Cement Screed	12	3000	4200	0.1512	2,407.32	363.98
Weather barrier (Air infiltration)	Breathable Waterproof Membrane	5	3000	4200	0.063	950.00	59.85
Insulation	Rigid polystyrene foam	150	3000	4200	1.89	35	66.15
Autoclaved aerated concrete block	Autoclaved aerated concrete	300	3000	4200	3.78	580	2192.40
Cement plaster	Cement Screed	15	3000	4200	0.189	1,090.00	206.01
Interior finish	Fire resistant gypsum board	13	3000	4200	0.1638	800.00	131.04
Total		500			6.3		3623.00
Exterior glazing	Curtain wall glazing	25	3000	2800	0.21	2500	525.00

As it was stated above, the interior wall loads were distributed evenly over the floor area, which resulted in:

$$Floor\ area\ =\ 1153.139\ m^2$$

$Distributed\ load\ =\ 0.771\ kN/m^2$

Also, the dead load from stairs was calculated which resulted in 93.1 kN per floor.

Overall, calculation of dead loads of non-structural components:

- First floor (finishing and slab) = 6.644 kN/m^2
- Typical floor (finishing and slab) = 5.954 kN/m^2
- Partition walls of the first floor = 0.816 $kN/m^2\ per\ floor\ area$
- Partition walls of the typical floor = 0.771 $kN/m^2\ per\ floor\ area$
- Exterior walls of the first floor = 0.507 $kN/m^2\ per\ floor\ area$
- Exterior walls of the typical floor = 0.381 $kN/m^2\ per\ floor\ area$
- Roof parapets = 0.518 $kN/m^2\ per\ roof\ area$
- Stairs = 93.1 $kN\ per\ floor$

3.2.1.2. Live Load Analysis

For the calculation of the minimum distributed live loads for office building ASCE 7 Chapter 4 (American Society of Civil Engineers) were investigated. According to table 4-1, the minimum concentrated live loads are listed below:

1. Lobbies and first-floor corridors: $L_0 = 4.79\ kN/m^2$
2. Stairs and exit ways: $L_0 = 4.79\ kN/m^2$
3. Offices: $L_0 = 2.4\ kN/m^2$
4. Corridors above the first floor: $L_0 = 3.8\ kN/m^2$
5. Ordinary flat roofs: $L_0 = 0.96\ kN/m^2$

Reduction for the uniformly distributed live load has to be applied and calculated by the following equation:

$$L = L_0(0.25 + \frac{4.57}{\sqrt{K_{LL} \times A_T}}) \quad [3]$$

Where:

- $K_{LL} - Live\ load\ element\ factor$
- $A_T - Tributary\ area$

Live load element factor (K_{LL}) is taken according to the table 4-2 from ASCE 7 (American Society of Civil Engineers) Chapter 4:

1. Interior columns: $K_{LL} = 4$
2. Exterior columns without cantilever slabs: $K_{LL} = 4$
3. Edge columns with cantilever slabs: $K_{LL} = 4$
4. Corner columns: $K_{LL} = 4$
5. Edge beams without cantilever slabs: $K_{LL} = 2$
6. Interior beams: $K_{LL} = 2$

Table 3.10 shows the floor live load reduction calculations.

Table 3.10. Floor live load reduction.

			Space, m	Span, m	At, m2	K_{LL}	Reduction	L_0, kN/m2	L, kN/m2
Typical floor	Offices	Exterior columns	3.5	7.0	24.5	4.0	0.7	2.4	1.7
		Interior columns	7.0	7.0	49.0	4.0	0.6	2.4	1.4
		Corner columns	3.5	3.5	12.3	4.0	0.9	2.4	2.2
		Edge beams	3.5	7.0	12.3	2.0	1.0	2.4	2.4
		Interior	3.5	7.0	24.5	2.0	0.9	2.4	2.2

		beams							
	Stairs and exit ways	Interior columns	7.0	7.0	49.0	4.0	0.6	4.8	2.8
		Exterior columns	3.5	7.0	24.5	4.0	0.7	4.8	3.4
		Interior beams	3.5	7.0	24.5	2.0	0.9	4.8	4.3
		Edge beams	3.5	7.0	12.3	2.0	1.0	4.8	4.8
	Corridors above the first floor	Exterior columns	3.5	7.0	24.5	4.0	0.7	3.8	2.7
		Interior columns	7.0	7.0	49.0	4.0	0.6	3.8	2.2
		Edge beams	3.5	7.0	12.3	2.0	1.0	3.8	3.8
		Interior beams	3.5	7.0	24.5	2.0	0.9	3.8	3.5
First floor		Exterior columns	3.5	7.0	24.5	4.0	0.7	4.8	3.4
		Interior columns	7.0	7.0	49.0	4.0	0.6	4.8	2.8
		Corner columns	3.5	3.5	12.3	4.0	0.9	4.8	4.3
		Edge beams	3.5	7.0	12.3	2.0	1.0	4.8	4.8
		Interior beams	3.5	7.0	24.5	2.0	0.9	4.8	4.3
Second Floor		Exterior columns	3.5	7.0	24.5	4.0	0.7	4.8	3.4
		Interior columns	7.0	7.0	49.0	4.0	0.6	4.8	2.8
		Corner columns	3.5	3.5	12.3	4.0	0.9	4.8	4.3

	Edge beams	3.5	7.0	12.3	2.0	1.0	4.8	4.8
	Interior beams	3.5	7.0	24.5	2.0	0.9	4.8	4.3

Next, reduced roof live load has to be calculated with the following formula:

$$L_r = L_0 \times R_1 \times R_2 \text{ where } 0.58 \leq L_r \leq 0.96 \quad [4]$$

Where

- $L_0 - Unreduced\ design\ roof\ live\ load$

The reduction factor R_2 for the flat roof is equal to 1 whereas the reduction factor R_2 needs to be evaluated accordingly to the ASCE 7:

$$R_1 = 1 \quad for\ A_T \leq 18.58\ m^2$$

$$R_1 = 1.2 - 0.011 \times A_T \quad for\ 18.58\ m^2 < A_T < 55.4\ m^2 \quad [5]$$

$$R_1 = 0.6 \quad for\ A_T \geq 55.74\ m^2$$

The following Table 3.11 shows the roof live load reduction calculations.

Table 3.11. Roof live load reduction.

	Space (m)	Span (m)	$A_T,\ m^2$	K_{LL}	R_1	R_2	$L_0,\ kN/m^2$	$L_r,\ kN/m^2$
Exterior columns	3.5	7.0	24.5	4.0	0.9305	1.0	0.960	0.8933
Interior columns	7.0	7.0	49.0	4.0	0.6610	1.0	0.960	0.6346
Corner columns	3.5	3.5	12.3	4.0	1.0000	1.0	0.960	0.9600

Edge beams	3.5	7.0	12.3	2.0	1.0000	1.0	0.960	0.9600
Interior beams	3.5	7.0	24.5	2.0	0.9305	1.0	0.960	0.8933

3.2.1.3. Snow Load Analysis

As indicated in ASCE 7, the city of Los Angeles is not subject to snow loads; hence snow load was not calculated for the design of this project.

3.2.2. Member Size Estimation

3.2.2.1 Structural layout

For this office building, spacing of 7 meters between the columns was selected to provide more space. Also, for large buildings spacing of 6 to 9 meters is usually recommended (Pooja, 2022).

For this structure, three different options of GLRS layouts were considered and to choose the suitable one for this project, economical aspects were crucial. To consider their potential costs, it was vital to determine the volume of all three cases. The cases that were considered are the following:

- Two-way slab with major beams
- One-way slab with major beams and one minor beam
- Two-way slab with major beams and two minor beams

General assumptions and statements taken from ASCE 7, Chapters 7-10 and used to calculate the member sizes:

- Thickness of major beams was taken as 10% of span for all cases
- The width of beams was calculated using $b = \frac{h}{2}$
- The thickness of simply supported one-way slab is $h = \frac{l}{20}$
- The thickness of simply supported minor beams is $h = \frac{l}{16}$

- Columns are square shaped
- Increment of 50 mm used for column sizing
- Reinforcement ratio is 1%

Case 1: Two-way slab with major beams

The span is 7 meters and therefore:

$$h_{major} = 10\% \, of \, L = 0.1 * 7 = 0.7 \, m$$

$$b_{major} = \frac{h}{2} = \frac{0.7}{2} = 0.350 \, m$$

The C40 grade concrete was selected for both slab and beams since this grade of concrete is often used for structures that carry heavy weights. This means that fc = 40 MPa.

For C40, modulus of elasticity was calculated using the following formula:

$E = 4700\sqrt{f_c}$ which resulted in E = 29730 MPa [6]

$$I_{b,cr} = 0.35 * \frac{1}{12} * b * h^3 = \frac{0.35}{12} * 0.350 * 0.7^3 = 0.003501 \, m^4$$

$$I_{s,cr} = 0.25 * \frac{1}{12} * L * h^3 = \frac{0.25}{12} * 7 * 0.200 = 0.001167 \, m^4$$

Next the stiffness ratio was calculated using next formula:

$$\alpha_{fm} = \frac{E_{cb} I_{b,cr}}{E_{cs} I_{s,cr}} \quad [7]$$

$$\alpha_{fm} = \frac{a_{f1} + a_{f2}}{2} = 5.52 > 2 \quad [8]$$

Since stiffness ratio is greater than 2, the following formula was used to determine the thickness of the slab:

$$h_{min} = \frac{l_n(0.8 + \frac{fy}{200000})}{36 + 9\beta} \geq 3.5 \, inches \quad [9]$$

Using all these above mentioned formulas, the thickness of the slab required was found to be

$$h_{min} = 0.163\, meters$$

It is important to mention that originally slab thicknesses were calculated as 0.163 mm. But since there is an increment of 50 mm, slab thicknesses were calculated as 200 mm. This increment of 50 mm that was mentioned in the assumptions, also applies on all other calculations too and was considered in the final calculations.

Next the volume for the first case was calculated:

$$V_{total} = V_{slab} + V_{beam} \quad [10]$$

$$V_{total} = 9.80 + 6.860 = 16.66\, m^3$$

Case 2: One-way slab with major beams and one minor beam

The same procedure was used to find thicknesses and width for slab and major beams. In the case of minor beams thickness, it was found in the following way

$$h_{minor\ beam} = \frac{l}{16} \quad [11]$$

$$h_{minor\ beam} = \frac{7}{16} = 0.438\, meters \approx 0.450\, meters \quad [12]$$

Other than that all calculations are the same, and the final values are the next

$$V_{total} = V_{slab} + V_{major\ beams} + V_{minor\ beams} \quad [13]$$

$$V_{total} = 9.80 + 6.860 + 0.788 = 17.45\, m^3$$

Case 3: Two-way slab with major beams and two minor beams

In the last case, we used the same assumptions and statements and thicknesses were found as previously mentioned.

Using the formula for minimum thickness of the slab, in this case it was

$$h_{min} = 0.163\,meters \approx 0.200\,meters \quad [14]$$

$$h_{minor\ beam} = \frac{L}{16} = 0.438\,meters \approx 0.450\,meters \quad [15]$$

$$b_{minor\ beam} = \frac{h}{2} = 0.219\,meters \approx 0.250\,meters \quad [16]$$

$$I_{slab} = 0.25 * \frac{1}{12} * L * h^3 = 0.001167\,m^4 \quad [17]$$

$$I_{major\ beam} = 0.35 * \frac{1}{12} * b * h^3 = 0.003501\,m^4 \quad [18]$$

$$I_{minor\ beam} = 0.35 * \frac{1}{12} * b * h^3 = 0.0006645\,m^4 \quad [19]$$

$$\alpha_{fm} = \frac{a_{f1}+a_{f2}}{2} = \frac{11.04+1.685}{2} = 6.363 \quad [20]$$

$$\beta = \frac{l_{yn}}{l_{xn}} = 1 \quad [21]$$

According to ASCE 7, the minimum thickness should be 0.089 meters, so the calculated thickness of 0.163 meters was taken. Next total volumes were calculated.

$$V_{total} = V_{slab} + V_{major\ beams} + V_{minor\ beams} = 18.235\,m^3 \quad [22]$$

All these calculations and final results are summarized in Table 3.12.

Table 3.12. Final results of volume calculations.

Option	Member	L, m	h, m	b, m	V, m3
Two-way slab	Slab	7.00	0.20	7.000	16.66
	Major beam	7.00	0.70	0.350	
Two-way slab with minor beams	Slab	3.50	0.20	3.500	18.24
	Major beam	7.00	0.70	0.350	
	Minor beam	7.00	0.45	0.219	
One-way with minors	Slab	7.00	0.20	3.500	17.45
	Major beam	7.00	0.70	0.350	
	Minor beam	7.00	0.45	0.219	

From Table 3.12, it is clearly seen that a two-way slab with major beams only is the best design choice for this office building.

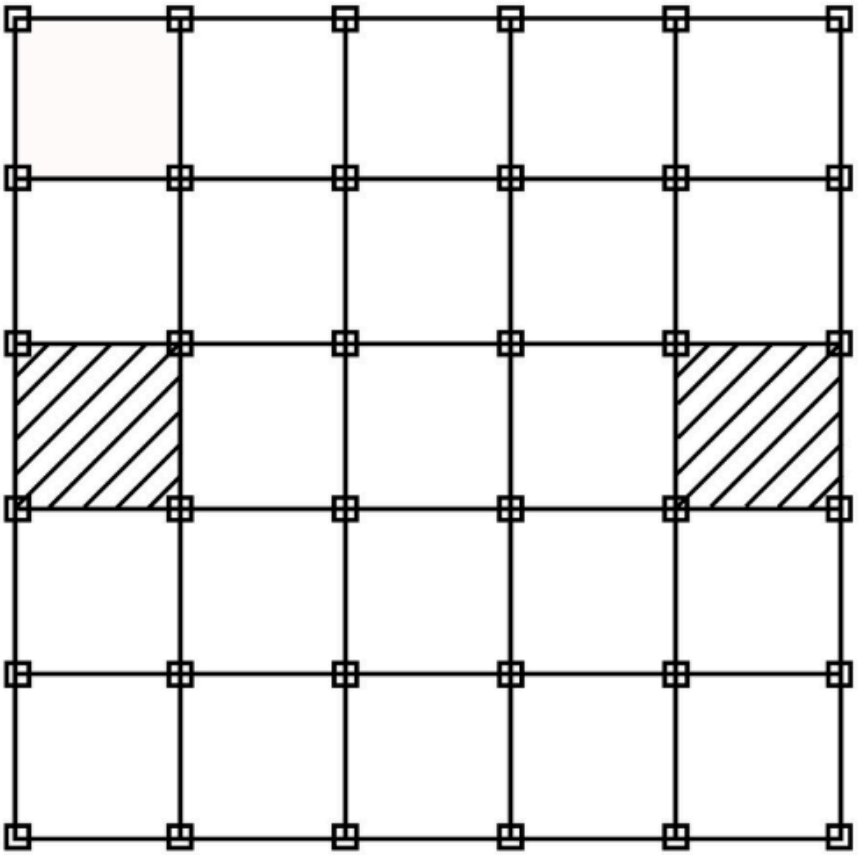

Figure 3.6 Structural layout of the building.

3.2.2.2. Estimation of Size Dimensions of Columns

Once the size dimensions for the slab, major and minor beams were calculated, column size estimations can be carried out based on the self-weight of these structural elements along with the already determined dead and live load calculations.

Firstly, the self-weight of the beams needs to be calculated:

$$SW_{slab} = \rho_{RC} \times V_{slab} \quad [23]$$

$$SW_{slab} = 2400\ kg/m^3 * 7\ m * 7\ m * 0.200\ m = 23520\ kg$$

$$SW_{major\ beam} = \rho_{RC} \times V_{major\ beam} \quad [24]$$

$$SW_{major\ beam} = 2400\ kg/m^3 * 7\ m * 0.7\ m * 0.350\ m = 4116\ kg$$

The following load combinations has to be applied to estimate the dimensions of the columns:

$$w_u = 1.2D + 1.6L + 0.5L_r \quad [25]$$

Total load transferred to the interior column are:

$D_{roof} = 5.914\ kN/m^2$

$L_{roof} = 0.960\ kN/m^2$

$L = 2.761\ kN/m^2$ (critical live load applied to interior column)

The following Table 3.13 was used to calculate the column sizing.

Table 3.13. Loads applied to columns and tributary areas.

	Dead load, kN/m2	Live load, kN/m2	Tributary area, m2
Exterior	9.117	3.41	25
Interior	8.292	2.76	49
Corner	9.941	4.325	12

This office building has a basement, hence the column sizes in the basement were also calculated. It is worth noting that the height of the first and second floor is 4 meters, while for the typical floor it is 3 meters.

Since our columns are square shaped, it was essential to find Ac (column area). Formulas used to calculate column sizes are the following:

$$P_u = w_u + A_T + w_{columns\ of\ above\ floor} \quad [26]$$

$$\phi P = 0.8\phi \times (0.85 \times f'_c \times A_c + f_y \times A_s) \quad [27]$$

$$\phi P_n \geq P_u \quad [28]$$

As an example, for the basement columns Ac was found to be equal to 0.549 m2 from calculations using formulas above. Then since it is a square shaped column, to find one side length we simply take a square root of that value. That results in 0.741 meters, then we take it as 0.750 meters. Therefore, the dimensions of columns of the basement are 0.750 m x 0.750 m.

Using the same procedure, column dimensions for all floors were calculated and final results are given in Table 3.14.

Table 3.14. Dimensions of columns

Floors	Column size, m
0-2	0.75
3-4	0.65
5-6	0.55
7-8	0.50
9-10	0.40
11-12	0.30

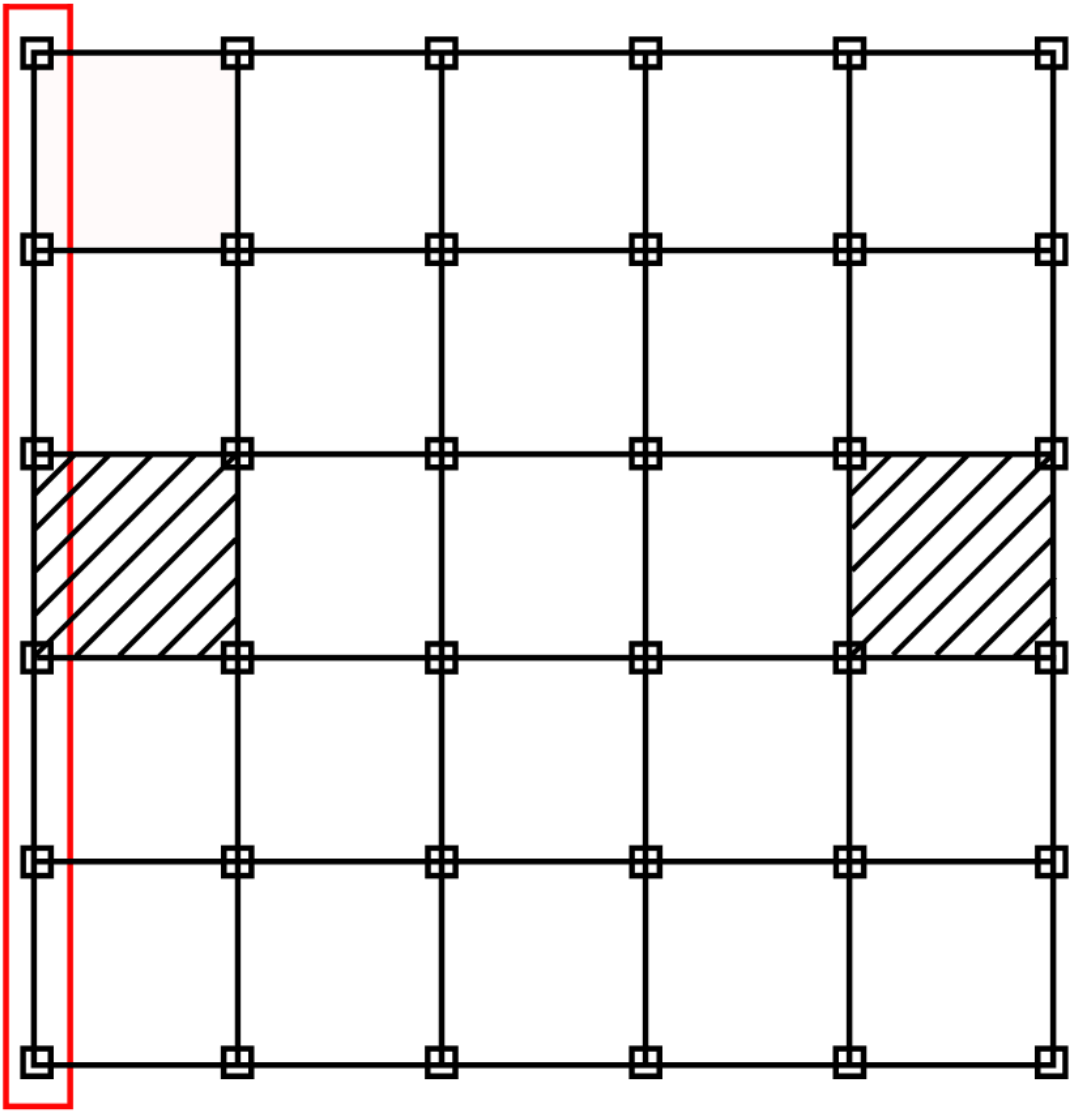

Figure 3.7. The chosen frame for assigning lateral forces.

3.2.3. Assigning Forces to SAP2000

3.2.3.1. Assigning forces to selected 2D frame

The selected 2D frame was built using SAP2000 software to analyze its structural behavior. In order to build the 2D frame the material type, its properties, and the frame had to be identified. All the structural members were designed with the same material type. They are C40 concrete and Grade 60 rebar which can be seen from the following Figure 35.

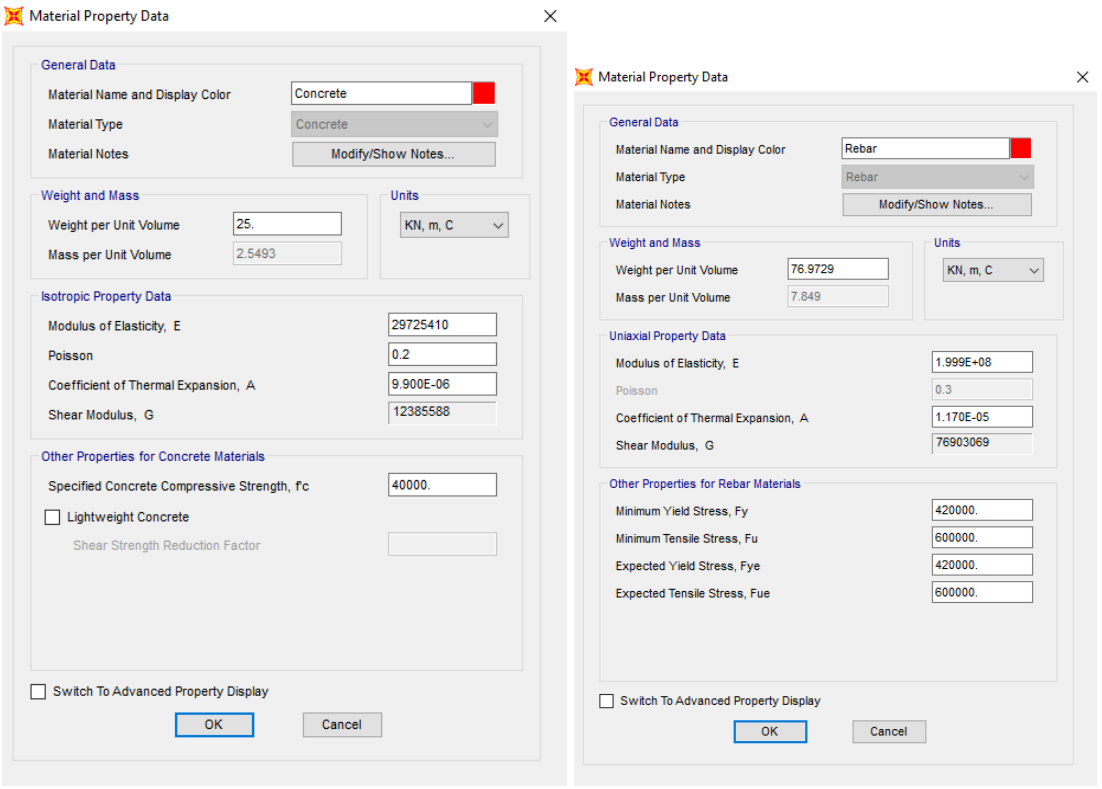

(a) (b)

Figure 3.8. SAP2000 Material Properties: (a) Concrete, (b) Rebar.

After that, the frame sections were defined. In particular, there are different columns with varying sizes on each respective level, as well as major beams. Figures 3.9-3.11 show the frame section properties and property modifiers, such as the coefficient for cracking moment of inertia.

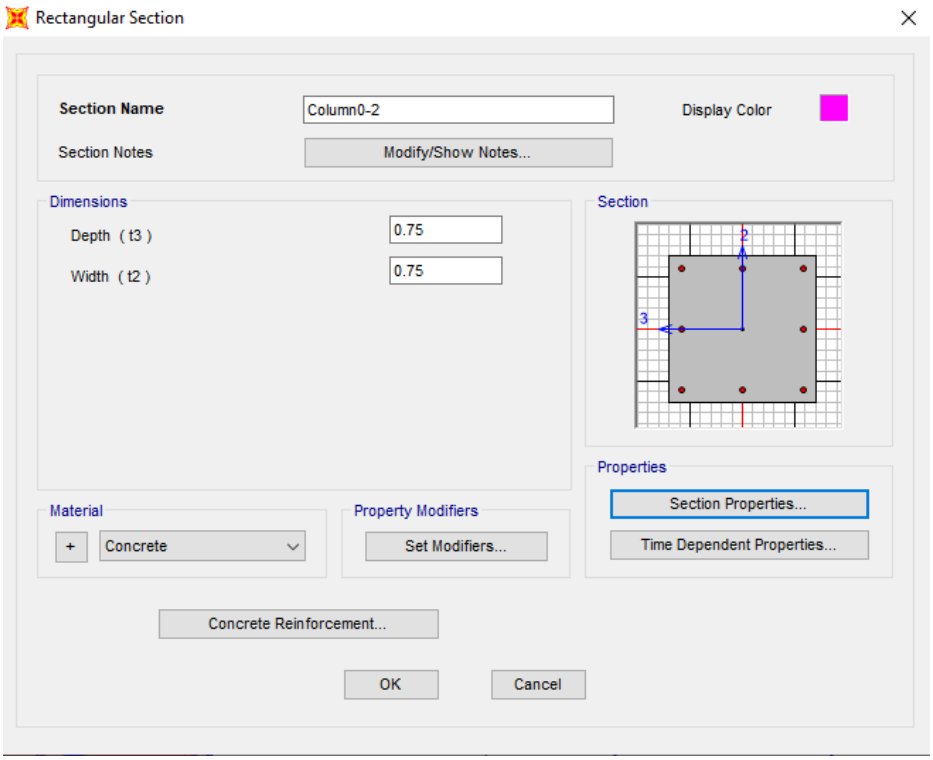

Figure 3.9. SAP2000: Column section properties.

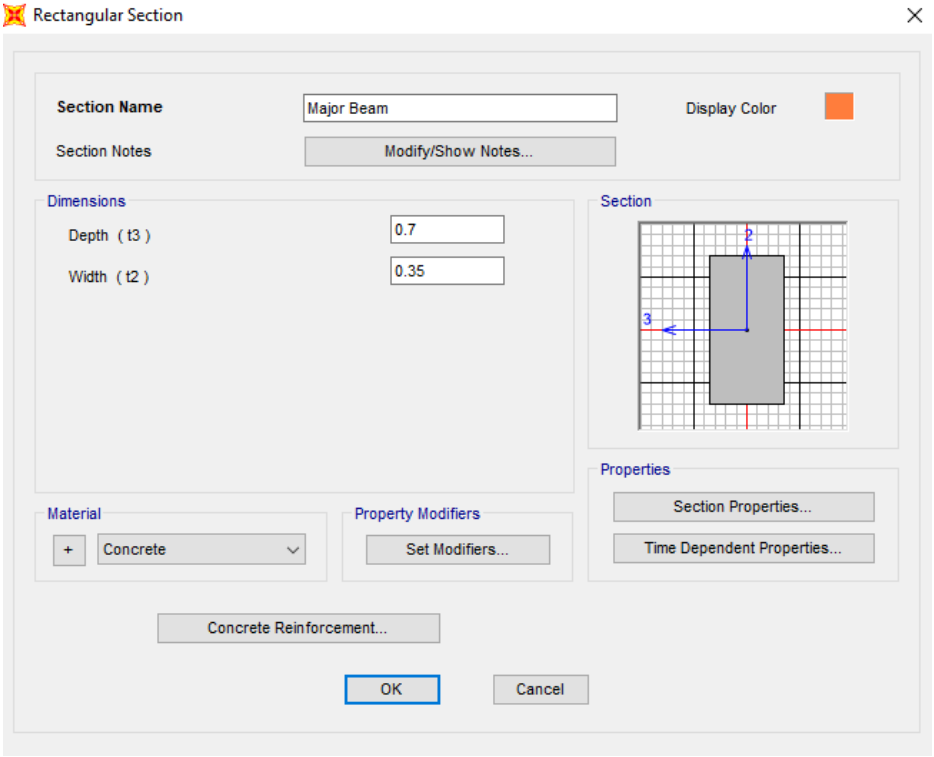

Figure 3.10. SAP2000: Major beam section properties.

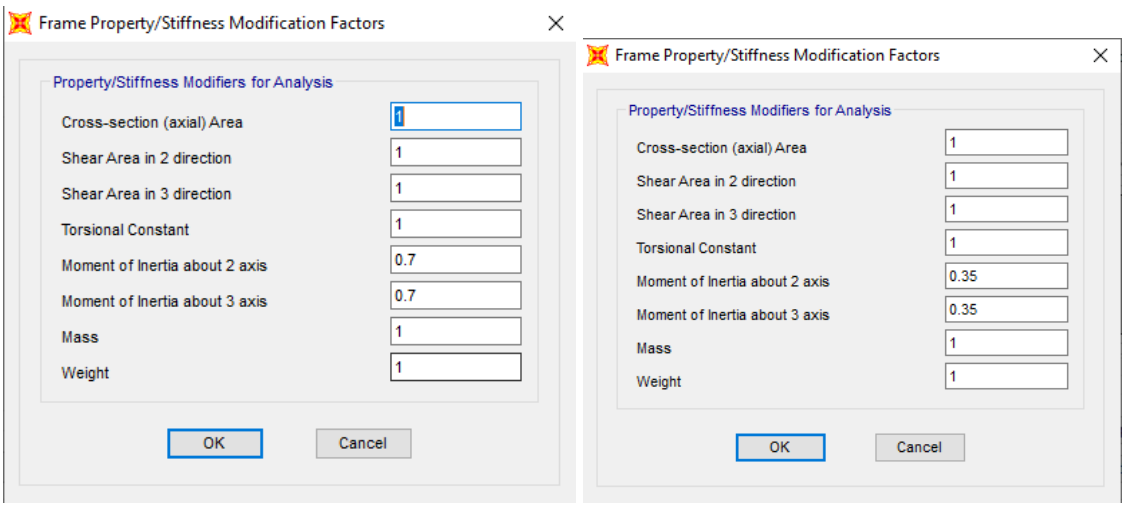

(a) (b)

Figure 3.11 SAP2000 Frame property/stiffness modification factors: (a) Column, (b) Beam.

Moreover, the joint restraints and also diaphragm constraints were applied. Below the first floor fixed support was applied to provide stability of the building and ensure that the structure is static. After that, diaphragm constraints were applied to cause all joints to move together as a planar diaphragm. These can be seen in Figures 3.12-3.13.

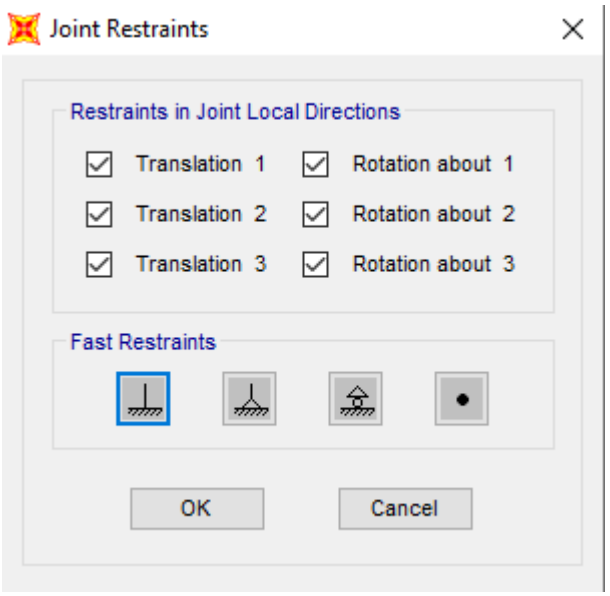

Figure 3.12 SAP2000 Joint Restraints: Fixed support.

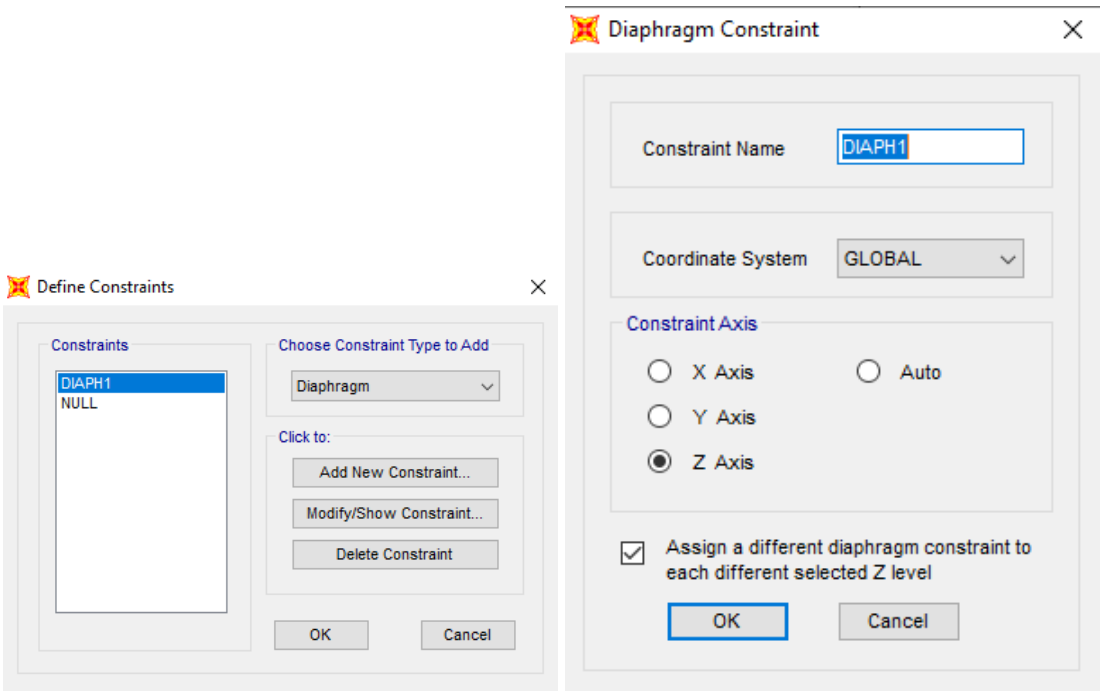

Figure 3.13 SAP2000: Diaphragm Constraint.

After defining the parameters, a building's 2D frame model was created. Unfactored dead loads, live loads, and roof live loads were then assigned to the model, as illustrated in following Figures 3.14-3.16.

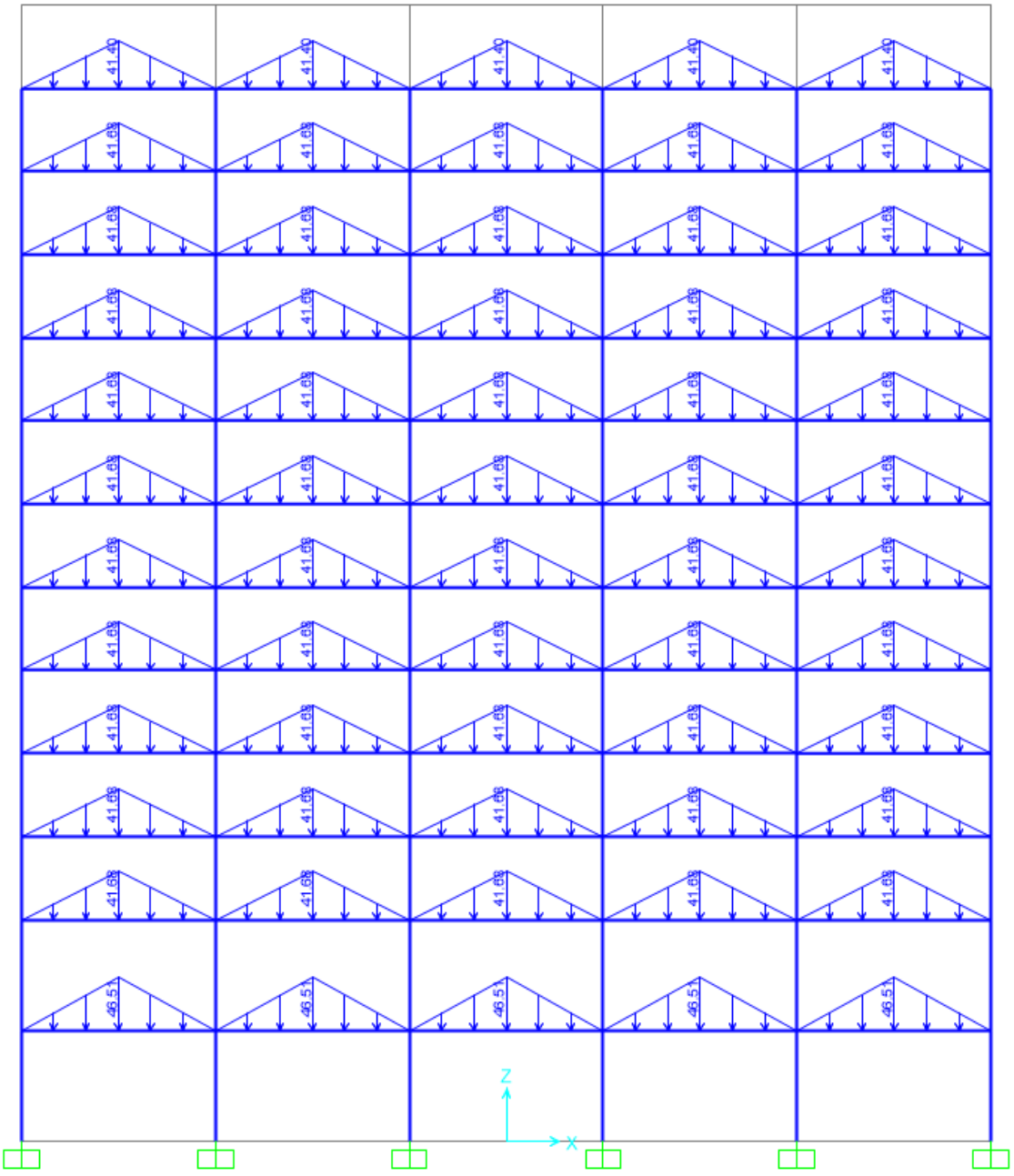

Figure 3.14. Assigned dead loads on 2D frames in SAP2000.

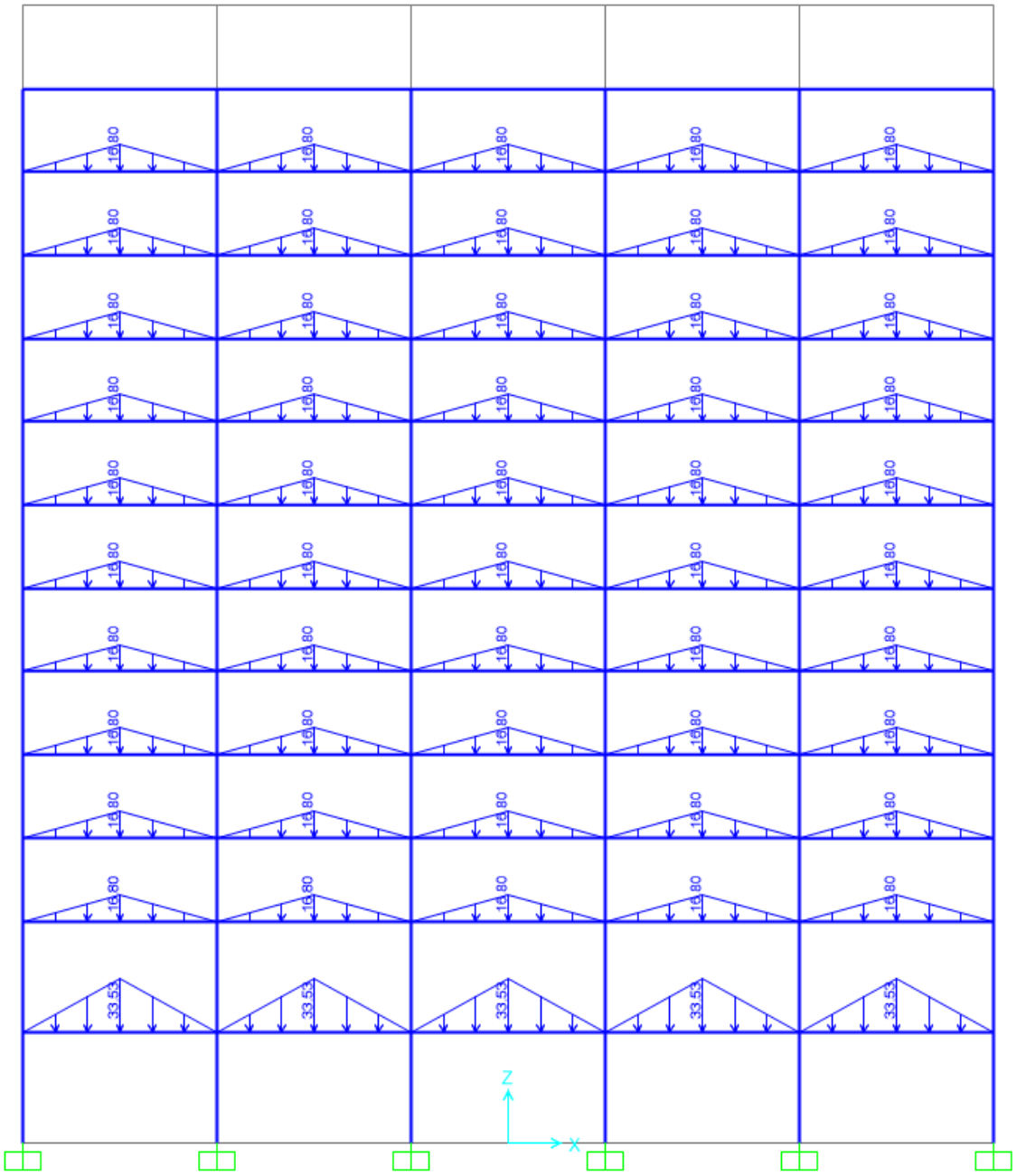

Figure 3.15. Assigned live loads on 2D frames in SAP2000.

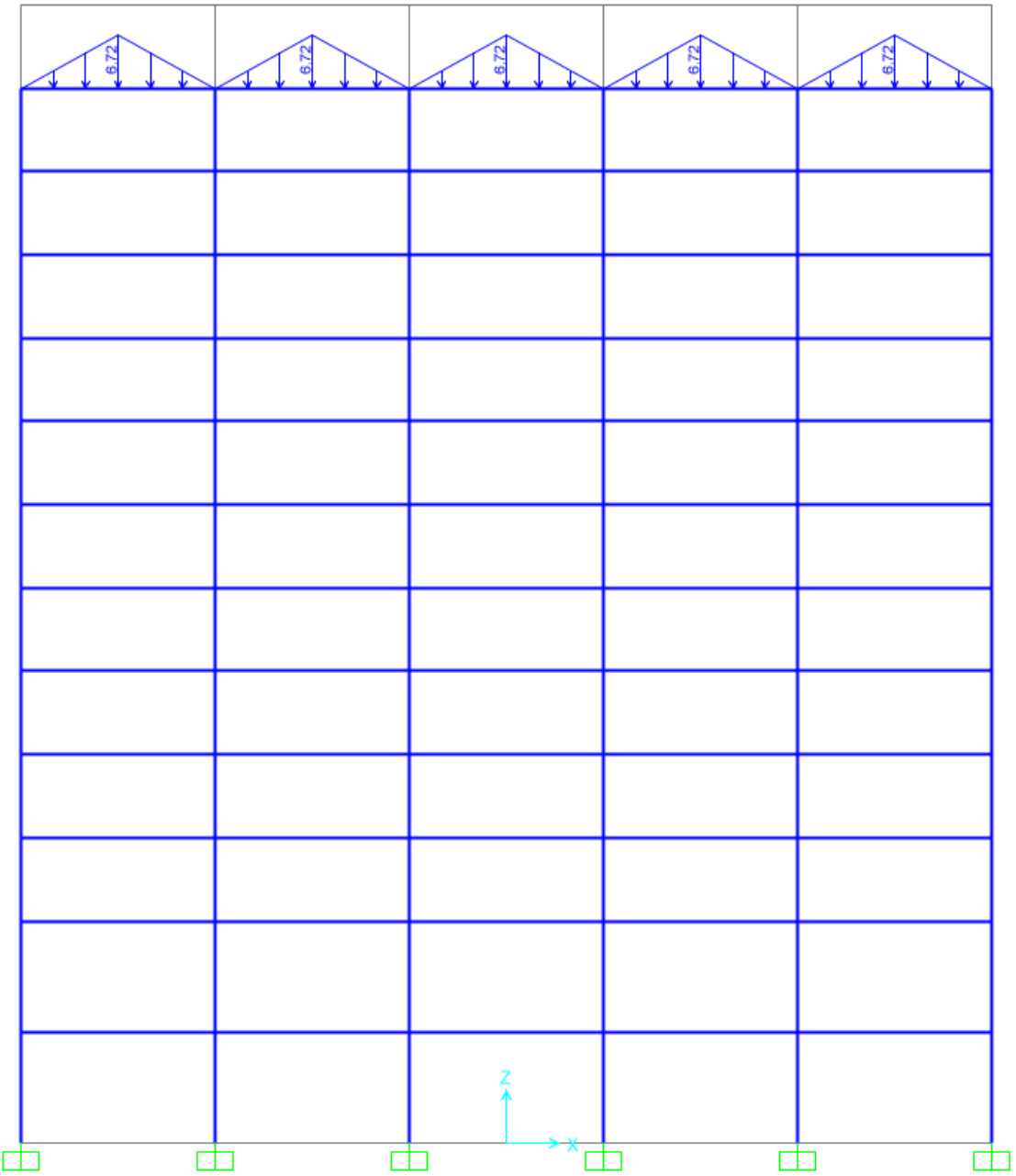

Figure 3.16. Assigned roof live loads on 2D frame in SAP2000.

3.2.3.2. Assigning forces to 3D frame

In similar specifications in terms of frame sections, materials and joint constraints, the 3D structure of the building was designed to determine its structural behaviour. The following Figures 3.17-3.18 display slab properties and stiffness modification factors that were defined for 3D analysis.

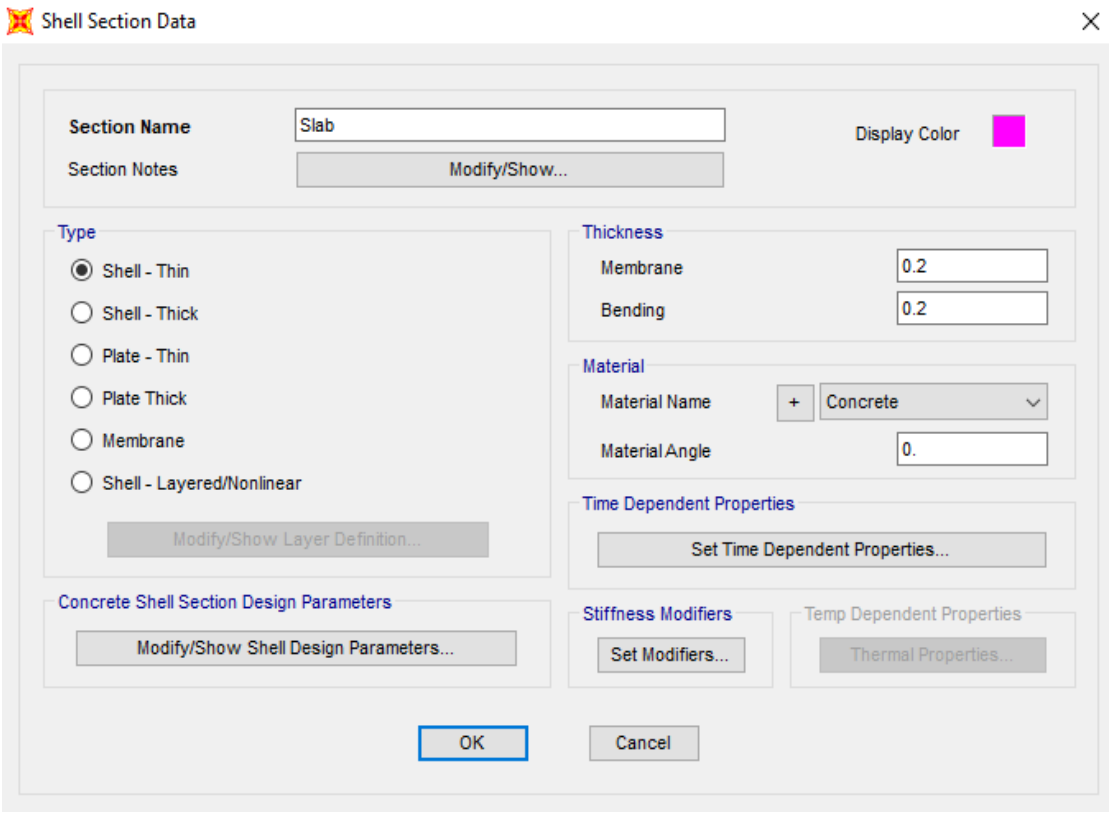

Figure 3.17 SAP2000: Slab Section.

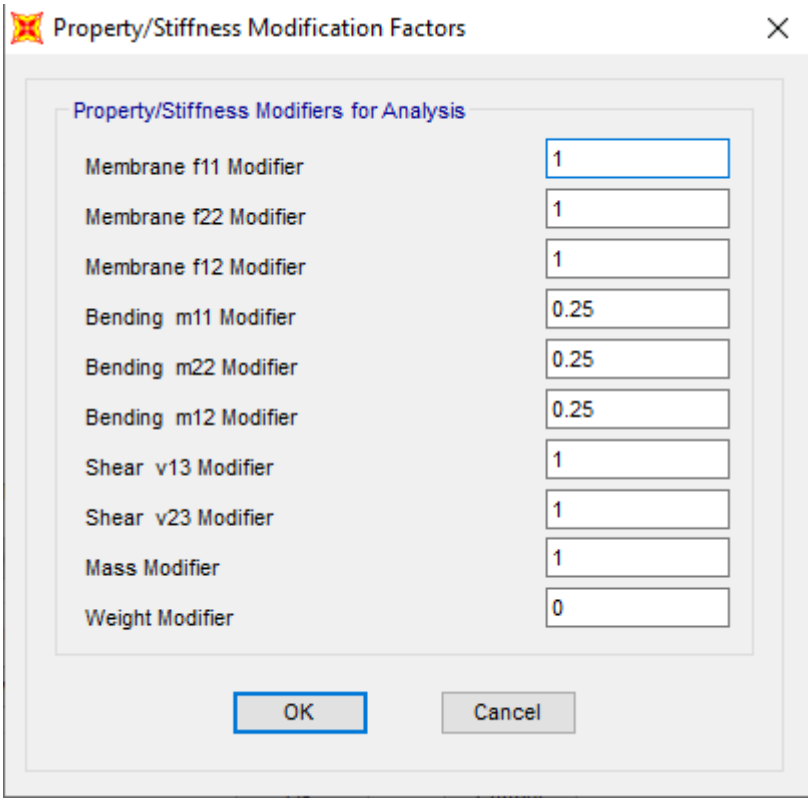

Figure 3.18 SAP2000: Slab property modifiers.

Next, all the loads were distributed and assigned on the slabs. The following Figures 3.19 to 3.23 display the dead loads, live loads, and roof live loads that are applied to the building's 3D model.

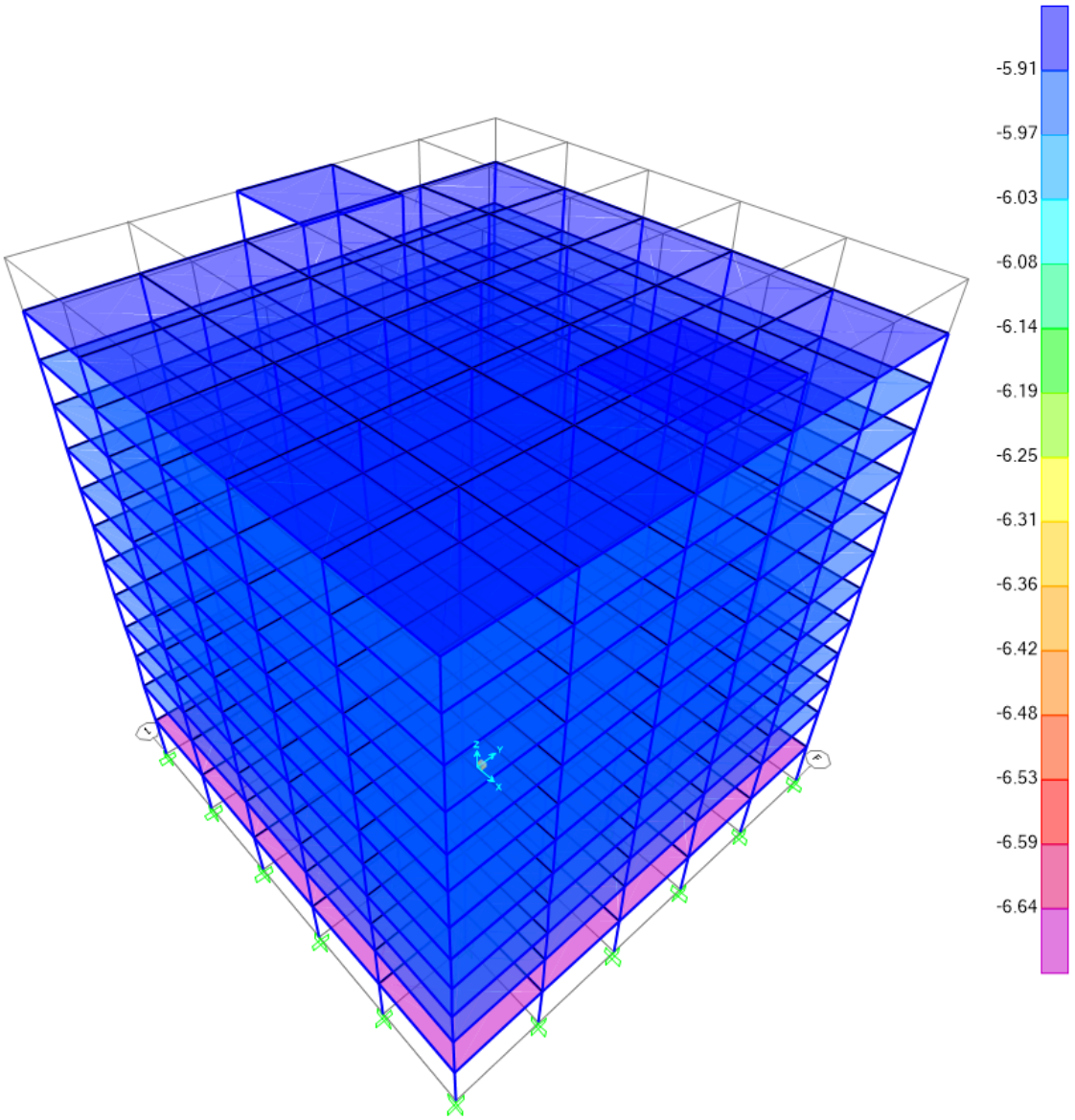

Figure 3.19 SAP2000: Dead area loads applied on 3D Model.

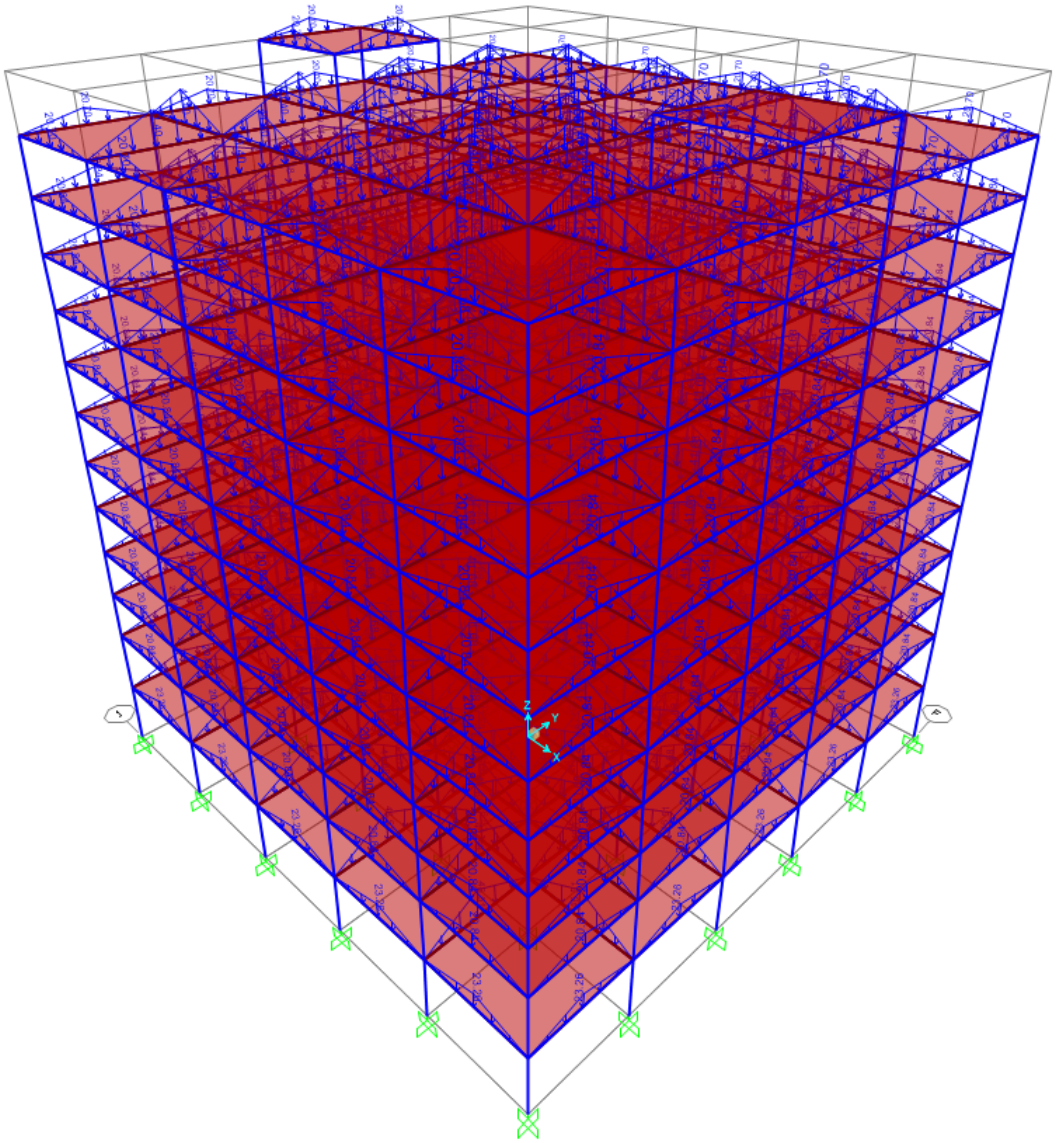

Figure 3.20 SAP2000: Dead frame loads applied on 3D Model.

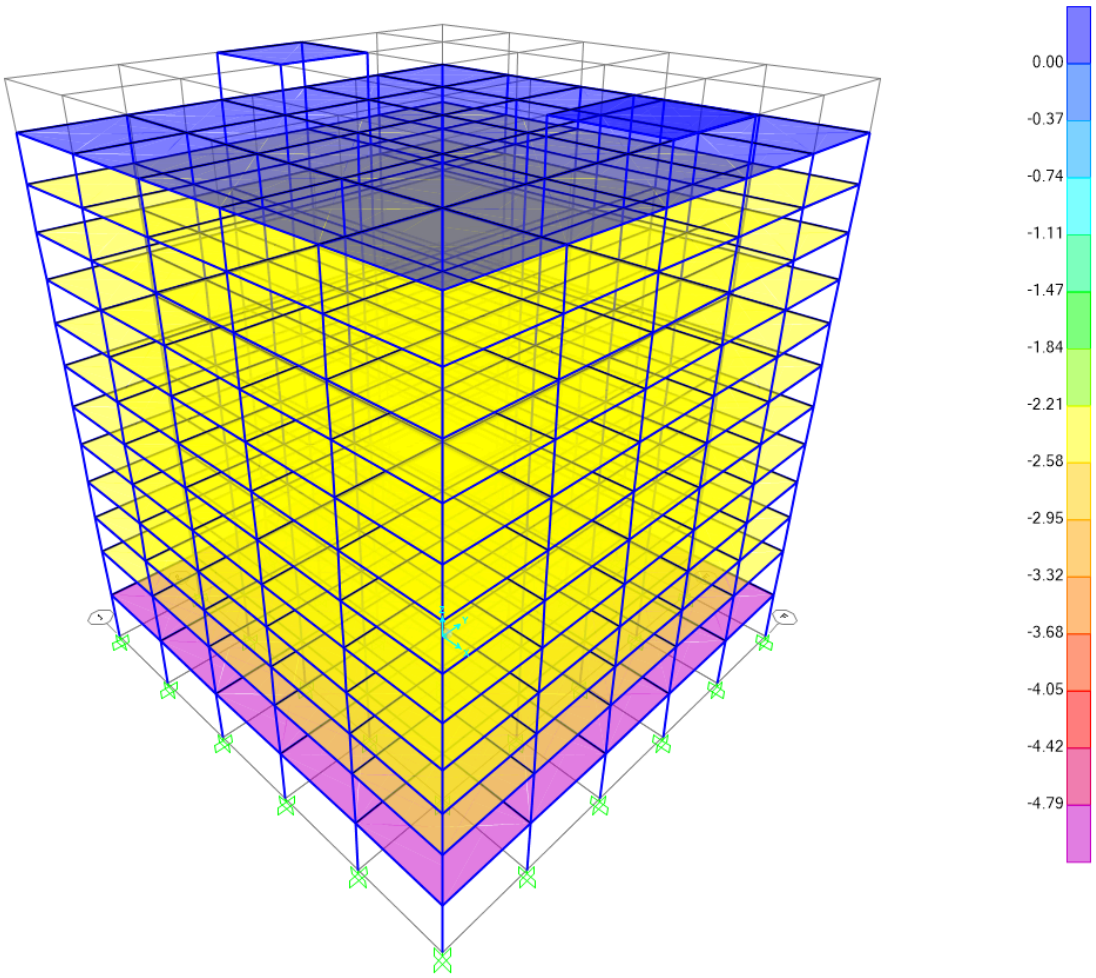

Figure 3.21 SAP2000: Live area loads applied on 3D Model.

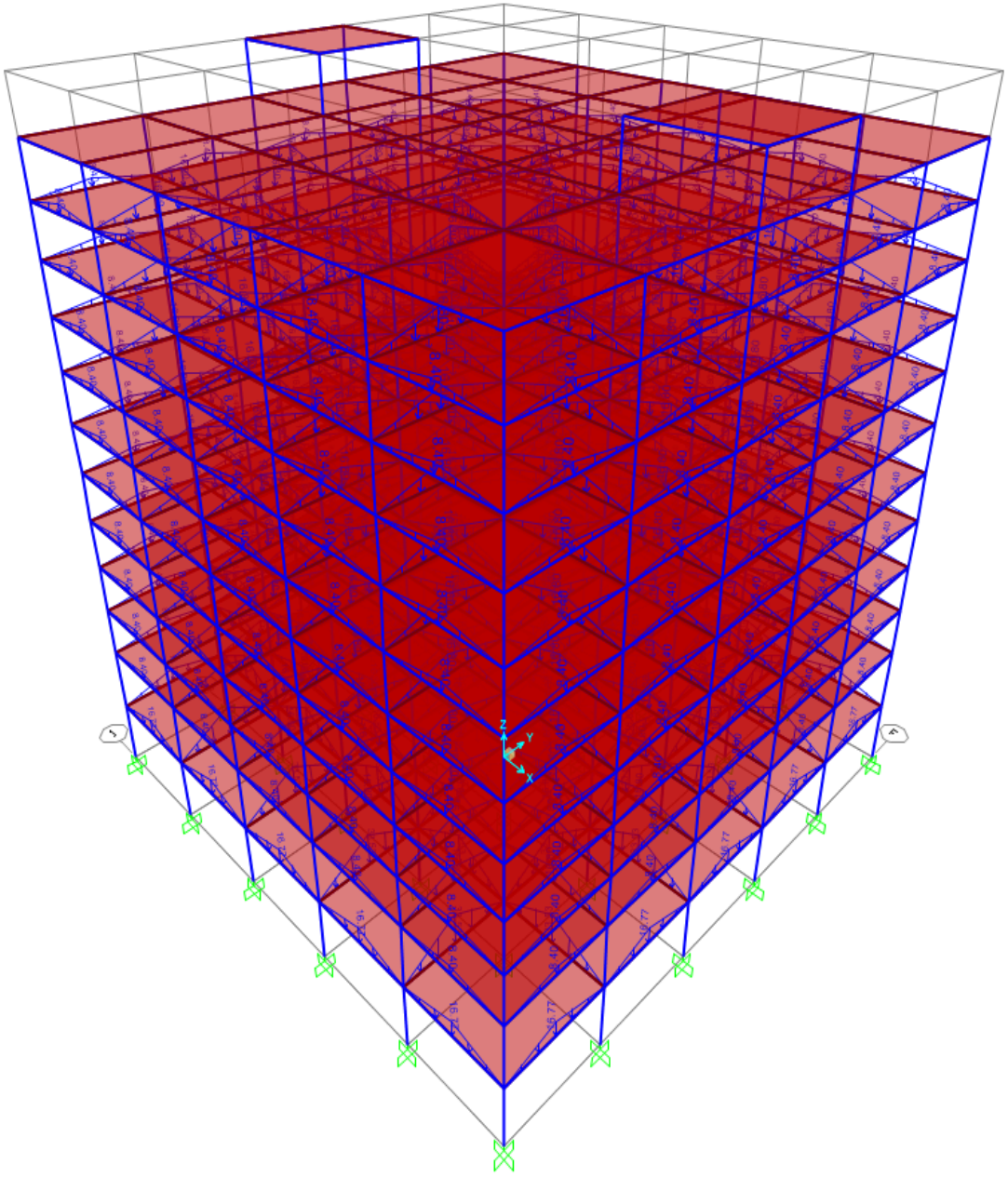

Figure 3.22 SAP2000: Live frame loads applied on 3D Model.

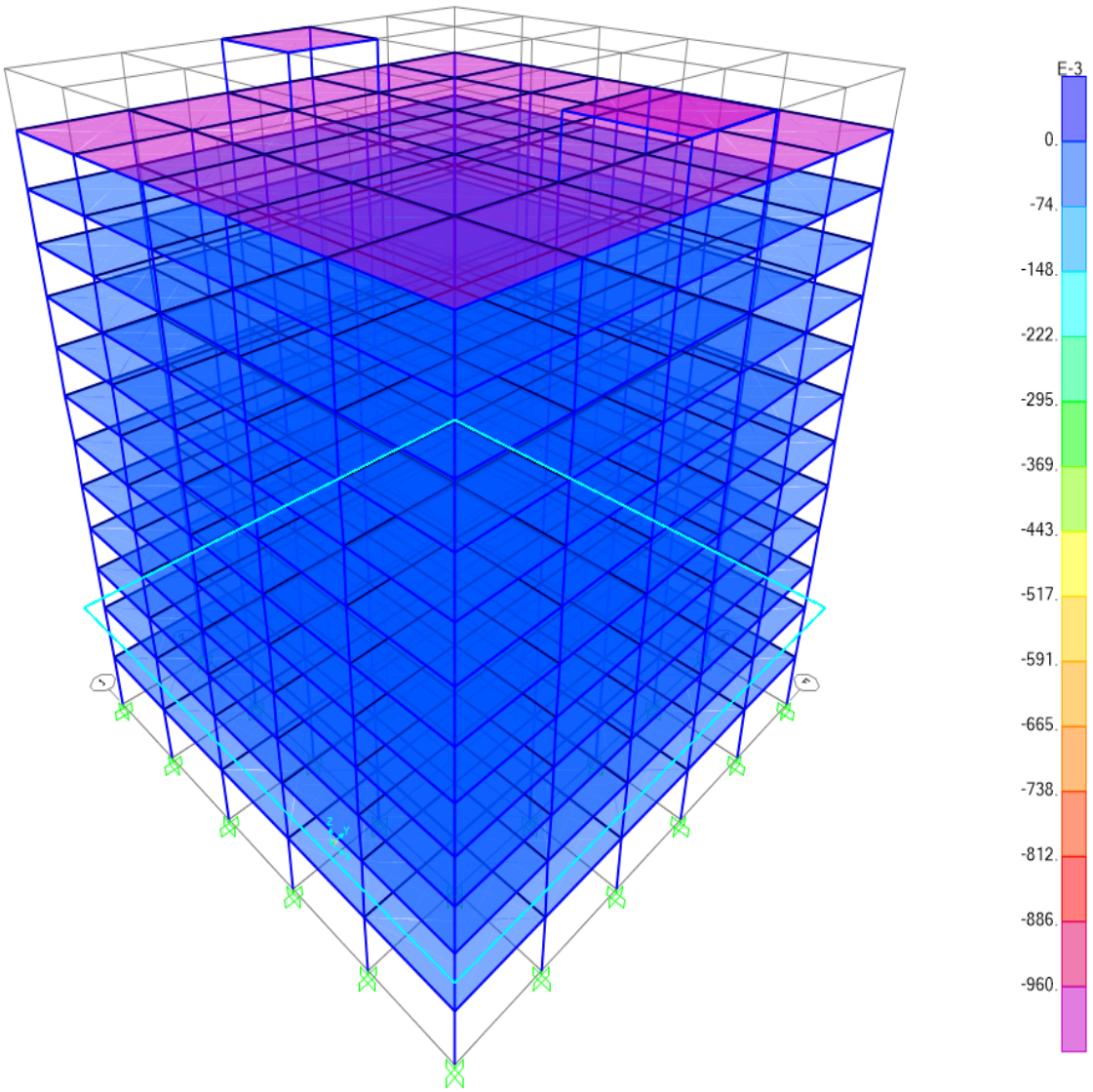

Figure 3.23 SAP2000: Roof live area loads applied on 3D Model ($L_r = 0.96\ kPa$)

3.3. Analysis and Design of Lateral Force Resisting System (LFRS)

3.3.1 Calculation of Seismic Loads

In order to calculate the seismic loads that will be applied to office building, American Society of Civil Engineers's standards need to be investigated. These standards are based on the equivalent lateral force (ELF) procedures. Additionally, it should be mentioned that for the calculations of the seismic loads we chose a special reinforced concrete moment frame.

In accordance with the site investigation report, the soil class was found to be classification C, which means that it will be used to evaluate the seismic design parameters for the site. The seismic parameters for the site were determined via ASCE Hazard Tool (ascehazardtool.org) website. According to the results from the map tool, the mapped acceleration parameters were identified as:

- Risk Category II - for office building

$$S_s = 2.35\ g,\ S_1 = 0.83\ g$$

Based on the site class, in order to find the adjusted parameters the soil condition correction factors were used:

$$F_a = 1.0,\ F_v = 1.3$$

$$S_{MS} = F_a \times S_s = 1.0 \times 2.35 = 2.35\ g \quad [29]$$

$$S_{M1} = F_v \times S_1 = 1.3 \times 0.83 = 1.079\ g \quad [30]$$

After that the maximum considered earthquake parameters were corrected to find the design acceleration values:

$$S_{DS} = \frac{2 \times S_{MS}}{3} = \frac{2 \times 2.35}{3} = 1.567\ g \quad [31]$$

$$S_{D1} = \frac{2 \times S_{M1}}{3} = \frac{2 \times 1.079}{3} = 0.719\ g \quad [32]$$

According to the seismic design calculations, the site was classified as Seismic Design Category D (American Society of Civil Engineers, 2017). For this certain category, a Special Reinforced Concrete Moment Frame was chosen as the Lateral Force Resisting System, with the following parameters:

$$Response\ modification\ factor,\ R = 8$$

$$Overstrength\ factor,\ \Omega = 3$$

$$Design\ amplification\ factor,\ C_d = 5.5$$

$$Importance\ factor,\ I_e = 1.0$$

Next, the periods of design spectrum were determined:

$$T_L = 8$$

$$T_0 = \frac{0.2 \times S_{D1}}{S_{DS}} = \frac{0.2 \times 0.719}{1.567} = 0.09177\ s \quad [33]$$

$$T_s = \frac{S_{D1}}{S_{DS}} = \frac{0.719}{1.567} = 0.4588\ s \quad [34]$$

The following equation was used to evaluate approximate fundamental period:

$$T_a = C^t \times h_n{}^x \quad [35]$$

Here,

T_a – *approximate fundamental period*

C^t, x – *values of approximate period parameters*

h_n – *building's structural height from ground to its highest elevation*

According to the American Society of Civil Engineers standards (ASCE 7-16), from the Table 12.8-2 for concrete moment-resisting frames the values are:

- $C_t = 0.0466$
- $x = 0.9$

So, the final value for the approximate fundamental period can be calculated:

$$T_a = 0.0466 \times 41^{0.9} = 1.318\ s$$

Next, the following equation was used to calculate the fundamental period of the structure:

$$T = C_u \times T_a \quad [36]$$

Where,

C_u – *Coefficient for Upper Limit on Calculated Period* (ASCE 7-16, Table 12.8-1)

In our case, since $S_{D1} = 0.719$, (C_u) the coefficient needs to be taken as 1.4 ($S_{D1} \geq 0.4$).

The final value for the fundamental period of the structure:

$$T = 1.4 \times 1.318 = 1.845\ s$$

Due to the fact that modal analysis in SAP 2000 was not conducted during this stage of project work, the period was assumed to be an approximate fundamental period, which is suitable for a conventional design procedure.

- $T = T_a = 1.318\ s$

The following formula needs to be used to determine the seismic base shear, for equivalent lateral force (ELF) procedures:

$$V = C_S \times W \quad [37]$$

Where,

C_s – *seismic response coefficient*

$W - effective\ seismic\ weight\ of\ the\ building$

The seismic response coefficient was found via next equation:

$$C_s = \frac{S_{DS}}{(\frac{R}{I_e})} = \frac{1.567}{(\frac{8}{1})} = 0.196 \quad [38]$$

Although there are a few conditions that have to be addressed.

1. $C_S = \frac{S_{D1}}{T\times(\frac{R}{I_e})}\ for\ T \leq T_L$ and it should not exceed this value

[36]

$$C_s = \frac{0.719}{1.845\times\frac{8}{1}} = 0.0487 < 0.196 \Rightarrow C_s = 0.0487\ is\ controlled$$

2. $C_s = \frac{0.5\times S_1}{(\frac{R}{I_e})}\ for\ S_1 \geq 0.6\ g$ and it should not be less than this value

[37]

$$C_s = \frac{0.5\times 0.83}{\frac{8}{1}} = 0.0519 > 0.0487 \Rightarrow C_s = 0.0519\ is\ controlled$$

After, with the weights of floor finishing, slab, beams, columns, stairs and partition and exterior walls the effective seismic weight was calculated. The values for the beams, columns and stairs were given in kN. However, for the rest of weights, the values were multiplied by the floor area which is 1153.14 m^2. The weights for each of the floors can be seen from the following table:

Table 3.15. Calculations of the Effective seismic weight.

Floor #	Floor finishing and slab (kN/m^2)	Column weight (kN)	Beam weight (kN)	Exterior/ Partition walls (kN/m^2)	Stairs (kN)	Floor weight (kN)
1	6.6444	1906.92	2422.68	1.3234	186.228	13703.8
2	6.6444	1906.92	2422.68	1.4947	186.228	13901.3
3	5.954	1074.24	2422.68	1.152	186.228	11877.4
4	5.954	1074.24	2422.68	1.152	186.228	11877.4

5	5.954	769.32	2422.68	1.152	186.228	11572.4
6	5.954	769.32	2422.68	1.152	186.228	11572.4
7	5.954	635.76	2422.68	1.152	186.228	11438.9
8	5.954	635.76	2422.68	1.152	186.228	11438.9
9	5.954	406.80	2422.68	1.152	186.228	11209.9
10	5.954	406.80	2422.68	1.152	186.228	11209.9
11	5.954	228.96	2422.68	1.152	186.228	11032.1
12	5.954	228.96	2422.68	1.152	186.228	11032.1
Roof	5.914	0.00	2422.68	0.518	186.228	10025.9
Effective Seismic Weight						**151892.3**

Since now the effective seismic weight is known, seismic base shear can be determined:

$$V = 0.0519 \times 151892.3 = 7883.21\ kN$$

Subsequently, the vertical distribution of seismic forces can be determined via following formula:

$$F_x = C_{vx} \times V \quad [39]$$

$$C_{vx} = \frac{w_x \times h_x^{\,k}}{\sum_{i=1}^{n} w_i \times h_i^{\,k}} \quad [40]$$

Here,

$C_{vx} - vertical\ distribution\ factor$

$w_x\ and\ w_i - portions\ of\ total\ effective\ seismic\ weight\ at\ corresponding\ levels\ x\ or\ i$

$k - structure\ period's\ exponent$:

$If\ T \leq 0.5\ s \Rightarrow k = 1$

$If\ T \geq 2.5\ s \Rightarrow k = 2$

$If\ 0.5\ s \leq T \leq 2.5\ s \Rightarrow k\ should\ be\ interpolated$:

$$k = \frac{2-1}{2.5-0.5} \times (1.318 - 0.5) + 1 = 1.659$$

The lateral seismic force at each floor can be seen from the following table. Additionally, it has to be noted that the weight of the roof was added to the 12th's floor.

Table 3.16. Lateral seismic force at each floor.

Floor #	$h_i\,(m)$	$W_x\,(kN)$	$W_x \times h_x^{\,k}$	C_{vx}	$F_x\,(kN)$
13	41	10025.9	1877054	0.146198	1151.96
12	38	11032.1	1855729	0.144537	1138.87
11	35	11032.1	1652695	0.128724	1014.27
10	32	11209.9	1480143	0.115284	908.37
9	29	11209.9	1288450	0.100354	790.73
8	26	11438.9	1127273	0.087800	691.81
7	23	11438.9	948436	0.073871	582.06
6	20	11572.4	788004	0.061375	483.60
5	17	11572.4	626733	0.048814	384.63
4	14	11877.4	489297	0.038110	300.28
3	11	11877.4	348340	0.027131	213.78
2	8	13901.3	260302	0.020274	159.75
1	4	13703.8	96632	0.007526	59.30
$Total\ W_x$		138188.5	12839088		

3.3.1.1. Calculation of seismic loads including the Torsional effects

Since our building is susceptible to torsional effects caused by differences in stiffness and the position of mass centers, it is important to account for torsional forces, and to determine the seismic forces acting on each frame.

The first step involved identifying the building's mass center. To find this, we considered the slabs, floor finishing, as well as interior partitions and exterior walls. The mass center was calculated after excluding the areas occupied by the elevator and stair shafts, since they lack slabs, while other elements were evenly spread across the floor's surface. The building is square shaped with both of the longitudinal and transverse directions being 35 meters. With the reference point established, we advanced with the calculations to locate the mass center.

$$x = 17.5\ m\ (since\ building\ is\ symmetrical)$$

$$y = \frac{A_{floor} \times y_{floor} - A_{stairs/elevator\ shaft} \times y_{stairs/elevator\ shaft}}{A_{floor} - A_{shaft}} \quad [41]$$

$$y = \frac{1225 \times 17.5 - 13.60 \times 16.73 - 34.15 \times 16.73}{1225 - 13.60 - 34.1502} = 17.53\ m$$

Hence, mass center: x = 17.5 m, y = 17.53 m.

After that, the stiffness center (SC) was also found by calculating the stiffness of the moment frame. First of all, the cracking moment of inertia of columns and beams were calculated using the following equations:

$$I_{b,cr} = \frac{1}{12} b h^3 * 0.35 \quad [42]$$

$$I_{c,cr} = \frac{1}{12} h^3 b * 0.70 \quad [43]$$

To calculate the stiffness of frame, the following formula was used:

$$D = \frac{12E}{h^2} \left(\frac{I_{c,cr} \cdot I_{b,cr}}{L \cdot I_{c,cr} + h \cdot I_{b,cr}} \right) \quad [44]$$

To find the force required to generate an inter-story rotation, the next equation was used:

$$C_F = h \cdot D \cdot \#\ of\ columns\ per\ frame \cdot \#\ of\ frames \quad [45]$$

Also it is important to mention that the exterior columns of the frame were calculated as 0.5.

Next, the stiffness center was calculated. Detailed calculations on frame stiffness are given in Appendix A. Stiffness center: x’ = 17.5 m, y’ = 17.5 m.
Both mass and stiffness centers can be seen in Figure 3.24.

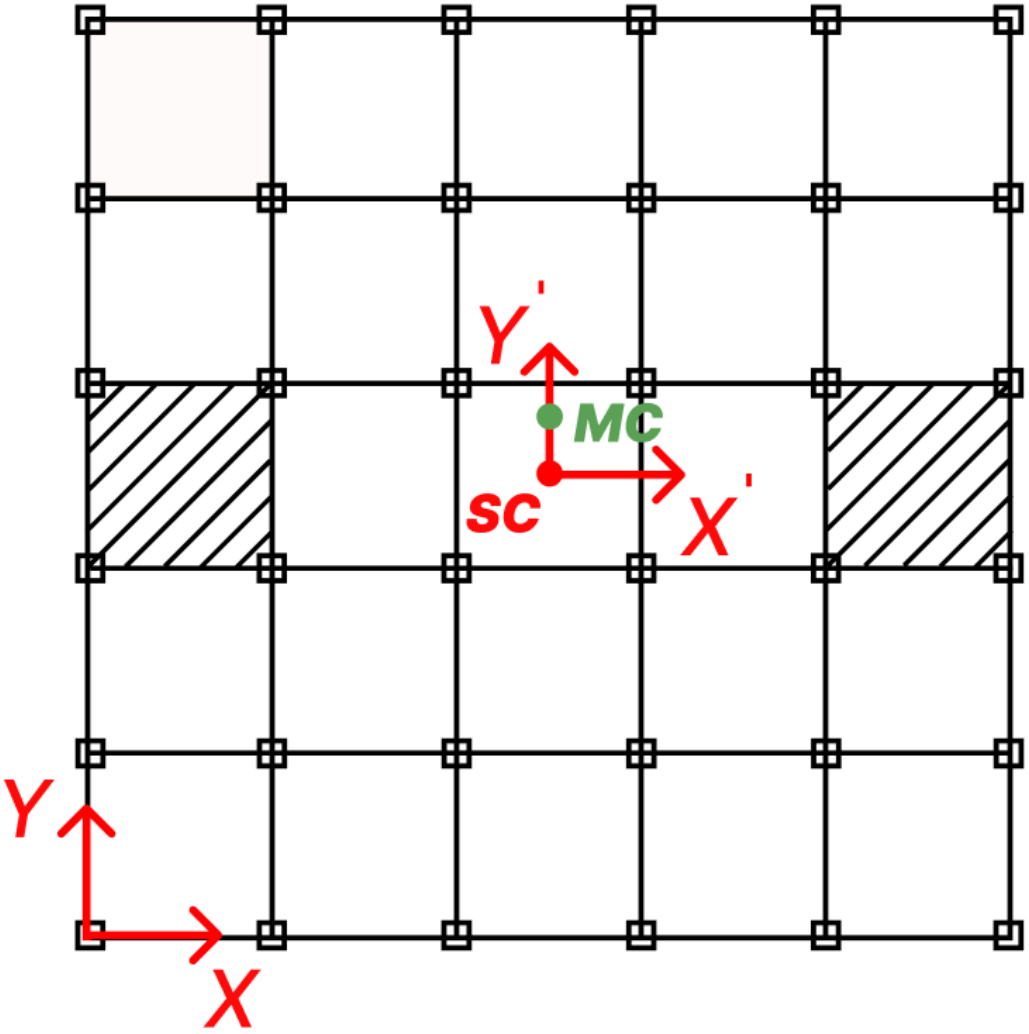

Figure 3.24 Mass and Stiffness centers.

The eccentricity was also calculated.

For the x-axis:

$$e_x = 17.5 - 17.5 = 0\,m$$

$$e_a = 5\% * L_x = 0.05 * 35 = 1.75\,m$$

$$e_{xt} = e_a + e_x = 1.75\,m$$

For the y-axis:

$$e_y = 17.53 - 17.5 = 0.03\,m$$

$$e_a = 5\% * L_y = 0.05 * 35 = 1.75\,m$$

$$e_{yt} = e_x + e_a = 1.78\,m$$

Consequently, torsion moment, torsional and direct forces, and total forces were calculated as:

$$T = eF \quad [46]$$

$$F_{direct} = \frac{F_x}{\#\ of\ frames} \quad [47]$$

$$F_{torsion} = \frac{T*C_f*(x_i\ or\ y_i)}{\Sigma C_f*(x_i^2\ or\ y_i^2)} \quad [48]$$

$$F_{total} = F_{direct} \pm F_{torsion} \quad [49]$$

The calculation of torsion and direct forces for both sides on each floor are presented in Table 3.14. Need to mention that there is a slight difference in torsion values because of the e_{xt} and e_{yt} difference which in turn differs due to the different area of shafts for elevators. But these dissimilarities are very little. Next, Table 3.18 presents readjusted seismic forces at each frame for the first floor of the building. Calculations for other floors are given in Appendix A.

Table 3.17. Direct forces and torsion for both axes with forces on each frame.

		Transverse		Longitudinal	
Floors	F_x, kN	F_{direct}, kN	T, kN-m	F_{direct}, kN	T, kN-m
13	1151.96	191.99	2015.93	191.99	2051.90
12	1138.87	189.81	1993.02	189.81	2028.59
11	1014.27	169.04	1774.97	169.04	1806.64
10	908.37	151.40	1589.65	151.40	1618.02
9	790.73	131.79	1383.77	131.79	1408.47
8	691.81	115.30	1210.67	115.30	1232.28
7	582.06	97.01	1018.61	97.01	1036.78

6	483.60	80.60	846.30	80.60	861.41
5	384.63	64.10	673.10	64.10	685.11
4	300.28	50.05	525.50	50.05	534.87
3	213.78	35.63	374.11	35.63	380.79
2	159.75	26.62	279.56	26.62	284.55
1	59.30	9.88	103.78	9.88	105.63

Table 3.18. Calculation of seismic loads on each frame for the first floor.

Floor #	Frame #	$F_{torsion}$, kN	F_{direct}, kN	F_{total}, kN
1	1	-1.0779	9.88	8.81
	2	-0.6467	9.88	9.24
	3	-0.2156	9.88	9.67
	4	-0.2156	9.88	10.10
	5	0.6467	9.88	10.53
	6	1.0779	9.88	10.96

3.3.2. Calculation of Wind Loads

3.3.2.1. Wind Loads with Torsional Effect

Wind load calculations were conducted following ASCE 7-16 standards. The basic wind speed in Los Angeles, California, was determined to be V = 95 mph = 42.5 m/s. Also, ASCE Hazard Tool showed these values. From both of these sources and using general knowledge, we have found the following information

- Exposure category - B

- Direction effect Kd = 0.85 - main wind load force resisting system (LFRS)
- Topographical effect Kzt = 1 - for flat land

Since our exposure category is B, we use values for B category from Table 3.19.

Table 3.19. Constants depending on exposure categories.

Exposure	α	z_g (m)	$\hat{a}$	$\hat{b}$	$\bar{\alpha}$	$\bar{b}$	c	ℓ (m)	$\bar{\in}$	z_{min} (m)*
B	7.0	365.76	1/7	0.84	1/4.0	0.45	0.30	97.54	1/3.0	9.14
C	9.5	274.32	1/9.5	1.00	1/6.5	0.65	0.20	152.4	1/5.0	4.57
D	11.5	213.36	1/11.5	1.07	1/9.0	0.80	0.15	198.12	1/8.0	2.13

To calculate the velocity pressure exposure coefficient, one of the two next formulas was used depending on the height of the point being considered.

$$K_z = 2.01\left(\frac{15}{z_g}\right)^{2/\alpha},\ for\ z < 15\ ft \quad [50]$$

$$K_z = 2.01\left(\frac{z}{z_g}\right)^{2/\alpha},\ for\ 15\ ft < z < z_g \quad [51]$$

Again depending on the exposure category some of the values change.

Table 3.20. Height effect constants depending on the exposure category of the site.

Exposure	α	$z_g,\ ft$	$z_g,\ m$
B	7.0	1200	365.76
C	9.5	900	274.32
D	11.5	700	213.36

Next the calculations for velocity pressure exposure coefficient values for our location are shown in Table 3.21.

Table 3.21. Results of Kz calculations.

Story	h (m)	z (m)	Kz
13	3	40	1.067
12	3	38	1.052
11	3	35	1.028
10	3	32	1.002
9	3	29	0.974
8	3	26	0.944
7	3	23	0.912
6	3	20	0.876
5	3	17	0.836
4	3	14	0.791
3	3	11	0.739
2	4	8	0.674
1	4	4	0.575

Then the Gust effect was calculated.

Generally Gust effect is calculated considering 2 possible wind directions, but not in our case. Since our building is square shaped, both distances B and L are the same.

So, B = L = 35 meters, number of frames = 6.

Since our building's height is more than 60 ft or 18 meters, it cannot be considered as a low rise or rigid building. This means that for flexible buildings gust effect factor should be calculated following all steps. Next formulas and values were determined to calculate the gust-effect factor.

$$n_a = 43.5/h^{0.9} = 43.5/134.5^{0.9} = 0.528 < 1\,Hz;\ flexible\ building \quad [52]$$

$$\bar{z} = 0.6 * h = 0.6 * 41 = 24.6\,m \quad [53]$$

$$I_z = c(\frac{10}{\bar{z}})^{1/6} = 0.3 * (\frac{10}{24.6})^{1/6} = 0.2582 \quad [54]$$

$$L_{\bar{z}} = l(\frac{\bar{z}}{10})^{\bar{\epsilon}} = 97.54 * (\frac{24.6}{10})^{1/3} = 131.67 \quad [55]$$

$$\overline{V_z} = \bar{b}(\frac{\bar{z}}{10})^{\bar{\alpha}} * V = 0.45 * (\frac{24.6}{10})^{0.25} * 42.5 = 23.951 \quad [56]$$

$$N_1 = \frac{n_1 L_{\bar{z}}}{\overline{V_z}} = \frac{0.528*131.67}{23.951} = 2.903 \quad [57]$$

$$R_n = \frac{7.47N_1}{(1+10.3N_1)^{5/3}} = \frac{7.47*2.903}{(1+10.3*7.47)^{5/3}} = 0.07127 \quad [58]$$

$$\eta_h = 4.6n_1 h/\overline{V_z} = 4.6 * 0.528 * 41/23.951 = 4.158 \quad [59]$$

$$\eta_B = 4.6n_1 B/\overline{V_z} = 4.6 * 0.528 * 35/23.951 = 3.549 \quad [60]$$

$$\eta_L = 15.4n_1 L/\overline{V_z} = 15.4 * 0.528 * 35/23.951 = 11.882 \quad [61]$$

$$R_h = \frac{1}{\eta_h} - \frac{1}{2\eta_h^2}(1 - e^{-2\eta_h}) = \frac{1}{4.158} - \frac{1}{2*4.158^2}(1 - e^{-2*4.158}) = 0.2116 \quad [62]$$

$$R_B = \frac{1}{\eta_B} - \frac{1}{2\eta_B^2}(1 - e^{-2\eta_B}) = \frac{1}{3.549} - \frac{1}{2*3.549^2}(1 - e^{-2*3.549}) = 0.242 \quad [63]$$

$$R_L = \frac{1}{\eta_L} - \frac{1}{2\eta_L^2}(1 - e^{-2\eta_L}) = \frac{1}{11.882} - \frac{1}{2*11.882^2}(1 - e^{-2*11.882}) = 0.0806 \quad [64]$$

$$R = \sqrt{\frac{1}{\beta}R_n R_h R_B(0.53 + 0.47R_L)} \quad [65]$$

$$R = \sqrt{\frac{1}{0.02}0.07127 * 0.2116 * 0.242(0.53 + 0.47 * 0.0806)} = 0.322$$

$$g_R = \sqrt{2ln(3600n_1)} + \frac{0.577}{\sqrt{2ln(3600n_1)}} \quad [66]$$

$$g_R = \sqrt{2ln(3600 * 0.528)} + \frac{0.577}{\sqrt{2ln(3600*0.528)}} = 4.034$$

$$Q = \sqrt{\frac{1}{1+0.63\left(\frac{B+h}{L_z}\right)^{0.63}}} = \sqrt{\frac{1}{1+0.63\left(\frac{35+41}{131.67}\right)^{0.63}}} = 0.8317 \quad [67]$$

$$G_f = 0.925\left(\frac{1+1.7I_z\sqrt{g_Q^2Q^2+g_R^2R^2}}{1+1.7g_vI_z}\right) \quad [68]$$

$$G_f = 0.925 * \frac{1+1.7*0.2582\sqrt{3.4^2*0.8317^2+4.034^2*0.322^2}}{1+1.4*3.4*0.2582} = 0.878$$

Then to calculate wind loads for four different cases, it is crucial to determine external pressure coefficients. For the windward wall, Cp = 0.8, whereas for the leeward wall it depends on the L/B ratio. In our case, this ratio is equal to 1, therefore Cp = -0.5.

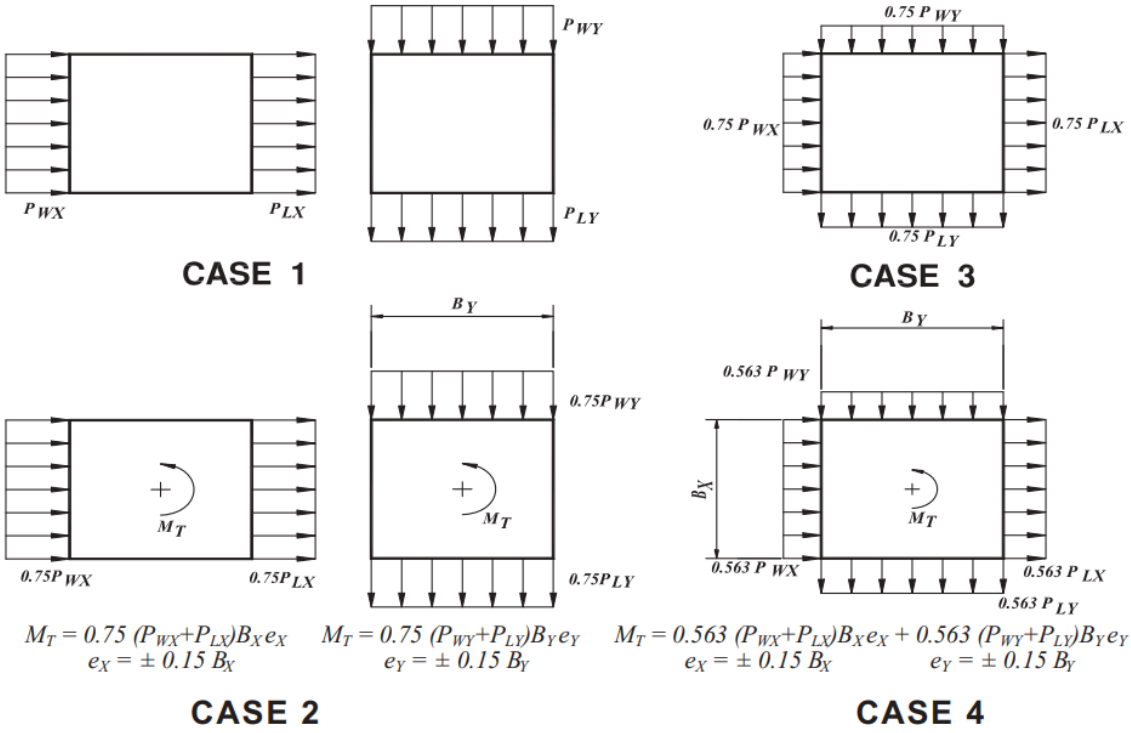

Figure 3.25 Design wind load cases.

There are 4 major cases that were considered in the design of the wind loads. They are taken from ASCE 7-16.

Case 1.

Next to find velocity pressure the following equation was used

$$q_z = 0.613 K_z K_{zt} K_d V^2 \quad (N/m^2) \qquad [69]$$

Then design wind pressures for the MWFRS was determined by the next formula

$$p = q_z GC_{p\,windward} - q_h GC_{pi\,leeward} \quad (N/m^2) \qquad [70]$$

To calculate forces at different floors two equations were used

$$F_{top\,floor} = (B/number\ of\ frames) * h_{13}/2 * P_{13} \qquad [71]$$

$$F_i = (B/number\ of\ frames) * (P_{i+1} * h_{i+1}/2 + P_i * h_i/2) \qquad [72]$$

Results of Case 1 calculations are in Table 3.22.

Table 3.22. Case 1 calculations results.

Story #	h (m)	Kz	q (Pa)	Pw, Pl (Pa)	P (Pa)	Fi (kN)	F per frame (kN)
13	3	1.067	1003.74	705.08	1139.97	59.85	29.92
12	3	1.052	990.55	695.77	1130.62	119.21	19.87
11	3	1.028	967.55	679.61	1114.46	117.87	19.64
10	3	1.002	943.09	662.43	1097.28	116.12	19.35
9	3	0.974	916.94	644.06	1078.91	114.2	19.04
8	3	0.944	888.77	624.27	1059.13	112.25	18.71
7	3	0.912	858.18	602.78	1037.64	110.08	18.35
6	3	0.876	824.58	579.19	1014.04	107.71	17.95
5	3	0.836	787.17	552.91	987.76	105.09	17.52
4	3	0.791	744.69	523.07	957.93	102.15	17.02
3	3	0.739	695.11	488.24	923.10	98.75	16.46

2	4	0.674	634.65	445.78	880.63	110.11	18.35
1	4	0.807	759.52	533.48	968.34	129.43	21.57

Case 2.

For this case, as it can be seen in Figure 3.23, firstly e_x and e_y values need to be found.

$$e_x = 0.15 * B_x = 0.15 * 35 = 5.25 \quad [73]$$

$$e_y = 0.15 * B_y = 0.15 * 35 = 5.25 \quad [74]$$

All calculations for this case are presented in Table 3.20.

Table 3.23. Case 2 calculation results.

Story #	Pw, Pl (Pa)	$M_T\ (kN - m)$	0.75Fi (kN)	F direct (kN)
13	705.08	157.10	44.89	22.44
12	695.82	155.83	89.41	14.90
11	679.66	153.60	88.41	14.73
10	662.48	151.23	87.09	14.52
9	644.11	148.70	85.69	14.28
8	624.32	145.97	84.19	14.03
7	602.83	143.01	82.57	13.76
6	579.23	139.76	80.79	13.47
5	552.95	136.14	78.83	13.14
4	523.11	132.02	76.62	12.77
3	488.28	127.22	74.07	12.35
2	445.81	121.37	82.59	13.76

1	533.53	133.46	97.08	16.18

For this case, we also had to find the total force which is the sum of torsional and direct forces. These results are given in Table 3.24. This presented table is the calculation results only for the first floor, for other floors tables are provided in Appendix.

Table 3.24. Calculation of wind loads on each frame for the first floor.

Floor #	Frame #	$F_{torsion}, kN$	F_{direct}, kN	F_{total}, kN
1	1	-1.3617	16.18	14.82
	2	-0.8170	16.18	15.36
	3	-0.2723	16.18	15.36
	4	0.2723	16.18	16.45
	5	0.8170	16.18	17.00
	6	1.3617	16.18	17.54

The same procedures were done for both cases.

Case 3.

Since the building is square shaped, results for frames from both sides should be the same.

Table 3.25. Case 3 calculation results.

Story #	$0.75F_1\ (kN)$	$F_1\ per\ frame\ (kN)$	$0.75F_2\ (kN)$	$F_2\ per\ frame\ (kN)$
13	44.89	22.44	44.89	22.44
12	89.41	14.90	89.40	14.90
11	88.41	14.73	88.40	14.73

10	87.09	14.52	87.09	14.51
9	85.69	14.28	85.69	14.28
8	84.19	14.03	84.19	14.03
7	82.57	13.76	82.56	13.76
6	80.79	13.47	80.78	13.46
5	78.83	13.14	78.82	13.14
4	76.62	12.77	76.61	12.77
3	74.07	12.35	74.07	12.34
2	82.59	13.76	82.58	13.76
1	97.08	16.18	97.07	16.18

Case 4.

Table 3.26. Case 4 calculation results.

Story #	Pw, Pl (Pa)	$M_T\ (kN\ -\ m)$	0.563F (kN)	$F_{direct}\ (kN)$
13	705.08	235.86	33.69	16.85
12	695.82	233.94	67.11	11.19
11	679.66	230.59	66.36	11.06
10	662.48	227.04	65.37	10.90
9	644.11	223.24	64.32	10.72
8	624.32	219.14	63.20	10.53
7	602.83	214.70	61.98	10.33
6	579.23	209.82	60.65	10.11

5	552.95	204.38	59.17	9.86
4	523.11	198.20	57.51	9.59
3	488.28	191.00	55.60	9.27
2	445.81	182.21	61.99	10.33
1	533.53	200.36	72.87	12.15

Table 3.2. Calculation of seismic loads on each frame for the first floor including the torsional effect.

Floor #	Frame #	$F_{torsion}$, kN	F_{direct}, kN	F_{total}, kN
1	1	-2.0445	12.14	10.10
	2	-1.2267	12.14	10.92
	3	-0.4089	12.14	11.74
	4	0.4089	12.14	12.55
	5	1.2267	12.14	13.37
	6	2.0445	12.14	14.19

3.3.3. Assigning Forces to SAP2000

3.3.3.1. Assigning forces to selected 2D frame

To apply and assign the lateral forces to the chosen first frame , the same technique which was outlined in “Assigning forces to selected 2D frame” was followed, involving the definition of material properties, frame sections, and constraints. The wind load for the selected frame was applied to each joint using ($F_{per\ frame}$) calculations from the Section 3.3.2, which was based on the Case 1 wind condition.

Furthermore, the wind load was applied similarly for the other Cases 2,3 and 4 for the selected first frame. All of the figures which show Case 2, 3 and 4 will be provided in the Section 9 Appendix part of the documentation. Similarly, seismic loads were assigned to each joint based on the (F_{total}) calculations provided in Section 3.3.1, with the torsional effect taken into consideration. The assigned forces are shown in the following Figures 3.26-3.27.

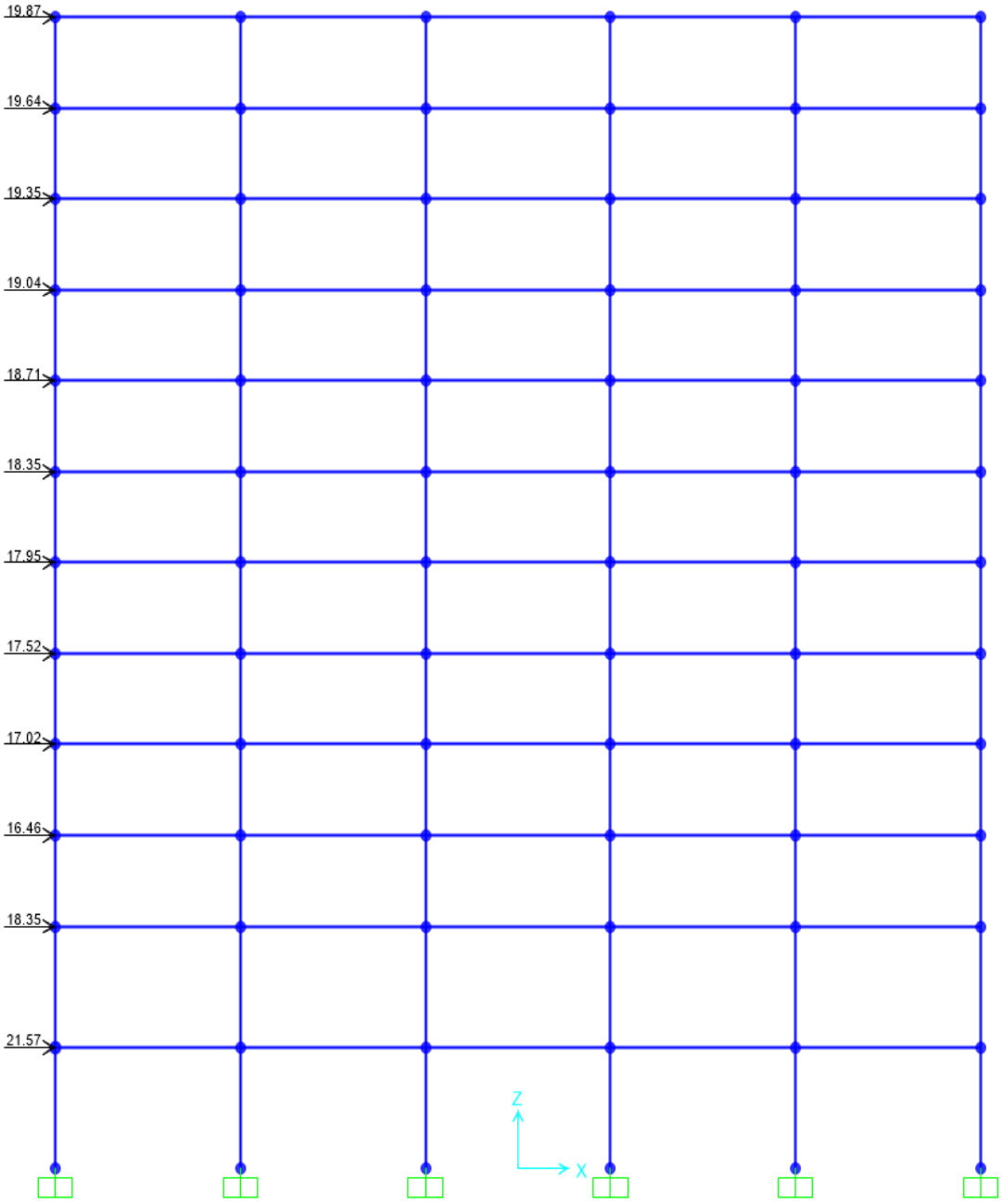

Figure 3.26. SAP2000: Assigned lateral forces for Case 1 wind loads on 2D frame.

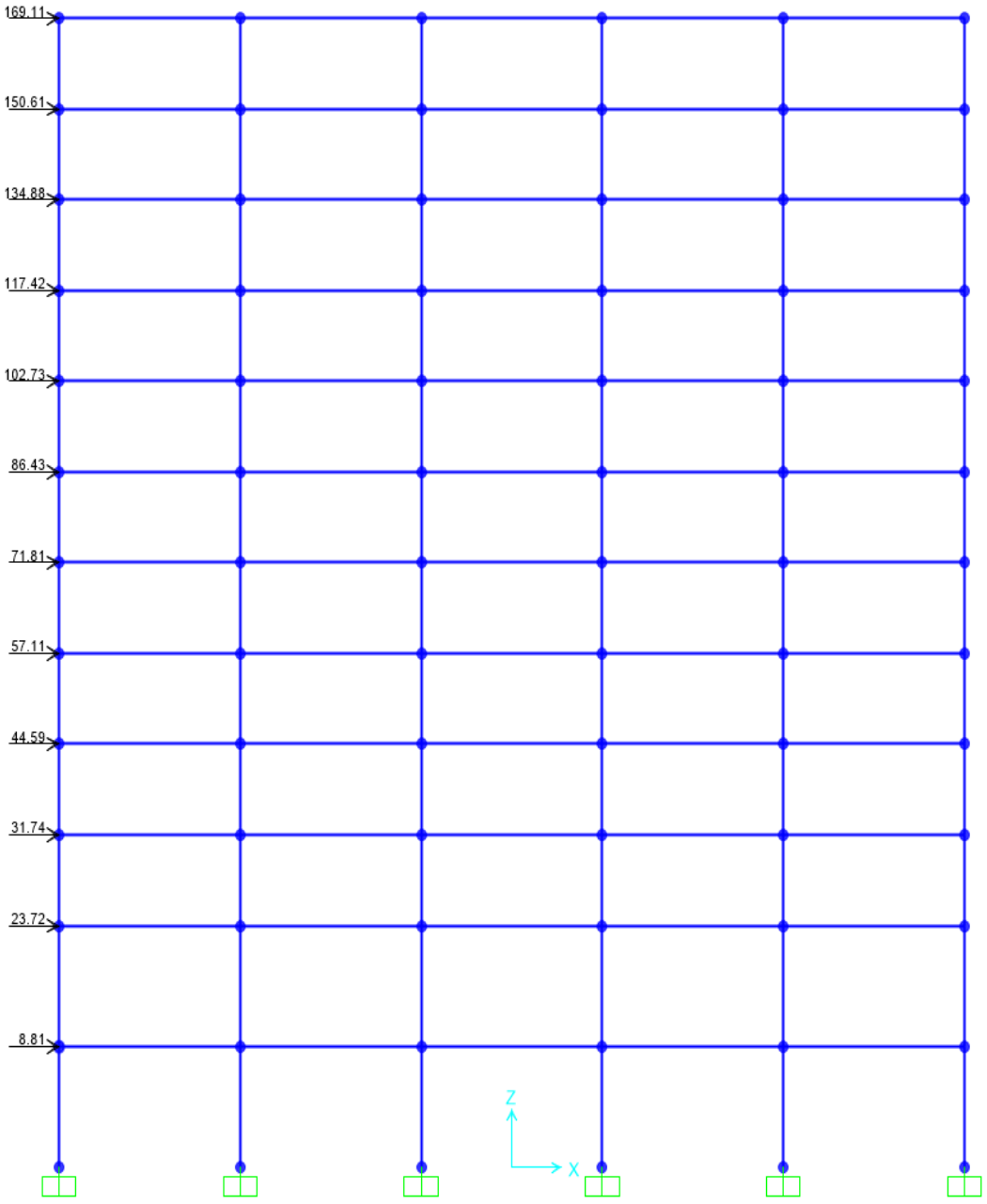

Figure 3.27. SAP2000: Assigned lateral forces for seismic loads on 2D frames.

3.3.3.2. Assigning forces to 3D frame

The lateral forces were assigned to the 3D frame of the building following the same procedure with 2D frames, to the same chosen first frame of our building. Following Figure 3.28 shows the assigned wind and seismic load patterns with the other load patterns such as dead, live and roof live load.

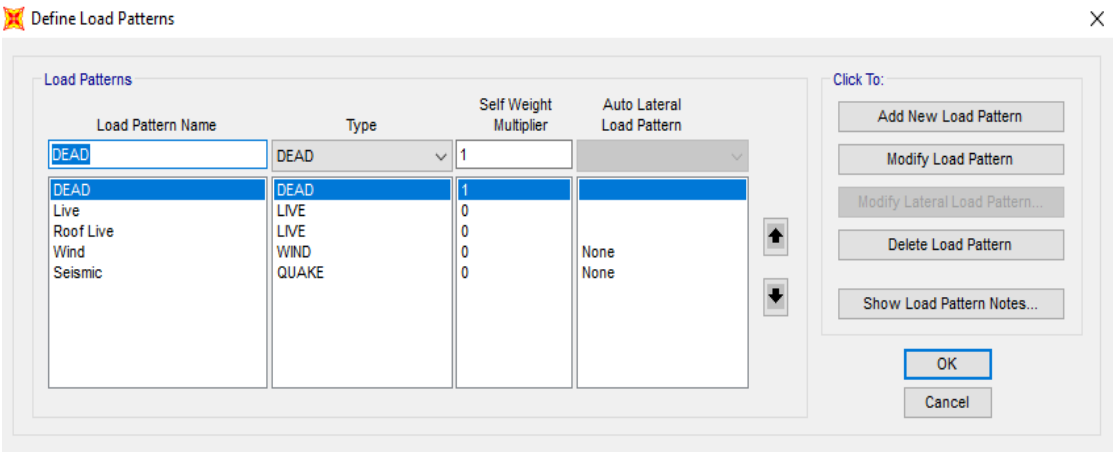

Figure 3.28. Assigned gravity loads and lateral forces load patterns in SAP2000.

The lateral forces assigned on the 3D frame of the building with the selected frame for the wind load Case 1 and as well as the seismic load can be seen in the Figures 3.29-3.30 below.

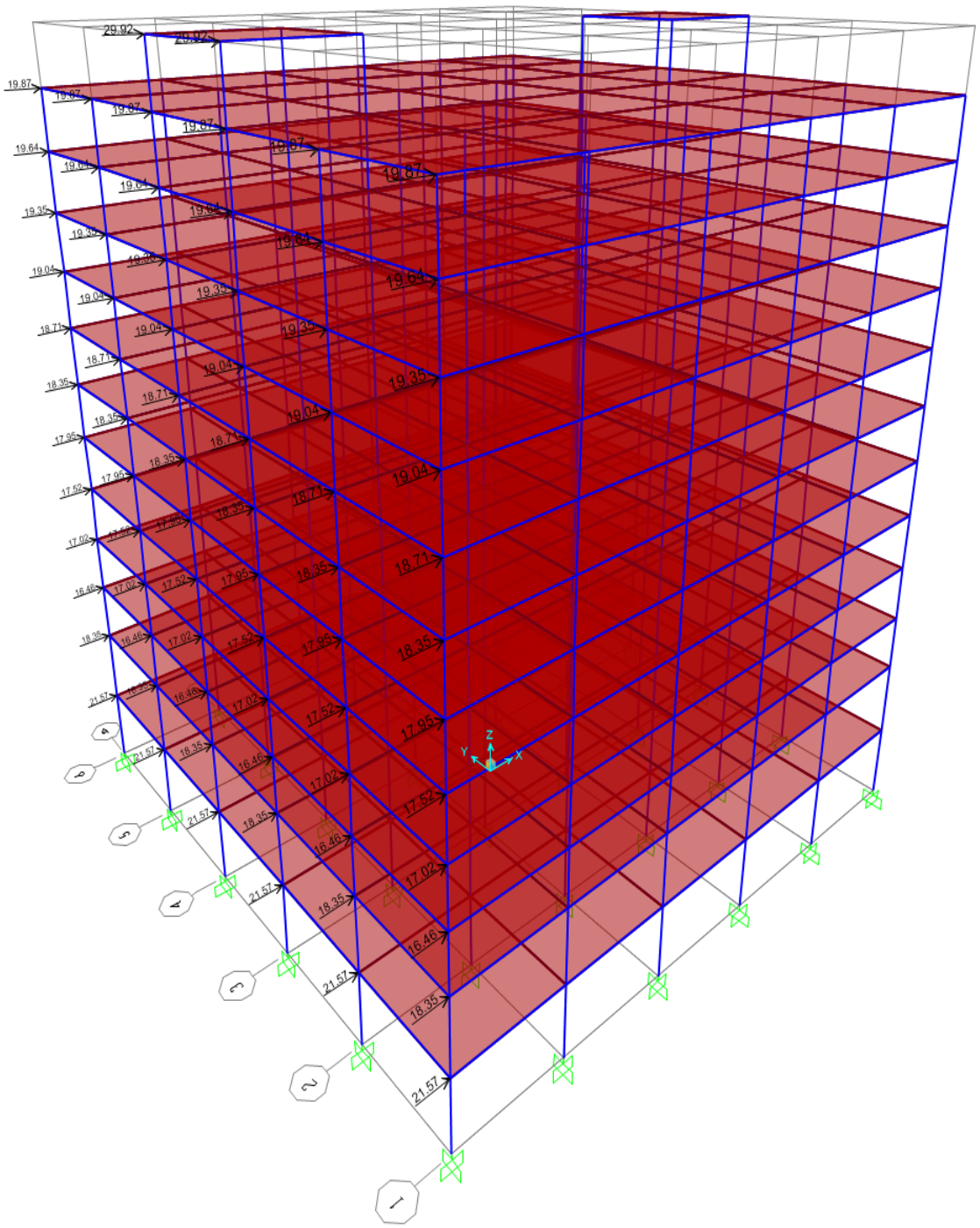

Figure 3.29. SAP2000: Assigned lateral forces for Case 1 wind loads on 3D frame.

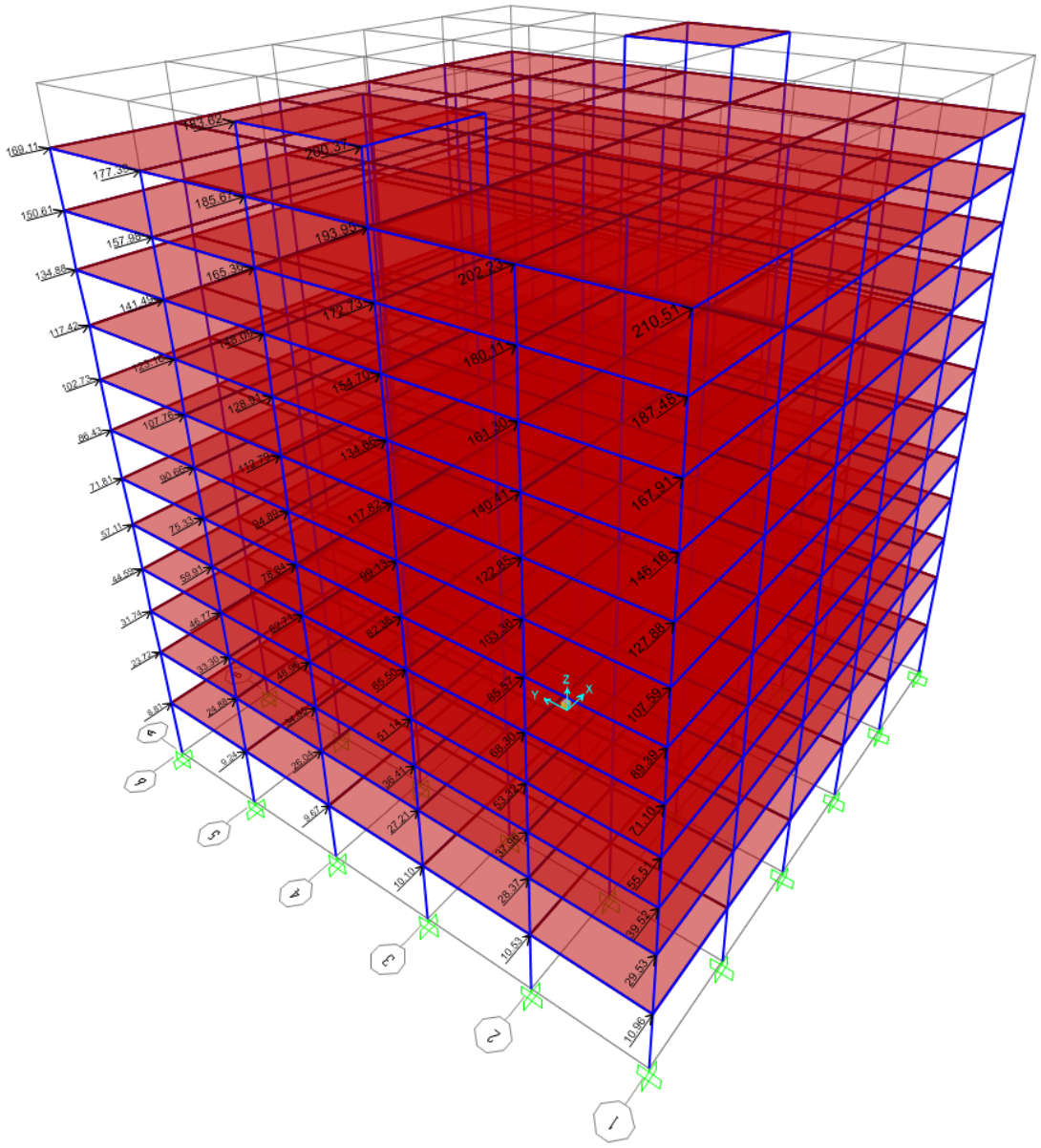

Figure 3.30. SAP2000: Assigned lateral forces for seismic loads on 3D frames.

3.4 Lateral Drift Analysis

3.4.1 Wind Drift Calculations

Table 3.21. Shear drift calculations

Story	h_i (mm)	Vavg (kN)	dt (mm)	Interstory (mm)	Absolute (mm)
13	3000	4.99	1.05	1.75	26.31
12	3000	6.64	1.40	1.75	24.56
11	3000	9.94	2.09	1.89	22.82
10	3000	13.19	1.68	1.67	20.93
9	3000	16.39	1.66	1.61	19.26
8	3000	19.53	1.56	1.59	17.65
7	3000	22.62	1.61	1.67	16.07
6	3000	25.64	1.73	1.79	14.40
5	3000	28.60	1.85	1.87	12.61
4	3000	31.48	1.89	1.93	10.74
3	3000	34.27	1.98	2.89	8.81
2	4000	37.17	3.80	3.91	5.92
1	4000	40.50	4.03	2.01	2.01

To calculate these drifts, first of all, the wind force per each floor was calculated. Then with the wind force, the acting force of V was determined. It is the summation of the wind force of the floor being calculated and the floor above. Then force per each frame was calculated. Since our building is square shaped, both longitudinal and transverse calculations are equal. To find the average force acting on the floor, we summed the force per frame of the above floor and the floor being

considered and then divided by 2. Then by using moments of inertia of columns and beams that we have calculated before, we used the formula for the drifts and got these results presented in Table 3.21.

Table 3.22. Flexural wind drift calculations

Story	M (N-mm)	a=b (m)	A (mm2)	Dqi (rad)	q_i (rad)	Interstory (mm)	Absolute (mm)
13	8.98E7	0.3	90000	1.64E-7	1.55E-5	0.05	0.41
12	2.39E8	0.3	90000	4.38E-7	1.54E-5	0.05	0.37
11	4.47E8	0.3	90000	8.19E-7	1.49E-5	0.04	0.32
10	7.14E8	0.4	160000	7.35E-7	1.41E-5	0.04	0.28
9	1.04E9	0.4	160000	1.07E-6	1.34E–5	0.04	0.23
8	1.42E9	0.5	250000	9.34E-7	1.23E-5	0.04	0.19
7	1.85E9	0.5	250000	1.22E-6	1.14E-5	0.03	0.16
6	2.34E9	0.55	302500	1.27E-6	1.01E-5	0.03	0.12
5	2.88E9	0.55	302500	1.57E-6	8.86E-6	0.03	0.09
4	3.47E9	0.65	422500	1.35E-6	7.3E-6	0.02	0.07
3	4.11E9	0.65	422500	1.60E-6	5.94E-6	0.02	0.04
2	5.04E9	0.75	562500	1.97E-6	4.34E-6	0.02	0.03
1	6.06E9	0.75	562500	2.37E-6	2.37E–6	0.01	0.01

We calculated the flexural wind drift to understand how the structure responds to lateral wind forces. To determine the interstory drift, we multiplied the height of each

floor by q_i (rad), which represents the rotational displacement at that level. This helps us assess how much the building shifts under wind loads and ensure it stays within safe limits. In order to get the total drift, the following equation was used:

$$Total\ drift\ =\ Shear\ Drift\ +\ Flexural\ Drift \quad [75]$$

3.4.2 Seismic Drift Calculations

By doing almost the same procedure, the following two tables for seismic drift were constructed.

Table 3.23. Shear Seismic Drift Calculations

Story	h_i (mm)	Vavg (kN)	dt (mm)	Interstory (mm)	Absolute (mm)
13	3000	32.00	2.97	8.00	171.96
12	3000	47.82	10.07	13.22	163.95
11	3000	77.72	16.37	14.84	150.73
10	3000	104.42	13.31	13.13	135.89
9	3000	128.02	12.95	12.41	122.76
8	3000	148.61	11.87	11.86	110.35
7	3000	166.31	11.84	12.01	98.50
6	3000	181.11	12.19	12.33	86.48
5	3000	193.17	12.48	12.33	74.15
4	3000	202.68	12.17	12.14	61.82
3	3000	209.82	12.11	17.03	49.68
2	4000	215.01	21.95	21.81	32.65
1	4000	218.05	21.67	10.84	10.84

Table 3.24. Flexural Seismic Drift Calculations

Story	M (N-mm)	a=b (m)	A (mm2)	Dqi (rad)	q_i (rad)	Interstory (mm)	Absolute (mm)
13	5.76E08	0.3	90000	1.05E-06	1.11E-04	0.33	2.89
12	1.72E09	0.3	90000	3.15E-06	1.09E-04	0.33	2.56
11	3.37E09	0.3	90000	6.18E-06	1.06E-04	0.32	2.23
10	5.48E09	0.4	160000	5.64E-06	1.00E-04	0.30	1.91
9	7.98E09	0.4	160000	8.22E-06	9.45E-05	0.28	1.61
8	1.08E10	0.5	250000	7.14E-06	8.63E-05	0.26	1.33
7	1.40E10	0.5	250000	9.21E-06	7.91E-05	0.24	1.07
6	1.74E10	0.55	302500	9.45E-06	6.99E-05	0.21	0.83
5	2.09E10	0.55	302500	1.14E-05	6.05E-05	0.18	0.62
4	2.46E10	0.65	422500	9.61E-06	4.91E-05	0.15	0.44
3	2.85E10	0.65	422500	1.11E-05	3.95E-05	0.12	0.29
2	3.37E10	0.75	562500	1.32E-05	2.84E-05	0.11	0.17
1	3.89E10	0.75	562500	1.52E-05	1.52E-05	0.06	0.06

3.4.3. Comparison of lateral drifts for hand, 2D and 3D SAP2000 Calculations

The following two figures show the lateral drifts for hand, 2D and 3D Model for the load cases between wind and seismic loads. The wind drift comparison shows that the 2D SAP2000 model and hand calculations align closely, whereas the 3D model deviates slightly. The problem can be in differences of how wind loads were applied in the 3D model. Even though there are some differences, they are considerably small so it

can be neglected. In case of seismic drift, all of the three methods produce similar results in the range of 10-20 mm. Additionally, it is important to note that all drift values fall within allowable limits, making sure that the office building meets design requirements.

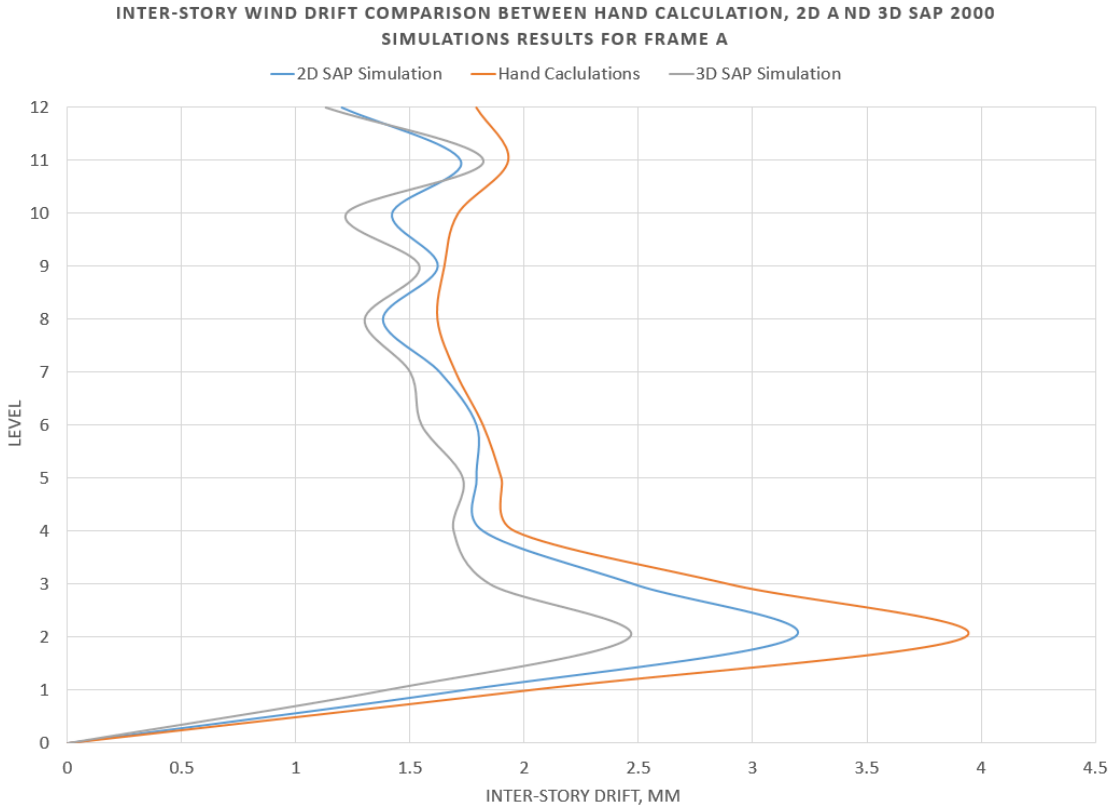

Figure 3.31. Internal forces for Frame A under Wind load condition

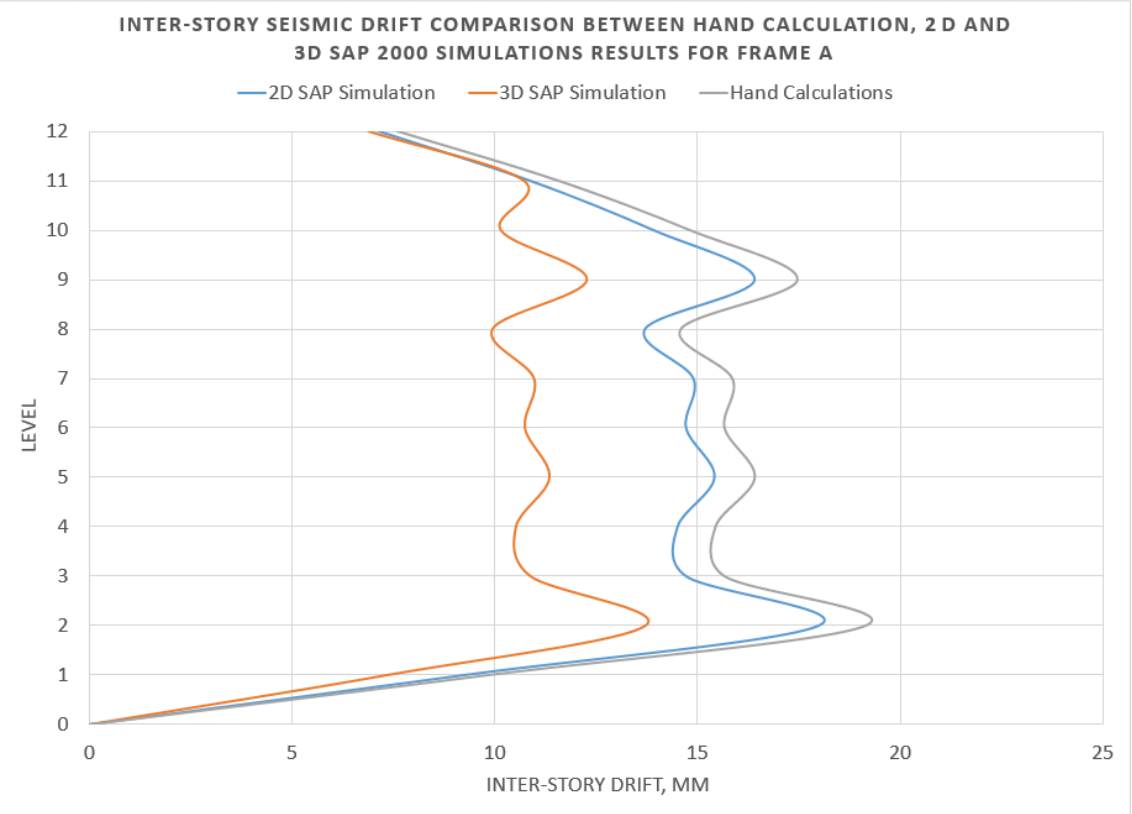

Figure 3.32. Internal forces for Frame A under Seismic load condition

3.4.4 Amplified inter-story seismic drift

Elastic story drift values from linear dynamic analysis need amplification through deflection amplification factor C_d in accordance with ASCE 7-16 Section 12.8.6 to reflect inelastic seismic behavior. The factor modifies elastic drifts to better represent the predicted inelastic deformation during design-level seismic forces.

To find the amplified interstory drift following equation will be used:

$$\Delta_s = C_d \times \Delta_e \qquad [76]$$

where,

$\Delta_s - amplified\ seismic\ inter\ -\ story\ drift\ (mm)$

$\Delta_e - elastic\ seismic\ inter\ -\ story\ drift\ (mm)$

$C_d - deflection\ amplification\ factor\ (C_d = 5.5\ according\ to\ the\ ASCE\ 7-16)$

The amplified drift values obtained through this process are analyzed against existing allowable drift levels.

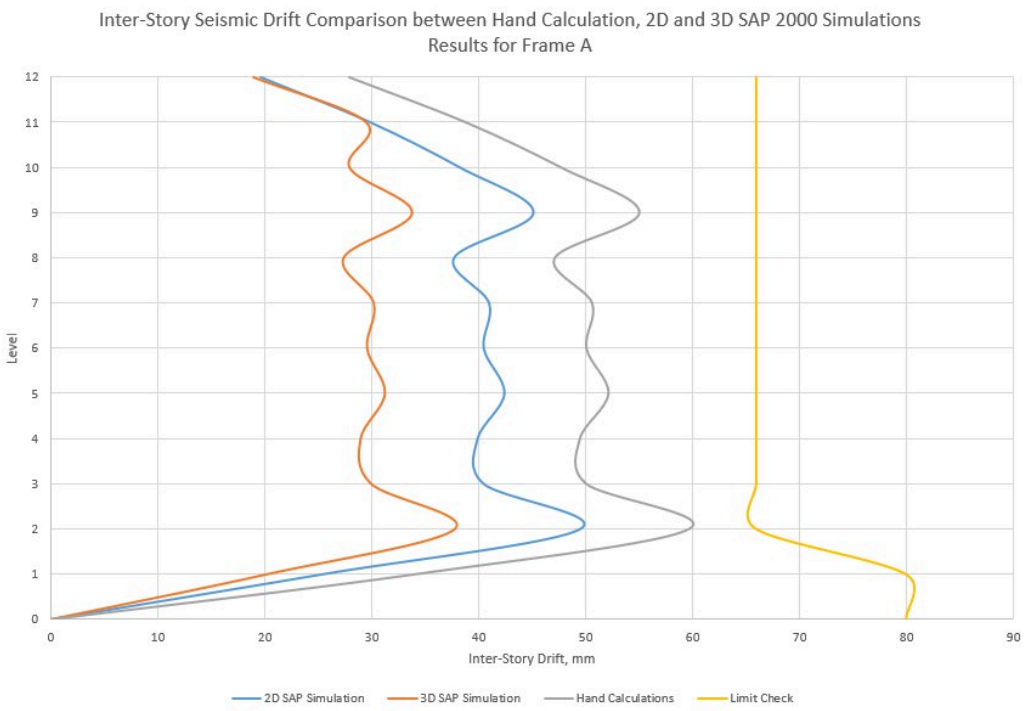

Figure 3.33 Inter-story seismic drift with limit checks.

The figure 3.33 demonstrates that all drift values from amplification stay within acceptable parameters according to code specifications.

3.4.5 Stability analysis

Seismic drift calculations use the stability coefficient to assess if second-order P-Δ effects can be ignored in accordance with ASCE 7-16 Section 12.8.7. The coefficient measures vertical load effects influenced through lateral displacements using the following formula:

$$\theta = \frac{P_x \Delta I_e}{V_x h_{ss} C_d} \qquad [77]$$

where,

$P_x -$ *total vertical design load* (kN)

$\Delta -$ *design story drift* (mm)

$I_e -$ *importance factor*

$V_x -$ *seismic shear force* (kN)

$h_{ss} -$ *story height* (mm)

$C_d -$ *deflection amplification factor*

The guideline of ASCE 7-16 allows neglecting P–Δ second-order effects when

stability coefficients stay below 0.1. The calculations for the selected frame can be seen below on Table 3.25.

Table 3.25. Stability coefficient calculations for selected Frame A

	Shear (mm)		Flexural (mm)		Total (mm)		$V_u\,(kN)$	$P_u\,(kN)$	θ
Story	Inter-story	Absolute	Inter-story	Absolute	Inter-story	Absolute			
13	8.00	171.96	0.33	2.890	8.33	174.85	768.0	11525.9	0.0076
12	13.22	163.95	0.33	2.559	13.55	166.51	1527.2	23051.8	0.0124
11	14.84	150.73	0.32	2.230	15.16	152.96	2203.4	34577.6	0.0144
10	13.13	135.89	0.30	1.911	13.43	137.80	2809.0	46103.5	0.0134
9	12.41	122.76	0.28	1.611	12.69	124.37	3336.1	57629.4	0.0133
8	11.86	110.35	0.26	1.328	12.12	111.68	3797.3	69155.3	0.0134
7	12.01	98.50	0.24	1.069	12.25	99.56	4185.4	80681.2	0.0143
6	12.33	86.48	0.21	0.831	12.54	87.31	4507.8	92207.0	0.0156
5	12.33	74.15	0.18	0.621	12.51	74.77	4764.2	103732.9	0.0165
4	12.14	61.82	0.15	0.440	12.29	62.26	4964.4	115258.8	0.0173
3	17.03	49.68	0.12	0.293	17.15	49.97	5106.9	126784.7	0.0258
2	21.81	32.65	0.11	0.174	21.93	32.82	5213.4	138310.6	0.0264
1	10.84	10.84	0.06	0.061	10.90	10.90	5252.9	154066.4	0.0145

The stability coefficient obtained for the frame demonstrates values lower than the established threshold of 0.1. The effects of P–Δ become insignificant enough to disregard them in structural drift analysis.

3.4.6 Irregularities check

The building received evaluation for seismic performance compliance by following the criteria established in ASCE 7-16 Table 12.3-1 for vertical and horizontal irregularity assessments.

The maximum and average story drifts were compared throughout the structure to perform its torsional irregularity check. The presence of torsional irregularity gets confirmed when the ratio surpasses 1.2. The ratios that appeared in Table 3.26. demonstrated values below 1.2 thus indicating no presence of torsional irregularities.

Table 3.26. Torsional irregularity check

Level	Ratio
12	1.184
11	1.171
10	1.167
9	1.115
8	1.092
7	1.062
6	0.893
5	0.742
4	0.590
3	0.461
2	0.328
1	0.245

The evaluation checked distribution patterns of deflection and stiffness to detect

soft story or stiffness irregularities. The analysis revealed negligible differences thus confirming that seismic forces produce no vertical irregularities within the structure.

3.4.7 Internal Forces Calculations

Figures 3.34 through 3.37 showcase the internal forces determined through SAP2000 software for the selected frame under various loading conditions.

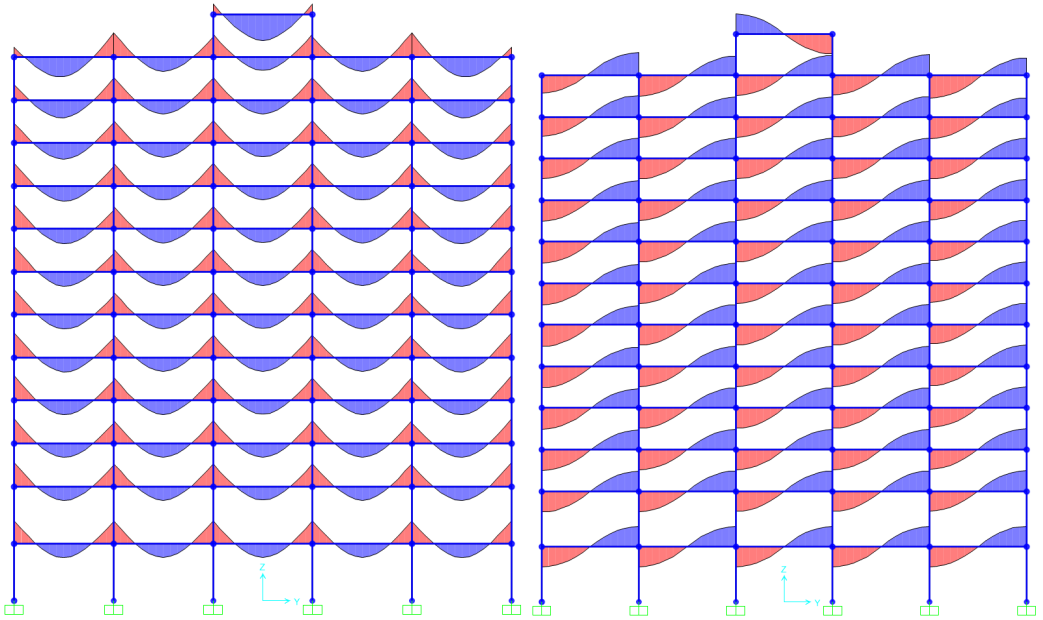

Figure 3.34 SAP2000: Moment and shear force diagram for dead load.

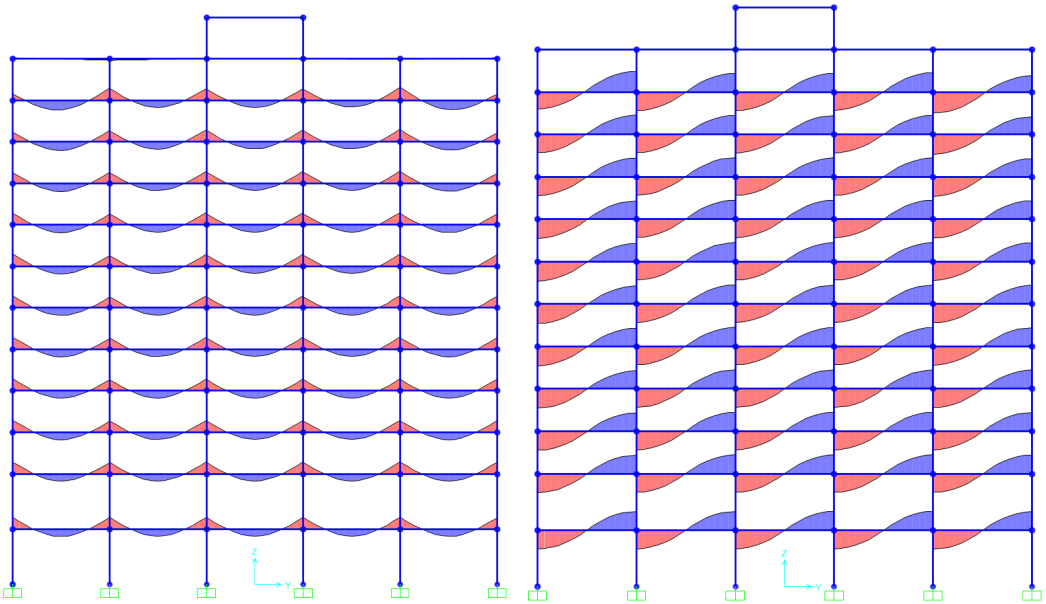

Figure 3.35 SAP2000: Moment and shear force diagram for live load.

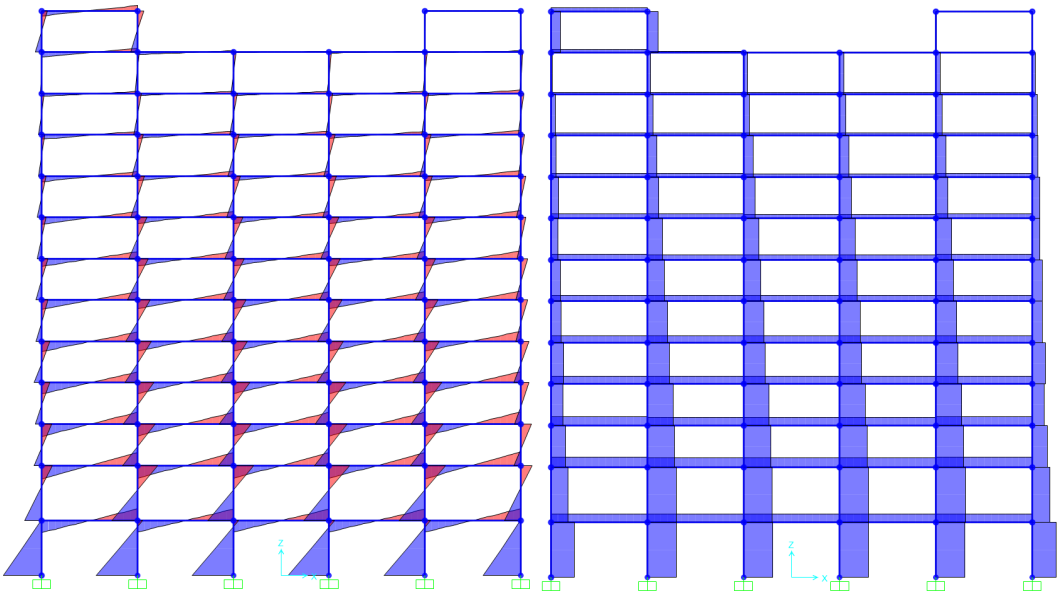

Figure 3.36 SAP2000: Moment and shear force diagram for wind load.

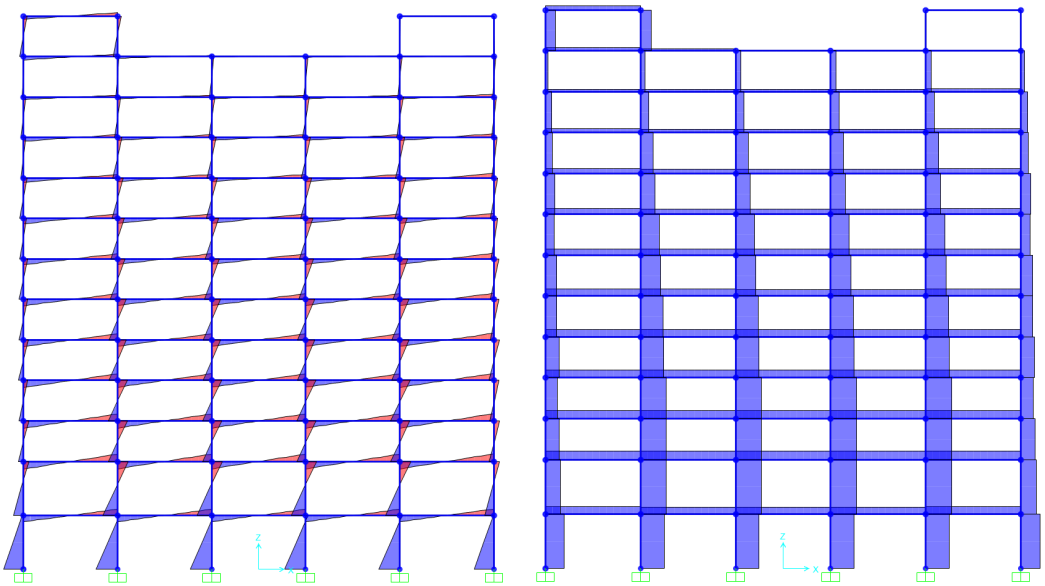

Figure 3.37 SAP2000: Moment and shear force diagram for seismic load.

Internal forces verifications under Dead load

In order to calculate the internal forces under the dead load, the approximate analysis was performed. Inflection point was taken as 0.1L to calculate all internal

forces. Arrangement of loads for internal beams and arrangement for approximate analysis method are presented in next figures.

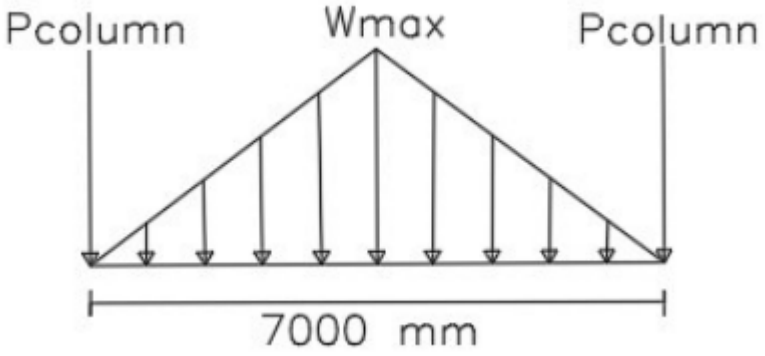

Figure 3.38 Load arrangement.

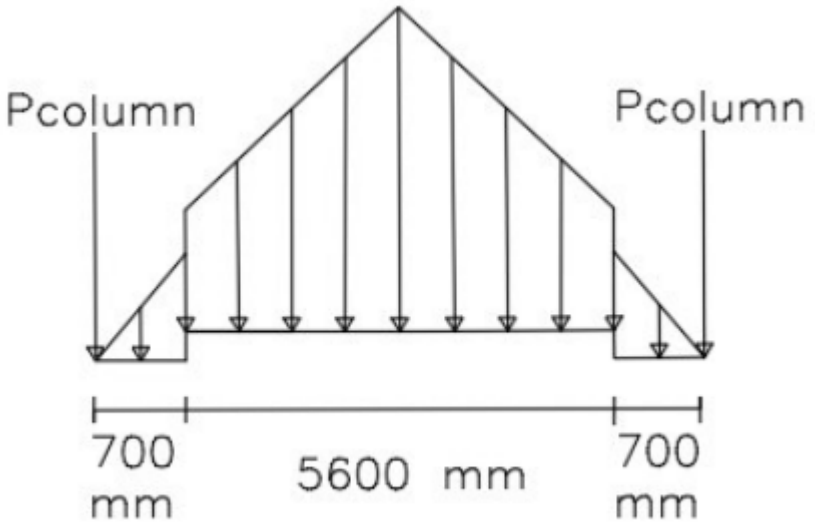

Figure 3.39 Approximate analysis method load arrangement.

Here 700 mm is 0.1L, where L is the span length which is equal to 7000 mm.

3.4.8 Comparison Internal force results for 2D, 3D and Hand calculations under Dead load

From the following Figure 3.40, it can be noted that the hand calculations and the 2D SAP2000 model give pretty similar axial force values, whereas the 3D SAP2000 model displays considerably lower results in comparison with those two. This might happen due to the fact that in the 3D model, the loads are spread across all the frames

and structural elements, which lead to each individual column carrying a less force. However in a real building, all the structural elements interact and share the applied loads altogether, rather than acting separately. On the other hand, the 2D model focuses on just one frame, making it behave more like a hand calculation, which does not consider how the entire structure distributes the forces.

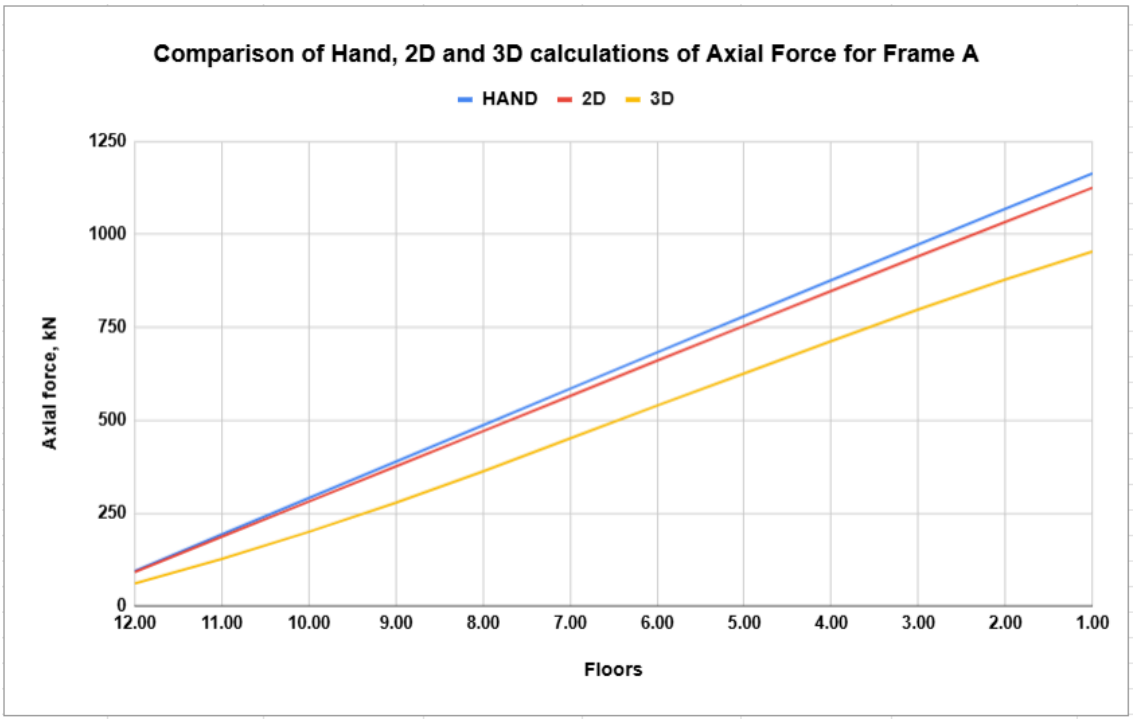

Figure 3.40 Internal forces for Frame A under dead load conditions: Axial force.

In case of shear forces, the values are reasonably similar between the 2D SAP2000 model and the hand computations, however there are notable changes in the 3D model. This occurs most likely due to uneven distribution of gravity loads applied to the whole system and structural elements. The inconsistent pattern may also indicate that the distribution of shear forces is being influenced by variations in stiffness. Another explanation for this can be improper configuration of the boundary conditions or diaphragm limits in SAP2000 software.

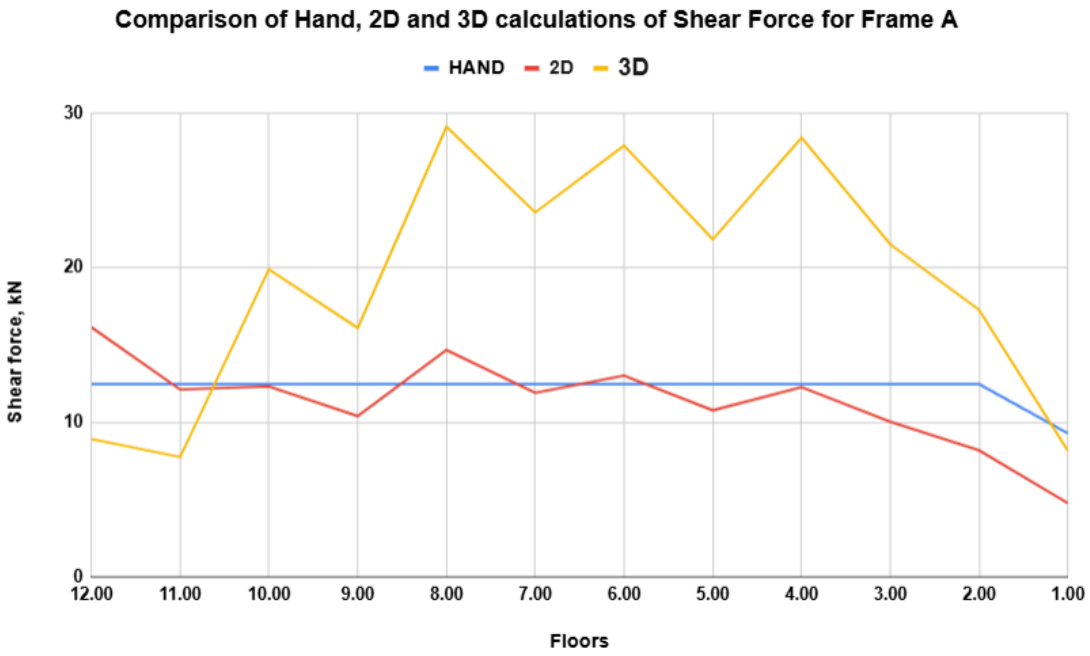

Figure 3.41 Internal forces for Frame A under dead load conditions: Shear force.

Next, regarding the bending moment reactions, the hand calculation was the most consistent, while the 2D results showed a slight decrease in moment values. Similarly with axial and shear forces the 3D model has some certain deviations, with some stories going through some bursts. This shows that the 3D model is taking into account other effects that the 2D model considers. It might be due to torsion, stiffness variations, and interactions between structural elements.

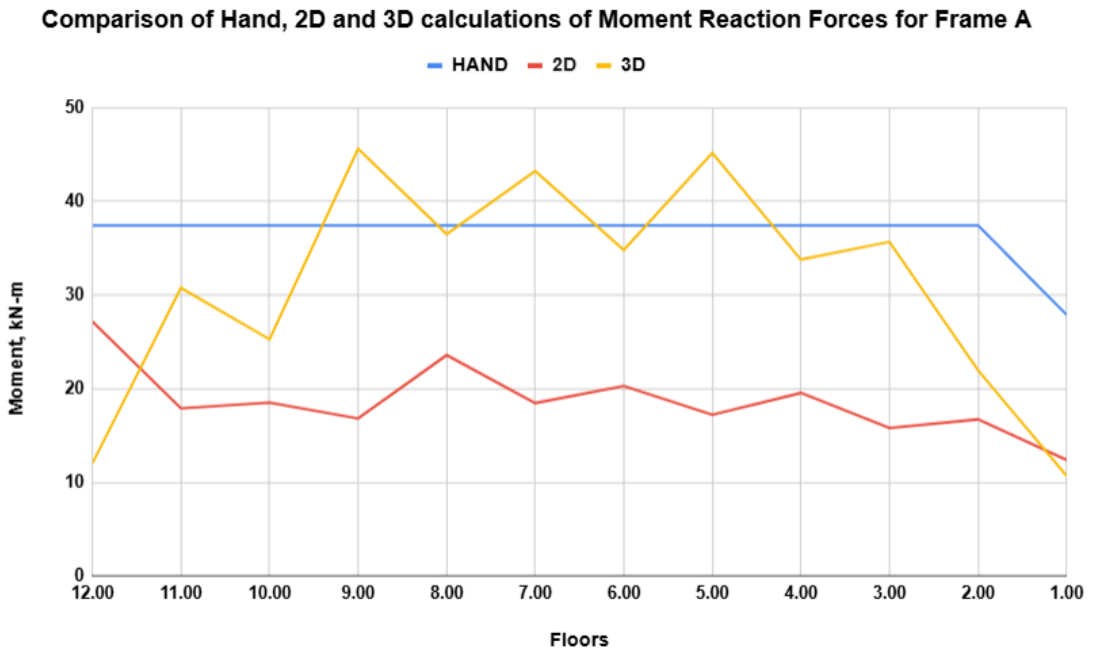

Figure 3.42. Internal forces for Frame A under dead load conditions: Moment diagram.

3.4.9 Internal forces verifications under Wind load

For the hand calculations of internal forces under wind load, the Portal Frame method was used. The following assumptions were made to use the Portal Frame method:

- A hinge is placed at the center of each girder because we assume that's where the moment is zero.
- Similarly, a hinge is placed at the center of each column, since we assume the moment there is also zero.
- At each floor level, the shear force at the interior column is twice as much as at the exterior column hinges, because we treat the frame as a combination of portals.

The results for all floors are given in the table below. The hand calculations are presented in Appendix A.

Table 3.27. The hand calculations results of internal forces under wind load

	Internal Column			External Column		
Story	Axial Force (kN)	Shear Force (kN)	Internal Moment (kN-m)	Axial Force (kN)	Shear Force (kN)	Internal Moment (kN-m)
13	0.00	5.98	8.98	-1.28	2.99	4.49
12	0.00	9.96	14.94	-4.70	4.98	7.47
11	0.00	13.89	20.83	-9.81	6.94	10.42
10	0.00	17.76	26.64	-16.59	8.88	13.32
9	0.00	21.57	32.35	-25.02	10.78	16.18
8	0.00	25.31	37.96	-35.06	12.65	18.98
7	0.00	28.98	43.47	-46.69	14.49	21.73
6	0.00	32.57	48.85	-59.88	16.28	24.43
5	0.00	36.07	54.11	-74.59	18.04	27.05
4	0.00	39.48	59.22	-90.78	19.74	29.61
3	0.00	42.77	64.15	-108.41	21.38	32.08
2	0.00	46.44	92.88	-133.90	23.22	46.44
1	0.00	50.76	101.51	-161.67	25.38	50.76

The following 3 figures are comparisons of 2D, 3D and Hand calculations of Axial, Shear Forces and Moments under the wind load. The hand calculations, 2D, and 3D SAP2000 models show similar results for axial, shear, and moment forces under wind load, meaning the lateral force-resisting system (LFRS) is working well. Axial forces align well, indicating that loads are distributed evenly. Shear forces exhibit a

similar pattern with only slight variations, indicating that the lateral loads are being transmitted appropriately. Moment forces rise as anticipated close to the base, and every method observes this trend. In general, the findings suggest that diaphragm modeling, boundary conditions, and structural interactions were managed effectively, resulting in reliable force distribution.

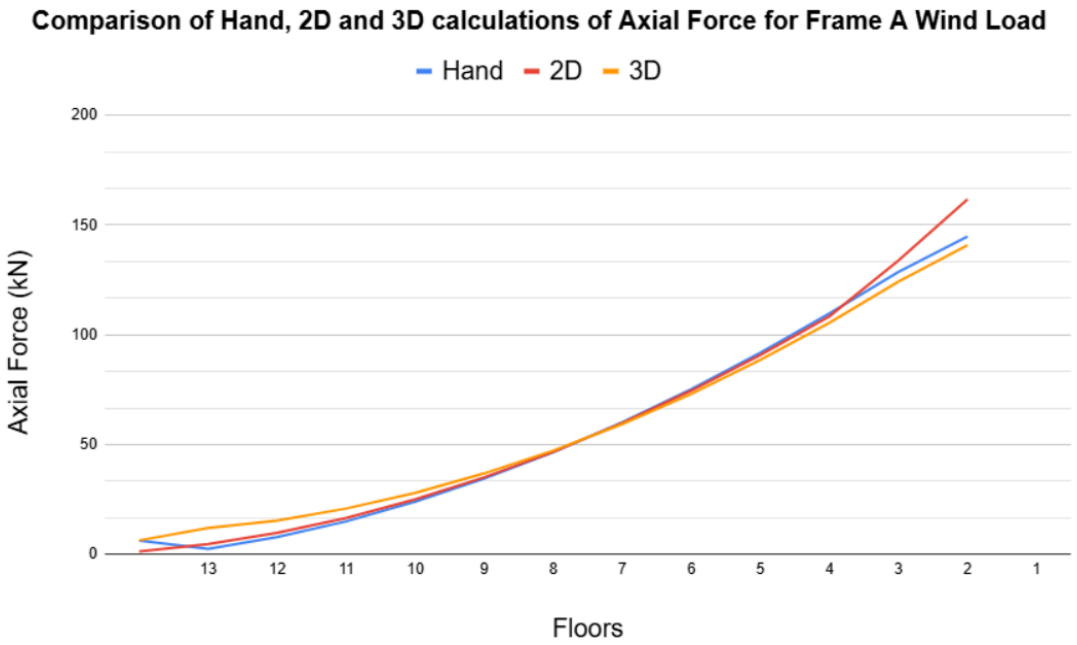

Figure 3.43 Internal forces for Frame A under wind load conditions: Axial force.

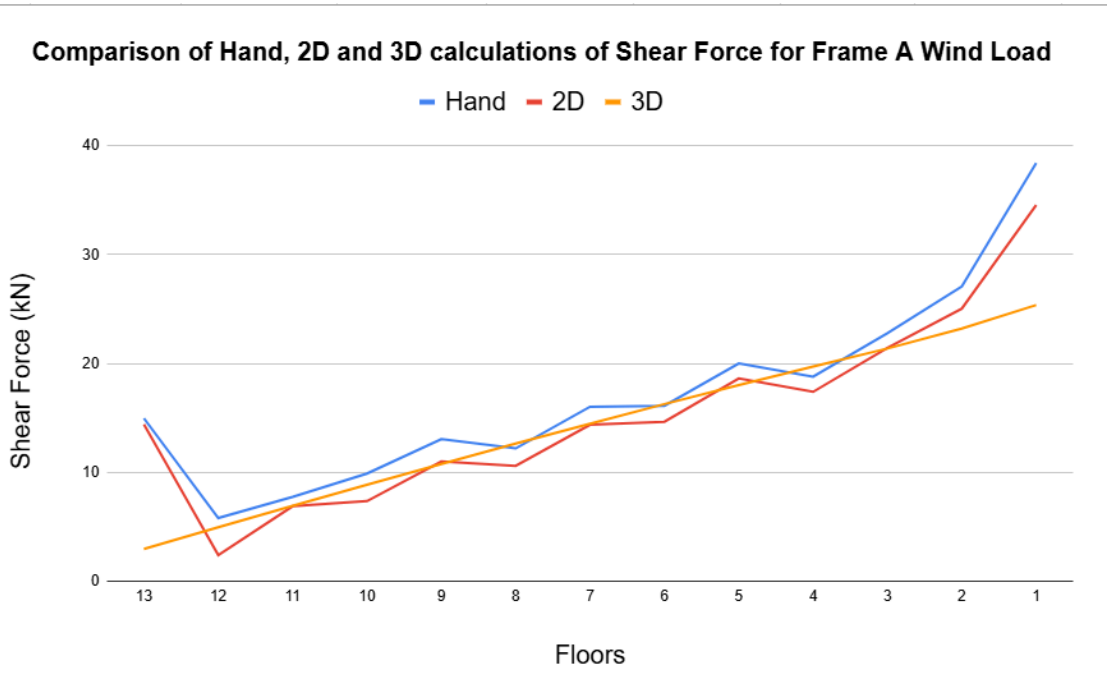

Figure 3.44 Internal forces for Frame A under wind load conditions: Shear force.

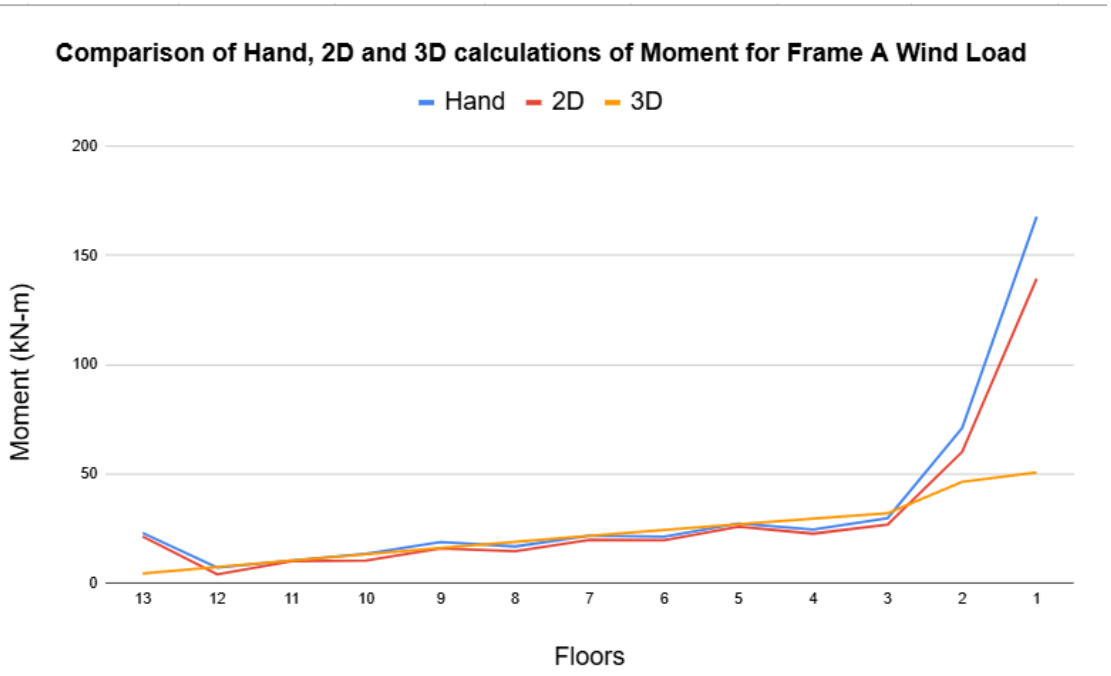

Figure 3.45 Internal forces for Frame A under wind load conditions: Moment diagram.

3.5 Structural Design

3.5.1 Structural member design using SAP2000

Structural building design work was accomplished through SAP2000 software. The software tool enables instant structural analysis while determining the necessary reinforcement ratios that follow the ACI 318 standard. The programming environment of SAP2000 enabled the entire design process to run in the software at once. A complete manual verification of essential results took place in the following hand calculations for the structural member design section. Figure 3.46 presents the outcome of the design process.

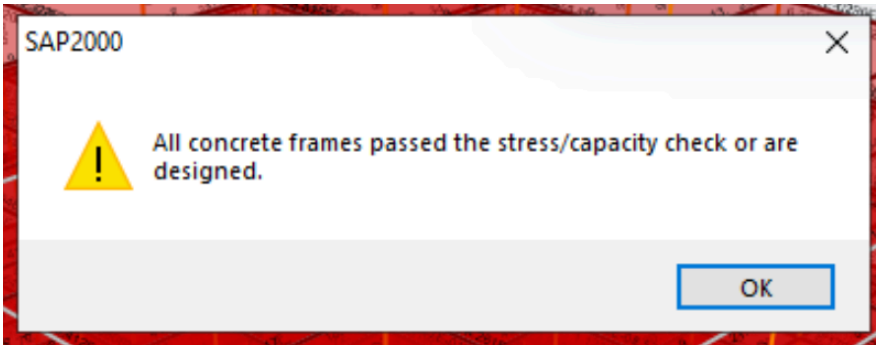

Figure 3.46 The structural design check in SAP2000 software.

3.5.1.1 Major Beams

To design major beams, the critical positive and negative moments were considered since our building is subject to seismic forces. Both these values were taken from the critical load combinations. For each floor, the beam with the highest moment values was selected from SAP2000 software. All these SAP2000 figures presented in Appendix D.

As an example below, I will provide the critical moment values of the second floor beam.

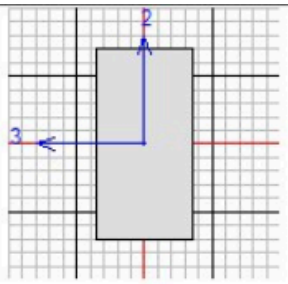

ACI 318-14 BEAM SECTION DESIGN Type:Sway Special Units: KN, m, C (Summary)

Element : 66	D=0.700	B=0.350	bf=0.350
Section ID : Major Beam	ds=0.000	dct=0.060	dcb=0.060
Combo ID : DCON8	E=29725410.0	fc=40000.000	Lt.Wt. Fac.=1.000
Station Loc : 0.000	L=7.000	fy=420000.000	fys=420000.000

Phi(Bending):	0.900
Phi(Shear):	0.750
Phi(Seis Shear):	0.600
Phi(Torsion):	0.750

Design Moments, M3

Positive Moment	Negative Moment	Special +Moment	Special -Moment
236.539	-473.077	236.539	-473.077

Flexural Reinforcement for Moment, M3

	Required Rebar	+Moment Rebar	-Moment Rebar	Minimum Rebar
Top (+2 Axis)	0.002	0.000	0.002	8.403E-04
Bottom (-2 Axis)	0.001	0.001	0.000	8.403E-04

Shear Reinforcement for Shear, V2

Rebar Av/s	Shear Vu	Shear phi*Vc	Shear phi*Vs	Shear Vp
0.001	258.886	0.000	258.886	136.402

Reinforcement for Torsion, T

Rebar At/s	Rebar Al	Torsion Tu	Critical Phi*Tcr	Area Ao	Perimeter Ph
0.000	0.000	0.766	44.909	0.136	1.744

Figure 3.47 Major beam design values of the 2nd floor beam from SAP2000.

3.5.1.2 Columns

In the same way, the values for columns were taken from SAP2000.

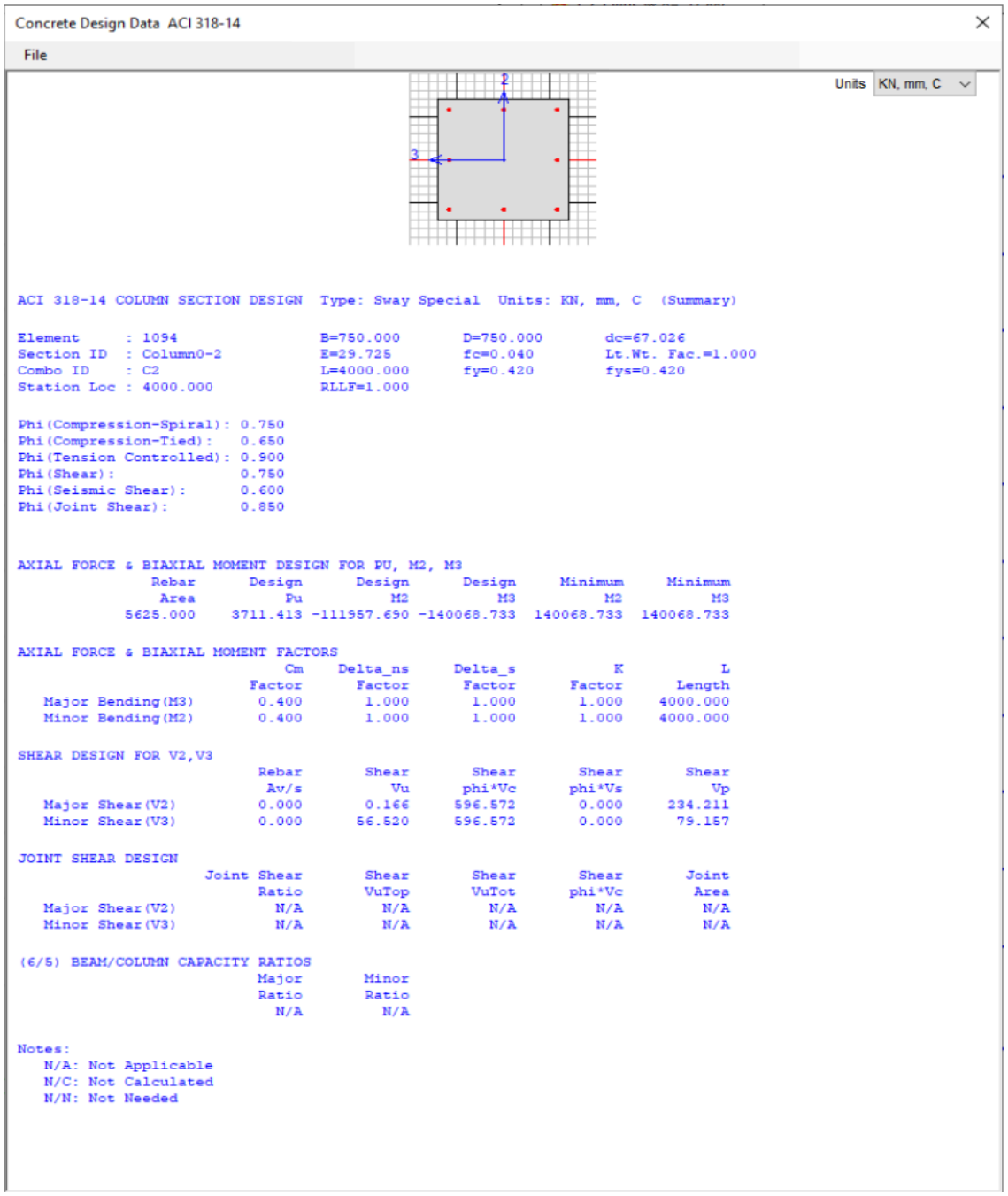

Concrete Design Data ACI 318-14

File

Units KN, mm, C

ACI 318-14 COLUMN SECTION DESIGN Type: Sway Special Units: KN, mm, C (Summary)

Element	: 1094	B=750.000	D=750.000	dc=67.026
Section ID	: Column0-2	E=29.725	fc=0.040	Lt.Wt. Fac.=1.000
Combo ID	: C2	L=4000.000	fy=0.420	fys=0.420
Station Loc	: 4000.000	RLLF=1.000		

Phi(Compression-Spiral):	0.750
Phi(Compression-Tied):	0.650
Phi(Tension Controlled):	0.900
Phi(Shear):	0.750
Phi(Seismic Shear):	0.600
Phi(Joint Shear):	0.850

AXIAL FORCE & BIAXIAL MOMENT DESIGN FOR PU, M2, M3

Rebar Area	Design Pu	Design M2	Design M3	Minimum M2	Minimum M3
5625.000	3711.413	-111957.690	-140068.733	140068.733	140068.733

AXIAL FORCE & BIAXIAL MOMENT FACTORS

	Cm Factor	Delta_ns Factor	Delta_s Factor	K Factor	L Length
Major Bending(M3)	0.400	1.000	1.000	1.000	4000.000
Minor Bending(M2)	0.400	1.000	1.000	1.000	4000.000

SHEAR DESIGN FOR V2,V3

	Rebar Av/s	Shear Vu	Shear phi*Vc	Shear phi*Vs	Shear Vp
Major Shear(V2)	0.000	0.166	596.572	0.000	234.211
Minor Shear(V3)	0.000	56.520	596.572	0.000	79.157

JOINT SHEAR DESIGN

	Joint Shear Ratio	Shear VuTop	Shear VuTot	Shear phi*Vc	Joint Area
Major Shear(V2)	N/A	N/A	N/A	N/A	N/A
Minor Shear(V3)	N/A	N/A	N/A	N/A	N/A

(6/5) BEAM/COLUMN CAPACITY RATIOS

Major Ratio	Minor Ratio
N/A	N/A

Notes:
N/A: Not Applicable
N/C: Not Calculated
N/N: Not Needed

Figure 3.48 Column values taken from SAP2000 software.

3.5.1.3 Two-way slab

SAP2000 software does not provide detailed information about the reinforcement of the slab, thus, the design of the reinforcement will be performed by hand.

3.5.2 Hand Calculations for structural member design.

3.5.2.1 Major Beams

As it was mentioned above, there will be two different calculations for negative and positive moments. Values will be taken from Figure 3.47.

Negative moment calculations

$$M_u = 473.1\ kN - m$$

$$b = 350\ mm,\ h = 700\ mm,\ d = 700 - 2.5 * 25.4\ mm = 636.5\ mm$$

$$f'_c = 40\ MPa;\ f_y = 420\ MPa$$

$$R_n = \frac{M_u}{\Phi bd^2} = 3335.77\ kN/m^2$$

$$\rho = \frac{0.85f'_c}{f_y}\left[1 - \sqrt{1 - \frac{2R_n}{0.85f'_c}}\right] = 0.0084$$

$$A_s = \rho bd = 0.0084 * 350 * 636.5 = 1865.873\ mm^2$$

$$A_s f_y = 0.85f'_c ab$$

$$a = \frac{A_s f_y}{0.85f'_c b} = 65.85\ mm$$

$$\beta_1 = 0.85 - 0.05\left(\frac{5801-4000}{1000}\right) = 0.76$$

$$c = \frac{a}{\beta_1} = 86.66\ mm$$

$$\varepsilon_t = 0.003\left(\frac{d-c}{c}\right) = 0.003\left(\frac{636.5-86.66}{86.66}\right) = 0.019 > 0.005$$

$$\varepsilon_t > 0.005 \rightarrow tension\ controlled\ and\ ductile$$

Hand calculated A_s is different from the value of SAP2000, that is why the error should be also calculated. The A_s value of SAP2000 is $0.002\ m^2$ which is equal to $2000\ mm^2$.

$$Error = \frac{2000-1865.873}{2000} * 100\% = 6.7\%$$

At first it can be seen as a huge error, but in fact it is not. The difference can be explained by the concrete cover assumptions and also the software calculates both compression and tension reinforcements. Next we can calculate the minimum steel area.

$$A_{s,\,min} = 3\sqrt{f'_c}bd/f_y \geq 200bd/f_y = 835.62\,mm^2 \geq 731.42\,mm^2$$

$$A_s = 2000\,mm^2 > 835.62\,mm^2 \rightarrow sufficient\ reinforcement$$

Based on above calculations, we can use the SAP2000 area values for all beams since the error is not too big and all areas are more than minimum steel area. For this case, 12th floor beams, $A_s = 2000\,mm^2$ ($3\,in^2$) will be used for the bar selection. At the negative moment locations, 3#9 bars ($A_s = 3\,in^2$) will be used for 2nd floor beams.

Positive moment calculations

$$M_u = 236.539\,kN - m$$

$$b = 350\,mm,\ h = 700\,mm,\ d = 700 - 2.5 * 25.4\,mm = 636.5\,mm$$

$$f'_c = 40\,MPa;\ f_y = 420\,MPa$$

$$R_n = \frac{M_u}{\Phi bd^2} = 1668.16\,kN/m^2$$

$$\rho = \frac{0.85f'_c}{f_y}\left[1 - \sqrt{1 - \frac{2R_n}{0.85f'_c}}\right] = 0.004$$

$$A_s = \rho bd = 0.004 * 350 * 636.5 = 907.66\,mm^2$$

$$A_s f_y = 0.85f'_c ab$$

$$a = \frac{A_s f_y}{0.85f'_c b} = 32\,mm$$

$$\beta_1 = 0.85 - 0.05\left(\frac{5801-4000}{1000}\right) = 0.76$$

$$c = \frac{a}{\beta_1} = 42.15mm$$

$$\varepsilon_t = 0.003\left(\frac{d-c}{c}\right) = 0.003\left(\frac{636.5-42.15}{42.15}\right) = 0.042 > 0.005$$

$$\varepsilon_t > 0.005 \rightarrow tension\ controlled\ and\ ductile$$

Hand calculated A_s is different from the value of SAP2000, that is why the error should be also calculated. The A_s value of SAP2000 is $1000\ mm^2$.

$$Error = \frac{1000-907.66}{1000} * 100\% = 9.23\%$$

The same explanation as in negative moments can be applied to this case also. Next we can calculate the minimum steel area.

$$A_{s,min} = 3\sqrt{f'_c}bd/f_y \geq 200bd/f_y = 835.62\ mm^2 \geq 731.42\ mm^2$$

$$A_s = 1000\ mm^2 > 835.62\ mm^2 \rightarrow sufficient\ reinforcement$$

Based on above calculations, we can use the SAP2000 area values for all beams since the error is not too big and all areas are more than minimum steel area. For this case, 12th floor beams, $A_s = 1000\ mm^2$ ($1.55\ in^2$) will be used for the bar selection. At the negative moment locations, 2#8 bars ($A_s = 1.57\ in^2$) will be used for 2nd floor beams.

Shear analysis

$$V_u = 258.886\ kN$$

$$\lambda = 1\ \ for\ normal\ weight\ concrete$$

$$\Phi V_c = \Phi * 2\lambda\sqrt{f'_c}b_w d = 0.75 * 2 * 1 * \sqrt{40000} * 350 * 636.5 = 66.83\ kN$$

$$V_u > V_c \rightarrow shear\ reinforcement\ is\ needed$$

$$V_{c1} = 4\sqrt{f'_c}b_w d = 178.22\ kN$$

$$V_{c2} = 8\sqrt{f'_c}b_w d = 356.44\ kN$$

$$V_s = \frac{V_u - \Phi V_c}{\Phi} = 254.89 < V_{c2}$$

$$\frac{A_v}{s} = \frac{V_s}{f_{yt}d} = 0.953\ mm^2/mm$$

From Figure 3.5.1.1.1 we can clearly see that that

$\frac{A_v}{s} = 0.001\ m^2/m = 1\ mm^2/mm$

$$Error = \frac{1-0.953}{1} * 100\% = 4.7\%$$

This error value shows that for the design of stirrups, the value of $\frac{A_v}{s}$ from SAP2000 can be used. For this major beam, #3 stirrups will be used. It also proves that for bars #9 and below, #3 stirrups can be used. The area of #3 stirrups is 71 mm^2 ($0.11\ in^2$).

Torsional analysis

Since this design is also subject to seismic forces, the torsion should be also checked. From the same figure, $T_u = 0.766\ kN - m$.

$$A_{cp} = 0.350 * 0.700 = 0.245\ m^2$$

$$P_{cp} = 2(0.35 + 0.7) = 2.1\ m$$

$$T_n = \Phi\lambda\sqrt{f'_c}\left(\frac{A_{cp}^{\ 2}}{P_{cp}}\right) = 4.2875\ kN - m$$

Since $T_u < T_n \rightarrow torsional\ reinforcement\ is\ not\ required$

Stirrups spacing: $S_1 = \frac{A_v f_{yt}}{V_s} = 0.764\ m \rightarrow \#3\ stirrups$

$$S_2 = \frac{d}{2} \leq 24\ in.\ if\ V_s \leq V_{c1} = (4\sqrt{f_c'})b_w d$$

$$S_3 = \frac{A_v f_{yt}}{50 b_w} \geq \frac{A_v f_{yt}}{0.75\sqrt{f_c'} b_w}$$

$$S = S_2 = 0.3\ m \rightarrow \#3\ stirrups\ at\ 300\ mm\ spacing$$

3.5.2.2 Columns

Slenderness ratio check

For this example, the first floor column (0.75 m x 0.75 m) was chosen for hand calculation verifications. To start with, using the slenderness ratio check we are able to identify if the column is short or slender. This slenderness ratio check is shown below:

Corner column:

$$\Psi_A = \frac{\Sigma(EI/l)\ columns}{\Sigma(EI/l)\ beams} = 9.22$$

$$\Psi_B = \frac{\Sigma(EI/l)\ columns}{\Sigma(EI/l)\ beams} = 9.22$$

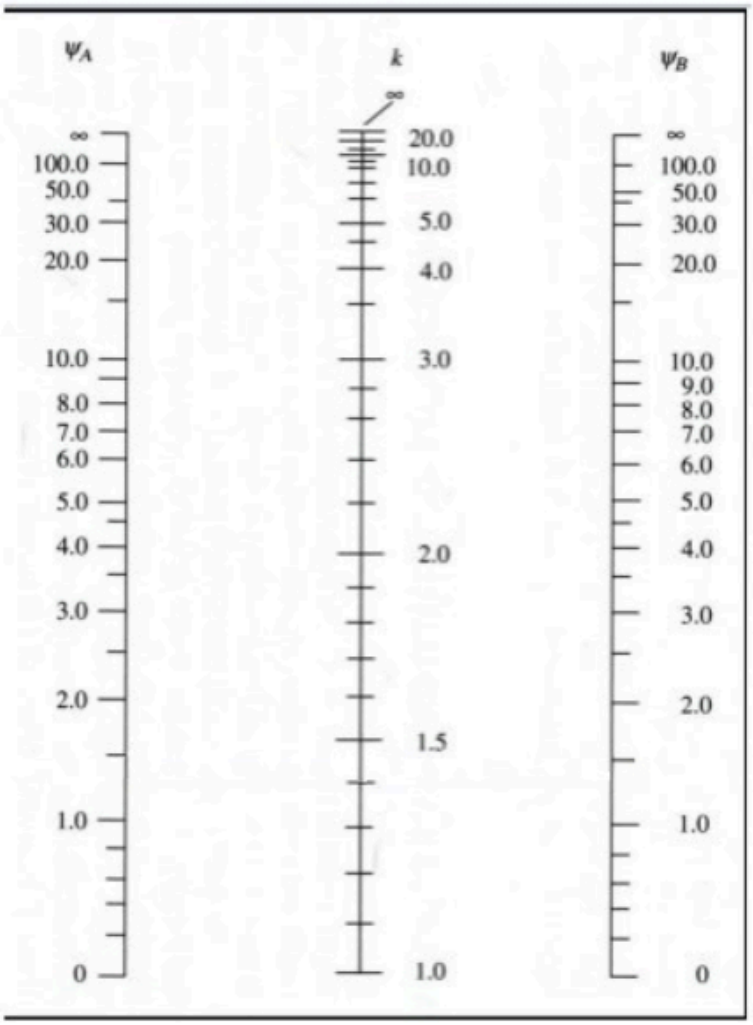

Figure 3.49 Slenderness ratio check chart.

Using Figure 3.49, Slenderness ratio check figure, we can see that our K value is 2.8.

Then by finding next values, we complete our calculations:

$$l_u = 3.3$$

$$r = 0.225$$

$$Slenderness = \frac{kl_u}{r} = 41.067 > 22 \rightarrow slender\ column$$

Internal column:

$$\Psi_A = \frac{\Sigma(EI/l)\ columns}{\Sigma(EI/l)\ beams} = 4.61$$

$$\Psi_B = \frac{\Sigma(EI/l)\ columns}{\Sigma(EI/l)\ beams} = 4.61$$

$$k\ from\ chart\ = \ 2.1$$

$$l_u = 3.3$$

$$r = 0.225$$

$$Slenderness = \frac{kl_u}{r} = 30.8\ >\ 22\ \rightarrow slender\ column$$

Edge column:

$$\Psi_A = \frac{\Sigma(EI/l)\ columns}{\Sigma(EI/l)\ beams} = 3.5$$

$$\Psi_B = \frac{\Sigma(EI/l)\ columns}{\Sigma(EI/l)\ beams} = 3.5$$

$$k\ from\ chart\ = \ 1.8$$

$$l_u = 3.3$$

$$r = 0.225$$

$$Slenderness = \frac{kl_u}{r} = 26.4\ >\ 22\ \rightarrow slender\ column$$

Since our columns were determined to be slender we have to amplify these values.

$$\delta_s = \frac{1}{[1-\frac{\Sigma Pf}{0.75\Sigma Pc}]} = 1.039 < 2.5$$

$$P_c = \pi^2 EI/(kl_u)^2 = 132758.75\ kN$$

$$\frac{l_u}{r} > \frac{35}{\sqrt{P_u/(f'_c A_g)}} \rightarrow\ if\ it\ is\ the\ case,\ further\ magnification\ is\ required$$

$$14.67 < 86.176 \rightarrow\ no\ further\ magnification\ is\ required\ for\ our\ case$$

Above magnification factor will be applied where it is necessary

$$M_1 = 111.957\ kN\ -\ m \rightarrow \delta M_1 = 116.29\ kN\ -\ m$$

$$M_2 = 140.068\ kN\ -\ m \rightarrow \delta M_1 = 145.49\ kN\ -\ m$$

Axial and moment analysis

$$M_u = 145.49\ kN\ -\ m$$

$$P_u = 3711.413\ kN$$

$$\varphi\ for\ tied\ columns\ is\ 0.65$$

$$P_n = \frac{P_u}{\Phi} = 5710\ kN$$

$$M_n = \frac{M_{crit}}{\Phi} = 223.8\ kN.m$$

$$e = \frac{M_n}{P_u} = 0.06\ m$$

$$K_n = \frac{P_n}{f_c' A_g} = 0.254$$

$$R_n = \frac{K_n e}{h} = 0.02$$

Using above values and interaction diagrams for rectangular columns from ACI 318-19, the reinforcement ratio was determined to be:

$$\rho = 0.01 \rightarrow A_S = 0.005625\ m^2$$

Bar selection:

8#9 ($A_s = 9\ in^2 = 0.0058\ m^2$)

Shear Strength Check

$$V_{u1} = 0.166\ kN;\ V_{u2} = 56.52\ kN;\ V_c = 8574\ kN$$

$$\Phi V_C = 6430\ kN$$

$$\frac{\Phi V_c}{2} = 3215\ kN$$

$$V_u < 0.5\Phi V_c \rightarrow Minimum\ reinforcement\ is\ required \rightarrow \#3\ ties$$

According to ACI code, the least column dimension should be 0.305 m. The least column size in this office building is 0.350 meters.

Biaxial Bending Check:

$$M_{ux} = 116.29\ kN.m \rightarrow M_{nx} = 178.91\ kN.m$$

$$M_{uy} = 145.5\ kN.m \rightarrow M_{yx} = 223.8\ kN.m$$

$$y_x = y_y = 0.82;\ e_x = 0.031m;\ e_y = 0.039\ m$$

Using the interaction diagram taken from ACI code, the next values were obtained.

$$P_{nx} = 128077\ kN;\ P_{ny} = 128077\ kN;\ P_o = 19133\ kN;\ P_{n0} = 27285\ kN$$

$$P_n > 0.1P_{n0} \rightarrow Valid\ method$$

$$\Phi P_n > P_u \rightarrow 17735\ kN > 3711\ kN \rightarrow Safe\ against\ biaxial\ bending$$

3.5.2.3 Two-way slab

Flexural Analysis

The slab panel dimensions are 3500 mm x 3500 mm. The column sizes differ at each floor. For the first two floors it is 750 mm x 750 mm. The slab thickness is 200 mm.

To complete both interior and exterior beam-supported panel designs, the following equations are used:

$$a_f = \frac{E_{cb}I_b}{E_{cs}I_s} = \frac{beam\ stiffness}{slab\ stiffness}$$

$$\beta_t = \frac{E_{cb}C}{2E_{cs}I_s} = \frac{torsional\ rigidity\ of\ edge\ beam\ section}{flexural\ rigidity\ of\ a\ slab\ of\ width\ equal\ to\ beam\ span\ length} = 0.24$$

$$C = torsional\ constant = \Sigma(1 - \frac{0.63x}{y})(\frac{x^3y}{3}) = 9.973 * 10^8$$

$$The\ interpolated\ coefficient = 97.61$$

Effective width for interior and exterior panels were found differently. It was taken as the least of 3 different ways of calculating this value.

Interior panel

$$b_w = b_w + 2 * \frac{s_w}{2} = 7750\ mm$$

$$b_w = b_w + 2 * (8h_f) = 3950\ mm$$

$$b_w = b_w + 2 * (\frac{l_n}{8}) = 2310\ mm$$

Exterior panel

$$b_w = b_w + \frac{s_w}{2} = 4250\ mm$$

$$b_w = b_w + 6h_f = 1950\,mm$$

$$b_w = b_w + \frac{l_n}{12} = 1270\,mm$$

Table 3.28. Summary of exterior slab design

Moment	Column Strip			Middle Strip		
	Negative	Positive	Negative	Negative	Positive	Negative
%	97.61	75.00	75.00	2.39	25.00	25.00
Moment distribution %	65	35	65	65	35	65
Mu (kN-m)	339.09	140.30	260.56	8.32	46.77	86.85
Mu slab (15%) (kN-m)	50.86	21.05	39.08	1.25	7.02	13.03
b (m)	1.27	1.27	1.27	1.27	1.27	1.27
Rn (kPa)	1633.06	675.68	1254.83	40.05	225.23	418.28
Ro	0.0040	0.0016	0.0030	0.0001	0.0005	0.0010
As (m2)	0.00084	0.00034	0.00064	0.00002	0.00011	0.00021
As min (m2)	0.000457	0.000457	0.000457	0.000457	0.000457	0.000457
Chosen A (m2)	0.00084	0.000457	0.00064	0.000457	0.000457	0.000457
Bar selection	3#6	4#4	6#4	4#4	4#4	4#4
Spacing (mm)	500	400	400	400	400	400
Min spacing (mm)	25.4	25.4	25.4	25.4	25.4	25.4

Table 3.29. Summary of interior slab design

Moment	Column Strip			Middle Strip		
	Negative	Positive	Negative	Negative	Positive	Negative
%	75.00	75.00	75.00	25.00	25.00	25.00
Mu (kN-m)	260.56	140.30	260.56	86.85	46.77	86.85
Mu slab (15%) (kN-m)	39.08	21.05	39.08	13.03	7.02	13.03
b (m)	2.30	2.30	2.30	2.30	2.30	2.30
Rn (kPa)	692.89	373.09	692.89	230.96	124.36	230.96
Ro	0.0017	0.0009	0.0017	0.0006	0.00011	0.00021
As (m2)	0.00063	0.00034	0.00063	0.00021	0.00011	0.00021
As min (m2)	1.283	1.283	1.283	1.283	1.283	1.283
Chosen A (m2)	1.283	1.283	1.283	1.283	1.283	1.283
Bar selection	3#6					
Spacing (mm)	800					
Min spacing (mm)	25.4					

3.5.2.4 Joint design

The joint design was carried out in accordance with Chapter 15 of ACI 318-19. The detailed calculation procedure followed the methodology outlined in the design book by Wight and MacGregor (Wight & MacGregor, 2009). The free body diagram of the interior beam-column joint is presented in Figure 3.5.2.4.1.

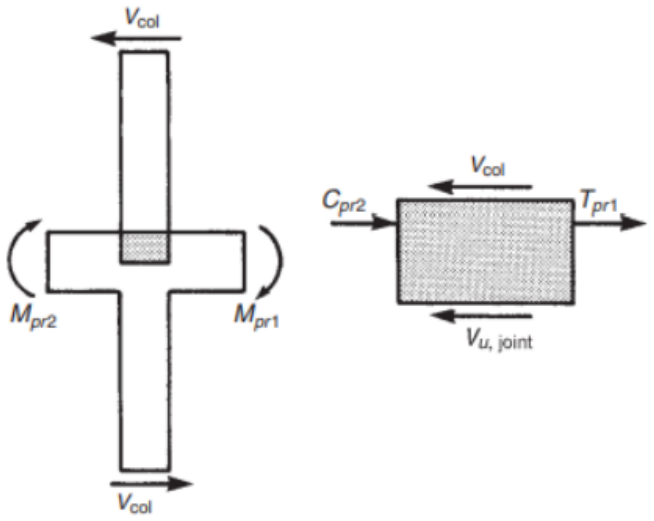

(c) Interior column-beam joint. (d) Top half of interior column-beam joint.

Figure 3.50 Beam-column joint free body diagram.

An interior beam-column joint shear was calculated using the following equation:

$$V_{u,\ joint} = T_{pr1} + C_{pr2} - V_{col}$$

$$T_{pr1} = \alpha A_s f_y = 1.25 * 1935.48 * 0.42 = 1016.127\ kN$$

$$C_{pr2} = \alpha A_s f_y = 1.25 * 851.6 * 0.42 = 447\ kN$$

$$V_{col} = 417\ kN \rightarrow From\ SAP2000$$

$$V_{u,\ joint} = 1016.127 + 447 - 417 = 1046\ kN$$

$$b_j = \frac{b_b + b_{col}}{2} = 550\ mm < b_b + h_{col} = 1100\ mm$$

$$V_n = \gamma \sqrt{f'_c} A_j = 1.7 * \sqrt{40} * 4125 = 4435.1\ kN$$

$$\Phi = 0.85 \rightarrow strain\ hardening\ of\ the\ reinforcement$$

$$\Phi V_n \geq V_u \rightarrow 0.85 * 4435.1 = 3769.8 \geq 1046\ kN$$

As we can see, the joint is safe against shear forces. To check for other directions, the same procedure can be repeated. According to ACI 15.4.2, the spacing requirement can be checked.

$$A_v = max\left(\frac{0.062\sqrt{f'_c} b_c s}{f_{yt}}, \frac{0.35 b_c s}{f_{yt}}\right)$$

$$s = min(\frac{A_v f_{yt}}{0.062\sqrt{f'_c} b_c}, \frac{A_v f_{yt}}{0.35 b_c})$$

To meet this requirements, #3 ties at 300 mm spacing will be provided.

3.5.2.5 Reinforcement detailing

Bar selection and spacing

The final bars and spacing selected for major beams and columns are presented in Tables 3.30 - 3.34.

Table 3.30. Final selected bars for major beams

Floor	Top reinforcement	Bottom reinforcement	Stirrups
1	5#7	3#6	#3 @ 300 mm
2	5#7	2#8	#3 @ 300 mm
3	5#7	2#8	#3 @ 300 mm
4	5#7	2#8	#3 @ 300 mm
5	3#9	5#5	#3 @ 300 mm
6	3#9	5#5	#3 @ 300 mm
7	3#9	3#6	#3 @ 300 mm
8	3#9	3#6	#3 @ 300 mm
9	3#9	3#6	#3 @ 300 mm
10	3#7	3#7	#3 @ 300 mm
11	5#5	2#7	#3 @ 300 mm
12	2#8	2#7	#3 @ 300 mm

Figure 3.31. Interior slab panel reinforcement bars.

Interior	
Bar selection	3#6
Spacing (mm)	800

Table 3.32. Exterior slab panel reinforcement bars.

Exterior						
Bar selection	3#6	4#4	6#4	4#4	4#4	4#4
Spacing (mm)	500	400	400	400	400	400

Table 3.33. Final selected bars for columns.

Floor	$a = b\ (m)$	Reinforcement
0-2	0.75	12#8
3-4	0.65	6#10
5-6	0.55	8#7
7-8	0.50	8#7
9-10	0.40	8#6
11-12	0.30	8#4

3.5.2.6 Development length

ACI 318-19 provides the method to determine reinforcing bar development lengths. The equation designed to determine tension bar development length is:

$$\frac{l_d}{d_b} = \frac{f_y \Psi_t \Psi_e \Psi_g}{20\lambda\sqrt{f_c'}} \quad (for\ bars\ larger\ than\ \#7)$$

Taking into consideration a certain conditions the development length of required bars in tension was calculated:

1) $Clear\ cover\ =\ 2.5\ -\ \frac{0.875}{2}\ =\ 2.0625\ in\ >\ d_b$

2) $Clear\ spacing\ of\ bars\ =\ 2.05\ in\ >\ d_b$

3) $minimum\ \#3\ stirrups\ were\ arranged$

$$l_d = 875\ mm\ >\ 750\ mm\ (column\ width) \rightarrow Hooked\ bars$$

Development length for hooked bars can be found via next equation:

$$l_{dh} = \left(\frac{f_y \Psi_e \Psi_r \Psi_o \Psi_c}{55\lambda\sqrt{f_c'}}\right) d_b^{1.5}\ (modification\ factor)$$

$$l_{dh} = 205\ mm\ >\ 8d_b = 177.8\ mm.$$

Subsequently, the 90° hook's parameters had to be determined:

$$D\ =\ 6d_b\ =\ 133.35\ mm,\ r\ =\ D/2\ =\ 66.675\ mm$$

The distance of the hook: $12d_b\ =\ 266.7\ mm$

In addition, stirrups will be placed along the development length at intervals of $\leq 3d_b$.

To calculate the development length for bars under compression, the following equation is applied:

$$l_{dc} = \left(\frac{f_y \Psi_r}{50\lambda\sqrt{f_c'}}\right) d_b \geq 0.0003 f_y \Psi_r d_b$$

Subsequently, the development length for bars under compression is:

$$l_{dc} = 250\ mm\ <\ 286\ mm$$

Lap slices

For the beams in tension:

$$l_{st} = l_{dh} = 205\ mm$$

For beams in compression:

$$l_{sc} = 0.0005 f_y d_b = 476\ mm$$

For columns:

As an example, column with $d_b = 0.875\ m$

$$l_{sc} = 0.0005 f_y d_b = 667\,mm$$

Table. 3.34. Lap slices for columns values

Floor	Reinforcement	d_b, in	Lap splices, mm
0-2	12#8	1	762
3-4	6#10	1.27	967.74
5-6	8#7	0.875	667
7-8	8#7	0.875	667
9-10	8#6	0.75	571.5
11-12	8#4	0.5	381

3.5.2.7 Special seismic provisions for reinforcement detailing

Beams

Since the building is in a high seismic risk area, special seismic detailing was included in the design. The beam's clear span and its width-to-depth ratio meet the requirements of Section 18.6 in ACI 318-19. To ensure strength and stability, at least two continuous longitudinal bars were placed at both the top and bottom of the beam, as required by Section 18.6.3.1. The beam was also designed so that the positive moment capacity at the joint face is more than half of the negative moment capacity. For added shear strength and ductility, hoops were installed over a length equal to twice the beam depth from the face of the support. The spacing of these hoops followed code limits—not exceeding d/4, 6 times the bar diameter (db), or 150 mm.

Columns

Seismic requirements for the columns were addressed following Section 18.7 of ACI 318-19. The reinforcement area in the columns was kept within the required range of 1-6 % of the cross-sectional area. Transverse reinforcement was placed on both sides

of the joint, extending a length l_0, which was taken as one-sixth of the column's clear span. All other relevant provisions from Section 18.7 were also considered during the design process to ensure the columns meet seismic performance standards.

Joints

The longitudinal reinforcement in the beams was extended all the way to the far face of the column at each joint. In joints where the reinforcement continued through the column, the column depth hhh was designed to be greater than 20 times the bar diameter ($20d_b$) to ensure proper anchorage. Additionally, the development lengths of the bars were checked and confirmed to meet the required criteria:

$$l_{\text{dh}} \geq \begin{cases} \dfrac{f_y d_b}{65\lambda\sqrt{f_c'}} \\ 8d_b \\ 6 \text{ in.} \end{cases}$$

3.5.2.8 Structural serviceability design

Deflection

Building structures need to be checked for deflection because it affects their serviceability. Different members must follow specific tabulated minimum thickness demands outlined in building codes. Deflection checks become redundant when the specified minimum thickness requirements for structural members are achieved or surpassed (Hassoun & Manaseer, 2020). The necessary minimum beam thickness for $f_y = 60000\ psi\ (413.7\ MPa)$ can be calculated through the following equation.

$$h_b = L/21$$

where,

$L - span\ length\ (m)$

For our case, the minimum thickness of the beam will be:

$$h_b = \frac{7000}{21} = 333\ mm < 350\ mm\ (actual\ depth\ of\ the\ beam)$$

As it can be seen, the selected beam member surpasses minimum requirements therefore the need for deflection calculations becomes unnecessary.

Crack width

The design of reinforced concrete structures depends fundamentally on crack control measures because these measures guarantee fundamental structural safety and durability together with reliability. The quantity of flexural cracking creates durability problems and visual concerns along with the deterioration of reinforcement materials. It is necessary to test that structural cracks stay within the boundaries defined by design standards. This empirical formula enables the assessment of maximum flexural crack width:

$$w = 0.076\beta_h f_s \sqrt[3]{d_c A}$$

where,

$w - estimated\ crack\ width\ (in)$

$\beta_h - ratio\ of\ the\ depth\ to\ the\ neutral\ axis\ and\ the\ cover\ to\ reinforcement\ (1.2)$

$f_s - stress\ in\ the\ steel\ (ksi)$

$d_c - cover\ (in)$

$A - effective\ tension\ area\ (in^2)$

$$w = 0.076 \times 1.20 \times 0.6 \times 60 \times \sqrt[3]{2.5 \times \frac{2.5\times(350/25.4)}{3}} = 0.01\ in\ < 0.016\ in$$

This building meets the allowable crack width standard of 0.016 inches since estimated crack dimensions stay below this threshold. The observed crack width meets the requirements.

The formula below determines the maximum allowable spacing of longitudinal reinforcement in the design.

$$s\ (in) = [15(\frac{40}{f_s}) - 2.5C_c]$$

$$s\ (in) = [15(\frac{40}{0.6\times60}) - 2.5 \times 2.5] = 10.42\ in = 264.67\ mm$$

The maximum distance between longitudinal reinforcement bars should be set at 264.67 mm.

4. Geotechnical Design

4.1. Site Description

The chosen site for construction of a 12 storey office building is located on 940 N Sycamore Avenue, Los Angeles, California in the USA. The area of the site is approximately 3995 square meters. The data related to characteristics of soil profile was retrieved from a geotechnical exploration report prepared by GeoPentech (2022). According to this report, the soil profile includes three layers: artificial fill, quaternary alluvium and Fernando Formation bedrock. The artificial fill is located at 3 m depth and contains stiff clay. Below this layer quaternary alluvium was found at 30.5-33.5 meters below ground surface. It consists of stiff to hard clay and medium dense-very dense sand. Fernando Formation bedrock is the last layer including hard siltstone and claystone. During the exploration groundwater was observed at 6 m depth below the ground surface.

4.1.1. Soil Profile

For soil characterization SPT and MC (modified California) tests were used, using automatic trip hammer, SPT sampler cutting shoe and barrel, hollow-stem auger, drilling mud. The tests were conducted on two boring logs at approximate depth 40.2 and 49.2 meters below ground surface. Also, the next laboratory tests were used to investigate soil: moisture content, dry density, Atterberg Limits, Passing No. 200 sieve and sieve distribution, corrosion suite, direct shear and consolidation. The information related to soil classification is demonstrated according to USCS (Unified Soil Classification System). For creating soil profile the data was extracted from a log of boring GP-1, as it has the least depth equal to 40.2 m.

Correction of SPT values based on field observations

For correction of SPT values for field procedures this formula was used:

$$N_{60} = \frac{\eta_H \eta_B \eta_S \eta_R N}{60} \quad [78]$$

Where

N_{60} – corrected SPT N-value for field procedures

η_H - hammer efficiency, %

η_B - borehole diameter correction

η_S - sampler correction

η_R - rod length correction

N - measured SPT value in the field

The values for η_H, η_B, η_S, η_R are taken from recommendations by Seed et.al. (1985) and Skempton (1986). (tables 3.5 by Das, 2019) Thus η_H=70%, η_B=1.15, η_S=1, η_R =1.

Table 4.1. Soil profile

Depth, m	Type of soil	N	N_{60}	γ, kN/m^3	σ_0', kN/m^2	C_N	$(N_1)_{60}$	c', kN/m^2	ϕ', deg
0.15-1.52	Fat CLAY (CH)	19	25	17.52	26.63	1.95	79.38	0	30
1.52-3.05	Lean CLAY (CL)	19	25	17.52	53.44	1.38	74.71	0	30
3.05-7.62	Lean CLAY (CL)	9	12	17.15	130.68	0.88	24.26	14.36	34
7.62-10.67	Fat CLAY (CH)	10	13	16.05	171.25	0.77	30.70	14.36	34
10.67-12.19	Clayey SAND (SC)	14	19	17.67	215.40	0.69	66.97	14.36	34
12.19-13.72	Lean CLAY (CL)	5	7	17.67	242.43	0.65	23.184	14.36	34
13.72-15.24	Clayey SAND (SC)	20	27	17.45	265.94	0.62	85.0	14.36	34
15.24-18.29	Lean CLAY (CL)	8	11	17.45	319.16	0.56	25.73	14.36	34
18.29-24.38	Clayey SAND (SC)	23	31	17.45	425.43	0.49	53.35	14.36	32

24.38-27.43	Poorly graded SAND with clay (SP-SC)	50	67	17.06	467.96	0.47	93.24	21.55	32
27.43-30.48	Clayey SAND (SC)	34	46	17.06	520.00	0.44	113.76	14.36	32
30.48-33.53	SILTSTONE	50	67	16.37	548.89	0.43	113.51	0	0
33.53-39.62	CLAYSTONE	23	31	16.37	648.58	0.40	44.28	0	0
39.62-40.23	SILTSTONE	50	67	15.47	622.36	0.40	268.07	0	0

Correction of SPT values for overburden pressure (for N_{60} in granular soils)

The granular soil layers are cohesionless which is why effective overburden pressure should be taken into account as it affects penetration resistance.
To correct SPT values for overburden pressure the next formula was used for calculations:

$$(N_1)_{60} = C_N * N_{60} \quad [79]$$

where,
C_N - overburden pressure correction factor
$(N_1)_{60}$ - value of N_{60} corrected to a standard value of $\sigma'_0 = p_a$ ($p_a \approx 101.3$ kN/m^2)

C_N value can be estimated by several relationships developed by Liao and Whitman, Skempton, Seed, Peck and Bazaraa. The magnitudes are nearly the same which is why the equation by Liao and Whitman was used to calculate the correction factor.
Liao and Whitman's relationship (1986):

$$C_N = \sqrt{\frac{1}{\frac{\sigma'_o}{p_a}}} \quad [80]$$

For calculation effective overburden pressure, the following formula was used:

$$\sigma_0' = \gamma H \quad [81]$$

Correlation between modulus of elasticity and SPT number:

To correlate elasticity modulus and SPT number, the following formula by Kulhawy and Mayne (1990) was used:

$$\frac{E_s}{p_a} = \alpha N_{60} \quad [82]$$

where,

E_s - modulus of elasticity for granular soil

α=5 for sands with fines

Table 4.2. Modulus of elasticity of sandy soils

Soil type	N_{60}	E_s, kN/m^2
Clayey SAND (SC)	14	9516.6
Clayey SAND(SC)	20	13595
Clayey SAND(SC)	23	15634
Poorly Graded SAND with Clay (SP-SC)	50	33988
Clayey SAND(SC)	34	23112

4.1.2. Seismic Analysis

Los Angeles is situated in the zone of high seismic activity, according to the USGS Seismic Hazard Map.

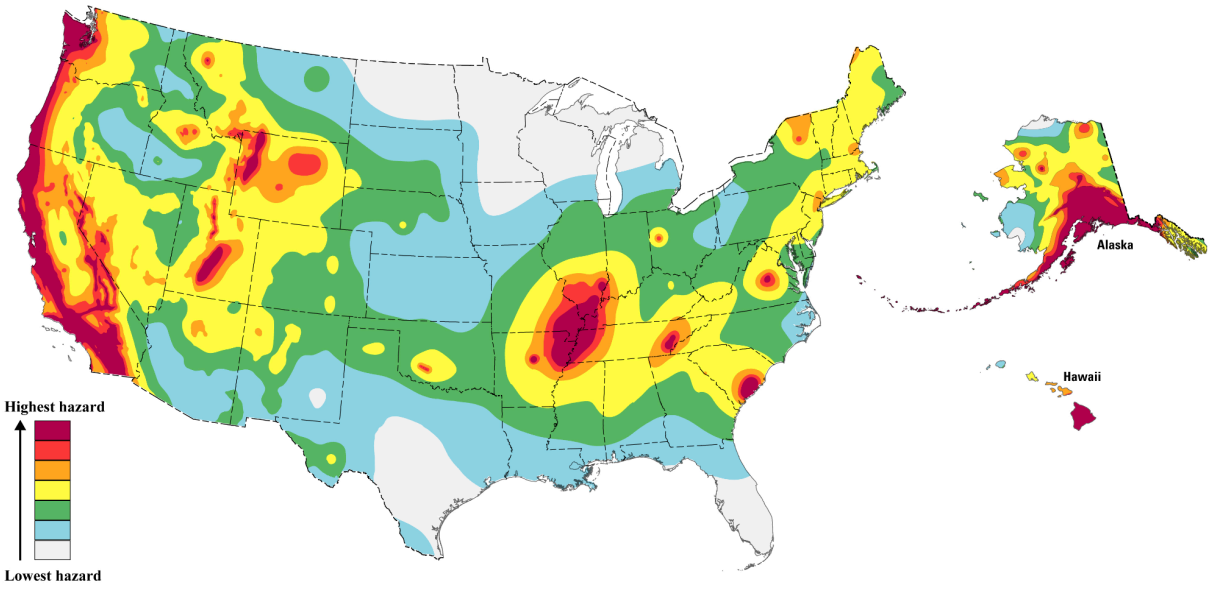

Figure 4.1. USGS Seismic Hazard map.

The Los Angeles region has a 60% chance of experiencing a magnitude 6.7 earthquake, a 46% chance of a magnitude 7 earthquake, and a 31% chance of a magnitude 7.5 earthquake within the next 30 years (USGS).

To assess the seismicity of the area, shear wave velocity value was used.

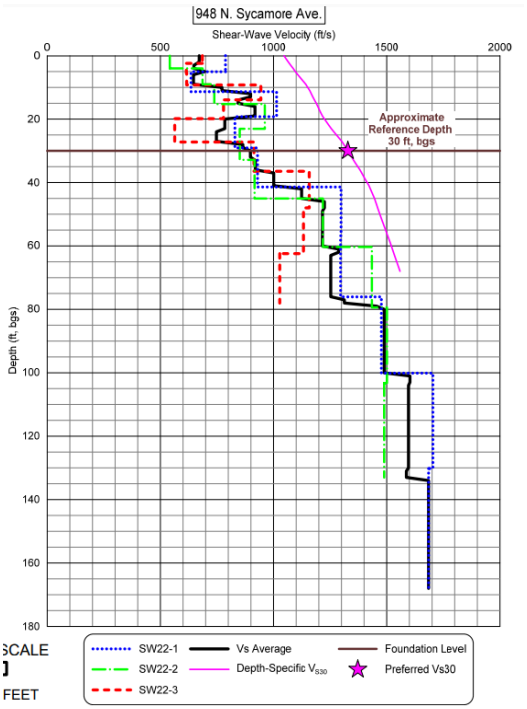

Figure 4.2. Shear-Wave Velocity Graph.

According to the GeoPentech (2022) report, shear wave velocity at 30 m depth (V_{S30}) is approximately 405 m/s. This value corresponds to the Site Class C - Very Dense Soil. Using guidelines from the 2019 California Building Code (CBC) and the American Society of Civil Engineers (ASCE), the study examined potential ground shaking in the area. The findings suggest that the region is classified as Seismic Design Category D, which means it requires stricter seismic design standards for buildings.

4.1.3. Water Level

Site investigation has shown that the water level is approximately 20-25 feet below the ground surface. However, in the prior exploration groundwater table was found to be 10 to 20 feet bgs. Variations in rainfall, tidal fluctuation, irrigation practices, and other factors not apparent at the time of measurements can cause fluctuations in groundwater levels. For this capstone project, the groundwater table will be taken to be 10 feet.

The presence of shallow groundwater will impose particular demands on our project, including the need for dewatering and the use of corrosion-resistant and waterproof materials. Throughout the building process, there will be a number of challenges, including grading delays, the possibility of damaging sensitive floor coverings, and vapor transmission through slabs, etc. The structure will take into account those requirements.

4.1.4. Liquefaction Potential Index Calculations.

The liquefaction potential index (LPI) was determined using a formula suggested by Luna & Frost (1998). The LPI is typically estimated for soil layers as deep as 20 meters. A weighting factor is used to prioritize the layers closest to the ground surface.

$$LPI = \sum_{i=1}^{n} w_i F_i H_i \quad [83]$$

$$F_i = 1 - FS \text{ for } FS < 1, \text{otherwise } FS = 0. \quad [84]$$

$$w_i = 10 - 0.5 z_i \text{ for } z < 20\,m, \text{ for depth more than 20 m, } w_i = 0. \quad [85]$$

Where,

w_i - weighting factor

F_i - liquefaction severity

H_i - thickness of soil layer

To find Factor of Safety, a correlation between the Cyclic Stress Ratio (CSR) and Cyclic Resistance Ratio (CRR) is utilized:

$$FS = \frac{CRR}{CSR} \times MSF \quad [86]$$

Where,

MSF - magnitude scaling factor

Seed and Idriss (1971) proposed the following formula for CSR:

$$CSR = 0.65 \times (\frac{a_{max}}{g}) \times (\frac{\sigma_v}{\sigma_v'}) \times r_d \times \frac{1}{MSF} \times \frac{1}{K_\sigma} \quad [87]$$

Where,

a_{max} - peak horizontal ground acceleration

r_d - stress reduction factor

K_σ - overburden correction factor

SPT N values for calculation of liquefaction need to be corrected by several factors.

$$(N_1)_{60} = N_m C_N C_E C_B C_R C_S \quad [88]$$

N_m - SPT N value

C_N - overburden correction factor

C_E - hammer energy ratio correction factor; 1.0 for automatic trip hammer.

C_B - borehole diameter correction factor; 1.15 for 8’ diameter borehole.

C_R - rod length correction factor; 1.0 for >30 m length.

C_S - sampler correction factor; 1.0 for standard tests.

Another value required for the calculation of CSR is magnitude scaling factor (MSF). For clay-like material, MSF recommended by Idriss & Boulanger (2014) is used:

$$MSF = 1.12 \times e^{(-M_w/4)} + 0.828 \leq 1.13 \quad [89]$$

M_w was taken as 6.7. This is based on a study by the U.S. Geological Survey (USGS). The study found that there is a 60% probability of an earthquake of this magnitude occurring within the next 30 years.

To find overburden correction factor K_σ, the following formulas were used:

$$C_\sigma = \frac{1}{18.9 - 2.5507\sqrt{(N_1)_{60}}} \leq 0.3 \quad [90]$$

$$K_\sigma = 1 - C_\sigma ln(\frac{\sigma_v'}{p_a}) \leq 1.0 \quad [91]$$

The stress reduction factor r_d is determined with the following equations:

$$r_d = exp(\alpha(z) + \beta(z) \times M_w) \quad [92]$$

$$\alpha(z) = -1.012 - 1.126 \times sin(\frac{z}{11.73} + 5.133) \quad [93]$$

$$\beta(z) = 0.106 + 0.118 \times sin(\frac{z}{11.28} + 5.142) \quad [94]$$

According to the GeoPentech (2022) report, a_{max} of the site is 0.33 g.

The results of the calculation of CSR is shown in the table below.

Table 4.3. CSR calculation results.

$Depth, m$	$Type\ of\ soil$	$(N_1)_{60}$	r_d	MSF	a_{max}	K_σ	CSR
1.52	Fat CLAY (CH)	44.57	0.99	1.04	0.33	0.63	0.01
3.05	Lean CLAY (CL)	41.95	0.97	1.04	0.33	0.58	0.03
7.62	Lean CLAY (CL)	11.7	0.89	1.04	0.33	1.04	0.03

10.67	Fat CLAY (CH)	16.45	0.83	1.04	0.33	1.15	0.06
12.19	Clayey SAND (SC)	30.91	0.8	1.04	0.33	0.34	0.1
13.72	Lean CLAY	11.04	0.77	1.04	0.33	1.2	0.12
15.24	Clayey SAND (SC)	44.16	0.74	1.04	0.33	0.72	0.09
18.29	Lean CLAY (CL)	12.6	0.68	1.04	0.33	1.11	0.08
24.38	Clayey SAND (SC)	25.66	0.59	1.04	0.33	0.78	0.05
27.43	Poorly graded SAND with clay (SP-SC)	79.93	0.56	1.04	0.33	0.89	0.13
30.48	Clayey SAND (SC)	54.35	0.53	1.04	0.33	0.92	0.01
33.53	SILTSTONE	81.08	0.52	1.04	0.33	0.92	0.15
39.62	CLAYSTONE	26.45	0.53	1.04	0.33	1	0.07
40.23	SILTSTONE	191.48	0.53	1.04	0.33	0.89	0.95

The next step is to calculate the cyclic resistance ratio (CRR). However, because the sample does not contain pure sand, the CRR calculation requires adjusted SPT N values. This adjusted value is called the clean sand equivalent $(N_1)_{60cs}$.

$$(N_1)_{60cs} = (N_1)_{60} + \Delta(N_1)_{60} \quad [95]$$

$$\Delta(N_1)_{60} = exp(1.63 + \frac{9.7}{FC+0.1} - \left(\frac{15.7}{FC+0.1}\right)^2) \quad [96]$$

FC value is given in the report by GeoPentech (2022).

$$CRR = exp\left[\left(\frac{(N_1)_{60cs}}{14.1}\right) + \left(\frac{(N_1)_{60cs}}{126}\right)^2 - \left(\frac{(N_1)_{60cs}}{23.6}\right)^3 + \left(\frac{(N_1)_{60cs}}{25.4}\right)^4 - 2.8\right] \quad [97]$$

The results of the CRR calculations are presented in Table 4.4.

Table 4.4. CRR calculation results.

Depth, m	$Type\ of\ soil$	$(N_1)_{60}$	$\Delta(N_1)_{60}$	$(N_1)_{60cs}$	FC	$CRR_{7.5}$
1.52	Fat CLAY (CH)	44.57	5.6	50.17	61.25	0.30

3.05	Lean CLAY (CL)	41.95	5.6	47.55	61.25	0.27
7.62	Lean CLAY (CL)	11.70	5.58	17.27	39.90	0.18
10.67	Fat CLAY (CH)	16.45	5.04	21.49	24.55	0.23
12.19	Clayey SAND (SC)	30.91	5.58	36.49	40.05	0.67
13.72	Lean CLAY	11.04	5.58	16.62	40.05	0.18
15.24	Clayey SAND (SC)	44.16	5.6	49.76	44.30	0.30
18.29	Lean CLAY (CL)	12.60	5.6	18.21	44.30	0.19
24.38	Clayey SAND (SC)	25.66	0.46	26.12	8.20	0.32
27.43	Poorly graded SAND with clay (SP-SC)	79.93	5.59	85.52	42.00	0.61
30.48	Clayey SAND (SC)	54.35	5.41	59.76	31.10	0.40
33.53	SILTSTONE	81.08	5.57	86.65	70.40	0.62
39.62	CLAYSTONE	26.45	5.53	31.98	84.60	0.73
40.23	SILTSTONE	191.48	5.53	197.00	84.60	1.45

Using formulas (4.1) and (4.4), FS and LPI were identified. The results are tabulated below.

Table 4.5. LPI calculation results.

Depth, m	$Type\ of\ soil$	H_i, m	$CRR_{7.5}$	CSR	LPI
1.52	Fat CLAY (CH)	1.52	0.30	0.01	0.00
3.05	Lean CLAY (CL)	1.53	0.27	0.03	0.00
7.62	Lean CLAY (CL)	4.57	0.18	0.03	0.00
10.67	Fat CLAY (CH)	3.05	0.23	0.06	0.00
12.19	Clayey SAND (SC)	1.52	0.67	0.10	0.00
13.72	Lean CLAY	1.53	0.18	0.12	0.00
15.24	Clayey SAND (SC)	1.52	0.30	0.09	0.00
18.29	Lean CLAY (CL)	3.05	0.19	0.08	0.00

24.38	Clayey SAND (SC)	6.09	0.32	0.05	0.00
27.43	Poorly graded SAND with clay (SP-SC)	3.05	0.61	0.13	0.00
30.48	Clayey SAND (SC)	3.05	0.40	0.01	0.00
33.53	SILTSTONE	3.05	0.62	0.15	0.00
39.62	CLAYSTONE	6.09	0.73	0.07	0.00
40.23	SILTSTONE	0.61	1.45	0.95	0.00

An LPI of 0 indicates a very low risk of liquefaction. According to the GeoPentech (2022) report, liquefaction is not considered a hazard on this site, and our calculations support this conclusion.

4.2. Site Response Analysis

To detect potential seismic hazards, such as damages to structure, liquefaction and landslides site response analysis is necessary to be done. This analysis allows us to see how seismic parameters change during propagation of seismic waves through deposit of soil (Laera & Brinkgreve). It can be performed by special software PLAXIS 2D. To model liquefaction onset engineers usually use two common methods, one of which is dynamic analysis using finite element code in PLAXIS 2D. To simulate soil behaviour with saturated conditions dynamic boundary conditions should be chosen properly. In the window called Phases a parameter of dynamic time interval was set as 42.7 seconds. Other values remained as default.

For the site response analysis, Landers earthquake (1992) with a magnitude of 7.3 was chosen. The strong motion data was retrieved from NCEI (National Centers for Environmental Information) website. Site response analysis was implemented using PLAXIS 2D software. All the necessary soil conditions and boundaries were entered. Site response analysis was used for the dynamic analysis in PLAXIS 3D. The following boundary conditions were entered:

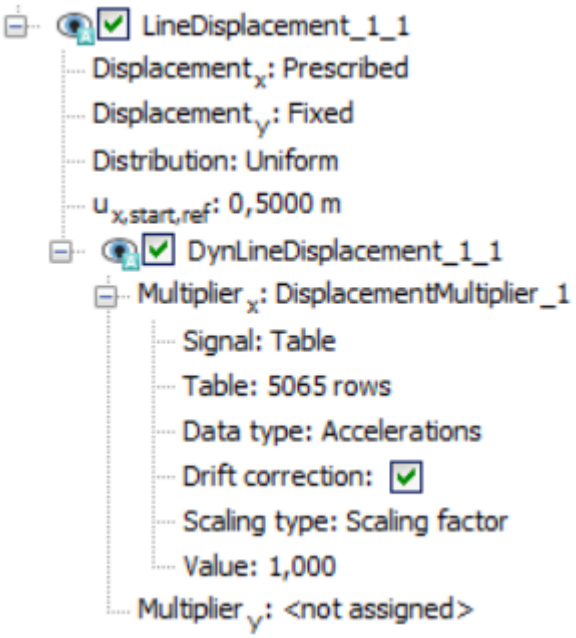

Figure 4.3. Boundary conditions.

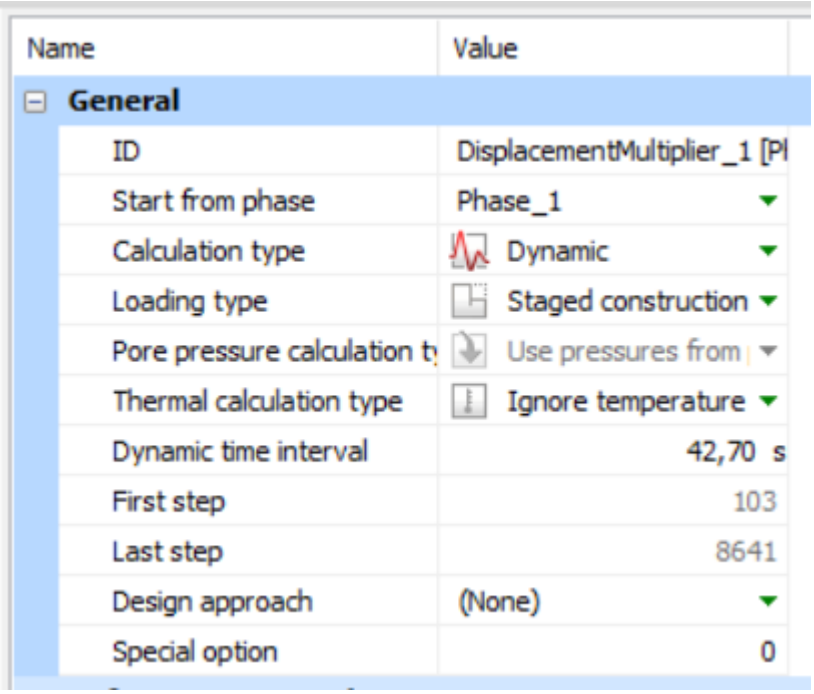

Figure 4.4. Configuration of Phase_1.

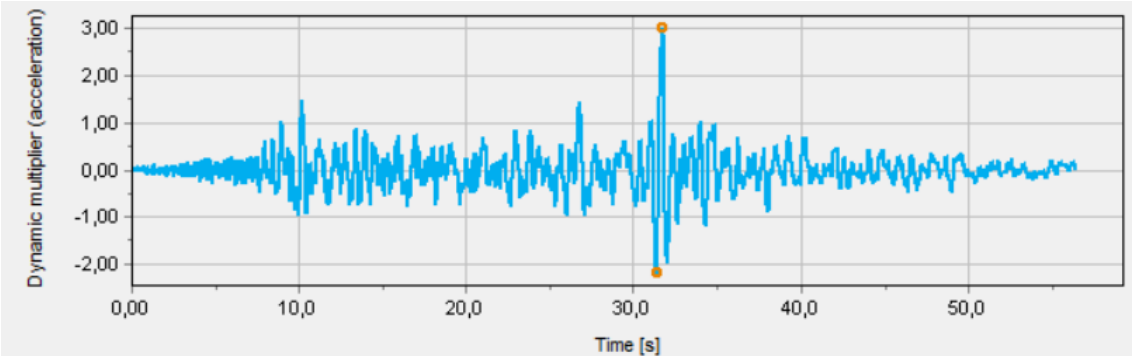

Figure 4.5. Accelerogram of Landers Earthquake.

As we can see from Figure 4.6, soil was displaced in x direction to 27.7 mm..

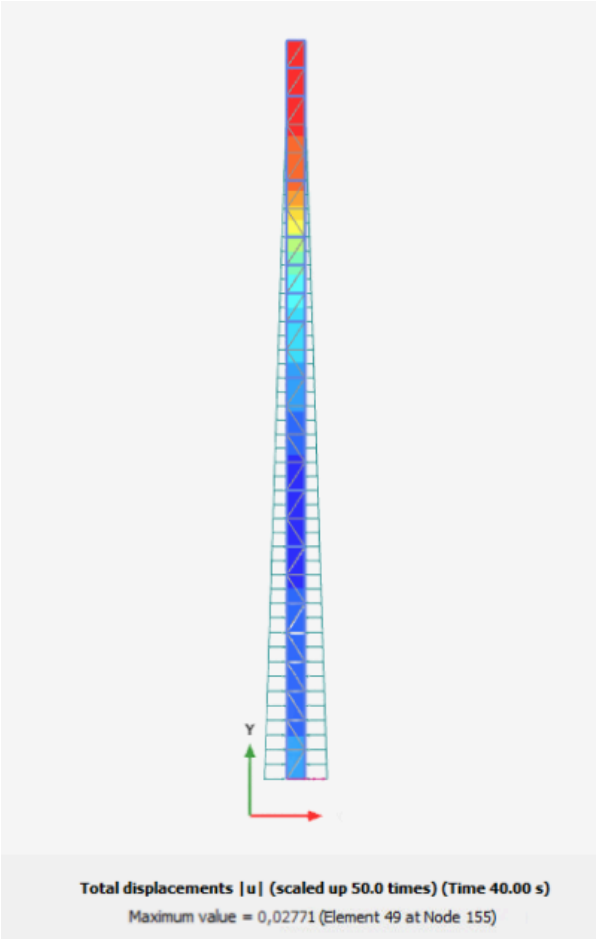

Figure 4.6. Soil deformation.

As a result of the site response analysis, the following data was obtained.

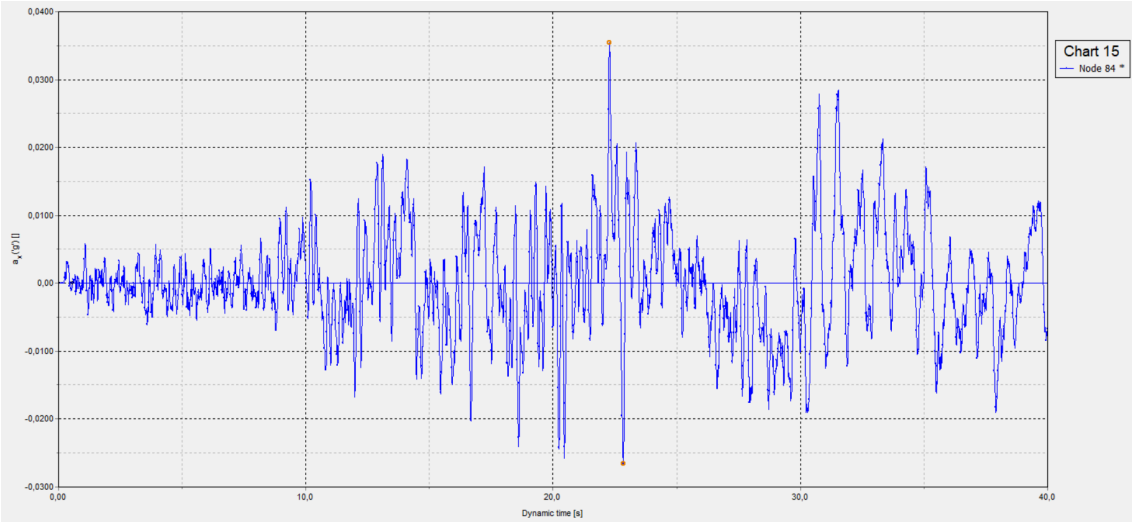

Figure 4.7. Acceleration along the x-axis.

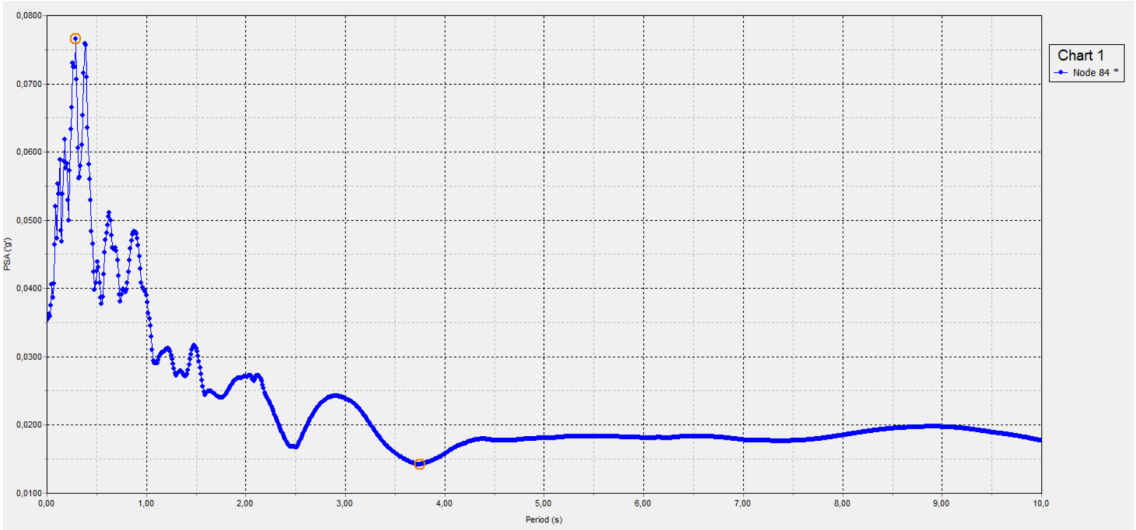

Figure 4.8. PSA.

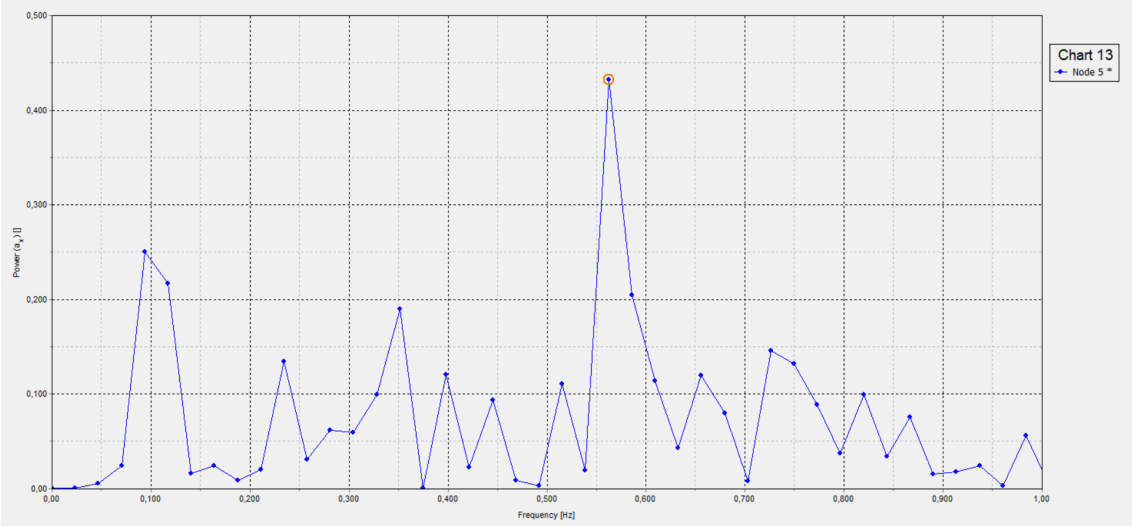

Figure 4.9. Fast Fourier transformation.

4.3. Foundation design

There are two types of foundation: shallow and deep. The average bearing pressure, based on the report, is 287.28 kN/m^2.

4.3.1. Shallow foundation

There are several types of shallow foundations, including pad, strip (continuous) and mat (raft) foundations. Pad foundations have circular, square or rectangular shapes. They carry column loads that spread evenly into the underlying ground. In strip

foundations wall loads are supported. Mat foundations can support wall loads or multiple columns.

4.3.2. Mat foundation

Mat or raft foundation is a type of shallow foundation for which a concrete slab supports more than one line of column. It is used for low-bearing capacity soil. The factor of safety required to be a minimum 3 under dead load or maximum live loads for mat foundation on clay. This design distributes the building's stress uniformly across the earth beneath, making it excellent for structures on weak or uneven ground. By covering the entire region, it prevents differential settling and ensures stability for huge constructions. Moreover, according to the geotechnical investigation report continuous mat foundation for settlement control was recommended.

To design the mat foundation, we will use the rigid method, which assumes that the entire slab is horizontal and rigid under stress. This method simplifies computations by treating the foundation as a single, unified structure. The figure below shows that the mat is divided into rectangular strips:

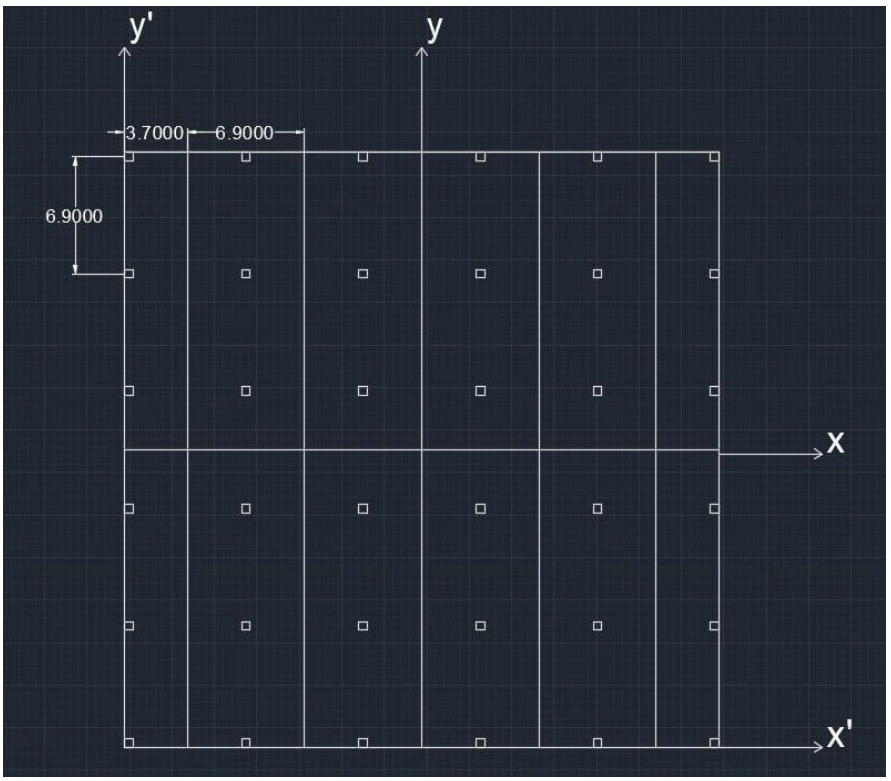

Figure 4.10. The separation of raft foundation into strips.

The figure also shows 3 types of columns, which are edge, inner and corner. In the case of office building with dimensions of $L \cdot B = 35\,m \cdot 35\,m$, the total load on raft foundation can be calculated as:

$$Q = Q_{corner} \times 4 + Q_{edge} \times 16 + Q_{inner} \times 16 \quad [98]$$

$$Q = 4209 \times 4 + 6781 \times 16 + 10895 \times 16 = 299652\,kN$$

where,

Q - total load on the raft foundation

Q_{corner} - load on corner columns: 4209 kN

Q_{edge} - load on edge columns: 6781 kN

Q_{inner} - load on inner columns: 10895 kN

To determine the load on the center of each column in the raft foundation next equation will be used:

$$q = \frac{Q}{A} + \frac{M_y}{I_y} + \frac{M_x}{I_x} \quad [99]$$

where,

A - area of footing

$$A = BL \quad [100]$$

I_x - moment inertia about x - axis

$$I_x = \frac{1}{12} \cdot BL^3 \quad [101]$$

I_y - moment inertia about y - axis

$$I_y = \frac{1}{12} \cdot LB^3 \quad [102]$$

M_x - moment of the column loads about x -axis

$$M_x = Q \cdot e_y \quad [103]$$

M_y - moment of the column loads about y -axis

$$M_y = Q \cdot e_x \quad [104]$$

e_x and e_y, load eccentricities, can be calculated as:

$$e_x = x - \frac{B}{2} \quad [105]$$

$$e_y = y - \frac{L}{2} \quad [106]$$

Table 4.6. Values for calculation of soil pressure

Area, m^2	I_x, m^4	I_y, m^4	x'	y'	e_x	e_y	M_x, kN	M_y, kN
1225	125052.08	125052.08	17.26	17.26	-0.24	-0.24	-14042.15	-14042.15

Table 4.7. Soil pressure below the mat for each column

Column name	Soil pressure	Column name	Soil pressure	Column name	Soil pressure	Column name	Soil pressure	Column name	Soil pressure	Column name	Soil pressure
A1	244.6	B1	240.6	C1	236.7	D1	232.4	E1	228.5	F1	224.5
A2	248.6	B2	244.6	C2	240.6	D2	236.4	E2	232.4	F2	228.5
A3	252.6	B3	248.6	C3	244.6	D3	240.4	E3	236.4	F3	232.4
A4	256.8	B4	252.8	C4	248.9	D4	244.6	E4	240.6	F4	236.7
A5	260.8	B5	256.8	C5	252.8	D5	248.6	E5	244.6	F5	240.6
A6	264.7	B6	260.8	C6	256.8	D6	252.6	E6	248.6	F6	244.6

The used equation to to calculate the soil pressure of the first strip in y-direction:

$$q_{av} = \frac{qA_1+qA_2+qA_3+qA_4+qA_5+qA_6}{2} \quad [107]$$

$$q_{av(strip\ A)} = 32915.015\ kN/m^2$$

The average load on each strip can be adjusted as:

$$Average\ load = \frac{q_{av} \times B_1 \times B + (Q_1+Q_2+Q_3+Q_4+Q_5+Q_6)}{2} \quad [108]$$

Average load = 17221.53 kN

The equation above consists of 2 parts which are:

Total reaction of soil $q_{av} \times B_1 \times B$

The total load on one strip $Q_1 + Q_2 + Q_3 + Q_4 + Q_5 + Q_6$

Modification factor can be calculated as:

$$F = \frac{Average\ load}{Q_1+Q_2+Q_3+Q_4+Q_5+Q_6} = 11.27 \quad [109]$$

$$q_{av(modified)} = 132.98\ kN/m^2$$

As all modified loads were calculated, bearing capacity can be calculated. Meyerhof's method was used to calculate the bearing capacity.

Meyerhof's method

To calculate ultimate bearing capacity, the general bearing capacity equation suggested by Meyerhof was used:

$$q_u = c'N_c F_{cs} F_{cd} F_{ci} + qN_q F_{qs} F_{qd} F_{qi} + \frac{1}{2}\gamma B N_\gamma F_{\gamma s} F_{\gamma d} F_{\gamma i} \quad [110]$$

where,

q_u - ultimate bearing capacity

c' - cohesion

q - effective stress at the level of the bottom of the foundation

γ - unit weight of soil

B - foundation width

$F_{cs}, F_{qs}, F_{\gamma s}$ - shape factors

$F_{cd}, F_{qd}, F_{\gamma d}$ - depth factors

$F_{ci}, F_{qi}, F_{\gamma i}$ - load inclination factors

N_c, N_q, N_γ - bearing capacity factors

For $\phi = 34$

$N_q = 29.44$, $N_c = 42.16$, $N_\gamma = 41.06$

To calculate shape factors, the following formulas by DeBeer (1970) are used:

$$F_{cs} = 1 + (\frac{B}{L})(\frac{N_q}{N_c}) \quad [111]$$

$$F_{qs} = 1 + (\frac{B}{L})tan\phi' \quad [112]$$

$$F_{\gamma s} = 1 - 0.4(\frac{B}{L}) \quad [113]$$

To calculate depth factors, the following formulas by Hansen (1970) are used.

if $\frac{D_f}{B} \leq 1, \phi' > 0$ then:

$$F_{cd} = F_{qd} - \frac{1-F_{qd}}{N_c tan\phi'} \quad [114]$$

$$F_{qd} = 1 + 2tan\phi'(1 - sin\phi')^2 \frac{D_f}{B} \quad [115]$$

$$F_{\gamma d} = 1$$

It was assumed that there is no load inclination (β), thus $F_{ci} = F_{\gamma i} = F_{qi} = 1$

For shallow foundations depth of foundation (D_f) is located within 0-2 m depth, which is why it was assumed that $D_f = 2$ m. According to the Building Code for City of Los Angeles developed in 2023 (ICC Digital Codes), the minimum requirements for depth and width of foundation are both 305 mm. The square foundation was chosen, thus B=L=2 m. Depth of the basement is 3.3 m. Thus, the bottom of the foundation is located in the lean clay soil layer. Friction angle in this layer is nearly 34 degrees.

Shape factors:

$$F_{cs} = 1 + \frac{29.44}{42.16} = 1.70$$

$$F_{qs} = 1 + tan34^\circ = 1.67$$

$$F_{\gamma s} = 1 - 0.4 = 0.6$$

Depth factors:

$$F_{qd} = 1 + 2tan34^\circ(1 - sin34^\circ)^2 \frac{2}{2} = 1.26$$

$$F_{cd} = 1.26 - \frac{1-1.26}{42.16*tan34} = 1.27$$

$$F_{\gamma d} = 1$$

$$\gamma = 17.52\ kN/m^3$$

The groundwater table is at 3.048 m.

$$\gamma' = \gamma - \gamma_w[1 - (\frac{D_w - D}{B})] = 17.52 - 9.81[1 - (\frac{3.048-2}{2})] = 12.85\ kN/m^3$$

As the soil is cohesionless (c'=0) the general bearing capacity equation becomes:

$$q_u = qN_q F_{qs} F_{qd} F_{qi} + \frac{1}{2}\gamma B N_\gamma F_{\gamma s} F_{\gamma d} F_{\gamma i} \quad [116]$$

$$q = \gamma D_f \quad [117]$$

$$q = 17.52 * 2 = 35.04\ kN/m^2$$

$$q_u = 35.04 * 29.44 * 1.67 * 1.26 + 0.5 * 12.85 * 2 * 41.06 * 0.6$$

$$q_u = 2170.65 + 316.57 = 2487.22\ kN/m2$$

Allowable bearing capacity is calculated using this formula:

$$q_{all} = \frac{q_u}{FS} \quad [118]$$

where,

q_{all} - allowable bearing capacity

FS - factor of safety

Minimum factors of safety for shallow foundations are 2.5-3.5. (Zhou, 2006) Thus, the value of 3 was selected.

$$q_{all} = \frac{2487.22}{3} = 829.07\ kN/m^2$$

To calculate gross allowable load, the next formula was used:

$$Q_{all} = q_{all} B^2 \quad [119]$$

$$Q_{all} = 829.07 * 2^2 = 3316.29\ kN$$

Terzaghi's bearing capacity equation for square foundation is calculated by this formula:

$$q_u = 1.3c' N_c + qN_q + 0.4\gamma B N_\gamma \quad [120]$$

The values for N_c, N_q, N_γ are 52.64, 36.50 and 38.04, respectively.

$$q_u = 35.04 * 36.5 + 0.4 * 12.85 * 2 * 38.04 = 1278.96 + 391.0512 = 1670.01\ kN/m^2$$

$$q_{all} = \frac{1670.01}{3} = 556.67\ kN/m^2$$

$$Q_{all} = 556.67 * 2^2 = 2226.68\,kN$$

4.3.3. Pile foundation design

4.3.3.1. Single pile design

Bearing capacity of the pile is defined as the sum of the skin friction of the soil layers and the bearing capacity at the pile point.

$$Q_u = Q_p + Q_s \quad [121]$$

where,

Q_u - ultimate bearing capacity of the pile

Q_p - point bearing capacity of the pile

Q_s - shaft resistance

It was initially decided that the pile should be made of precast concrete, because they can endure high loads and resist corrosion. For the sample calculation, we assumed the diameter to be 0.61 meters. From that, we calculated the cross-sectional area and the perimeter of the pile.

$$A = \frac{\pi D^2}{4} = \frac{\pi \times 0.61^2}{4} = 0.292\,m^2$$

$$P = \pi D = 0.61\pi = 1.916\,m$$

The soil profile shows that the site's soil is mostly composed of layers of clay, sand, and stone. Therefore, we computed bearing capacities in three different instances: when the pile tip is in stone, clay, and sand.

Point bearing capacity in Clay

The depth of the pile tip was selected at 10.3 meters to demonstrate the calculations. Basement depth is 3.300 m. Then, the depth of the pile is 7 m.

Meyerhof's End Bearing Capacity in Clay

$$Q_p \approx N_c^* c_u A_p = 9 c_u A_p \quad [122]$$

where,

c_u - soil's undrained cohesion beneath the pile tip

N_c^* - bearing capacity factor

$$Q_p = 9 \times 14.36\, kN/m^2 \times 0.292\, m^2 = 37.738\, kN$$

Bearing capacity of the clay layers are relatively low.

Vesic's End Bearing Capacity in Clay

The formula of the bearing capacity of the clay soil according to Vesic is given below.

$$Q_p = A_p c_u N_c^* \quad [123]$$

$$I_{rr} = I_r = \frac{E_s}{3c_u} \quad [124]$$

where,

I_{rr} - reduced rigidity index

I_r - rigidity index

Then, the value of reduced rigidity index is:

$$I_{rr} = \frac{19500.00}{3 \times 14.36} = 452.646$$

Bearing capacity factor can be found using the following formula:

$$N_c^* = 4/3 \times (ln(I_{rr}) + 1) + \pi/2 + 1 = 12.057 \quad [125]$$

Substituting the values in the Formula 119, we get:

$$Q_p = 0.292\, m^2 \times 14.36\, kN/m^2 \times 12.057 = 50.556\, kN$$

Average of the two methods is taken to ensure more accurate results.

$$Q_{p,\,ave} = \frac{37.738+50.556}{2} kN = 44.147\, kN$$

The end bearing capacities for each layer are presented in Table 4.8.

Table 4.8. Point Bearing Capacity calculations for piles in Clay layers.

Depth, m	Type of soil	Q_p, kN (Meyerhof's)	Q_p, kN (Vesic's)	Q_p, kN (average)
0.15-1.52	Fat CLAY (CH)	0.000	0.000	0.000
1.52-3.05	Lean CLAY (CL)	0.000	0.000	0.000
3.05-7.62	Lean CLAY (CL)	37.738	50.108	43.923

7.62-10.67	Fat CLAY (CH)	37.738	50.556	44.147
12.19-13.72	Lean CLAY (CL)	37.738	47.095	42.416
15.24-18.29	Lean CLAY (CL)	37.738	49.622	43.680

Frictional Resistance Clay

There are three methods to find the frictional resistance of a clay layer: α, β, and λ methods.

λ ***method***

$$f_{av} = \lambda(\overline{\sigma_0}' + 2c_u) \quad [126]$$

where,

f_{av} - average unit frictional resistance

$\overline{\sigma_0}'$ - mean effective vertical stress

Variation of λ with Pile Embedment Length was found using Table 12.10 from Das & Sivakugan (2019). The bearing capacity in this method is:

$$Q_s = pLf_{av} \quad [127]$$

Calculating the values of c_u and $\overline{\sigma_0}'$, we get:

$$c_u = \frac{(c_{u(1)}L_1 + c_{u(2)}L_2 + \ldots)}{L} \quad [128]$$

$$c_u = \frac{45.486\times(10.30-7.62)+45.486\times(7.30-3.05)+0+0}{10.30-7.62} = 45.49\ kN/m^2$$

$$\overline{\sigma_0}' = \frac{(A_1 + A_2 + \ldots)}{L} \quad [129]$$

$$\overline{\sigma_0}' = \frac{20.239+20.506+179.088+74.653}{10.3} = 28.591\ kN/m^2$$

Now having found all necessary values, we can find f_{av}, and then Q_s:

$$f_{av} = 0.185 \times (28.591 + 2 \times 45.49) = 41.865\ kN/m^2$$

$$Q_s = 1.916 \times 7 \times 41.865 = 561.493\ kN$$

β ***method***

In this method, the formula for skin resistance is as follows:

$$Q_s = \sum fp\Delta L \quad [130]$$

The unit frictional resistance can be found using:

$$f = (1 - sin\phi'_R) \times tan\phi'_R \times \sigma_0' \quad [131]$$

Calculating all the values:

$$f = (1 - sin(34^o)) \times tan(34^o) \times 61.256 = 18.213\ kN/m^2$$

$$Q_s = 18.213 \times 1.916 \times (10.300 - 7.620) = 93.522\ kN$$

α ***method***

The α method uses the following formula to find frictional resistance:

$$Q_s = \sum \alpha c_u p \Delta L \quad [132]$$

where,

α - empirical adhesion factorTo find the α, the next formula is suggested by Sladen (1992):

$$\alpha = C\left(\frac{\overline{\sigma_0'}}{c_u}\right)^{0.45} \quad [133]$$

So the value of α is:

$$\alpha = 0.5 \times \left(\frac{42.069}{71.478}\right)^{0.45} = 0.483$$

Substituting values in Formula 128, skin friction is:

$$Q_s = 0.483 \times 71.478 \times 1.916 \times 7 = 241.535\ kN$$

The results of calculation for all clay layers are tabulated below.

Table 4.9. Calculation results for the skin friction of piles in the Clay layers.

Depth, m	Type of soil	α *method*	β *method*	λ *method*	Average
0.15-1.52	Fat CLAY (CH)	0.00	7.585	0.00	2.53
1.52-3.05	Lean CLAY (CL)	0.00	33.753	0.00	11.25
3.05-7.62	Lean CLAY (CL)	99.06	132.396	444.11	225.19
7.62-10.67	Fat CLAY (CH)	241.54	93.522	561.49	298.85
12.19-13.72	Lean CLAY (CL)	415.94	60.381	748.00	408.11
15.24-18.3	Lean CLAY (CL)	655.86	55.455	828.01	513.11

Point Bearing Capacity in Sand

The depth was chosen to be 14.3 m, the basement is 3.3 m, so the depth of the pile is 11 m. To estimate the point bearing capacity of the pile in sand, we used 5 methods: Meyerhof's, Vesic's, Coyle & Castello's, Meyerhof's based on SPT, and Braudi's based on SPT.

Meyerhof's End Bearing Capacity in Sand

According to Meyerhof, Q_p can be found using:

$$Q_p = A_p q_p = A_p q' N_q^* \leq A_q q_l \quad [134]$$

$$q_l = 0.5 p_a N_q^* tan\varphi' \quad [135]$$

where,

q' - effective vertical stress at the pile tip

q_l - limiting point resistance

N_q^* - bearing capacity factor for pile

Calculation of the q' for Clayey Sand layer is given in Table 4.10.

Table 4.10. q' estimation.

Type of soil	$\gamma - \gamma_w$, kN/m^3	H_i, m	$\gamma' \times H_i$, kN/m^2
Fat CLAY (CH)	17.52	1.52	26.630
Lean CLAY (CL)	17.52	1.53	26.806
Lean CLAY (CL)	7.34	4.57	33.544
Fat CLAY (CH)	6.24	3.05	19.032
Clayey SAND (SC)	7.86	1.52	11.947
Lean CLAY (CL)	7.86	1.53	12.026
Clayey SAND (SC)	7.64	1.52	11.613
q'			137.166

Bearing capacity factor $N_q^* = 115$ is found using Table 12.6 from the friction angle

(34°) values (Das & Sivakugan, 2019).

$$Q_p = 0.292\,m^2 \times 137.166\,kN/m^2 \times 115 = 4606.048\,kN$$

$$Q_l = 0.292\,m^2 \times 0.5 \times 100\,kN/m^2 \times 115 \times tan(34^\circ) = 1132.688\,kN$$

$$\text{Since } Q_p > Q_l,\ Q_p = 1132.688\,kN$$

Vesic's End Bearing Capacity in Sand

Vesic proposed the following formula to find Q_p:

$$Q_p = A_p q_p = A_p \overline{\sigma_0'} N_\sigma^* \quad [136]$$

where,

N_σ^* - bearing capacity factor, found using table 12.8 from Das & Sivakugan (2019).

$$\sigma_0' = \left(\frac{1+2K_0}{3}\right) \times q' \quad [137]$$

$$K_0 = 1 - sin\varphi' \quad [138]$$

$$I_{rr} = \frac{I_r}{1+I_r\Delta} \quad [139]$$

$$I_r = \frac{E_s}{2(1+\mu_s)\times q' tan\varphi'} \quad [140]$$

$$E_s = m \times p_a \text{, m = 750 for dense soil} \quad [141]$$

$$\mu_s = 0.1 + 0.3\left(\frac{\varphi'-25}{20}\right) \text{ - for } 25^\circ \leq \varphi' \leq 45^\circ \quad [142]$$

where,

$\overline{\sigma_0'}$ - mean effective normal ground stress at the level of the pile tip

K_0 - earth pressure coefficient at rest

Δ - average volumetric strain in the plastic zone below the pile point

E_s - modulus of elasticity of soil

μ_s - Poisson's ratio of soil

Calculating these values:

$$\Delta = 0.005\left(1 - \frac{\varphi' - 25}{20}\right) \times \frac{q'}{p_a} \quad [143]$$

$$E_s = 750 \times 100 = 75000\, MPa$$

$$\mu_s = 0.1 + 0.3\left(\frac{34-25}{20}\right) = 0.235$$

$$\Delta = 0.005\left(1 - \frac{34-25}{20}\right) \times \frac{137.166}{100} = 0.004$$

$$I_r = \frac{75000}{2(1+0.235)\times 137.166 \times tan34} = 328.406$$

$$I_{rr} = \frac{328.406}{1+328.406\times 0.004} = 146.690$$

$$N_\sigma^* = 90.96 \text{ from Table 12.8.}$$

$$K_0 = 1 - sin34^\circ = 0.441$$

$$\overline{\sigma_0}' = \left(\frac{1+2\times 0.441}{3}\right) \times 137.166 = 86.054\, kN/m^2$$

Therefore, the value of Q_p is:

$$Q_p = 0.292 \times 86.054 \times 90.96 = 2285.628\, kN$$

Coyle and Castello's End Bearing Capacity in Sand

Coyle and Castello's method suggests that:

$$Q_p = A_p q' N_q^* \quad [144]$$

where,

N_q^* bearing capacity factor

The value of N_q^* can be found using Figure 12.20 in the book by Das & Sivakugan (2019). It depends on the embedment ratio L/D ratio and friction angle of the soil.

$$L/D = \frac{11}{0.5} = 22 \quad [145]$$

N_q^* for the pile at the depth of 14.3 m is 45.

$$Q_p = 0.292 \times 137.166 \times 45 = 1802.366\, kN$$

End Bearing Capacity in Sand based on SPT

Meyerhof's bearing capacity formula based on SPT-N is as follows:

$$q_p = 0.4 p_a N_{60} \frac{L}{D} \leq 4 p_a N_{60} \quad [146]$$

where,

N_{60} - average value of the SPT-N near the pile point (10D above to 4D below the pile point)

$$q_p = 0.4 \times 100 \times 22 \times \frac{13+19+7+27+11}{5} = 13\,552\ kN/m^2$$

$$Q_p = q_p A_p = 13552 \times 0.292 = 2957.184\ kN$$

Braudi's bearing capacity based on SPT values is expressed as:

$$q_p = 19.7 p_a (N_{60})^{0.36} \quad [147]$$

$$q_p = 19.7 \times 100 \times \left(\frac{13+19+7+27+11}{5}\right)^{0.36} = 5271.979\ kN/m^2$$

$$Q_p = A_p q_p = 5271.979 \times 0.292 = 1539.418\ kN$$

Summary of all bearing capacity calculation results is given below.

Table 4.11. Q_p estimation results for piles in Sand.

Qp in SAND						
Depth, m	Type of soil	Meyerhof	Vesic	Coyle & Castello	Meyerhof SPT	Briaudi SPT
10.67-12.19	Clayey SAND (SC)	3794.782	2068.549	1418.918	3208.107	1532.191
13.72-15.24	Clayey SAND (SC)	4606.048	2285.628	1802.366	3957.184	1539.418
18.29-24.38	Clayey SAND (SC)	4637.467	2311.394	2118.349	9133.760	1923.716
24.38-27.43	Poorly graded SAND with clay (SP-SC)	5194.445	2335.536	1731.482	19600.000	2098.194
27.43-30.48	Clayey SAND (SC)	5897.501	2651.646	1747.408	19200.000	2253.756

For further calculations, we chose to use values of the Coyle & Castello method. Because the range of results is wide, we decided to use the lowest numbers.

Frictional Resistance in Sand

Frictional resistance in sand was calculated using 4 methods: using general formula for skin friction, Coyle & Castello's, Meyerhof's and Braudi's based on SPT results.

General Formula

The formula of skin resistance is:

$$Q_s = \sum fp\Delta L \quad [148]$$

$$f = (1 - sin\phi'_R) \times tan\phi'_R \times \sigma_0' \quad [149]$$

The calculated results are shown in the table below:

Table 4.12. Calculation of the frictional resistance in Sand using the general formula.

Depth, m	Type of soil	σ_0', $\frac{kN}{m^2}$	f	Q_s, kN
12.190	Clayey SAND (SC)	26.858	20.693	60.264
15.240	Clayey SAND (SC)	26.524	20.435	59.514
24.380	Clayey SAND (SC)	106.271	76.330	890.653
27.430	Poorly graded SAND with clay (SP-SC)	52.033	37.373	218.402
30.480	Clayey SAND (SC)	52.033	37.373	218.402

Coyle and Castello's method

According to Coyle and Castello, Q_s can be found using the following formula:

$$Q_s = K\overline{\sigma_0'}tan(\delta')pL \quad [150]$$

Table 4.13. Calculation of Q_s in Sand using the method of Coyle and Castello.

Type of soil	Length, m	$\overline{\sigma_0'}$, $\frac{kN}{m^2}$	K	Q_s, kN

Clayey SAND (SC)	8.00	553.25	1.50	578.18
Clayey SAND (SC)	11.00	635.18	1.20	577.00
Clayey SAND (SC)	17.00	1242.45	0.50	511.97
Poorly graded SAND with clay (SP-SC)	23.00	1483.86	0.47	600.62
Clayey SAND (SC)	25.00	1529.13	0.47	625.22

Frictional Resistance in Sand based on SPT

The formula for finding frictional resistance using SPT is as follows:

$$Q_s = pLf_{av} \quad [151]$$

Meyerhof and Braudi proposed their formulas for average unit frictional resistance:

Meyerhof's:

$$f_{av} = 0.02p_a(\overline{N_{60}}) \quad [152]$$

For Braudi's:

$$f_{av} = 0.224p_a(\overline{N_{60}})^{0.29} \quad [153]$$

Table 4.14. Results of the calculation of skin resistance in Sand using SPT-N values.

Length, m	Type of soil	$\overline{N_{60}}$	f_{av}	Meyerhof	f_{av}	Braudi
8.00	Clayey SAND (SC)	18.800	37.976	60.264	52.976	812.01
11.00	Clayey SAND (SC)	18.286	36.937	59.514	52.551	1107.57
17.00	Clayey SAND (SC)	18.889	38.156	890.653	53.048	1727.88
23.00	Poorly graded SAND with clay (SP-SC)	23.700	47.874	218.402	56.656	2496.72

25.00	Clayey SAND (SC)	25.727	51.969	218.402	58.021	2779.20

The frictional resistances of each layer were calculated and tabulated. Then, the cumulative frictional resistance was found at different depths. The results are shown in Table 4.15.

Table 4.15. Total frictional resistance at different depths.

Depth, m	Type of soil	Q_s, kN
0.15-1.52	Fat CLAY (CH)	2.53
1.52-3.05	Lean CLAY (CL)	13.78
3.05-7.62	Lean CLAY (CL)	238.97
7.62-10.67	Fat CLAY (CH)	537.82
10.67-12.19	Clayey SAND (SC)	1159.53
12.19-13.72	Lean CLAY (CL)	1567.64
13.72-15.24	Clayey SAND (SC)	2213.41
15.24-18.29	Lean CLAY (CL)	2726.52
18.29-24.38	Clayey SAND (SC)	3849.89
24.38-27.43	Poorly graded SAND with clay (SP-SC)	5459.03
27.43-30.48	Clayey SAND (SC)	7294.48

Negative Skin Friction

Negative skin friction can happen when clay layers are located above granular soil. In our case, the clay layer is located above sand. Therefore, the piles will be subjected to negative skin friction.

The formula for negative skin friction is:

$$Q_n = \frac{pK'\gamma'_f H^2_f tan\delta'}{2} \quad [154]$$

Table 4.16. Calculation results of the negative skin friction.

Depth, m	Type of soil	γ_f', $\frac{kN}{m^3}$	K'	$0.6\phi'$, deg	Q_n, kN
1.52	Fat CLAY (CH)	17.520	1.000	0.000	0.000
3.05	Lean CLAY (CL)	17.520	1.000	0.000	0.000
7.62	Lean CLAY (CL)	7.340	0.441	20.400	66.955
10.67	Fat CLAY (CH)	6.240	0.441	20.400	111.606
12.19	Clayey SAND (SC)	7.860	0.441	20.400	183.487
13.72	Lean CLAY (CL)	7.860	0.441	20.400	232.437
15.24	Clayey SAND (SC)	7.640	0.441	20.400	278.765
18.29	Lean CLAY (CL)	7.640	0.441	20.400	401.510
24.38	Clayey SAND (SC)	7.640	0.470	19.200	712.390
27.43	Poorly graded SAND with clay (SP-SC)	7.250	0.470	19.200	855.750
30.48	Clayey SAND (SC)	7.250	0.470	19.200	1056.635
33.53	SILTSTONE	6.560	0.369	23.467	1132.663
39.62	CLAYSTONE	6.560	0.369	23.467	1581.476
40.23	SILTSTONE	5.660	0.369	23.467	1406.845

4.3.3.2. Group of piles

Since a single pile could bear a load of 10 000 kN, it was necessary to prepare a design for a group of piles. Ultimate bearing capacity of the group of piles can be calculated using the formula:

$$Q_{g(u)} = \Sigma Q_u \quad [155]$$

where,

$Q_{g(u)}$ - ultimate load-bearing capacity of the group pile

Q_u - ultimate load-bearing capacity of each pile

The formula for ΣQ_u:

$$\Sigma Q_u = (n_1 \times n_2) \times Q_u \quad [156]$$

where,

n_1, n_2 - number of piles

For example, for the configuration 3 to 2:

$$\Sigma Q_u = 3 \times 2 \times 3737.012 = 22422.073\ kN/m^2$$

For the safety purposes, the ultimate bearing capacity of the group is divided by the Factor of Safety (FS=3):

$$Q_{g(all)} = \frac{Q_{g(u)}}{FS} \quad [157]$$

Another point to consider is the efficiency of the group of piles:

$$\eta = \frac{2(n_1+n_2-2)d+4D}{p \times n_1 \times n_2} \quad [158]$$

If the value of $\eta \geq 1$, the group of piles act as individual piles.

Then, $Q_{g(u)} = \Sigma Q_u$

If the value of $\eta < 1$, the group of piles acts as a block.

Then, $Q_{g(u)} = \eta \Sigma Q_u$

Also, to design the pile cap, the dimensions of it needs to be calculated:

$$L_g = (n_1 - 1)d + 2(D/2) \quad [159]$$

$$B_g = (n_2 - 1)d + 2(D/2) \quad [160]$$

After analyzing many a number of possible variations, including changing the diameter size of the pile from 0.406 to 0.610 m, the length from 8 to 23 m, checking different configurations, and altering center-to-center spacing, the following layout was chosen:

Table 4.17. Group pile design parameters.

	Interior	Exterior	Corner
Configuration	3x3	3x2	2x2

Diameter, m	0.610	0.610	0.610
Length, m	11.00	11.00	11.00
Spacing, m	1.83	1.83	1.83
n1	3.00	3.00	2.00
n2	3.00	2.00	2.00
Bg, m	4.27	2.44	2.44
Lg, m	4.27	4.27	2.44
p, m	1.917	1.917	1.917
A, m^2	0.292	0.292	0.292

The following table shows the allowable bearing capacities of the piles and column loads:

Table 4.18. Bearing capacities of the pile groups and exerted column loads.

Column	Chosen configuration	Q_u, kN	Group efficiency	Q_g, kN	Q_{all}, kN	P_u, kN
Interior	3x3	3737.012	0.990	33313.240	11104.413	10895.21
Exterior	3x2	3737.012	1.167	22422.073	7474.024	6780.850
Corner	2x2	3737.012	1.273	14948.049	4982.683	4209.220

The piles will be placed under each column in the following arrangement:

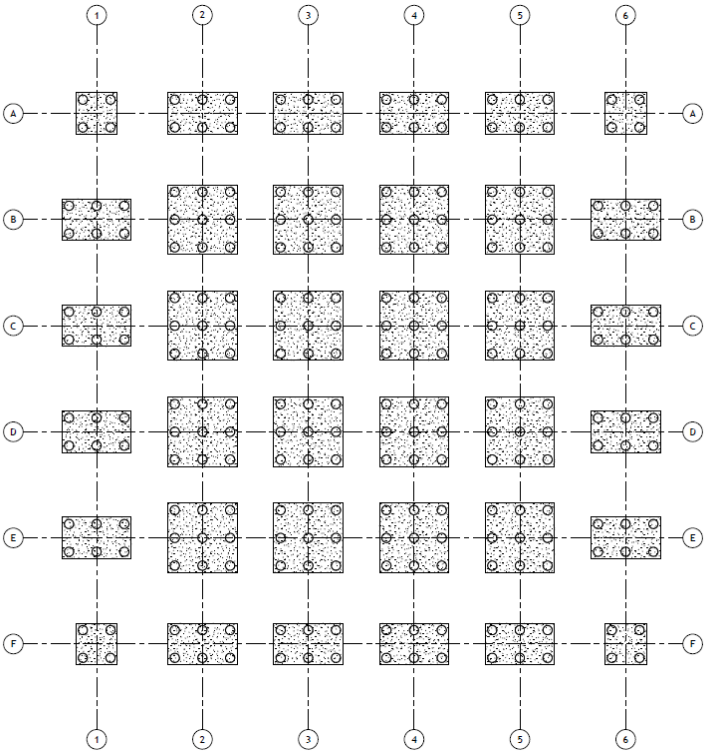

Figure 4.11. Pile layout.

4.3.4. Settlement

4.3.4.1. Elastic Settlement

Elastic Settlement for Single pile

Length and diameter of the pile are 0.61 m and 12.7 m.

According to the method of Vesic (1977), there are three components to find total settlement of the pile head.

To estimate total elastic settlement of pile head under working load of Q_w the following formula was used:

$$s_e = s_{e(1)} + s_{e(2)} + s_{e(3)} \quad [161]$$

Firstly, the elastic shortening with skin friction taken into consideration is estimated by this equation:

$$s_{e(1)} = \frac{(Q_{wp} + \xi Q_{ws})L}{A_p E_p} \quad [162]$$

where,

Q_{wp} - working load at pile point

Q_{ws} - working load along the pile shaft

A_p - cross-sectional area of pile point

L - length of pile

E_p - elasticity modulus of pile material

ξ - constant which depends on skin friction distribution

$$Q_{wp} = \frac{1418.918}{3} = 472.97\ kN$$

$$Q_{ws} = \frac{578.18}{3} = 192.727\ kN$$

$A_з$=0.292 m2

L=11 m

$E_з$=$4700\sqrt{30} = 25743\ MPa$ - for normal weight concrete (civil engineering portal)

Average compression strength for normal concrete was taken as 30 MPa.

ξ=0.67, as the skin friction increases with depth.

$$s_{e(1)} = \frac{(472.97+0.67*192.727)*11}{0.292*25743000} = 0.00088108 \text{ m}$$

The formula for the pile settlement caused by load carried at pile point is given by:

$$s_{e(2)} = \frac{q_{wp}D}{E_s}(1 - \mu_s^2) \qquad [163]$$

$$q_{wp} = \frac{Q_{wp}}{A_p} = 1619.76 \text{ kN/m2}$$

where,

D - diameter of pile

q_{wp} - point load per unit area at pile point

E_s - elasticity modulus of soil at/below pile point =9623.5 kN/m2

μ_s - Poisson's ratio of soil=0.205

I_{wp} - influence factor ≈0.85

$$s_{e(2)} = \frac{1619.76*0.61}{9623.5}(1 - 0.042)0.85 = 0.0836\ m$$

Pile settlement caused by load carried by pile shaft was calculated by the following equation:

$$s_{e(3)} = (\frac{Q_{ws}}{pL})\frac{D}{E_s}(1 - \mu_s^2)I_{ws} \qquad [164]$$

$$s_{e(3)} = (\frac{192.797}{1.917*12.7})\frac{0.61}{9623.5}(1 - 0.205)3.597 = 0.00144\ m$$

where,

p - pile perimeter = 1.917 m

L - embedded pile length

I_{ws} - influence factor

The influence factor can be calculated by relationship proposed by Vesic (1977):

$$I_{ws} = 2 + 0.35\sqrt{\frac{L}{D}}=3.597 \quad [165]$$

$$s_e = s_{e(1)} + s_{e(2)} + s_{e(3)}=0.00088108+0.0836+0.00144=0.0859 \text{ m}$$

Elastic Settlement for Group of piles

Vesic (1969) suggested simplified formula for settlement of group of piles:

$$s_{g(e)} = \sqrt{\frac{B_g}{D}} \quad [166]$$

where,

B_g - group pile section width

D - each pile's width/diameter

S_e - each pile's elastic settlement

L - embedment length of piles

Table 4.19. Elastic settlement of group piles.

	D (m)	B_g (m)	s_e(m)	$S_{g(e)}$ (m)
Exterior	0.61	2.75	0.0859	0.1824
Interior	0.61	4.88	0.0859	0.243
Corner	0.61	2.75	0.0859	0.1824

4.3.4.2. Consolidation settlement of group piles

For calculation of consolidation settlement 2:1 stress distribution method was used (Das, 2019).

Increase in effective stress caused at the middle of each layer of soil by load Q_g can be computed by the following formula:

$$\Delta\sigma_i' = \frac{Q_g}{(B_g+z_i)(L_g+z_i)} \quad [167]$$

where,

$\Delta\sigma'_i$-increase in effective stress at middle of layer i

B_g, L_g - width and length of group piles

z_i - distance from z=0 to middle of clay layer i

To calculate consolidation settlement of each layer caused by increased stress next relationship was used:

$$\Delta s_{c(i)} = [\frac{\Delta e_{(i)}}{1+e_{o(i)}}]H_i \quad [168]$$

where,

$\Delta s_{c(i)}$- consolidation settlement of layer i

$\Delta e_{(i)}$- change in void ratio

$e_{o(i)}$-initial void ratio of layer i

H_i-thickness of layer i

Eventually, total consolidation settlement found in the following way:

$$\Delta s_{c(g)} = \sum \Delta s_{c(i)} \quad [169]$$

Settlement for clay layer 1:

$$\Delta\sigma'_{(1)} = \frac{22422.073}{(2.75+1.525)(4.88+1.525)} = 818.88\ kN/m^2$$

$$\Delta\sigma'_{o(1)} = 17.15 * 4.57 + (16.05 - 9.81) * 3.05 = 97.408\ kN/m^2$$

$$\Delta s_{c(1)} = \frac{C_{c(1)}H_1}{1+e_{o(1)}} log[\frac{\sigma'_{o(1)}+\Delta\sigma'_{(1)}}{\sigma'_{o(1)}}] = \frac{0.11*3.05}{1+0.63} log[\frac{97.408+818.88}{97.408}] = 0.20\ mm$$

Settlement for clay layer 2:

$$\Delta\sigma'_{(2)} = \frac{22422.073}{(2.75+0.765)(4.88+0.765)} = 1130\ kN/m^2$$

$$\Delta\sigma'_{o(2)} = 17.15 * 4.57 + (16.05 - 9.81) * 3.05 + 0.765 * (17.45 - 9.81) =$$

$$= 103.252\ kN/m^2$$

$$\Delta s_{c(1)} = \frac{0.11*1.53}{1+0.63} log[\frac{103.252+1130}{103.252}] = 0.11\ mm$$

$$\Delta s_{c(g)} = 0.20 + 0.11 = 0.31\ mm$$

Void ratio and compression index values were taken from the report.

4.3.5. Lateral Earth Pressure

To properly design such structures as sheet-pile walls, retaining walls, braced cuts and others lateral earth pressure needs to be calculated. Here, several factors are significant including wall movement type and amount, soil's parameters of shear strength, soil's unit weight and backfill's conditions of drainage. There are three different special cases of lateral earth pressure: at-rest earth pressure, active earth pressure and passive earth pressure. In this project, only active earth pressure will be considered.

Active earth pressure:

Basement depth at 3.3 m was chosen for this project.

$$\sigma_a' = \sigma_o' K_a \quad [170]$$

$$K_a = tan^2(45 - \frac{\phi'}{2}) \quad [171]$$

$$P_a = A_1 + A_2 + A_3 + A_4 \quad [172]$$

Table 4.20. Active earth pressure calculations.

Depth (m)	γ (kN/m^3)	ϕ (degrees)	σ_0' (kN/m^2)	K_a	σ_a' (kN/m^2)	P_a (kN/m)	Distance of line of action
0	17.52	30	0	0.33	0	27.287	1.11
1.52-	17.52	30	26.6304	0.33	8.788		
1.52+	17.15	34	26.0680	0.28	7.30		
3.05-	17.15	34	52.3075	0.28	14.646		
3.05+	17.15	34	52.3075	0.28	14.646		
3.3	17.15	34	56.595	0.28	15.847		

$$P_a = 0.5 * 1.52 * 7.3 + 1.53 * 8.7880 + 0.5 * 1.53 * (14.646 - 8.788) + 0.25 * 14.646 +$$

$$+ 0.5 * 0.25 * (15.847 - 14.646) = 5.548 + 13.44564 + 4.48137 + 3.6615 + 0.150125$$

$$= 27.287\ kN/m$$

Distance of line of action:

$$z = \frac{A_1(1.78+\frac{1.52}{3})+A_2(1.015)+A_3(0.25+\frac{1.53}{3})+A_4(\frac{0.25}{2})+A_5(\frac{0.25}{3})}{P_a} =$$

$$= \frac{5.548*2.287+13.44564*(1.015)+4.48137(0.76)+3.6615*0.125+0.150125*0.083}{27.287} = 1.11m$$

4.4. Retaining wall design

Cantilever wall was chosen, as this is a cost-saving option. First, approximate dimensions were taken from the following figure.

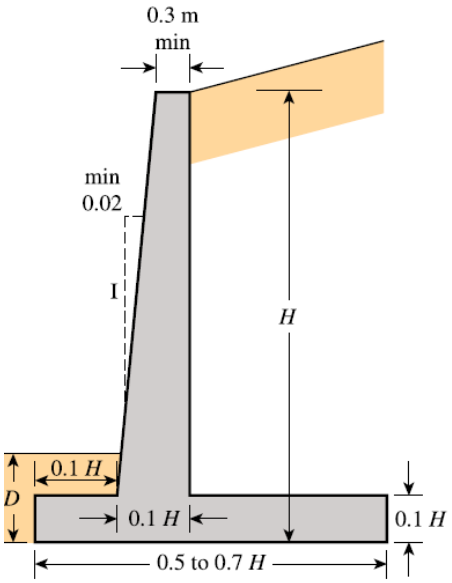

Figure 4.12. Approximate dimensions for cantilever wall.

Using AutoCAD, a preliminary design of the retaining wall was drawn. For D a minimum value of 0.6 m was chosen. Top of stem=0.3 m, which is a minimum value.

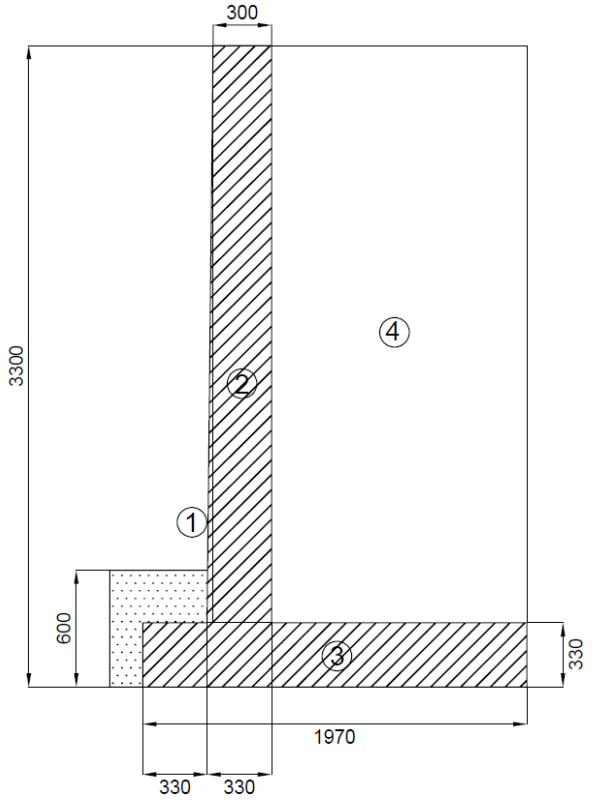

Figure 4.13. Retaining wall design.

Next, moments of forces resisting overturning were calculated. Area of each section was found, then weight per unit length was determined. The calculated values are presented in the table below.

$$A_1 = 0.5 * 0.03 * 2.97 = 0.045\, m^2$$

$$A_2 = 2.97 * 0.30 = 0.891\, m^2$$

$$A_3 = 1.97 * 0.33 = 0.650\, m^2$$

$$A_4 = 1.31 * 2.97 = 3.891\, m^2$$

$$W = A * \gamma \qquad [173]$$

Where,

W - weight per unit length, kN/m

Unit weight of concrete and unit weight of backfill are 24 kN/m^3 and 17.52 kN/m^3 respectively.

$$W_1 = 0.04455 * 24 = 1.069\, kN/m$$

$$W_2 = 0.891 * 24 = 21.384\, kN/m$$

$$W_3 = 0.6501 * 24 = 15.602\ kN/m$$

$$W_4 = 3.8907 * 17.52 = 68.165\ kN/m$$

$$\Sigma V = W_1 + W_2 + W_3 + W_4 \quad [174]$$

$$\Sigma V = 1.069 + 21.384 + 15.602 + 68.165 = 106.221\ kN/m$$

$$M = W * X \quad [175]$$

Where,

X - moment arm from C, m

Moment arm is a horizontal distance from point C to section centroid.

$$M_1 = 1.0692 * 0.35 = 0.374\ kN * m/m$$

$$M_2 = 21.384 * 0.51 = 10.906\ kN * m/m$$

$$M_3 = 15.6024 * 0.985 = 15.368\ kN * m/m$$

$$M_4 = 68.165064 * 1.315 = 89.63\ kN * m/m$$

$$\Sigma M_R = M_1 + M_2 + M_3 + M_4 \quad [176]$$

$$\Sigma M_R = 0.374 + 10.906 + 15.368 + 89.63 = 116.285\ kN * m/m$$

Table 4.21. Calculation of moments of forces resisting overturning about C

Section	Area (m^2)	Weight/unit length (kN/m)	Moment arm from C (m)	Moment about C (kN*m/m)
1	0.045	1.069	0.350	0.374
2	0.891	21.384	0.510	10.906
3	0.650	15.602	0.985	15.368
4	3.891	68.165	1.315	89.637
		ΣV=106.221		ΣM_R=116.285

Check for overturning

Overturning moment is calculated via the next formula:

$$\Sigma M_o = P_a cos\alpha(\frac{H}{3}) \quad [177]$$

$$\Sigma M_o = 27.287 * 1 * \frac{3.3}{3} = 30.0157\ kN * m/m$$

Then, factory of safety was found:

$$FS_{(overturning)} = \frac{\Sigma M_R}{\Sigma M_o} \quad [178]$$

$$FS_{(overturning)} = \frac{116.2854832}{30.0157} = 3.87 > 2 \text{ (OK)}$$

Minimum value for desired factor of safety against overturning is 2-3, which is why the calculated value is acceptable.

Check for sliding along the base

A minimum required value of factor of safety against sliding is 1.5. To reach the desired factor of safety, a key to the base slab was used.

The following formula was used to calculate passive force per unit length:

$$P_p = \frac{1}{2}\gamma_2 D_1^2 K_p + 2c_2' D_1\sqrt{K_p} \quad [179]$$

$$K_p = tan^2(45 + \frac{34}{2}) = 3.537$$

$$P_p = \frac{1}{2} * 17.52 * 0.6^2 * 3.537 = 11.154\ kN/m$$

Factor of safety against sliding is calculated below. k_1 and k_2 values usually range from ½ to ⅔. For the calculation ⅔ value was taken.

$$FS_{(sliding)} = \frac{(\Sigma V)tan(k_1\phi_2') + Bk_2c_2' + P_p}{P_a cos\alpha} \quad [180]$$

$$FS_{(sliding)} = \frac{106.221*tan(\frac{2}{3}*34)+11.154}{27.287} = 2.034 > 1.5 \text{ (OK)}$$

The calculated value is acceptable.

Check for bearing capacity failure

Distance from toe C $\overline{X}$ is determined:

$$\overline{X} = \frac{\Sigma M_R - \Sigma M_O}{\Sigma V} \quad [181]$$

$$\overline{X} = \frac{116.285-30.0157}{106.221} = 0.812 \text{ m}$$

Width of the cantilever wall, B is equal to 1.970 m.

Eccentricity of the resultant force R is found in the following way:

$$e = \frac{B}{2} - \overline{X} \quad [182]$$

$$e = \frac{1.970}{2} - 0.812 = 0.173\,m < \frac{B}{6} = \frac{1.970}{6} = 0.328\,m$$

Calculated eccentricity value is acceptable, which is why there is no need to unproportionate the retaining wall and reduce eccentricity.

$$q_{toe} = \frac{\Sigma V}{B}(1 + \frac{6e}{B}) \quad [183]$$

$$q_{heel} = \frac{\Sigma V}{B}(1 - \frac{6e}{B}) \quad [184]$$

Maximum and minimum pressures are calculated:

$$q_{toe} = \frac{106.221}{1.970}(1 + \frac{6*0.173}{1.970}) = 82.330\,kN/m^2$$

$$q_{heel} = \frac{106.221}{1.970}(1 - \frac{6*0.173}{1.970}) = 25.509\,kN/m^2$$

The formula for ultimate bearing capacity of shallow foundation is used, as the retaining wall is considered as continuous foundation.

$$q_u = c_2' N_c F_{cd} F_{ci} + qN_q F_{qd} F_{qi} + \frac{1}{2}\gamma_2 B' N_\gamma F_{\gamma d} F_{\gamma i} \quad [185]$$

Where,

$$q = \gamma_2 D \quad [186]$$

$$B' = B - 2e \quad [187]$$

For $\phi_2' = 34°$ bearing capacity factors are: N_c=42.16, N_q=29.44, N_γ=41.06.

$$q = 17.52 * 0.6 = 10.512\,kN/m^2$$

$$B' = 1.970 - 2 * 0.173 = 1.624\,m$$

First, depth factors are found using equations for $\frac{D}{B} \leq 1$, $\phi_2' > 0$:

$$F_{qd} = 1 + 2tan\phi_2'(1 - sin\phi_2')^2(\frac{D}{B}) \quad [188]$$

$$F_{qd} = 1 + 2tan34^\circ(1 - sin34^\circ)^2(\frac{0.6}{1.970}) = 1.080$$

$$F_{cd} = F_{qd} - \frac{1-F_{qd}}{N_c tan\phi_2'} \quad [189]$$

$$F_{cd} = 1.080 - \frac{1-1.080}{42.16*tan34} = 1.083$$

$$F_{\gamma d} = 1$$

Then, inclination factors are calculated:

$$F_{ci} = F_{qi} = (1 - \frac{\psi}{90})^2 \quad [190]$$

$$F_{\gamma i} = (1 - \frac{\psi}{\phi_2})^2 \quad [191]$$

Where,

ψ - load inclination

$$\psi = tan^{-1}(\frac{P_a cos\alpha}{\Sigma V}) \quad [192]$$

$$\psi = tan^{-1}(\frac{27.287}{106.221}) = 14.407$$

$$F_{ci} = F_{qi} = (1 - \frac{14.407}{90})^2 = 0.705$$

$$F_{\gamma i} = (1 - \frac{14.407}{34})^2 = 0.332$$

$$q_u = 10.512 * 29.44 * 1.080 * 0.705 + \frac{1}{2} * 17.52 * 1.624 * 41.06 * 1 * 0.332$$

$$q_u = 429.564\ kN/m^2$$

The required value for factor of safety is 3. To find safety factor against bearing capacity failure next formula is used:

$$FS_{(bearing\ capacity)} = \frac{q_u}{q_{max}} \quad [193]$$

$$FS_{(bearing\ capacity)} = \frac{429.564}{82.330} = 5.217$$

Selection of foundation

It was concluded that the most optimal option is pile foundation due to a number of reasons, namely high capacity of bearing loads, adaptability to various soil types and control of settlement. Also, piles are able to reach deeper layers of soil or bedrock and provide more stability to a building against earthquake forces which increases overall safety of structure (civiltoday.com).

4.5. Software analysis of bearing capacities

4.5.1. Axial Bearing Capacity

The bearing capacity and settlement of groups of piles were calculated for soil foundations using Geo5. The results then were compared with hand calculations. Then, Plaxis was used for more accurate modeling of the settlement of all pile groups, because

it takes into account the complex interaction of soil and structures. This allowed the settlement to be estimated while considering a group efficiency, vertical load, and soil's deformation characteristics. The results are presented in Table 4.22.

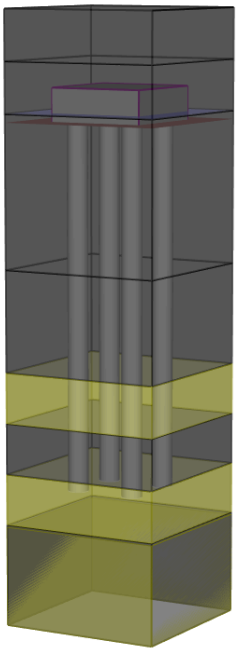

Figure 4.14. Soil profile in GEO5.

In Geo5 Soil analysis type was chosen as cohesive, because mainly the piles interact with clay soil. The results of the bearing capacity check and settlement are shown below.

Analysis of bearing capacity of pile group in cohesionless soils

Max. vertical force includes self-weight of pile cap.

Pile skin bearing capacity	R_s	=	2328,36 kN
Pile base bearing capacity	R_b	=	2853,80 kN
Vertical bearing capacity of single pile	R_c	=	5182,16 kN
Vertical bearing capacity of pile group	R_g	=	16482,73 kN
Maximum vertical force	V_d	=	5233,92 kN

Safety factor = 3,15 > 3,00

Vertical bearing capacity of pile group is SATISFACTORY

Figure 4.15. Bearing capacity check in GEO5.

Analysis of settlement of pile group in cohesive soils
Max. vertical force includes self-weight of pile cap.

The depth of substitute found.	d	=	7,33	m
Maximum service load	N	=	3004,18	kN
Depth of influence zone	h	=	6,38	m
Settlement of pile group	s	=	6,6	mm

Figure 4.16. Settlement analysis in GEO5.

In order to analyze pile groups in PLAXIS 3D a three-dimensional model of the soils and pile groups were created, taking into account the piles' actual geometry as well as their interactions with loads and soils. In calculations, Mohr-Coulomb models in drained conditions were used to analyze pile groups. This approach was chosen because the Mohr-Coulomb model takes into account the soil's strength properties. Drained conditions were used because the calculation considers long-term soil consolidation, when the pore pressure will be dissipated and the settlements will stabilize. This approach helps to obtain realistic results of the settlement under our operational loads.

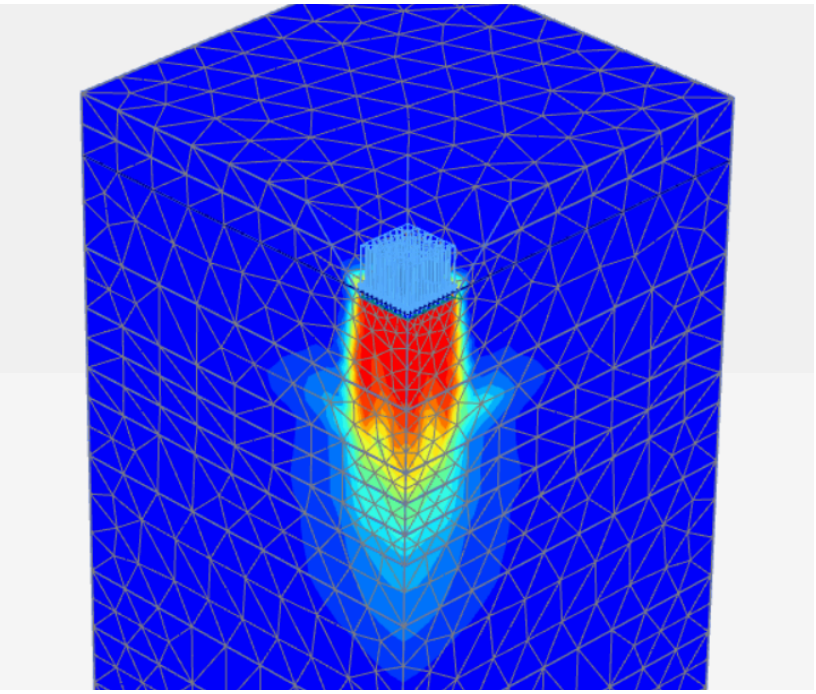

Figure 4.17. Displacement of corner piles in PLAXIS 3D under axial load.

Table 4.22. Comparison of settlement and bearing capacities.

	Applied Load, kN	Group Axial Bearing Capacity, kN		Settlement, mm		
		Hand Calculations	GEO5	Hand Calculations	GEO5	Plaxis 3D
Interior	10895	33633	31809	18.5	6.6	30.2
Exterior	6780	22422	23856	24.8	8.9	42.4
Corner	4209	14948	16482	18.5	8.6	38.1

The results of calculations of the bearing capacity and settlement of pile groups differ due to the different accuracy of the methods. Manual calculations give the highest values of the bearing capacity, since we used simplified formulas. In Geo5, these values are lower, because the program performs more detailed calculations and considers more parameters of the soil and piles. The settlement, on the contrary, is the smallest in Geo5, since not all properties are taken into account. Plaxis 3D shows the greatest settlement, since it models the interaction of piles with each other and with the soil. The differences are due to the level of detail of the calculations.

4.5.2. Lateral bearing capacity of pile foundation

There are two types of laterally loaded piles: short or rigid and long or elastic piles (Das & Sivakugan, 2019). Distribution degree of reaction of soil is affected by several factors, including pile stiffness, soil stiffness and fixity of pile ends. Currently, elastic solution and ultimate load analysis are suggested as solutions for laterally loaded piles. Ultimate load analysis, also referred to as the method of Brom assumes shear failure in soil pile bending.

Calculated lateral loads are presented in the following table. The values for vertical and horizontal forces are taken from the structural part.

Table 4.23. Calculations of lateral loads

Type of	Load	F_x (kN)	F_y (kN)	Pile number	Lateral load

column	combination				(kN)
Interior	1.2D+1L+1Ey	0.503	0.098	9	0.057
Exterior		0.228	-49.410	6	8.235
Corner		-194.132	-32.845	4	49.220

Constant modulus of subgrade reaction η_h and subgrade modulus at depth z, k_z for sandy soil layers are calculated. The results are in the table below.

Table 4.24. Constant modulus of subgrade reaction and subgrade modulus at depth values

Depth (m)	Type of soil	n_h (kN/m^3)	k_z (kN/m^2)
1.52	Clayey sand	4000	6080
1.52	Clayey sand	4000	6080
6.09	Clayey sand	4000	24360
3.05	Poorly graded sand with clay	11000	33500
3.05	Clayey sand	11000	33500

To find numerical value of characteristic length of pile, next relationship is used:

$$T = \sqrt[5]{\frac{E_p I_p}{n_h}} \qquad [194]$$

Where,

E_p - elasticity modulus

I_p - inertia moment

n_h - constant modulus of horizontal subgrade reaction

$E_p = 27806 * 10^3\ kPa$

$$I_p = \frac{\pi D^4}{64} \quad [195]$$

$$I_p = 0,0068\, m^4$$

Constant modulus of horizontal subgrade reaction for submerged, dense sand was found from table 12.16 (Das & Sivakugan, 2019).

$$n_h = 10500$$

$$T = 1.78\, m$$

To find coefficient of rankine passive earth pressure , the following formula was applied:

$$K_p = tan^2(45 + \frac{\phi'}{2}) \quad [196]$$

$$K_p = 1.20$$

Pile length is 11 m and diameter is 0.61m. This means that piles are long because L>5T.

To determine section modulus the next equation is used:

$$S = \frac{I_p}{\frac{d_1}{2}} \quad [197]$$

$$S = 0,0223\, m^3$$

Piles' yield moment was identified in the following way:

$$M_y = SF_Y \quad [198]$$

Where,

S - section modulus of pile section

F_Y - yield stress of pile material

$$M_y = 0.0223 * 35000 = 780kN * m$$

$$\frac{M_y}{D^4 \gamma K_p} = \frac{780}{0.61^4 * 17.15 * 1.20} = 273.73$$

According to the graph of ultimate lateral resistance graph for long piles in sand:

$$\frac{Q_{u(g)}}{K_p D^3 \gamma} = 85$$

$$Q_{u(g)} = 85 K_p D^3 \gamma \quad [199]$$

$$Q_{u(g)} = 85 * 1.20 * 0.61^3 * 17.15 = 397.06\, kN$$

The pile is restrained. Factor of safety is equal to 3.

$$Q_{all} = \frac{Q_{u(g)}}{FS} \qquad [200]$$

$$Q_{all} = \frac{397.06}{3} = 132.35\ kN$$

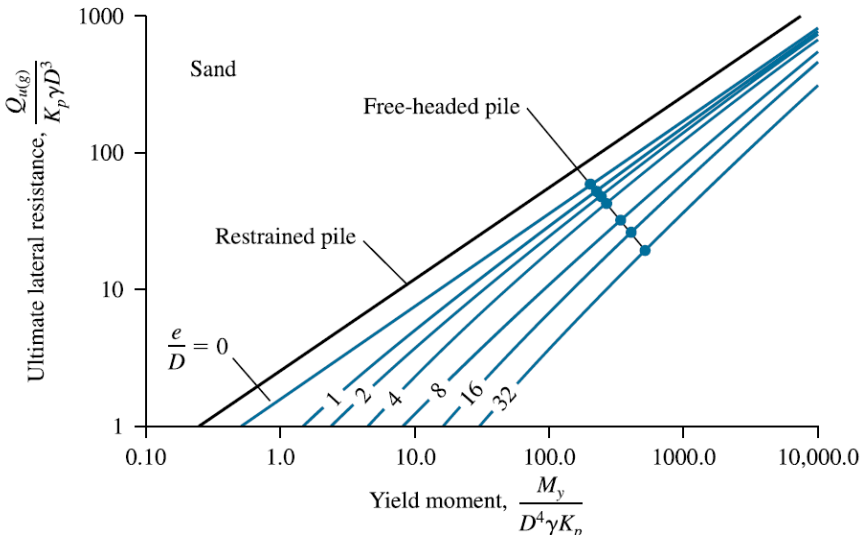

Figure 4.18. Ultimate lateral resistance versus yield moment for long piles in sandy soil.

Table 4.25. Lateral load bearing capacity and lateral load values

Type of column	**Q_{ug} (kN)**	**Q_{all} (kN) Qg**	**$Q_{lateral}$ (kN)**
Interior	1276.38	425.46	0.0569
Exterior	850.92	283.64	8.235
Corner	567.28	189.09	49.22

According to the table, $Q_{lateral} < Q_{all}$.

Lateral deflection

The relationship by Davisson and Gill (1963) was used to calculate deflection for pile foundation incorporated into cohesive soil:

$$x_z(z) = A_x' \frac{Q_g R^3}{E_p I_p} + B_x' \frac{M_g R^2}{E_p I_p} \qquad [201]$$

Where,

A'_x, B'_x - coefficients

R - characteristic length

Coefficients for long piles were taken from the table 12.15 (Das & Sivakugan, 2019).

M_g was taken as zero.

Table 4.26. Pile deflection values and coefficients

Depth (m)	A_x	B_x	x_z (interior)	x_z (exterior)	x_z (corner)
1,52	1.151	0.494	1.46	0.974	0.649
1,52	1.151	0.494	1.46	0.974	0.649
6,09	0.063	0.059	0.080	0.053	0.036
3,05	0.314	-0.0005	0.398	0.266	0.177
3,05	0.314	-0.0005	0.398	0.266	0.177

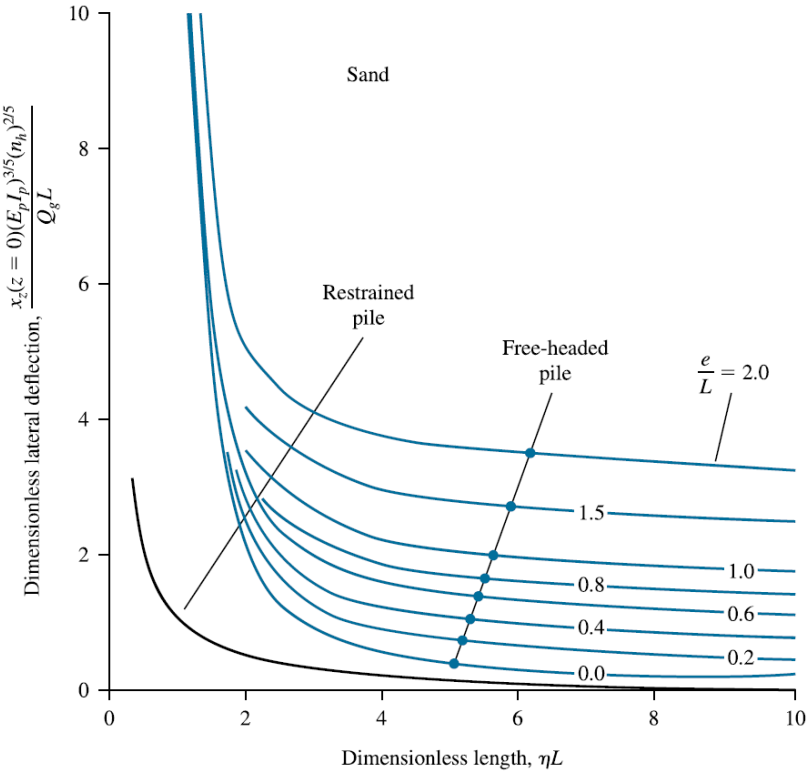

Figure 4.19. Brom's solution for calculation of pile head deflection.

To check for pile head deflection, next formula was used:

$$\eta = \sqrt[5]{\frac{n_h}{E_p I_p}} \qquad [202]$$

$$\eta = \sqrt[5]{\frac{10500}{27806*10^3*0{,}0068}} = 0.561\, m^{-1}$$

$$\eta L = 0.561 * 11 = 6.171$$

According to the figure, dimensionless lateral deflection for the restrained pile is approximately equal to 0.1.

$$\frac{x_z (E_p I_p)^{3/5} (n_h)^{2/5}}{Q_g L} = 0.1$$

4.6. Reinforcement design of a Pile Cap.

4.6.1. Pile cap

Proper pile cap design ensures that loads are distributed uniformly on piles, preventing excessive deformation and settlement, which is critical for overall structural stability. The pile cap calculations use ACI 318-19 for bending, shear and punching

failure, IS 2911: Part 1 for minimum cap thickness, and Eurocode 2 (EN 1992-1-1:2004) for punching strength and load-bearing capacity verification.

$$h_{min} = \frac{largest\ pile\ spacing}{4} + D \quad [203]$$

$$h_{min} = \frac{1.830}{4} + 0.61 = 1.0675\ m$$

$$M = \frac{P_u \times L_g}{4} \quad [204]$$

$$M' = \frac{4209.22 \times 2.44}{4} = 2566.84\ kNm$$

$$A_s = \frac{M'}{0.87 f_y d} \quad [205]$$

$$A_s = 8647,6\ mm^2$$

$$z = 239.923$$

$$A_{st} = 49437.71$$

$$Number\ of\ bars = \frac{A_s}{A_{bar}} \quad [206]$$

$$Number\ of\ bars = \frac{8647,6}{491} = 18$$

$$v_u = \frac{V_u}{bd} \quad [207]$$

$$v_u = \frac{2104.61 \times 10^3}{2440 \times 997} = 0.86\ MPa$$

$$U_1 = 2(B + H) \quad [208]$$

$$U_1 = 2(700 + 700) = 2800\ mm$$

Punching Shear Stress calculations:

$$v_{punch} = \frac{P_u}{U_1 d} \quad [209]$$

$$v_{punch} = \frac{4209.22 \times 10^3}{2800 \times 1} = 1.52\ MPa$$

$$v_{punch} = \frac{P_u}{U_1 d} \leq v_{c,allowable} = 1.8\ MPa$$

If the pile cap's thickness of reinforcement is insufficient, failure may occur, reducing the foundation's bearing capacity resulting in an emergency. So, the new thickness for the pile cap should be calculated.

$$d = \frac{P_u}{U_1 \times v_c} \quad [210]$$

Substituting values:

$$d = \frac{4209.22 \times 10^3}{2800 \times 1.8}$$

$$d = 833.4\, mm$$

$$h_{new} = d + 75 = 833.4 + 75 = 911\, mm \approx 1.0\, m$$

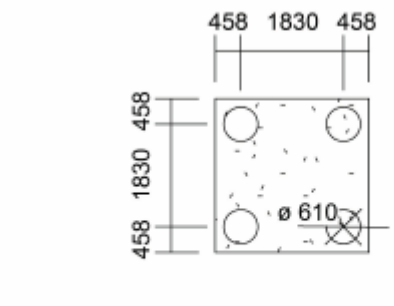

Figure 4.20. Pile group for corner column.

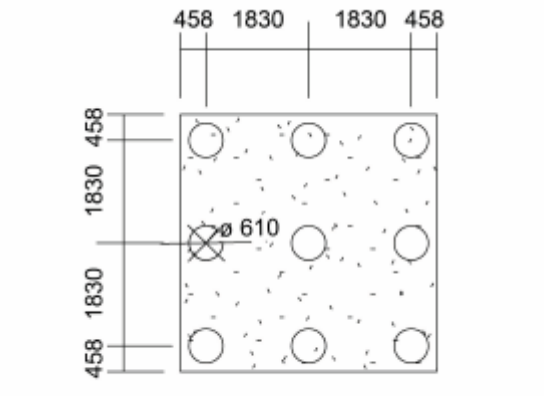

Figure 4.21. Pile group for interior column.

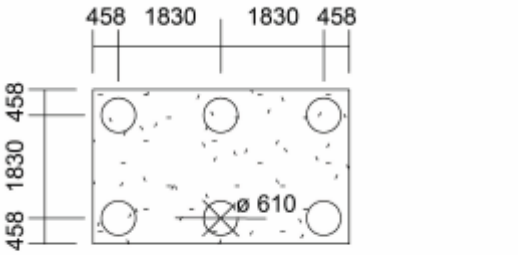

Figure 4.22. Pile group for exterior column.

Table 4.27. Reinforcement configuration for groups of piles.

	Interior	**Exterior**	**Corner**
Configuration	3x3	3x2	2x2
Diameter, m	0.610	0.610	0.610
Length, m	11.00	11.00	11.00
Bg, m	4.27	2.44	2.44
Lg, m	4.27	4.27	2.44
B, m	5.000	3.000	3.000
L, m	5.000	5.000	3.000
h, m	0.915	0.915	0.915
d, m	1.830	1.830	1.830
D (bar), mm	32	30	25
dx, mm	826	826	826
# of bars	22	20	18
Spacing of bars, mm	106	96	87
dy, mm	798	798	798
# of bars	46	40	32
Spacing of bars, mm	112	110	98

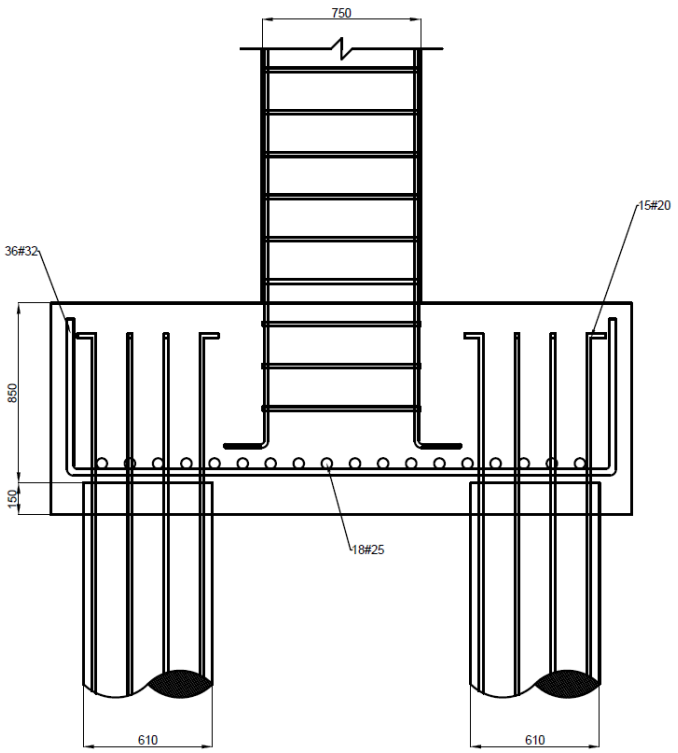

Figure 4.23. Cross section of a Pile Cap.

4.6.2. Single pile

Firstly, the pile should be checked for slenderness.

$$l_e = \beta l_0 = 1.2 \times 11 = 13.2\,m \quad [211]$$

Where,

l_e - effective length of a pile

l_o - unsupported length of a pile

$\beta = 1.2$, since the pile cap is fixed.

$$\frac{l_e}{h} = \frac{13.2}{0.61} = 21.64\,m > 10 \rightarrow Slender\ pile \quad [212]$$

Since the piles are slender, magnified moments will be used for the calculations.

$$a = \frac{l_e^2}{2000h} K = \frac{13.2^2}{2000 \times 0.61} \times 1 = 0.143\,m \quad [213]$$

$$M_{add} = Q_{min} a = 1312.60\,kN \times 0.143\,m = 187.70\,kNm \quad [214]$$

$$M_{mag} = M + M_{add} = 97.32 + 187.70 = 285.02\,kNm \quad [215]$$

$$e = \frac{M_{mag}}{Q_{min}} = \frac{285.02}{1312.60} = 0.217\,m \quad [216]$$

$$\frac{e}{R} = \frac{0.217}{0.305} = 0.711 \quad [217]$$

$$\frac{M}{h^3} = \frac{285.02}{0.61^3} = 1.256\,kN/m^2 \quad [218]$$

$$k = \frac{h_e}{h} = 0.75 \quad [219]$$

$$A_{st} = \frac{A_c \times 1}{100} = \frac{\pi \times 0.305^2 \times 1.6}{100} = 4675.9\,mm^2 \quad [220]$$

Table 4.28. Pile Reinforcement Design for each pile group.

Pile Group	Madd (kNm)	Mmag (kNm)	M/h3 (kN/m²)	ρ (%)	Asc (mm²)	Design
Exterior	132.65	197.49	0.871	1.6	4675.9	15 #20 mm
Interior	187.70	285.02	1.256	1.6	4675.9	15 #20 mm
Corner	121.29	191.16	0.842	1.6	4675.9	15 #20 mm

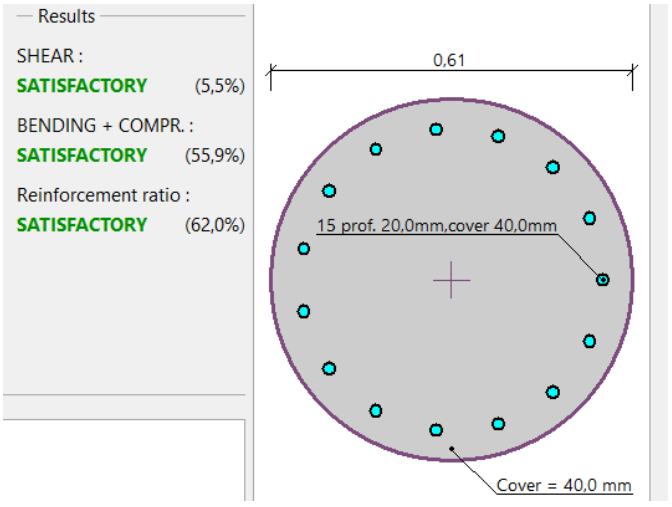

Figure 4.24. Reinforcement of a single pile in Geo5.

4.8. Sheet pile design

Sheet piles are used for support of excavation walls when excavation works occur on a large area (Das & Sivakugan, 2019). There are types of sheet piles based on depth: cantilever and anchored. Based on material they can be classified as following: wooden, precast concrete, steel.

4.8.1. Hand calculations

Basement depth is 3.3 m. The sheet pile is located fully in clayey soil.

φ=34 degrees and γ=17.15 kN/m^3

Firstly, coefficients of rankine earth pressure were found:

$$K_p = tan^2(45 + \frac{\phi'}{2}) \quad [221]$$

$$K_p = 3.537$$

$$K_a = tan^2(45 - \frac{\phi'}{2}) \quad [222]$$

$$K_a = 0.283$$

$$K_{p(design)} = \frac{K_p}{FS} \quad [223]$$

$$K_{p(design)} = 1.7690$$

Then, the next equation was applied to find active pressure at L=3.3 m:

$$\sigma'_2 = \gamma L K_a \quad [224]$$

$$\sigma'_2 = 16.02\ kN/m^2$$

To determine L_3, the following formula was used:

$$L_3 = \frac{LK_a}{K_{p(design)} - K_a} \quad [225]$$

$$L_3 = 0.628\ m$$

After that, σ'_5 was found:

$$\sigma'_5 = \gamma L K_{p(design)} + \gamma L_3 (K_{p(design)} - K_a) \quad [226]$$

$$\sigma'_5 = 116.12\ kN/m^2$$

To identify pressure diagram area, next relationship was used:

$$P = 0.5\sigma'_2 L + 0.5\sigma'_2 L_3 \quad [227]$$

$$P = 31.46\ kN/m$$

Centroid of pressure diagram was then found:

$$\bar{z} = \frac{L(2K_a - K_{p(design)})}{3(K_{p(design)} - K_a)} \quad [228]$$

$$\bar{z} = 0.891\ m$$

Next, A'_1, A'_2, A'_3, and A'_4 were determined:

$$A'_1 = \frac{\sigma'_5}{\gamma(K_{p(design)} - K_a)} \quad [229]$$

$$A'_1 = 4.56$$

$$A'_2 = \frac{8P}{\gamma(K_p - K_a)} \quad [230]$$

$$A'_2 = 4.510$$

$$A'_3 = \frac{6P[2\bar{z}\gamma(K_p - K_a) + \sigma'_5]}{\gamma^2(K_p - K_a)^2} \quad [231]$$

$$A'_3 = 13.066$$

$$A'_4 = \frac{P[6\bar{z}\sigma'_5 + 4P]}{\gamma^2(K_p - K_a)^2} \quad [232]$$

$$A'_4 = 7.54$$

L_4 was calculated via the following formula:

$$L_4^4 + A'_1 L_4^3 - A'_2 L_4^2 - A'_3 L_4 - A'_4 = 0 \quad [233]$$

$$L_4 = 1.986\ m$$

$$D_{theory} = L_3 + L_4 \quad [234]$$

$$D_{theory} = 2.614\ m$$

$$\sigma'_3 = L_4(K_p - K_a)\gamma \quad [235]$$

$$\sigma'_3 = 110.83\ kN/m^2$$

$$\sigma'_4 = \sigma'_5 + \gamma L_4(K_p - K_a) \quad [236]$$

$$\sigma'_4 = 226.95\ kN/m^2$$

$$L_5 = \frac{\sigma'_3 L_4 - 2P}{\sigma'_3 + \sigma'_4} \quad [237]$$

$$L_5 = 0.465\, m$$

Point of zero shear force is found in the next way:

$$z' = \sqrt{\frac{2P}{\gamma(K_p - K_a)}} \quad [238]$$

$$z' = 1.127\, m$$

Then, maximum bending moment was calculated:

$$M_{max} = P(\bar{z} + z') - [0.5\gamma z'^2(K_p - K_a)]\frac{1}{3}z' \quad [239]$$

$$M_{max} = 50.172\, kN * m/m$$

Next, section modulus was determined:

$$S = \frac{M_{max}}{\sigma_{all}} \quad [240]$$

$$S = 2.23 * 10^{-4}\, m^3/m$$

Based on maximum bending moment and section modulus, according to the table 18.1 PZ-22 section designation was chosen (Das & Sivakugan, 2019). Section properties are as follows: H=235 mm, L=558.8 mm, f=9.53 mm, w=9.53 mm Steel was chosen for material of sheet pile for its convenience due to being resistant to high driving stress. In the US, the thickness of sheet piles ranges from 10 to 13 mm. ASTM A-572 is a higher-strength section. Allowable stress for this steel type is 225 MN/m2.

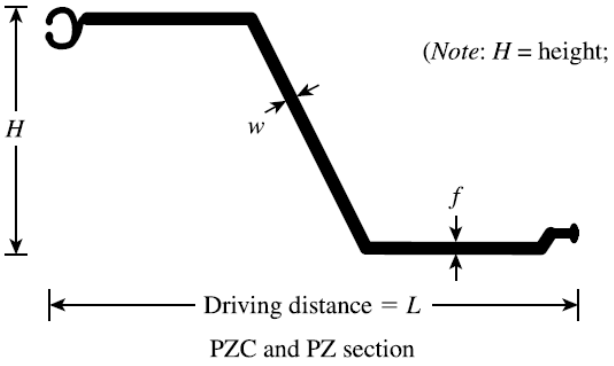

Figure 4.25. PZ section.

4.8.2. Numerical analysis on PLAXIS

To find maximum displacement and maximum pressure values, Geo5 software was used. Bending moment and shear force values are presented in the figure below.

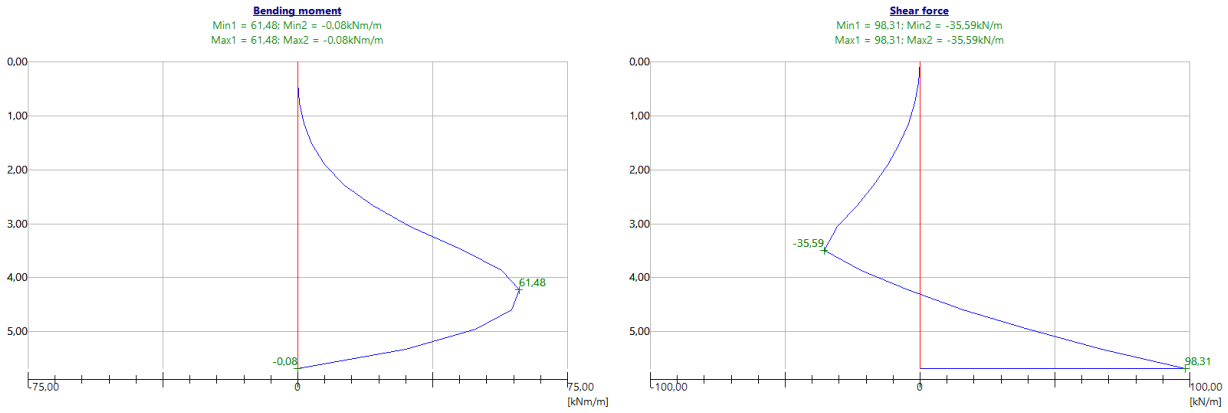

Figure 4.26. Bending moment and shear force.

Analysis in the software showed that the results of bending and shear force are both satisfactory, basen on the figure below.

Results

BENDING : SATISFACTORY (26,4%)
SHEAR : SATISFACTORY (15,4%)

Figure 4.27. Results of check for bending and shear.

Slope stability verification (Bishop)

Sum of active forces : F_a = 265,80 kN/m
Sum of passive forces : F_p = 718,27 kN/m

Sliding moment : M_a = 3099,29 kNm/m
Resisting moment : M_p = 8375,06 kNm/m
Utilization : 37,0 %

Slope stability ACCEPTABLE

Figure 4.28. Slope stability verification.

It was decided to use sheet piles as a retaining wall for this project, as it can be used as a permanent structure. The main benefits are high-strength to low weight ratio, sustainability - possibility to recycle and reuse, wide availability of various sizes and lengths, longevity and cost-effectiveness (aarsleff.co.uk).

4.9. Software analysis of pile foundation under loading

PLAXIS 3D was used to check the settlement of the designed foundation. Pile layout was created in the software. We used embedded beams for piles, plates for pile caps, and point loads for column loads. Sheet piles were also designed. The layout can be seen from Figure 4.29.

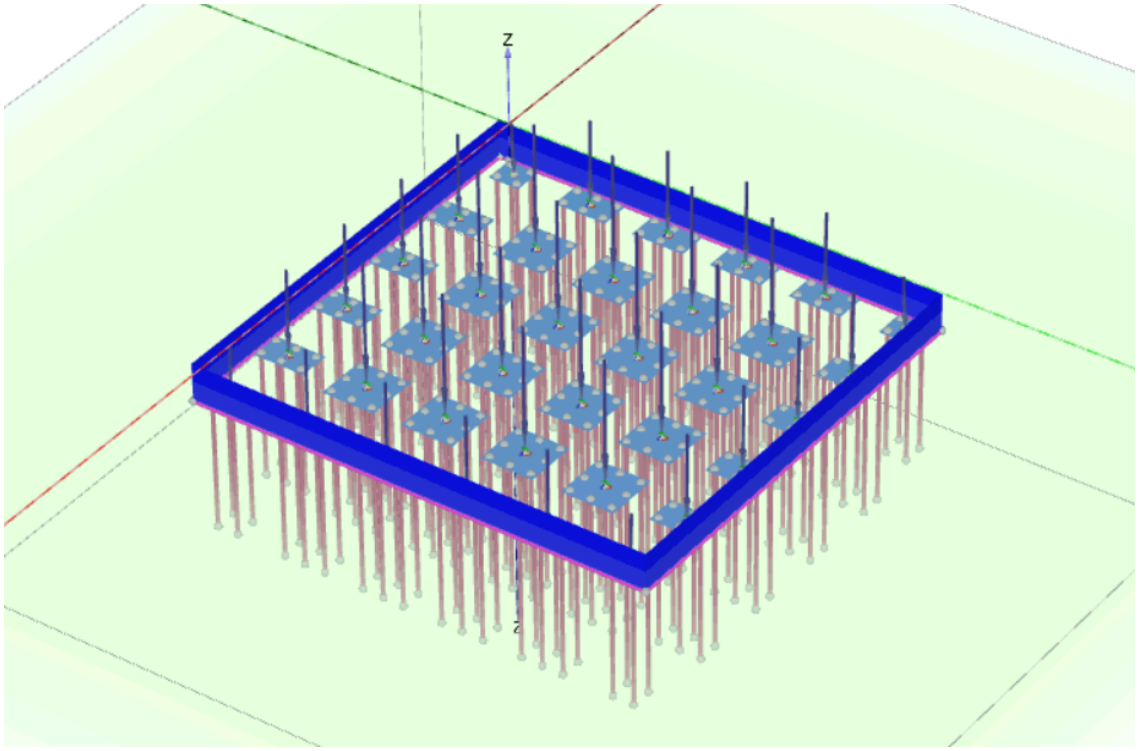

Figure 4.29. Pile layout in PLAXIS 3D.

The simulation was conducted in 5 phases; initial, excavation, sheet pile installation, pile cap and pile installation, applying loads, and dynamic analysis.

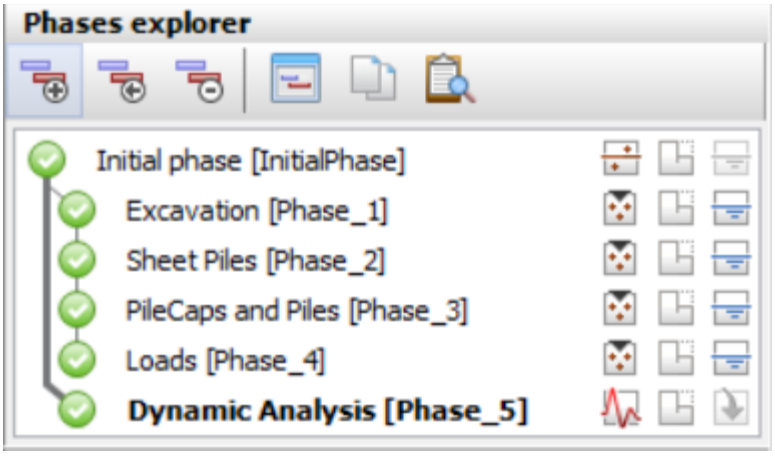

Figure 4.30. Phases of the construction.

The result for the displacement of the soil is given in the figure below.

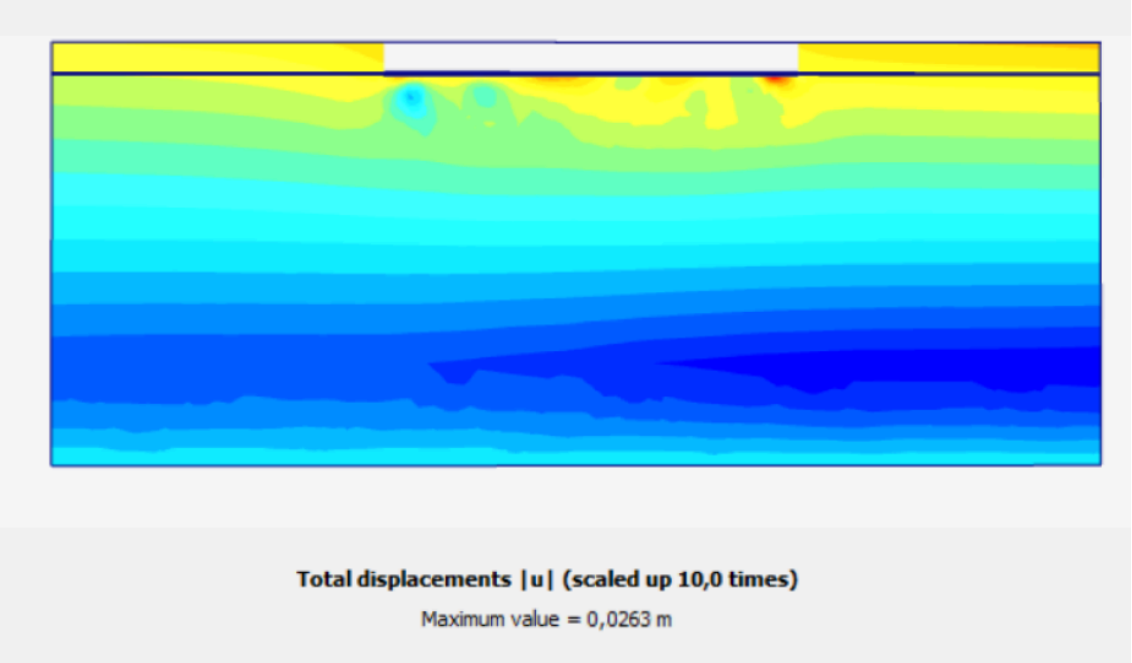

Figure 4.31. Total displacement of the foundation in PLAXIS 3D.

The displacements are all in range of allowable displacement for pile foundation.

4.10. Construction procedure

Site Clearing

Any unwanted objects such as trees, rocks, vegetation, remnants of old structures are removed to make a building area safe and easy to access. To perform this step a mechanical method of clearing which uses heavy machinery is selected. Before site clearing some pre-clearing considerations should be made. Site should be thoroughly assessed in terms of debris and any hazard to the environment. Also, site clearing should be done in accordance with local, state and federal regulations to avoid project delays and fines.

Site Surveying, Testing, and Plan Design

Site survey is important because on this step topography, type of soil, climatic conditions, and existing structures are evaluated. Any documents including zoning maps, geological surveys are collected to obtain valuable information. After site analysis all boundaries of the property are labelled and all control points are set. Control points are beneficial for creating plans, maps and integrating erosion control solutions. After that existing utilities - drainage, gas lines, electrical cables should be identified.

Soil testing focuses on evaluating rock, water and compactibility. Various tests, such as Atterberg limit, Proctor's compaction, moisture content, specific gravity, dry density are conducted.

Site Investigation

Geotechnical investigation, focused on study of GWT, soil properties, is of high importance as it prevents unnecessary expenses, ensures stable foundation, evaluates appropriateness of specific methods of construction and reduces geotechnical risks. Also, soil investigation is a mandatory requirement of building codes and regulations. Significant information, including load bearing capacity, soil types and properties, water content, permeability, conditions of GWT, and possible geotechnical risks can be obtained from soil investigation reports.

Sheet Pile Installation

Before installation it is important to examine sheet piles conditions on presence of cracks and integrity of components of interlocking. Sheet piles should be arranged in sections to check if piles are interlocked in a proper way. First sheet pile is hammered to the chosen depth, 3.3 m. Then it is installed by an impact hammer, as the soil is very stiff. After that the second one is driven in the way that it can interlock with the first one. To ensure wall integrity connectors are used. When installing piles thorough monitoring is required because there is a possibility that piles would not penetrate soil. In addition to it, deviation of sheet piles from vertical planes due to obstacles should also be controlled.

Steel sheet piles are chosen for their ability to withstand high driving stresses, extend via welding or bolting and good water-tightness.

As a method of installation pitch and drive is used. In this method, a sheet pile is threaded and driven to its final depth. The main advantage is that it is fast and cheap. As the selected sheet pile is short, and no risk of leaning pitch and drive approach is a good option.

Excavation

It is important to make proper excavation work to ensure that the structure will be stable and long-standing. Excavation is done via special equipment such as excavators, backhoes, bulldozers and skid steers. Depth of excavation is 3.3 m. Soil layers are removed by excavators and backhoes. Based on OSHA guidelines, one of the soil layers is Type C - submerged soil, which is why bending cannot be done. Other available systems are sloping, shoring and shielding. These systems aim to provide workers with safety, by preventing cave-ins and soil movement. To make the foundation surface smooth and even bulldozers and skid steers are employed. Also, preventive measures are needed to minimize potential harm to the environment, including soil erosion, soil contamination, groundwater pollution, noise, waste and air contaminants. Areas needed for pile caps should also be excavated.

Pile Installation

Precast pile from concrete was selected, as it is resistant to corrosion, and is able to be subjected to hard driving. Piles can be driven using an impact hammer or a vibratory hammer. Vibratory hammer was chosen because less noise generated, so that residential buildings surrounding the construction site are not disturbed.

Pile Cap Construction

Before installment, a piling mat consisting of crushed aggregate is needed to be established in order to support rigs and vehicles. Thickness of the mat is 300 mm. Piling is done by three workers: first man is responsible for running the machine, second - for hooking up cages from steel, auger bit and concrete pump and third - for shovel.

Filling with Concrete

At this stage concrete is poured and set for the pile cap.

Backfilling the Excavation

Backfilling is when an excavated area is filled in using any material, including sand, crushed stone and gravel. After adding each layer of backfill material, compaction should be done to ensure stable foundation. For compaction hand tampers, plate compactors, or roller compactors can be employed. Backfill is used for building

insulation and enhancement of drainage systems as well. As a backfill material coarse-grained soil is chosen for its ease in compaction (Paredes, 2024).

Quality Assurance

Quality assurance is setting a minimum quality standard to avoid potential risks. It ensures that materials of proper dimensions and shape are used, equipment works correctly, workers have necessary skills and project management goes well. For this purpose special software such as PlanRadar can be used (Lehner, 2021).

5. Construction Management

5.1. Charter

Project Charter			
Project Title	Design of a 12-story Office Building in Los Angeles, CA, USA		
Description	The aim of the project is to design and construct a cost-effective 12-story high-rise office building located at 940 N Sycamore Avenue, Los Angeles, California, USA. Numerous popular tourist attractions are within walking distance of the address, including Celebration Theatre, The Hudson Theatres, The Complex Theatres and Studios, Casita Hollywood, LIVE HOUSE, and Plummer Park.		
Start Date	September 2024	End date	August 2027
Project Manager	Malika Sissenova		
Project Sponsor	Nazarbayev University		
Purpose	The aim of the project is to design and construct a high-rise office building at 940 N Sycamore Avenue, Los Angeles, California, USA that meets the environmental standards and construction regulations.		
Project Deliverables	1. 12-story office building 2. Parking space		

<table>
<tr><td></td><td colspan="3">3. Comfortable working area
4. Design documentation</td></tr>
<tr><td>Risk and Issues</td><td colspan="3">1. Financial Risks. Unexpected increases in material costs, equipment rentals can lead to budget overruns.
2. Schedule Delays. Unforeseen soil conditions and weather events can cause delays.
3. Quality Issues. Using low-quality materials and poor execution can result in poor quality.
4. Safety risks. Accidents on construction sites can result in injuries or fatalities.
5. Legal risks. Disagreements between project parties can lead to legal disputes.</td></tr>
<tr><td>Estimated budget</td><td colspan="3">$34,966,501.74</td></tr>
<tr><td>Main Stakesholders</td><td colspan="3">Local Government and regulatory bodies
Sustainability consultants
Material suppliers
Investors and Financial Institutions
Local community
Future clients</td></tr>
<tr><td rowspan="6">Milestones</td><td>Stage</td><td>Deadline</td><td>Status</td></tr>
<tr><td>Project Initiation</td><td>04.10.2024</td><td>Completed</td></tr>
<tr><td>Pre-Construction Planning</td><td>15.05.2025</td><td>In Progress</td></tr>
<tr><td>Construction</td><td>02.03.2027</td><td>Not Started</td></tr>
<tr><td>Finishes</td><td>13.07.2027</td><td>Not Started</td></tr>
<tr><td>Closeout</td><td>31.08.2027</td><td>Not Started</td></tr>
<tr><td>Team members</td><td colspan="3">Tangguli Zhubanysh
Alibi Seitkaliyev
Amirmagruf Amantay
Bekbarys Aidaraliyev</td></tr>
</table>

	Malika Sissenova Aruzhan Gabit

5.2. Feasibility study

When constructing a high-rise building, it is important to take into account economic feasibility: compare the expected income from sale or rent with the costs in order to calculate the payback period and profitability of the project.

We determined how much we could earn from renting a high-rise building. To do this, we conducted a market analysis, studying current market rates for similar properties. The typical annual renting rate for office space in Los Angeles ranges between $30 and $70 per square foot. We decided to choose 50$ per square foot as a rental price.Then, the Revenue will be:

Rental Revenue = 50*13 200*10 = $7 260 000 per year

The payback period can be calculated as follows:

Payback Period = 34 966 502 / 7 260 000 = 4.82 years

The payback period of the project is 4.97 years. Considering the fact that the payback period ranges from 4 to 10 years, our project can be considered acceptable. Therefore, the project can be considered economically feasible.

5.3. Cost/benefit estimation

Cost estimation of a construction project plays a key role in ensuring accurate financial planning, cost control and resource management. It helps to prevent budget overruns, ensure accountability to customers and investors, and compare contractors' proposals to select the best option. For this project, we calculated the cost of the building using RSMeans, which is a professional tool used for estimating the construction costs.

RSMeans provides access to a large database that contains information about the costs of materials, labor, equipment, and other aspects of construction. We entered the basic parameters of the project, such as the type of the building, its area, number of floors and location. The program calculated how much material would be needed for

construction and added the cost of labor and equipment. The results are presented in Table 5.1.

Table 5.1. Building cost estimation from RSMeans.

		Quantity	% of Total	Cost per S.F.	Cost
A	**Substructure**		**4.33%**	**$25.60**	**$337,946.92**
A1010	Standard Foundations			$0.69	$9,158.77
	Pile caps, 12 piles, 11' - 6" x 8' - 6" x 49", 40 ton capacity, 19" column size, 900 K column	1.01		$0.33	$4,366.15
	Pile caps, 14 piles, 11' - 6" x 10' - 9" x 55", 80 ton capacity, 29"column size, 2155 K column	0.81		$0.36	$4,792.62
A1020	Special Foundations			$11.76	$155,270.46
	Steel H piles, 50' long, 800K load, end bearing, 12 pile cluster	1.01		$2.05	$27,110.77
	Steel H piles, 50' long, 1600K load, end bearing, 10 pile cluster	0.81		$1.60	$21,099.69
	Grade beam, 30' span, 52" deep, 14" wide, 12 KLF load	530		$8.11	$107,060.00
A1030	Slab on Grade			$0.45	$5,889.23
	Slab on grade, 4" thick, non industrial, reinforced	1015.38		$0.45	$5,889.23
A2010	Basement Excavation			$0.29	$3,858.46
	Excavate and fill, 10,000 SF, 8' deep, sand, gravel, or common earth, on site storage	1015.38		$0.29	$3,858.46
A2020	Basement Walls			$12.41	$163,770.00

	Foundation wall, CIP, 12' wall height, pumped, .591 CY/LF, 28.79 PLF, 16" thick	530		$12.41	$163,770.00
B	**Shell**		**66.11%**	**$390.78**	**$5,158,293.49**
B1010	Floor Construction			$254.49	$3,359,330.29
	Cast-in-place concrete column, 24" square, tied, 900K load, 12' story height, 567 lbs/LF, 4000PSI	1120.61		$16.55	$218,519.26
	Cast-in-place concrete column, 12", square, tied, minimum reinforcing, 150K load, 10'-14' story height, 135 lbs/LF, 4000PSI	1060		$5.59	$73,776.00
	Cast-in-place concrete column, 16", square, tied, minimum reinforcing, 300K load, 10'-14' story height, 240 lbs/LF, 4000PSI	1192.5		$8.63	$113,883.75
	Cast-in-place concrete column, 20", square, tied, minimum reinforcing, 500K load, 10'-14' story height, 375 lbs/LF, 4000PSI	1590		$16.44	$217,035.00
	Concrete I beam, precast, 18" x 36", 790 PLF, 25' span, 6.44 KLF superimposed load	7679.7		$189.81	$2,505,502.13
	Flat slab, concrete, with drop panels, 6" slab/2.5" panel, 12" column, 15'x15' bay, 75 PSF superimposed load, 153 PSF total load	1015.38		$1.14	$15,078.46
	Precast concrete double T beam, 2" topping, 24" deep x 8' wide, 50' span, 30 PSF superimposed load, 120 PSF total load	12184.61		$15.02	$198,243.69

	Precast concrete double T beam, 2" topping, 24" deep x 8' wide, 50' span, 75 PSF superimposed load, 165 PSF total load	1015.38		$1.31	$17,292.00
B2010	Exterior Walls			$108.78	$1,435,876.00
	E.I.F.S., CMU, 8" x 8" x 16", 2" EPS	55120		$108.78	$1,435,876.00
B2020	Exterior Windows			$24.23	$319,868.25
	Aluminum flush tube frame, thermo-break frame, 2.25" x 4.5", 5'x6' opening, no intermediate horizontals	3445		$8.03	$105,933.75
	Glazing panel, plate glass, 1/4" thick, clear	10335		$16.21	$213,934.50
B2030	Exterior Doors			$0.87	$11,529.69
	Door, aluminum & glass, without transom, full vision, double door, hardware, 6'-0" x 7'-0" opening	0.81		$0.48	$6,336.00
	Door, aluminum & glass, with transom, non-standard, double door, hardware, 6'-0" x 10'-0" opening	0.6		$0.39	$5,193.69
B3010	Roof Coverings			$2.34	$30,901.22
	Roofing, single ply membrane, EPDM, 60 mils, loosely laid, stone ballast	1015.38		$0.13	$1,705.85
	Insulation, rigid, roof deck, extruded polystyrene, 40 PSI compressive strength, 4" thick, R20	1015.38		$0.32	$4,274.77
	Roof edges, aluminum, duranodic, .050" thick, 6" face	530		$1.13	$14,946.00

	Flashing, aluminum, no backing sides, .019"	530		$0.23	$2,978.60
	Gravel stop, aluminum, extruded, 4", duranodic, .050" thick	530		$0.53	$6,996.00
B3020	Roof Openings			$0.06	$788.04
	Roof hatch, with curb, 1" fiberglass insulation, 2'-6" x 3'-0", galvanized steel, 165 lbs	0.3		$0.03	$355.79
	Smoke hatch, unlabeled, galvanized, 2'-6" x 3', not incl hand winch operator	0.3		$0.03	$432.25
C	**Interiors**		**18.32%**	**$108.28**	**$1,429,356.16**
C1010	Partitions			$9.81	$129,514.40
	Concrete block (CMU) partition, light weight, hollow, 6" thick, no finish, foamed in insulation	1320		$1.20	$15,892.80
	Metal partition, 5/8"fire rated gypsum board face, no base,3 -5/8" @ 24" OC framing, same opposite face, no insulation	1760		$0.60	$7,955.20
	Metal partition, 5/8"fire rated gypsum board face, no base,3 -5/8" @ 24" OC framing, same opposite face, sound attenuation insulation	1320		$0.59	$7,748.40
	Furring 1 side only, steel channels, 3/4", 24" OC	1320		$0.19	$2,534.40
	Gypsum board, 1 face only, exterior sheathing, fire resistant, 5/8"	55120		$4.26	$56,222.40

	Gypsum board, 1 face only, exterior sheathing, fire resistant, 5/8"	1320		$0.10	$1,346.40
	Add for the following: taping and finishing	1320		$0.07	$884.40
	Add for the following: taping and finishing	55120		$2.80	$36,930.40
C1020	Interior Doors			$3.43	$45,310.11
	Door, single leaf, kd steel frame, hollow metal, commercial quality, flush, 3'-0" x 7'-0" x 1-3/8"	37.07		$3.43	$45,310.11
C1030	Fittings			$0.19	$2,462.05
	Toilet partitions, cubicles, ceiling hung, plastic laminate	2.69		$0.19	$2,462.05
C2010	Stair Construction			$79.00	$1,042,800.00
	Stairs, steel, pan tread for conc in-fill, picket rail,16 risers w/ landing	66		$79.00	$1,042,800.00
C3010	Wall Finishes			$4.31	$56,888.80
	Painting, interior on plaster and drywall, walls & ceilings, roller work, primer & 2 coats	8800		$0.59	$7,832.00
	Painting, interior on plaster and drywall, walls & ceilings, roller work, primer & 2 coats	55120		$3.72	$49,056.80
C3020	Floor Finishes			$5.24	$69,220.80
	Carpet tile, nylon, fusion bonded, 18" x 18" or 24" x 24", 35 oz	7920		$3.13	$41,263.20
	Vinyl, composition tile, maximum	3960		$0.92	$12,117.60
	Tile, ceramic natural clay	1320		$1.20	$15,840.00
C3030	Ceiling Finishes			$6.30	$83,160.00

	Acoustic ceilings, 3/4" fiberglass board, 24" x 48" tile, tee grid, suspended support	13200		$6.30	$83,160.00
D	**Services**		**11.24%**	**$66.43**	**$876,891.93**
D1010	Elevators and Lifts			$7.77	$102,553.85
	Traction, geared passenger, 3500 lb,15 floors, 10' story height, 2 car group, 350 FPM	0.2		$7.77	$102,553.85
D2010	Plumbing Fixtures			$1.42	$18,688.15
	Water closet, vitreous china, bowl only with flush valve, wall hung	2.69		$0.69	$9,148.62
	Urinal, vitreous china, wall hung	0.91		$0.10	$1,352.49
	Lavatory w/trim, vanity top, PE on CI, 20" x 18"	1.72		$0.18	$2,399.35
	Service sink w/trim, PE on CI,wall hung w/rim guard, 24" x 20"	0.81		$0.24	$3,147.69
	Water cooler, electric, wall hung, wheelchair type, 7.5 GPH	1.32		$0.20	$2,640.00
D2020	Domestic Water Distribution			$0.37	$4,822.44
	Gas fired water heater, commercial, 100< F rise, 300 MBH input, 278 GPH	0.25		$0.37	$4,822.44
D2040	Rain Water Drainage			$1.19	$15,712.96
	Roof drain, CI, soil,single hub, 4" diam, 10' high	0.25		$0.05	$607.96
	Roof drain, CI, soil,single hub, 5" diam, for each additional foot add	201.4		$1.14	$15,105.00
D3020	Heat Generating Systems			$2.71	$35,747.88

	Plate heat exchanger, 1800 GPM	0.05		$0.92	$12,138.92
	Utility fan set system, belt drive, 7500 CFM	0.05		$0.17	$2,255.42
	Boiler, cast iron, gas & oil, hot water, 6000 MBH	0.1		$1.43	$18,886.15
	Pump, base mounted with motor, end-suction, 6" size, 25 HP, to 1550 GPM	0.05		$0.19	$2,467.39
D3030	Cooling Generating Systems			$16.83	$222,156.00
	Packaged chiller, water cooled, with fan coil unit, offices, 60,000 SF, 190.00 ton	14520		$16.83	$222,156.00
D4010	Sprinklers			$2.95	$38,922.23
	Wet pipe sprinkler systems, steel, light hazard, 1 floor, 10,000 SF	792		$0.23	$3,001.68
	Wet pipe sprinkler systems, steel, light hazard, each additional floor, 10,000 SF	12408		$2.62	$34,618.32
	Standard High Rise Accessory Package 16 story	0.05		$0.10	$1,302.23
D4020	Standpipes			$3.11	$41,020.25
	Wet standpipe risers, class III, steel, black, sch 40, 6" diam pipe, 1 floor	0.12		$0.15	$1,955.63
	Wet standpipe risers, class III, steel, black, sch 40, 6" diam pipe, additional floors	0.97		$0.32	$4,264.62
	Fire pump, electric, with controller, 5" pump, 100 HP, 1000 GPM	1		$2.35	$31,000.00
	Fire pump, electric, for jockey pump system, add	1		$0.29	$3,800.00

D5010	Electrical Service/Distribution			$11.09	$146,371.00
	Underground service installation, includes excavation, backfill, and compaction, 100' length, 4' depth, 3 phase, 4 wire, 277/480 volts, 1200 A	1		$2.45	$32,400.00
	Feeder installation 600 V, including RGS conduit and XHHW wire, 60 A	100		$0.15	$1,990.00
	Feeder installation 600 V, including RGS conduit and XHHW wire, 200 A	100		$0.36	$4,750.00
	Feeder installation 600 V, including RGS conduit and XHHW wire, 1200 A	234		$5.48	$72,306.00
	Switchgear installation, incl switchboard, panels & circuit breaker, 277/480 V, 1200 A	1		$2.65	$34,925.00
D5020	Lighting and Branch Wiring			$13.40	$176,933.30
	Receptacles incl plate, box, conduit, wire, 16.5 per 1000 SF, 2.0 W per SF, with transformer	13200		$5.01	$66,132.00
	Miscellaneous power, 1.2 watts	13200		$0.35	$4,620.00
	Central air conditioning power, 4 watts	13200		$0.63	$8,316.00
	Motor installation, three phase, 460 V, 15 HP motor size	4		$0.79	$10,480.00
	Motor feeder systems, three phase, feed to 200 V 5 HP, 230 V 7.5 HP, 460 V 15 HP, 575 V 20 HP	200		$0.17	$2,274.00

	Motor connections, three phase, 200/230/460/575 V, up to 5 HP	1		$0.01	$132.50
	Motor connections, three phase, 200/230/460/575 V, up to 100 HP	1		$0.04	$578.00
	Fluorescent fixtures recess mounted in ceiling, 1.6 watt per SF, 40 FC, 10 fixtures @32watt per 1000 SF	15180		$6.39	$84,400.80
D5030	Communications and Security			$5.60	$73,960.62
	Telephone wiring for offices & laboratories, 8 jacks/MSF	9900		$1.72	$22,671.00
	Communication and alarm systems, fire detection, addressable, 100 detectors, includes outlets, boxes, conduit and wire	0.33		$1.96	$25,872.00
	Fire alarm command center, addressable with voice, excl. wire & conduit	0.1		$0.10	$1,261.62
	Internet wiring, 8 data/voice outlets per 1000 S.F.	9.9		$1.83	$24,156.00
D5090	Other Electrical Systems				$3.25
	Uninterruptible power supply with standard battery pack, 15 kVA/12.75 kW	2.53			$3.25
E	**Equipment & Furnishings**		**0%**		
E1090	Other Equipment				
F	**Special Construction**		**0%**		
G	**Building Sitework**		**0%**		
	SubTotal		**100%**	**$591.10**	**$7,802,488.50**

	Contractor Fees (GC,Overhead,Profit)		**25.00%**	**$147.77**	**$1,950,622.13**
	Architectural Fees		**6.00%**	**$44.33**	**$585,186.64**
	User Fees		**0.00%**	**$0.00**	**$0.00**
	Total Building Cost			**$783.20**	**$10,338,297.26**

From the table 5.1, the total cost of the building is $10,338,297.26 and cost per square foot is $783.20. The cost per square foot of a high-rise office building in the USA ranges from $430 to $1001. Therefore, our calculations can be considered appropriate. These values were calculated using data from the year 2018. Therefore, the future work should include updated cost estimation of the building.

To calculate the overall cost of the project, several factors were considered. First, the preliminary cost of the building was calculated using RSMeans platform. As a result, a 12-story structure with a basement and a floor area of 13,200 square feet in Los Angeles will cost a total of $10,338,297.26. To determine the cost of the land, we found the nearest land for sale, which costs $982.5 per square meter, and applied the same cost to our land (Loopnet, 2024). According to the internet sources, the labor costs are approximately 30% of the total project cost (Bridgit, 2024). Equipment and Insurance costs were assumed. Taxes in California for Construction Projects is 7.5% of the total costs (CDTFA, 2024). The total cost calculations are shown in the table below.

Table 5.2. Total Cost Calculation for the project.

Expenses Type	**Cost**
Land	$3,925,171.39
Materials	$10,338,297.26
Labor	$7,763,880.60
Equipment	$5,000,000.00
Insurance	$500,000.00
Other	$5,000,000.00
Taxes	$2,439,152.49
Total	**$34,966,501.74**

5.4. Work breakdown structure

Work Breakdown Structure in construction management is a project management approach based on subdividing the project into smaller activities that are more manageable. It supports the structuring and definition of the total scope of work for planning and monitoring, including the financial, operational, and organizational parts of the project. The WBS in Figure 5.2. is a hierarchical representation of the work that needs to be executed in constructing a 12-storey office building.

The major characteristics of WBS include hierarchy, orientation towards outcome, exact levels, unique identifiers, and function of defining the project scope. It starts with a general description of the project and breaks it down into stages, tasks, and subtasks. The highest level consists of major project stages, which include planning, design, and construction. These phases are then broken down into foundations, structural elements, and electrical systems at the second level. Specific activities at the third tier refer to laying reinforcement or pouring concrete. The work breakdown structure emphasizes the products or deliverables from the action that produces the intended output.

WBS can aid in enhancement of planning and communication. It can allow more effective comprehensive budgeting and resource allocation, as well as some risk management support. A properly designed work breakdown structure aids in progress tracking and task completion documentation, and in staying on schedule should there be delays.

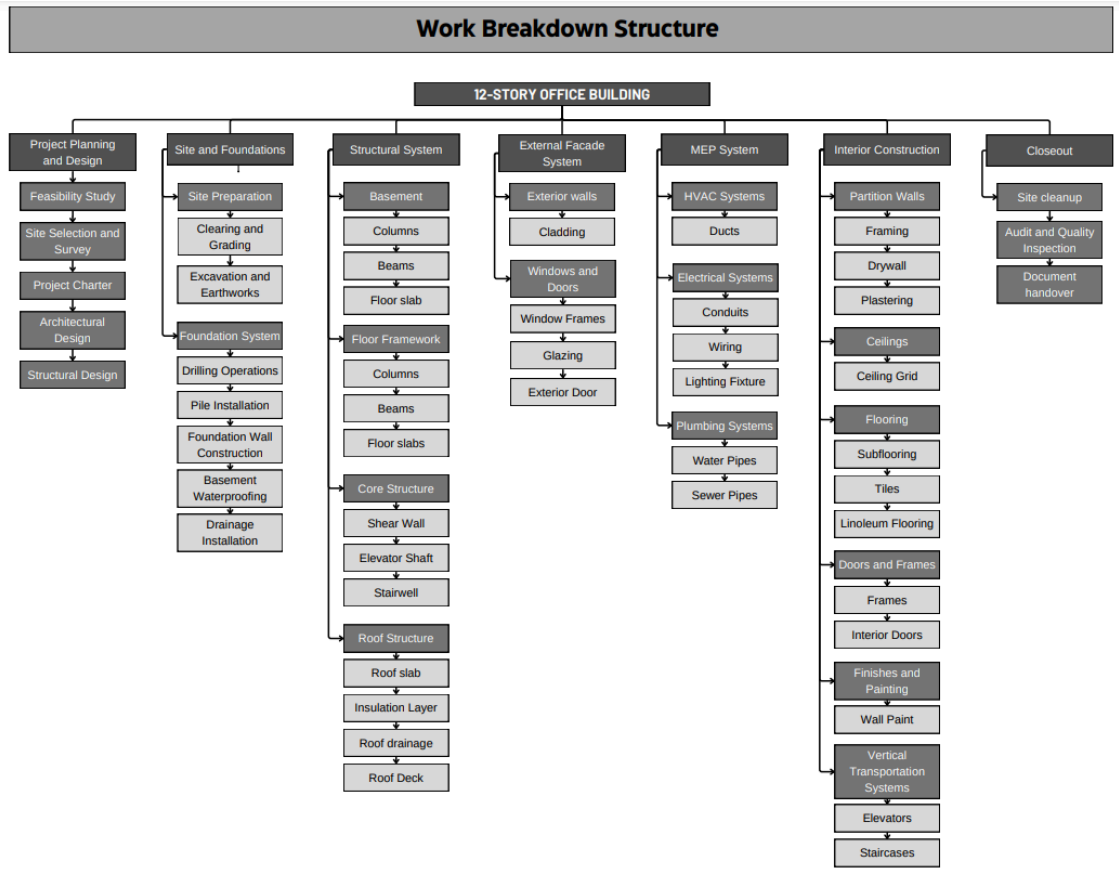

Figure 5.1. WBS of a 12-storey Office Building.

5.5. Scheduling

The construction schedule proposes a detailed plan for a 12-story office building, extending from the November of 2024 and running up to November 2027. For this project, a Gantt chart was created using a program Primavera P6. It was based on the WBS of the project.

As it can be seen from the Figures 5.2-5.5, The project is planned to be executed in 3 years. Major site preparation, excavation, and foundation in chronological order will be followed by basement and floors; it is estimated that each floor will take approximately 2-3 months. Also, the schedule incorporates roofing, facade installation, and MEPs into the timeline to ensure that parallel progress is achieved in both structural and systems installation. All these activities planned are meant to depict efficiency in the task sequence and, where necessary, overlap them so as to save time and resources.

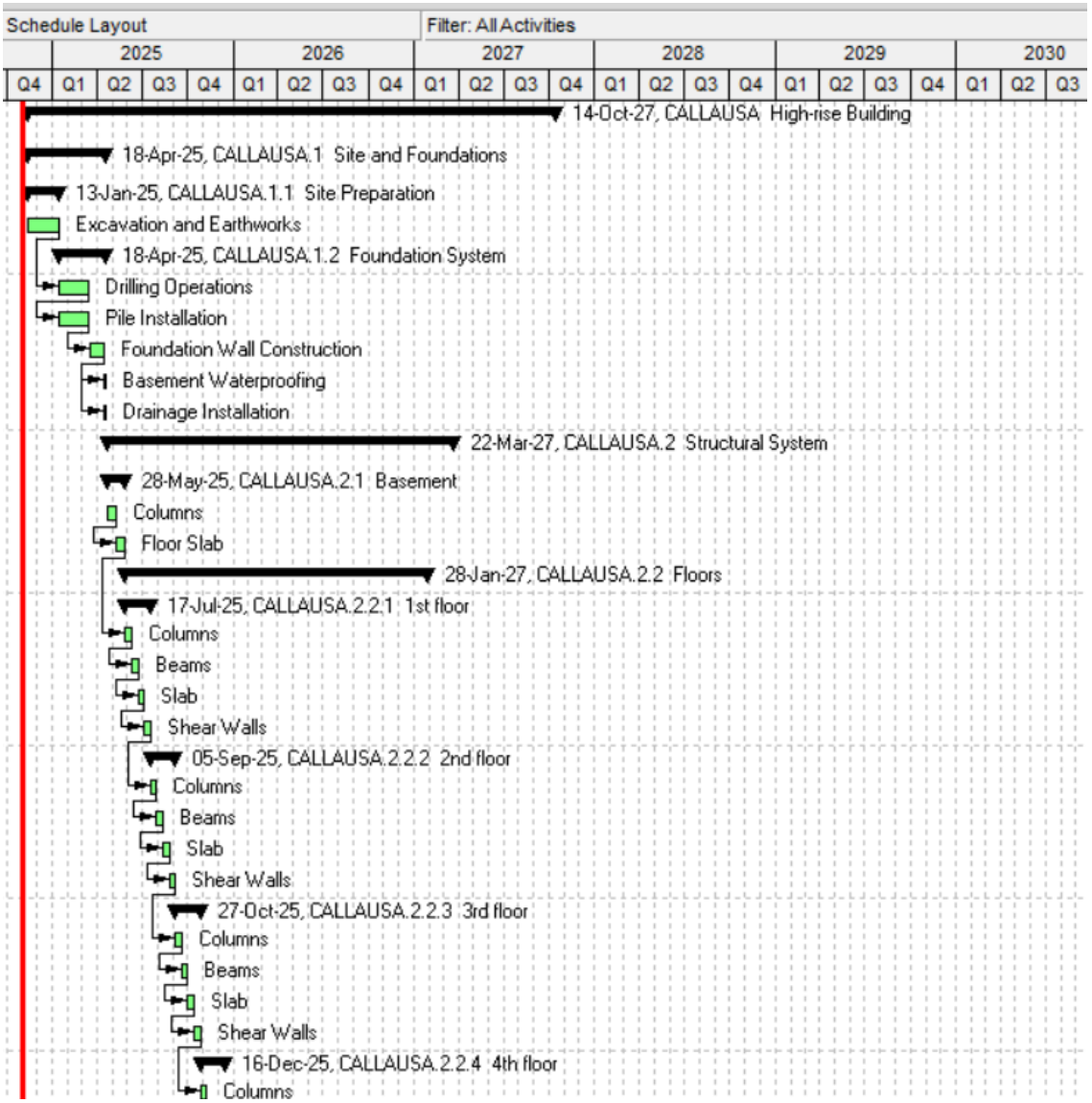

Figure 5.2. Schedule of the Project (November 2024 - December 2025).

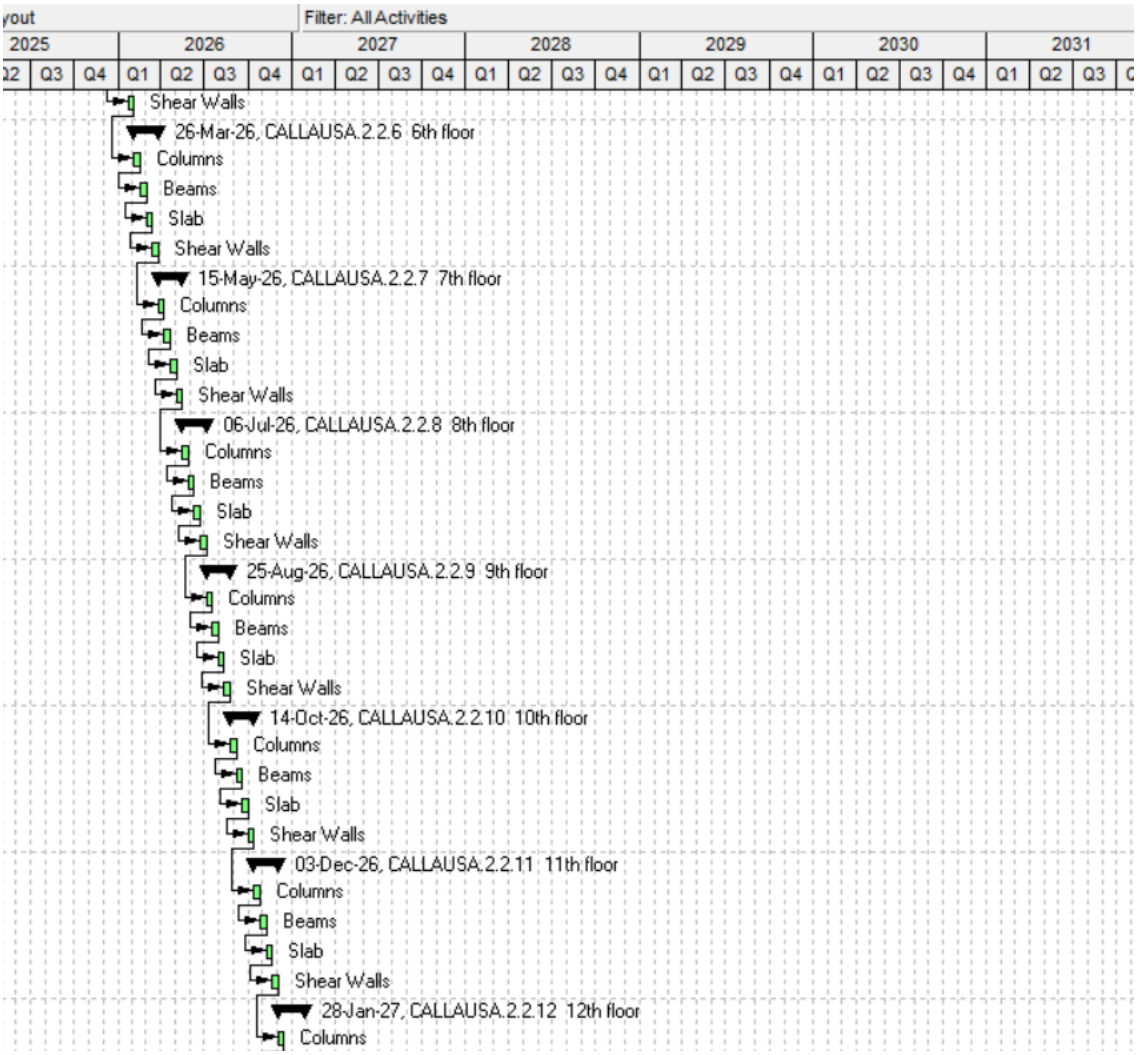

Figure 5.3. Schedule of the Project (December 2025 - January 2027).

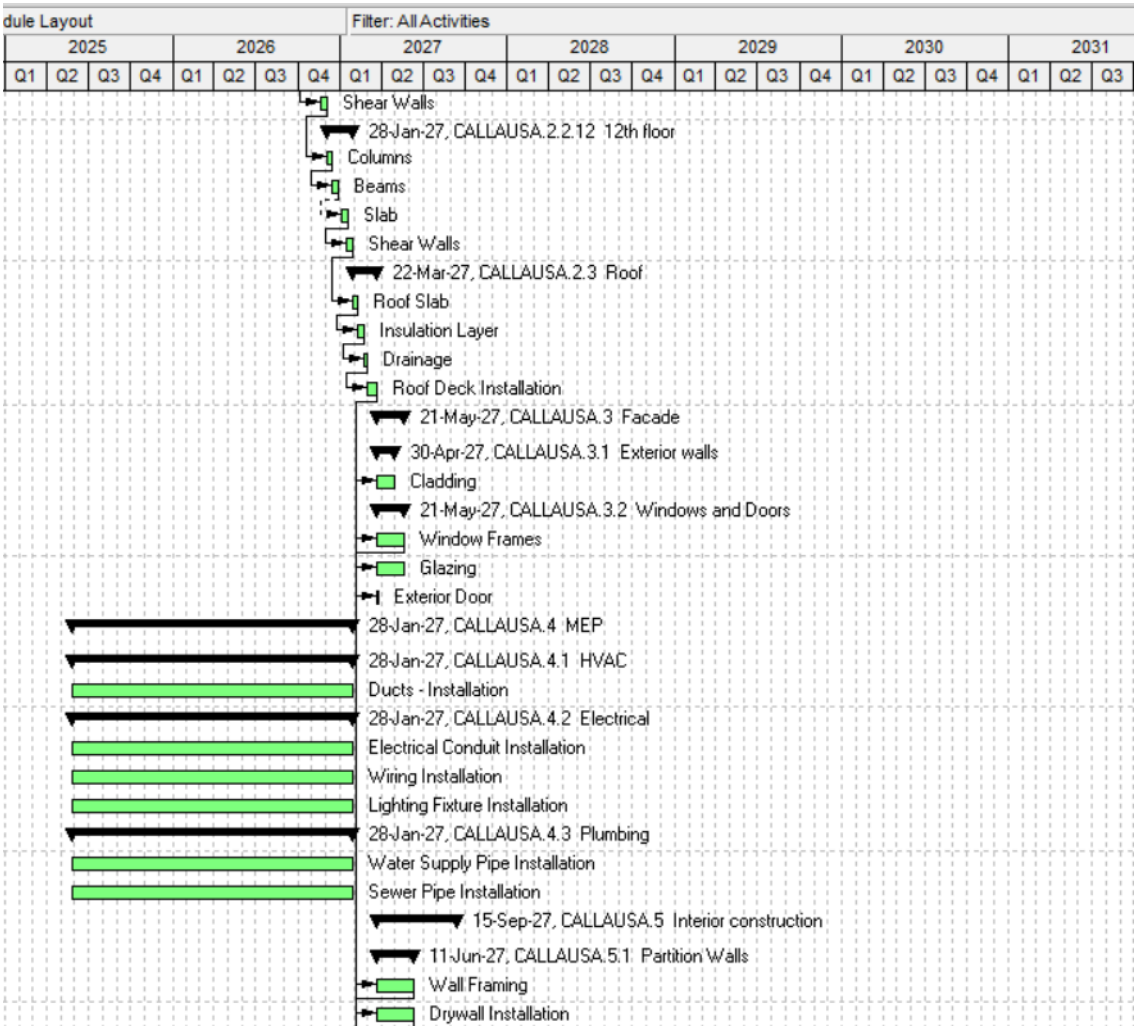

Figure 5.4. Schedule of the Project (January 2027 - June 2027).

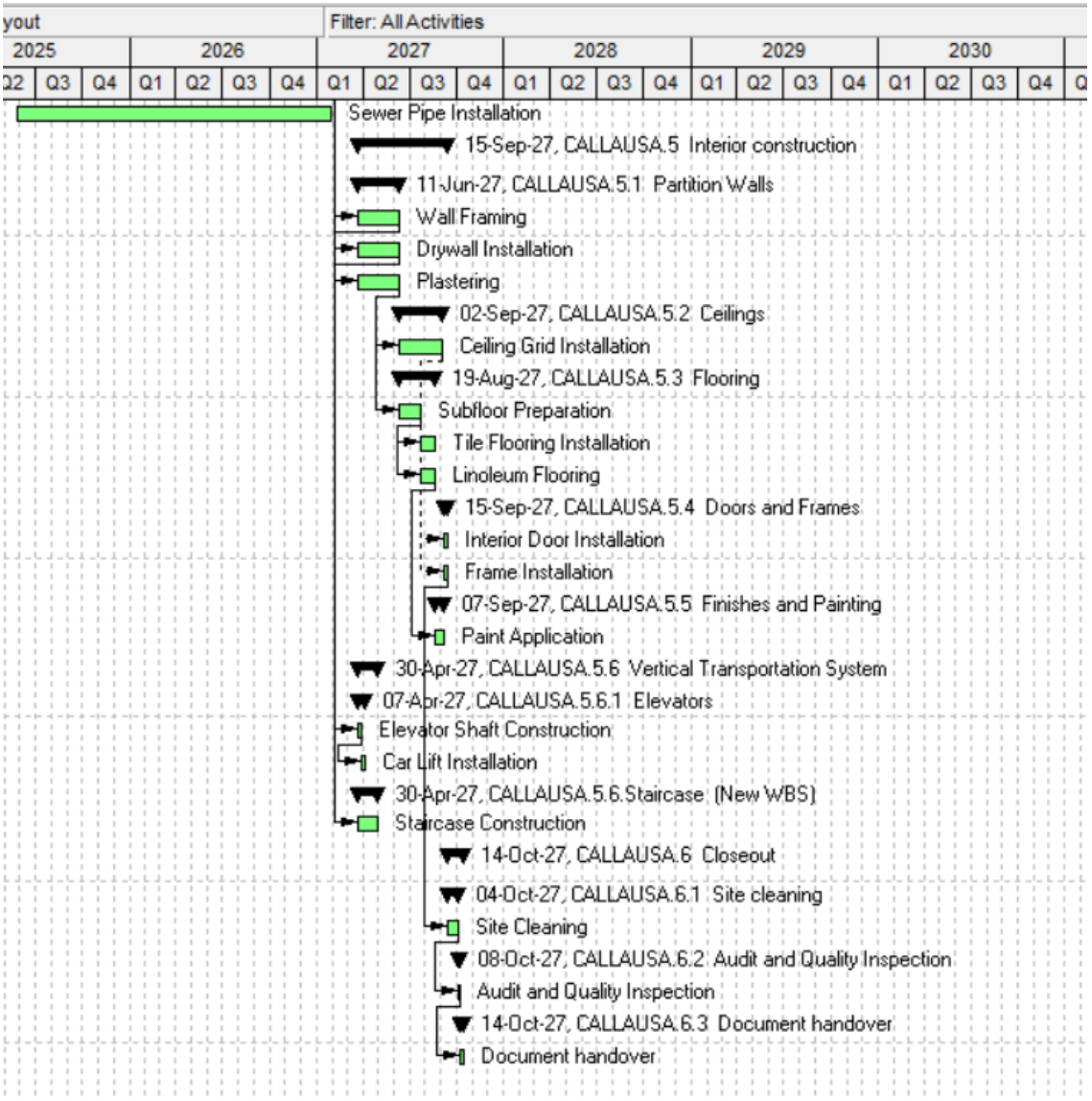

Figure 5.5. Schedule of the Project (June 2027 - November 2027).

5.6. Risk management

Risk assessment of a construction project is the process of identifying, analysing and managing potential risks that may affect the project. There might be some situations that can cause delays in the schedule, changes in budget plans, affect the quality or safety of the project. Therefore, effective risk assessment can help to prepare for unexpected circumstances, minimize losses and ensure the successful completion of the project.

Table 5.3 presents the risk analysis for our construction project. We have categorised potential threats into structural, geotechnical, safety, financial, management, environmental and external categories. We have rated each risk by probability and impact level and developed specific measures to minimize them.

Table 5.3. Risk Assessment.

Risk	Risk Element	Likelihood	Impact	Action Measures
Structural / Architectural	Errors in design	6	8	- Conduct design reviews - Use design software with error detection capabilities
	Design changes during construction	5	7	- Ensure effective collaboration during design approval
	Changes in building code standards	2	6	- Regularly check local building codes for updates - Engage code compliance consultants - Leave space for compliance updates
Geotechnical	Unforeseen soil conditions	5	8	- Conduct soil testings and geotechnical assessments before starting the construction - Consider emergency plans for foundation design modifications
	Soil erosion, landslides, subsidence	2	8	- Construct retaining walls and drainage systems
	Seismic risks	7	10	- Design structures to meet seismic safety standards - Use structural reinforcements
Safety	Accidents, injuries	8	9	- Regularly conduct safety trainings - Ensure all safety standards are met at the construction site
	Use of hazardous materials	3	7	- Use safe materials, substitute hazardous materials - Ensure proper storage and disposal of hazardous materials
	Breakdown of	6	6	- Regularly conduct maintenance checks

	equipment/material			- Purchase only high-quality, durable equipment
Financial	Budget Overrun	6	8	- Track and monitor the expenses - Reserve budget for contingency funds
	Fluctuating materials' costs	7	7	- Sign long-term contracts with suppliers - Prepare a list of alternative materials
	Unexpected project expenses	5	8	- Reserve budget for contingency funds - Perform thorough risk assessment to identify potential expenses
Management	Delays in project schedule	7	8	- Use project management software to track the construction process - Plan realistic timelines with buffer time in case of delays
	Conflicts with contractors	5	7	- Clearly define expectations in contracts - Maintain open and effective communication with contractors
	Labor shortage	6	6	- Offer competitive wages and benefits - Build a network of contractors
Environmental	Soil Contamination	3	6	- Perform environmental assessment - Use remediation techniques
	Pollution	4	6	- Adhere to environmental regulations - Implement waste management measures
	Weather Delays	7	6	- Schedule realistic timelines with buffer time in case of delays - Consider seasonal changes and climate when preparing a schedule
External	Changes in government policies or regulations	4	8	- Stay updated about the political situation in the world
	Geopolitical factors affecting the supply chain	4	9	- Have diverse suppliers from different countries - Buy essential materials in surplus

5.7. Quality management

Pre-Construction Phase

- Double-check that all design plans have been thoroughly evaluated and approved by the quality team.
- Ensure that any essential permits and compliance documentation (such as IBC, CBC, etc.) are secure and up to date.
- Ensure that material specifications, supplier certificates, and testing techniques are well-recorded and easily available.

Site Preparation and Foundation Work

- Analyze soil test data and geotechnical assessments to ensure they are consistent with the design specifications.
- Oversee excavation and compaction work to ensure retaining structures and drainage systems match design specifications.
- Ensure that foundation reinforcement and concrete pours adhere to the specified mix and placement criteria.

Building Construction Quality Checklist

Project Information

Project name: Civillians Inc. 12-story office building

Project location: 940 N Sycamore Avenue in Los Angeles, California

Project manager: Malika Sissenova

Inspection team: Alibi Seitkaliyev
Amirmagruf Amantay

Date: 25.02.2025

Phase 1. Pre construction checklist

1. Pre-Construction Phase
□ Verify that design documents are reviewed and approved.
□ Confirm that all permits and approvals are obtained.
□ Ensure material specifications and procurement plans are documented.
□ Conduct contractor and subcontractor qualifications.
□ Develop a site-specific quality management plan.
2. Foundation and Site Preparation
□ Inspect soil compaction and verify geotechnical reports.
□ Confirm rebar placement according to structural drawings.
□ Ensure concrete mix meets strength specifications.
□ Monitor curing process and perform compression tests.
□ Verify proper installation of drainage and waterproofing systems.

Figure 5.6 Construction Quality Checklist.

Structural Construction

- Inspect the positioning of rebar in columns, beams, and slabs to ensure it corresponds to the design drawings.
- Monitor concrete curing processes and ensure structural elements match the expected load estimates (as detailed in the GLRS and column design sections).
- Ensure that the formwork and scaffolding are stable and safe for workers to complete their tasks.

Non-Structural Elements and Finishes

- Check the quality and consistency of interior and exterior wall finishes (based on the chosen autoclaved aerated concrete system).
- Confirm that floor finishes, waterproofing, insulation, and ceiling installations are completed according to specifications.
- Validate that elevator installations and emergency exits meet the required clearance and safety standards as per architectural calculations.

Risk Management and Corrective Actions

- Keep a close eye on potential issues like material defects, poor workmanship, or delays that could impact quality.
- Document any problems and ensure corrective measures are implemented promptly.
- Periodically review risk areas, incorporating lessons learned and updating quality protocols as needed.

Final Inspection and Commissioning

Perform a thorough final walkthrough to confirm all construction work meets the project's quality standards.

Test and verify that all systems (structural, MEP, safety) are functioning correctly and have passed commissioning tests.

Create a detailed punch list and ensure all items are addressed before the project is handed over.

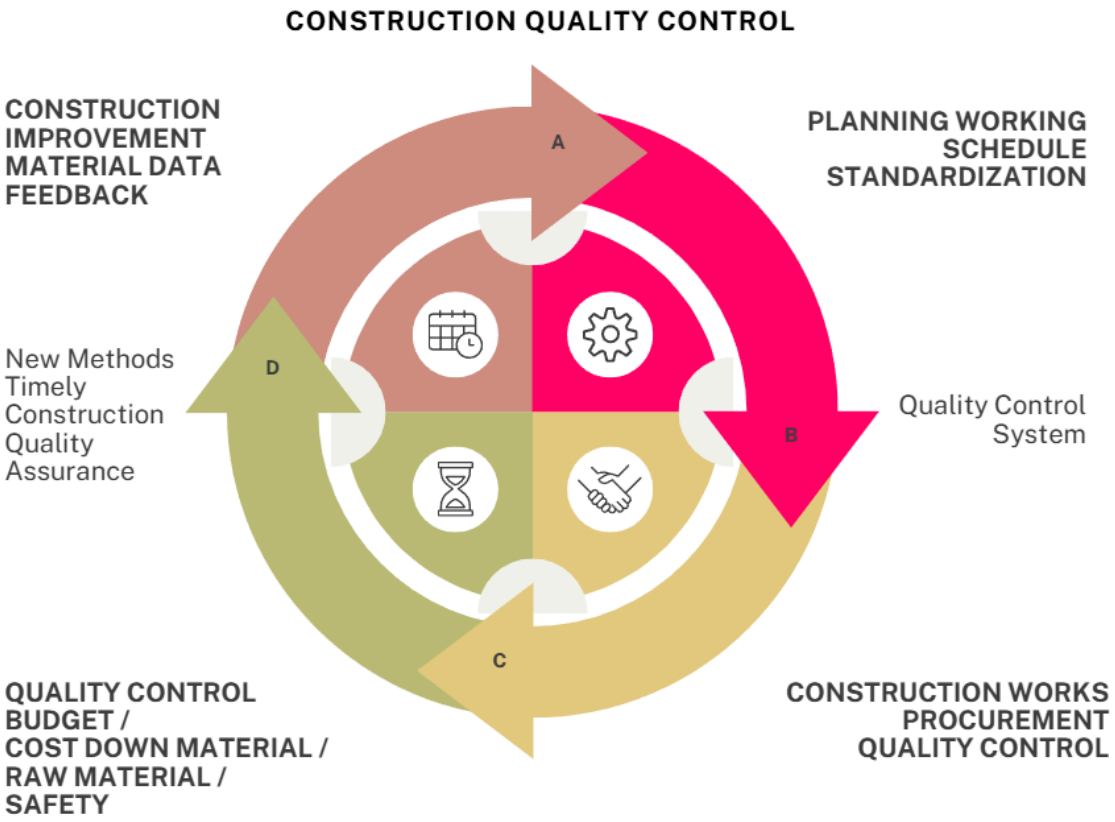

Figure 5.7. Quality metrics.

5.8. Procurement planning/ Stakeholder analysis

Procurement Process

A well-organized procurement process helps ensure that materials, equipment, and services are sourced efficiently and cost-effectively. Here's a breakdown of the typical steps involved:

1. Initiation and Planning

- Identify what's needed for the project, including materials, equipment, services, and labor.
- Develop a procurement strategy that aligns with the project's timeline and budget.
- Set clear evaluation criteria and performance metrics to guide decision-making.

2. Vendor Sourcing and Prequalification

- Research and identify potential vendors through market analysis or recommendations.
- Send out pre qualification questionnaires to assess vendors' capabilities, financial health, and track record.
- Create a shortlist of vendors that meet the project's technical and quality requirements.

3. Solicitation and Bidding

- Prepare and send out detailed Requests for Proposals (RFPs), Invitations to Bid (ITBs), or Requests for Quotations (RFQs).
- Host pre-bid meetings, if needed, to clarify project requirements and answer vendor questions.
- Collect and document all vendor bids for evaluation.

4. Evaluation and Award

- Evaluate bids based on factors like cost, quality, delivery timelines, and vendor reliability.
- Conduct technical and financial reviews to ensure vendors can meet project demands.
- Award the contract to the best-fit vendor and negotiate final terms.

5. Contract Negotiation and Finalization

- Finalize contract details, including scope, pricing, delivery schedules, quality standards, and penalties for non-compliance.
- Obtain necessary approvals from legal and management teams.
- Sign contracts and communicate expectations clearly to all parties involved.

6. Order Management and Execution

- Issue purchase orders and monitor delivery timelines.
- Inspect delivered goods to ensure they meet quality standards.
- Coordinate logistics and align deliveries with the construction schedule.

7. Performance Monitoring and Closure

- Track vendor performance against agreed milestones and quality benchmarks.
- Address any issues through corrective actions or contract adjustments.
- Conduct final inspections and formally close the procurement process once all deliverables are received and approved.

Table 5.4. Vendor list for construction materials.

Vendor Name	Products/Services Provided	Contact Information
Cemex USA	Ready-mix concrete, cement, aggregates	(855) 292-8453, www.cemexusa.com
California Steel Services	Structural steel, rebar, fabrication	(562) 941-0328, www.calsteel.com
United Rentals	Heavy equipment rental	(800) 877-3687, www.unitedrentals.com
Grainger	Safety equipment, tools, MEP supplies	(888) 361-8649, www.grainger.com
HD Supply Construction & Industrial	Building materials, tools, fasteners	(800) 431-3000, www.hdsupply.com
LA Steel Services	Custom steel fabrication, welding	(323) 585-2332, www.lasteel.com
Ferguson Enterprises	Plumbing, HVAC, waterworks supplies	(800) 721-2590, www.ferguson.com
Sunbelt Rentals	Construction equipment, generators	(800) 667-9328, www.sunbeltrentals.com
GCP Applied Technologies	Waterproofing, concrete additives	(877) 423-6491, www.gcpat.com

Table 5.5. Stakeholder matrix.

Stakeholder	Role/Responsibility	Level of Interest

Property Owner	Provides funding, defines project scope, and makes key decisions.	High
Architect	Designs the building layout, aesthetics, and compliance with zoning laws.	High
Civil Engineer	Ensures structural integrity, material selection, and site grading.	High
Construction Contractor	Manages construction activities, labor, materials, and scheduling.	High
Subcontractors/Suppliers	Provide materials, labor, and specialized construction services.	High
Governmental Authorities	Oversee regulatory compliance, issue permits, and conduct inspections.	High
Financial Institutions	Provide project financing, loans, and investment oversight.	Medium
Utility Companies	Install and maintain power, water, gas, and telecommunications infrastructure.	Medium
Environmental Consultants	Ensure compliance with environmental regulations and sustainability standards.	Medium

Legal Advisors	Handle contracts, dispute resolution, and regulatory compliance.	Medium
Future Residents	End users who will live in the property and assess livability.	Low

5.9. Construction safety

Improving site safety is a primary concern for global construction businesses. A positive and mature safety culture is becoming increasingly critical for facilitating such improvement. Anecdotal evidence reveals that in many big accidents, the safety management system's defenses failed due to the prevailing safety culture in which safety management operations were carried out (ACSNI 1993).

The industry's characteristics, such as dynamic work locations heavy equipment use, and seemingly inescapable worker-hazard interactions, all lead to disproportionate injury and illness rates when compared to other work industries. Regardless of these features, organizations that demonstrate and convey commitment to well-structured and well-funded safety programmes can successfully reduce incident rates (Hinze 1997).

The table below represents a phased project-specific accident prevention plan which was based on a thorough risk analysis

Table 5.6. Phased Project-Specific Accident Prevention Plan.

Phase	Construction Tasks	Potential Hazards	Equipment to be used	Prevention Measures

Site Preparation	Clearing, grading, excavation	- Uneven terrain - Falling objects - Underground utilities	- Excavators - Bulldozers - Dump trucks	- Conduct site survey - Mark utilities - Use spotters for heavy equipment
Foundation Work	Pouring concrete, rebar installation	-Falls from height - Chemical exposure - Strains & sprains	- Concrete mixers - Rebar cutters - Cranes	- Guardrails & harnesses - Proper ventilation - Manual handling training
Structural Framing	Steel/wood framing, welding	- Falling objects - Fire hazards - Electrocution	- Cranes - Welding machines - Nail guns	- Secure materials - Fire extinguishers on-site -Lockout/Tagout (LOTO) procedures
Electrical & Plumbing	Wiring, piping, HVAC	- Electrical shocks - Confined space hazards - Chemical leaks	- Drills - Pipe cutters - Testing equipment	- De-energize circuits before work - Confined space permits - Proper PPE (gloves, masks)

Finishing Work	Drywall, painting, flooring	- Dust inhalation - Slips & trips - Repetitive motion injuries	- Sanders - Paint sprayers - Tile cutters	- Use respirators - Keep walkways clear - Ergonomic tools & breaks

5.10. Construction site planning

The site has been carefully designed to maximise productivity, safety and efficiency. Key features include a dedicated employee and vehicle park for staff parking and equipment storage, a clearly defined vehicle circulation area to control the flow of trucks and heavy equipment and a secure materials storage area for the storage of construction materials including concrete, steel and timber.

The site will be accessed primarily via North Sycamore Avenue, with additional entry points along North Orange Drive to accommodate material deliveries. Pedestrian access will be segregated from the roadways to enhance worker safety and emergency evacuation routes will be clearly visible. The employee/vehicle park will be paved and fitted with security lights, while materials storage will be protected from the elements and theft by a covered storage area and fence. The vehicle circulation area will enforce speed limits and use spotters to direct vehicles to reverse, reducing the likelihood of accidents.

Safety and logistics were considered during the planning stages. To prevent congestion, internal traffic will be restricted to one direction and local authorities will be notified of any road closures or planned deliveries. Waste management plans will include dedicated waste disposal and recycling bins. Temporary facilities such as an on-site office, toilets and a first aid station will be installed near the officers' area for convenience. All underground utilities will be clearly marked to avoid accidental impacts during excavation.

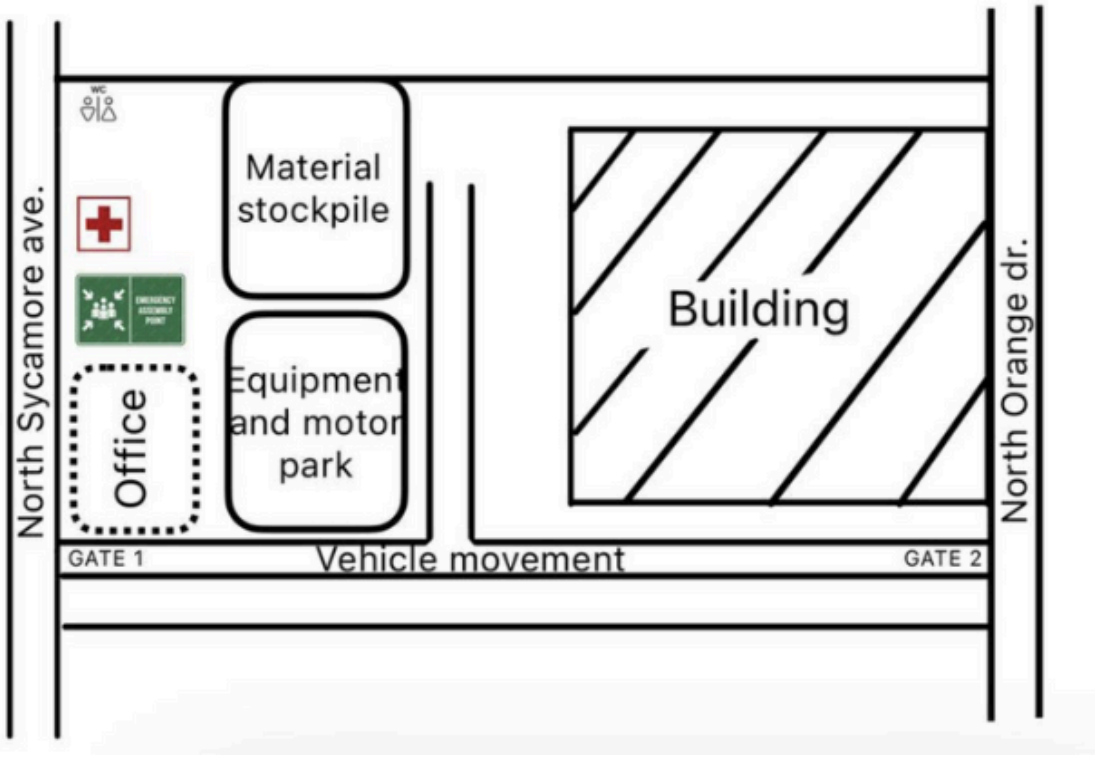

Figure 5.8.Construction site planning.

6. Environmental engineering

6.1. Introduction

Stormwater management is an essential aspect of urban development, ensuring effective handling of rainfall to prevent flooding, reduce environmental degradation, and promote sustainable land use. This report presents the analysis and design of a stormwater sewage system for the project area, focusing on grading, drainage, and environmental sustainability.

The project is located in a densely developed urban region characterized by varying topography and existing drainage infrastructure. The aim is to design a system that effectively manages stormwater runoff while adhering to regulatory standards and ensuring environmental sustainability. The report includes topographic analysis, slope evaluation, grading and drainage plans, and a sustainability-focused design.

6.2 Site Analysis

The project began with a detailed analysis of the topographic data of the area. The data was obtained by Contour Map Creator. The project area's topography, as illustrated in Figure 6.1, demonstrates significant elevation variations, with contour lines indicating natural flow patterns. Higher elevations in the northwest slope down toward the southeast, influencing the stormwater runoff direction. This variability in elevation necessitates careful grading to achieve effective drainage. Elevations on our site range between 84.063 - 85.256 m.

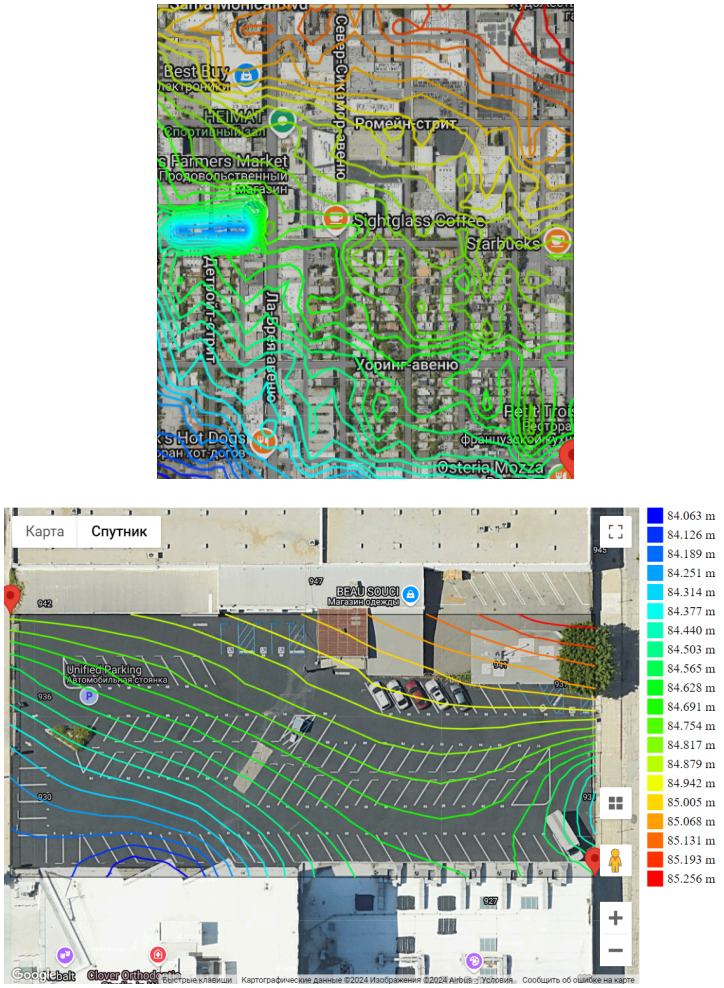

Figure 6.1. Topographic map of Project Area.

6.2.1 Existing Drainage System

This figure 6.2 shows a map of the Los Angeles County storm drain system in the site area (Los Angeles County Public Works, 2024). The surrounding area is serviced by a storm drain network with major stormwater flow directed along pre-existing pipelines. However, the existing infrastructure has limitations in handling peak rainfall, necessitating additional measures to prevent localized flooding within the project boundaries.

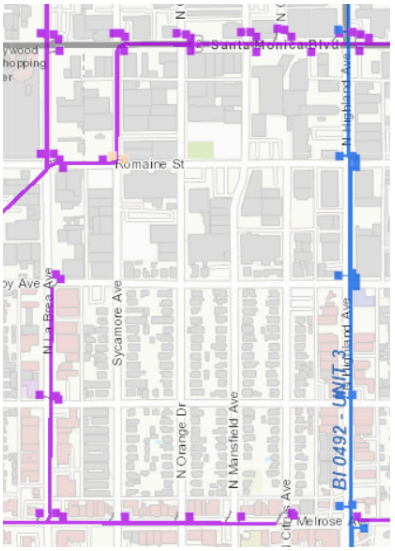

Figure 6.2. Los Angeles County Storm drain system.

6.2.2 Slope Analysis

By using a topographic map, the surface was created using the Civil 3D Autodesk program. By using this program slope, slope arrow, cut and fill analysis was held. Figure 6.3 highlights the slope distribution across the site. Areas with steeper slopes (6.91%–28.98%) present challenges for erosion control, while flatter areas (0%–1.34%) require enhanced drainage to prevent water pooling. The site grading will balance these variations, ensuring safe and efficient stormwater flow.

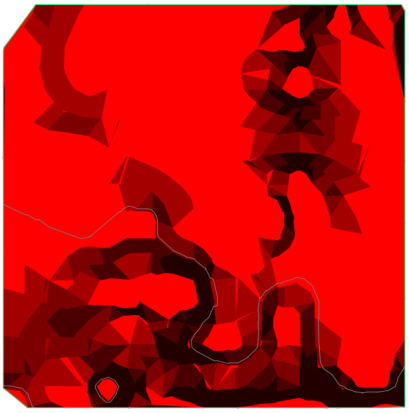

Slopes Table

Number	Minimum Slope	Maximum Slope	Area	Color
1	0.00%	1.34%	11767.13	
2	1.34%	2.15%	9221.30	
3	2.15%	2.92%	5488.99	
4	2.92%	3.67%	3948.21	
5	3.67%	4.77%	3035.13	
6	4.77%	6.91%	2051.16	
7	6.91%	28.98%	1298.96	

Figure 6.3. Slope analysis of the site.

6.3 Grading and Drainage Design

6.3.1 Slope Arrow Analysis

As shown in Figure 6.4, slope arrows indicate natural water flow paths across the site. High-density arrows in certain areas suggest potential zones of water accumulation, requiring strategic placement of catch basins and drainage inlets.

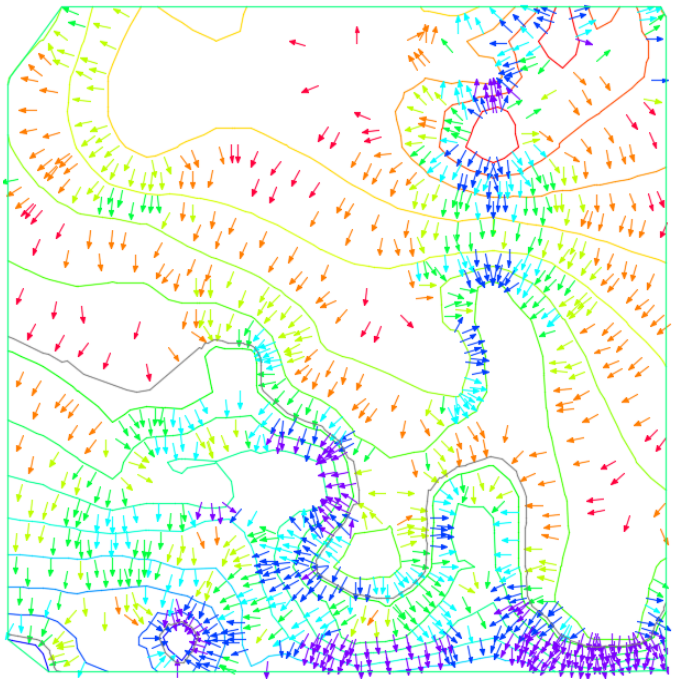

Figure 6.4 Slope arrow analysis of the site.

6.3.2 Grading Plan

Figure 6.5 presents the proposed grading design with specified elevations and slope percentages. Key considerations include:

Cut and Fill Requirements: Adjustments to the terrain are necessary to level the site while maintaining natural drainage paths.

Design Elevations: Critical points were assigned elevations to ensure water flows toward designated drainage outlets.

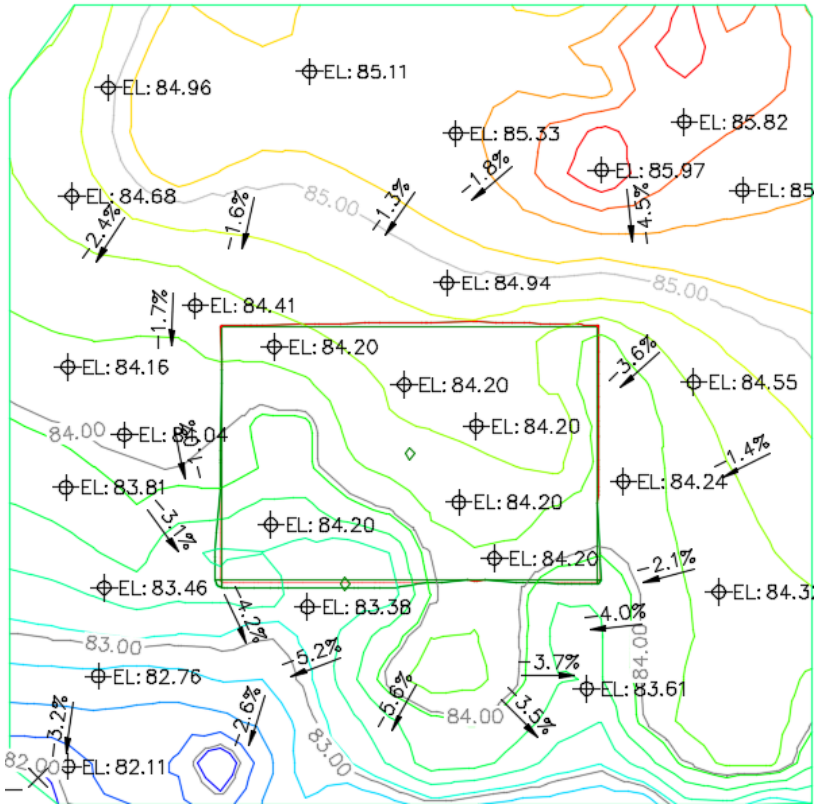

Figure 6.5 Grading of the site with elevations and slopes.

6.3.3 Cut and Fill Analysis

The cut and fill analysis, detailed in Figure 6.6, quantifies the earthwork required:

Cut Volume: 827.83 m³

Fill Volume: 1153.00 m³

Net Fill: 325.17 m³

This analysis ensures that earthworks are balanced, reducing material transport costs and environmental impacts.

Cut(adjusted)(Cu. ...	Fill(adjusted)(Cu. M.)	Net(adjusted)(Cu. ...	Net Graph
827.83	1153.00	325.17<Fill>	

Figure 6.6 Cut and fill analysis of the site.

6.4 Drainage Plan

6.4.1 Proposed Drainage System

The proposed grading and drainage plan (Figure 6.7) integrates porous concrete parking areas and green zones to enhance water infiltration. The design ensures:

- Slopes of 1.0%–1.5% direct water toward the drainage system.
- Permeable pavements minimize runoff, promoting infiltration.
- Green areas act as natural detention basins, improving sustainability.

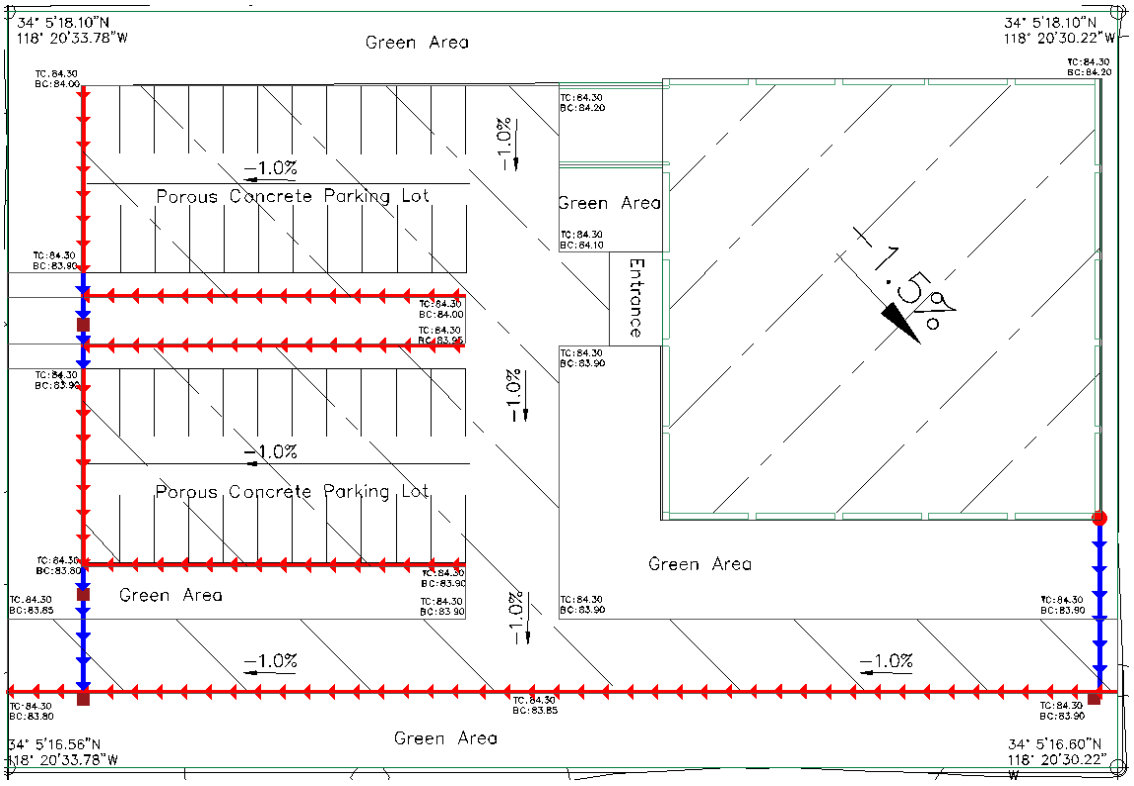

Figure 6.7 Preliminary grading and drainage plan of the site.

Key components of the stormwater sewage system include:

Catch Basins: The dark red squares represent inlets where stormwater enters the system. This placement ensures effective water collection, minimizing the risk of flooding during heavy rain.

Rooftop Catchment System: The red circle denotes a rooftop catching gutter system. This system is designed to capture runoff from the building's roof, which is significant in managing the volume of stormwater, especially during heavy rainfall. The roof is designed with a slight incline towards the gutter, facilitating the gravity-led flow of water and enhancing drainage efficiency.

Drains (Red Lines): The red lines represent drains that collect rainwater runoff from the building roof and paved areas. These drains are crucial for capturing and directing water to the sewer system, preventing water from accumulating and causing surface flooding. Alongside the red lines, which also denote drainage pathways, trees and other vegetation have been planted. These green infrastructure elements are crucial as they help absorb and filter stormwater, reducing runoff and improving water quality. The trees also provide additional benefits such as enhancing air quality, cooling the urban environment, and improving aesthetic value.

Routing: The blue lines in the diagram represent the pipes that connect catch basins.

In figure 6.8 red lines represent proposed stormwater pipes designed to connect with the existing city system (shown in purple and blue lines). This integration is crucial for dispersing water flow during peak conditions and preventing localized flooding.

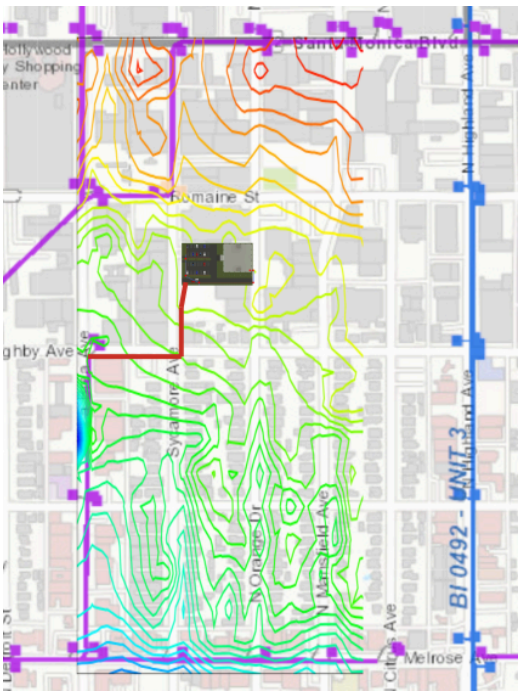

Figure 6.8. Design of tubes to the city storm drain system.

6.5 Stormwater Quantity Estimation

6.5.1 The Rational Method

The Rational Method estimates peak discharge based on rainfall intensity, land use, and area. It is suitable for urban and suburban areas with small drainage catchments. The governing equation is:

$$Q = C \cdot I \cdot A \quad [241]$$

Where:

Q - Peak runoff (cubic feet per second, cfs)

C - Runoff coefficient (dimensionless, based on surface type)

I - Rainfall intensity (inches per hour) for a given return period

A - Drainage area (acres)

Runoff coefficients are selected based on surface characteristics. Values were chosen according to

Asbestos sheet roof – 0.8 (Kumar, 2004)

Parking Lot – 0.9 (PDH, 2020)

Grass Area – 0.15 (Tsutsumi et al., 2004)

6.5.2 Area Classification

To enhance water management, the total area was subdivided into distinct surface types based on drainage patterns:

Grass area – 2109.76 m^2

Roof – 1267.36 m^2

Parking Lot – 2108.38 m^2

This classification helps accurately assess runoff potential by recognizing differences in infiltration and imperviousness.

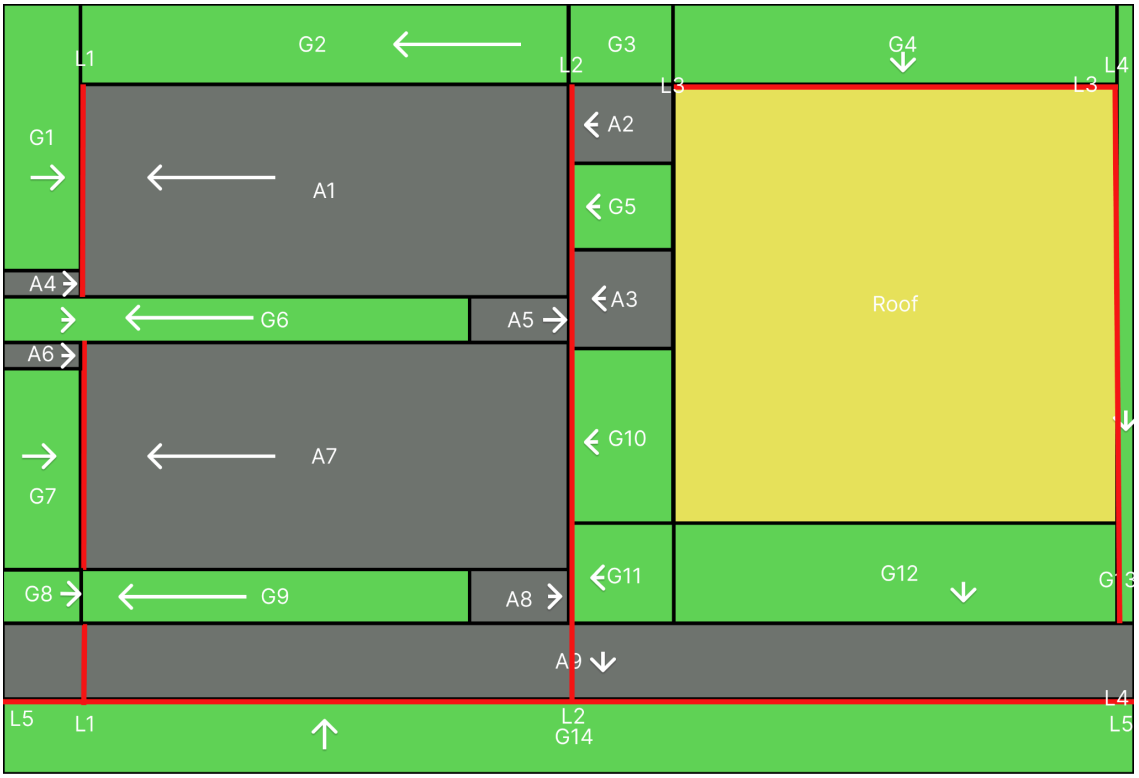

Figure 6.9. Division to small areas.

6.5.3 Rainfall Intensity

The rainfall intensity was derived based on a 10-year return period and a 24-hour storm duration. According to the NOAA Atlas 14 data (NOAA, 2023), the total precipitation for this event is 4.99 inches. The intensity is calculated as:

Intensity:

$$I = \frac{4.99\ in}{24hr} = 0.2079\ in/hr = 98.76mm/hr$$

This uniform intensity assumption is consistent with Rational Method applications for small sites.

6.5.4.Time of Concentration (T_c)

Time of concentration is the time required for water to flow from the furthest point of the catchment to the outlet. It is crucial in selecting the appropriate rainfall intensity for the Rational Method. The total time of concentration was computed using a combination of overland flow (sheet flow) and shallow concentrated flow.

Two formulas were used:

Sheet Flow Time (T_{t1}):

$$T_{t1} = \frac{0.933}{I^{0.4}} \left(\frac{nL}{\sqrt{S}}\right)^{0.6} \quad [242]$$

Where:

n - Manning's roughness coefficient

L - Length of flow path

S - Slope

I - Rainfall intensity

Shallow Concentrated Flow Time (T_{t2}):

$$V = 3.28\, k\, S_p^{0.5} \quad [243]$$

$$T_{t2} = \frac{L}{V} = \frac{L}{3.28\, k\, S_p^{0.5}} \quad [244]$$

Then:

$T_c = T_{t1} + T_{t2}$

Each sub-area's values were calculated individually in following Table 6.1.

Table 6.1. Calculation of each area time of concentration and runoff quantity.

	Width(mm)	Length(mm)	Slope Width %	Slope Length %	Area m2	Tt1	Tt2	Tc	Q(cfs)
G1	5969	21100	1	0	125,95	13,29	2,12	15,41	0,0009706
G2	38730	6003	1	0	232,50	40,81	0,60	41,42	0,0017917

G3	8370	6003	0	1	50,25	13,33	0,84	14,18	0,0003872
G4	35600	6003	0	1	213,71	13,33	3,57	16,91	0,0016469
G5	8370	6748	1	0	56,48	16,28	0,68	16,96	0,0004353
G6	37100	3691	0	1	136,94	9,96	3,72	13,68	0,0010553
G7	5969	16000	1	0	95,50	13,29	1,61	14,90	0,0007360
G8	5969	4238	1	1	25,30	10,82	0,43	11,25	0,0001949
G9	31179	4238	0	1	132,14	10,82	3,13	13,95	0,0010183
G10	8370	14129	1	0	118,26	16,28	1,42	17,70	0,0009113
G11	8370	7870	1	1	65,87	15,69	0,79	16,48	0,0005076
G12	35600	7870	0	1	280,17	15,69	3,57	19,26	0,0021591
G13	1329	49000	0	1	65,12	47,00	0,13	47,13	0,0005018
G14	90000	5950	0	1	535,50	13,26	9,03	22,30	0,0041267
A1	38730	17096	1	1	662,13	24,99	2,32	27,31	0,0306154
A2	8370	6650	1	0	55,66	16,28	0,90	17,18	0,0025736
A3	8370	7600	1	0	63,61	16,28	1,03	17,31	0,0029413
A4	5969	2000	1	0	11,94	13,29	0,27	13,56	0,0005520
A5	6197	3691	1	0	22,87	13,59	0,50	14,09	0,0010576
A6	5969	2000	1	0	11,94	13,29	0,27	13,56	0,0005520
A7	38779	18000	1	1	698,02	25,77	2,45	28,22	0,0322751
A8	7600	4238	0	1	32,21	10,82	1,03	11,85	0,0014893
A9	90000	6000	0	1	540,00	13,33	12,24	25,57	0,0249685
Roof	35600	35600	1,5	1,5	1267,36	34,36	4,84	39,20	0,0520890
								Total	0,1655566

Peak runoff values for all sub-areas were obtained by applying the Rational Method after computing the time of concentration. This process was repeated for all areas including grass patches, roof areas, and impervious zones like parking lots. The total peak runoff from all catchments summed up to 0.1656 cfs.

6.6 Drainage Design

6.6.1 Manning's Equation

$$Q = \frac{1.486}{n} A R^{2/3} S^{1/2} \quad [245]$$

Where:

Q - Flow rate (m^3/s)

n - Manning's roughness coefficient (assumed 0.010 for HDPE pipes)

A - Flow cross-sectional area (m^2)

R - Hydraulic radius

S - Slope (2%, chosen to meet velocity requirements in 4-inch pipes)

High-Density Polyethylene (HDPE) pipes were selected for the storm sewer system due to their excellent hydraulic performance, durability, and ease of installation. HDPE offers a low Manning's roughness coefficient (n = 0.010), which allows for higher flow capacities compared to traditional materials under similar slope and diameter conditions. This contributes to more compact and cost-effective pipe sizing while maintaining efficient flow. In addition, HDPE is highly resistant to corrosion, chemical attack, and abrasion, making it particularly suitable for stormwater applications where variable water quality and sediment loads are expected. The flexibility of HDPE also allows for easier handling during installation, reduces the need for extensive jointing, and helps accommodate slight ground movements, minimizing the risk of cracking or leakage over time. These combined properties make HDPE a sustainable and reliable choice for long-term infrastructure performance.

For simplicity and efficiency, drainage was modeled using an optimum rectangular channel, where:

$$Width(w) = 2 * Depth\,(d) \quad [246]$$

This shape yields the minimum wetted perimeter for a given flow area, maximizing hydraulic efficiency. Therefore, the cross-sectional area becomes:

$$A = 2d^2 \quad [247]$$

Using the calculated flow rate Q, slope S = 0.02, and Manning's n, we computed the corresponding depth and width for each drainage line to ensure adequate capacity. Calculations are shown in following Table 6.2.

Table 6.2. Calculation of each pipe sizes.

Drains	Areas	Q(m3/s)	Estimated Area (m2)	depth of pipe(mm)	Width (mm)
L1	G1+A4+G2+A1+G6+ A6+A7+G7+G8+G9	0,001975419933	0,001316946622	25,66073481	51,32146963
L2	G3+A2+G5+A3+A5+ AG10+G11+A8	0,0002917551137	0,0001945034091	9,861627886	19,72325577
L3	G4	0,00004663485041	0,00003108990027	3,942708477	7,885416955
L4	G13+Roof	0,001489207064	0,0009928047093	22,28008875	44,5601775
L5	G12+A9+G14	0,004688041009	0,003125360672	39,53075178	79,06150356

Although the above calculations provide theoretically sufficient dimensions for each drain line based on hydraulic requirements, many of the resulting cross-sections - particularly for minor flow areas - are too small for practical construction and maintenance. Several computed depths and widths fall below 25 mm and 50 mm respectively, which are not suitable for standard construction practices.

According to local stormwater design guidelines (Los Angeles County Department of Public Works [LACDPW], 2006), the minimum allowable pipe diameter for storm drains is 4 inches (approximately 100 mm). This minimum ensures structural integrity, ease of installation, and maintenance accessibility, and also provides a safety margin to handle sediment deposition or minor increases in flow.

Therefore, to comply with these local regulations and ensure long-term reliability, all pipe segments have been resized to a minimum diameter of 4 inches, regardless of the initially calculated flow capacity.

6.6.2 Final Cross-Sectional Views of Drainage Channels

To illustrate the final channel designs, cross-sectional views were developed based on the calculated dimensions and adjusted to comply with local minimum requirements. The flow-carrying channels are modeled as optimum rectangular sections, where the width is twice the depth to maximize hydraulic efficiency while simplifying construction.

Since some of the calculated dimensions resulted in very narrow and shallow channels, all pipe sections were adjusted to the minimum required size of 4 inches (100 mm) in depth, with corresponding widths of 200 mm. This ensures compliance with Los Angeles County drainage standards, which mandate a minimum pipe diameter of 4 inches for stormwater systems (LACDPW, 2006). Figure 6.10 shows the cross-section facing the direction of flow, including depth, width, and pipe material (HDPE).

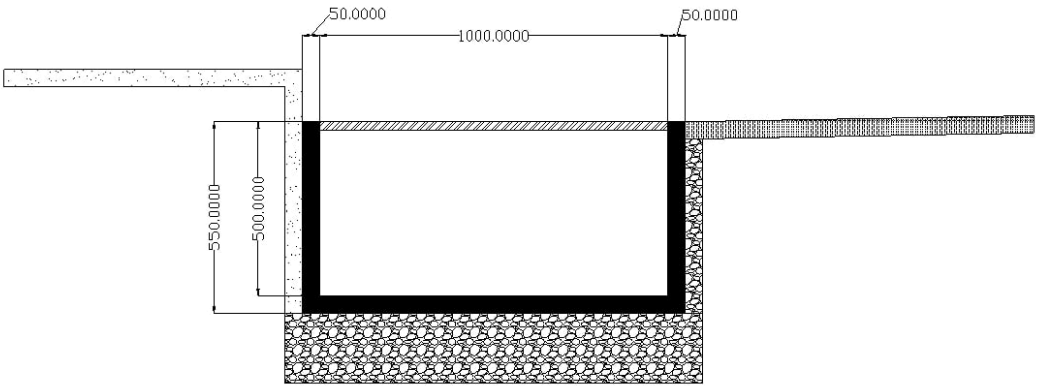

Figure 6.10. Front View.

Figure 6.11 Displays the longitudinal profile of the pipe with an applied slope of 2% (20 mm per meter), indicating the direction of flow and connection to inlet or outlet structures.

Figure 6.11. Side View.

The final drainage plan was developed based on updated hydraulic calculations and feedback received during the design review process. Adjustments were made to the original layout to better reflect realistic runoff conditions, improve flow efficiency, and address concerns raised during evaluation. These refinements included modifying pipe sizes, reassessing drainage subareas, and confirming that all components complied with both hydraulic principles and **local regulations** (Los Angeles County Department of Public Works, 2006). The updated design ensures that the stormwater system is both functionally effective and compliant with regulatory and practical standards.

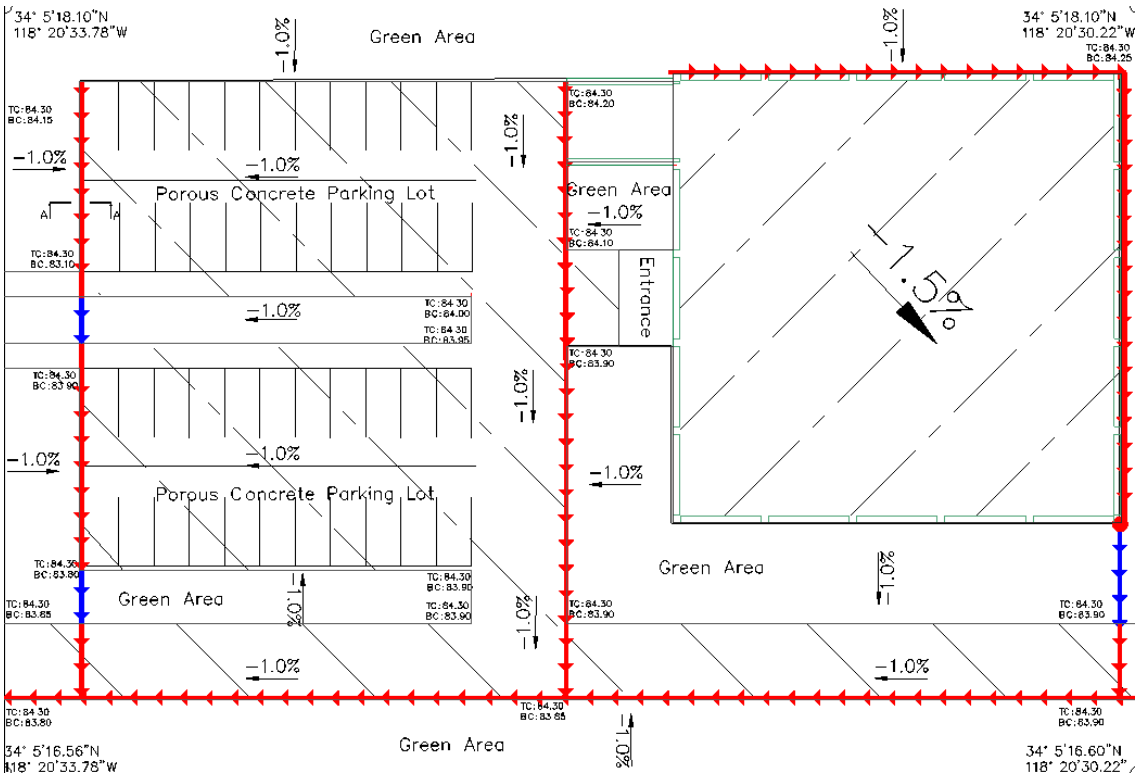

Figure 6.12. Final Drainage plan

This capstone project successfully fulfilled the objective of designing a comprehensive storm sewer system for the designated project area by progressing through a series of methodical and interrelated design phases over two academic semesters.

During the first semester, the focus was on laying the foundational aspects of the design. A preliminary horizontal layout was developed based on the site's topography and existing infrastructure. This helped define the most efficient drainage paths while minimizing conflicts with existing utilities..

In the second semester, the project advanced to the analytical and technical design stages. The Rational Method was used to estimate peak stormwater runoff, considering the specific surface types and a 10-year return period rainfall event. These flow rates informed the hydraulic design of the storm sewer system using Manning's equation, assuming HDPE material and a minimum slope of 2% to ensure self-cleansing velocities. Although some calculated pipe dimensions were minimal, all were adjusted to meet local regulatory standards, with a minimum pipe diameter of 4 inches, ensuring constructability and long-term system performance. Furthermore, a rainwater collection system was designed for rooftops and parking areas, integrating sustainability through runoff management and structural adequacy.

The final design meets all required components of the assignment, including a detailed layout, hydraulic calculations, and compliance with engineering standards. In addition to meeting performance objectives, the system was developed with an emphasis on practicality, regulatory compliance, and sustainability, aligning with the evaluation criteria of the capstone project.

This project not only strengthened technical competencies in stormwater system design but also encouraged critical thinking, teamwork, and a deeper understanding of sustainable infrastructure planning — valuable skills for future engineering practice.

7. Conclusion

The successful completion of this capstone project demonstrates the comprehensive effort involved in designing a 12-story high-rise office building in Los Angeles, California. This endeavor integrates architectural innovation, structural integrity, geotechnical precision, environmental responsibility, and effective construction management.

By adhering to local building codes such as the International Building Code (IBC), California Building Code (CBC), and ASCE guidelines, the project ensures safety, functionality, and resilience, particularly in a seismically active region. The use of reinforced concrete as the primary material provides cost-effectiveness, durability, and adaptability, meeting both economic and structural needs.

The geotechnical analysis led to the selection of a pile foundation system, optimizing the building's support on the site’s soil conditions. The environmental engineering aspects focused on sustainable practices, including efficient stormwater management, energy conservation, and the adoption of LEED principles to reduce the building's ecological footprint.

This project exemplifies the harmonious integration of technical expertise and innovative design, contributing to urban development in Los Angeles. Future work may focus on refining construction techniques, exploring additional sustainable practices, and enhancing occupant amenities. This report serves as a foundation for realizing a safe, efficient, and modern office space that aligns with the city’s growth and sustainability goals.

8. References

Aarsleff. (n.d.). Available at: https://aarsleff.co.uk/company-news/top-10-advantages-of-sheet-piling/#:~:text=1)%20Sheet%20piles%20are%20recyclable,silent%20and%20vibration%2Dfree%20methods.

Admane, H. and Murnal, P. (2017). Analysis of masonry structures: A review. *International Journal of Engineering Research and Applications, 63*(1), pp. 68-78. Available at: https://www.researchgate.net/publication/345710631_ANALYSIS_OF_MASONRY_STRUCTURES_A_REVIEW

Autodesk. (2024). Commercial Construction Cost Per Square Foot. Available at: https://www.autodesk.com/blogs/construction/commercial-construction-cost-per-square-foot/

ArcelorMittal Sheet Piling. (n.d.). Installation method. Available at: https://sheetpiling.arcelormittal.com/installation-method

California Building Standards Commission. (n.d.) *Building Standards Commission*. Available at: https://www.dgs.ca.gov/BSC (Accessed: 27 September 2024).

CDTFA. (2024). Tax Guides for Construction Contractors. Available at: https://www.cdtfa.ca.gov/industry/construction-contractors/industry-topics.htm#:~:text=Currently%20the%20state%20rate%20is,then%20you%20owe%20the%20difference.

City of Los Angeles. (n.d.). Sewer structures. *GeoHub*. Available at: https://geohub.lacity.org/datasets/lahub::sewer-structures/explore?location=34.087197%2C-118.343112%2C16.50

Civiltoday.com. (n.d.). Advantages and Disadvantages of Pile Foundation. Available at: https://civiltoday.com/geotechnical-engineering/foundation-engineering/deep-foundation/449-advantages-and-disadvantages-of-pile-foundation

CivilWeb Spreadsheets. (n.d.). Terzaghi Bearing Capacity. Available at: https://civilweb-spreadsheets.com/foundation-design-spreadsheet/soil-bearing-capacity-calculation-excel/terzaghi-bearing-capacity/

Contour Map Creator. (n.d.). *Contour Map Creator*. Retrieved 27 September 2024, from https://contourmapcreator.urgr8.ch/.

Copper Development Association, 2025. *Architectural Handbook*. Available at: https://copper.org/publications/pub_list/pdf/A4050-Architectural-Handbook.pdf [Accessed 22 April 2025].

Das, B.M. and Sivakugan, N. (2019). Principles of foundation engineering. Boston, Cengage Learning.

Designing Buildings. (2022). Sheet piles. Available at: https://www.designingbuildings.co.uk/wiki/Sheet_piles#Steel_sheet_piles

Different types of concrete grades and their uses (2023) Base Concrete. Available at: https://www.baseconcrete.co.uk/different-types-of-concrete-grades-and-their-uses/ (Accessed: 24 April 2025)

Encardio Rite. (n.d.). Soil Investigation: Ensuring Structural Stability and Cost Efficiency. Available at: https://www.encardio.com/blog/soil-investigation-construction-guide

Hassoun, M.N. and Al-Manaseer, A.A. (2020) Structural concrete: Theory and design. Hoboken, NJ: Wiley.

ICC Digital Codes. (2023). *2023 City of Los Angeles Building Code (2 Volumes) - Full Code*. Available at: https://codes.iccsafe.org/content/CACLABC2023P1/chapter-18-a-soils-and-foundations#CACLABC2023P1_Ch18A_Sec1809A

International Code Council, 2021. *Chapter 15: Roof Assemblies and Rooftop Structures*. In: *2021 International Building Code*. Available at: https://codes.iccsafe.org/content/IBC2021P1/chapter-15-roof-assemblies-and-rooftop-structures [Accessed 22 April 2025].

International Code Council, 2021. *Section 713.4: Fire-Resistance Rating of Shaft Enclosures*. In: *2021 International Building Code, Chapter 7: Fire and Smoke Protection Features*. Available at: https://codes.iccsafe.org/s/IBC2021P1/chapter-7-fire-and-smoke-protection-features/IBC2021P1-Ch07-Sec713.4 [Accessed 22 April 2025].

Kalpana, M. and Mohith, S. (2020). Study on autoclaved aerated concrete: Review. *Materials Today: Proceedings, 22*(3), pp. 894-896. https://doi.org/10.1016/j.matpr.2020.03.171

Kumar, M. D. (2004). Roof water harvesting for domestic water security: Who gains and who loses? *Water International*, *29*(1), 43–53. https://doi.org/10.1080/02508060408691747

Laera, A., & Brinkgreve, R.B.J. (2016). Site response analysis and liquefaction evaluation. Available at: https://bentleysystems.service-now.com/community?id=kb_article_view&sysparm_article=KB0110096

LEED. (n.d.). Available at: https://www.usgbc.org/leed

Lehner, T. (2021). Quality assurance in construction: 5 golden rules. Available at: https://www.planradar.com/quality-assurance-in-construction-5-golden-rules-saving-money/

Los Angeles County Department of Public Works. (2006). *Hydrology Manual* (2nd ed.). https://dpw.lacounty.gov/wrd/publication/engineering/2006_Hydrology_Manual/

Los Angeles County Public Works. (n.d.). Storm Drain System Maps. Retrieved 27 September 2024, from https://pw.lacounty.gov/fcd/StormDrain/index.cfm.

Los Angeles Fire Department. (n.d.). Fire zone map. Available at: https://lafd.org/fire-prevention/brush/fire-zone/fire-zone-map

Modulus of Elasticity of Concrete. (n.d.). Available at: https://www.engineeringcivil.com/modulus-of-elasticity-of-concrete.html/comment-page-2

NFSA (2024). Occupancy Classifications in the IBC. Available at: https://nfsa.org/2024/01/08/occupancy-classifications-in-the-ibc/ (Accessed: 23 November 2024).

OSHA (n.d.) Soil Classification Outline. Available at: https://www.osha.gov/sites/default/files/2020-06/Soil%20Classification%20Training%20Outline.pdf

Paredes, R. (2024). What is Backfill and Why is It Important? Available at: https://safetyculture.com/topics/backfilling/

Pooja. (2022, January 11). Column layout for residential building - 4 important points. *Civil Engineering, Building/Structure Engineering*. Available at: https://www.gcelab.com/blog/column-layout-for-residential-building-4-important-points

Q Green Techcon. (n.d.). Normal Concrete vs High-Strength Concrete Properties and Differences. Available at: https://qgreentech.com/normal-concrete-vs-high-strength-concrete/#:~:text=The%20compressive%20strength%20of%20normal,high%20strength%20concrete%20also%20changes.

REGA Engineering. (2023). Steps of a Site Survey. Available at: https://www.regaeng.com/steps-of-a-site-survey

Reinforcement products online. (2024). What Is a Pile Cap? A Brief Introduction. Available at: https://www.reinforcementproductsonline.co.uk/news/pile-cap-reinforcement/

Scoutred. (n.d.). Zoning information for 3855. Available at: https://scoutred.com/zoning/3855

Stormwater drainage design for parking lots. (n.d.-b). https://pdhonline.com/courses/c201/c201content.pdf

SW Funk (2024). Foundation Excavation: Understanding The Process and Best Practices. Available at: https://swfunk.com/news/foundation-excavation-process-best-practices/

Thapa, I., Bhandari, A. and Subedi, B. (2020). Comparative study of structural analysis between reinforced cement concrete structure and steel framed structure. *International Journal of Engineering Research & Technology, 07*(08), pp. 3633-3637. Available at: https://www.researchgate.net/publication/343857703_Comparative_Study_of_Structural_Analysis_between_Reinforced_Cement_Concrete_Structure_and_Steel_Framed_Structure

Tradesafe. (2024). Guide to Site Clearing in Construction: Importance & How It's Done. Available at: https://trdsf.com/blogs/news/what-is-site-clearing#:~:text=Site%20clearing%20is%20a%20fundamental%20part%20of%20the%20construction%20process,safe%20and%20accessible%20work%20area

Tsutsumi, A., Jinno, K., & Berndtsson, R. (2004). Surface and subsurface water balance estimation by the groundwater recharge model and a 3-D two-phase flow model/estimation de Bilan hydrologique de surface et de subsurface à l'aide de modèles de recharge de nappe et d'écoulement diphasique 3-D. *Hydrological Sciences Journal*, *49*(2). https://doi.org/10.1623/hysj.49.2.205.34837

U.S. Department of Justice. (2010). *2010 ADA Standards for Accessible Design*. Available at: https://www.ada.gov/regs2010/2010ADAStandards/2010ADAstandards.htm (Accessed: 27 September 2024).

U.S. Geological Survey. (2020). What is the probability that an earthquake will occur in the Los Angeles Area? Available at: https://www.usgs.gov/faqs/what-probability-earthquake-will-occur-los-angeles-area-san-francisco-bay-area

U.S. Green Building Council. (n.d.). Water strategies in LEED v4. *U.S. Green Building Council*. Available at: https://www.usgbc.org

Using wood as a new generation building material in the context of sustainable development. (2022). Available at: https://www.researchgate.net/publication/359137232_Using_wood_as_a_new_generation_building_material_in_the_context_of_sustainable_development

9. Appendix

9.1 Appendix A

Table 9.1 Frame Stiffness Calculations.

Floor	$I_{c,cr}$, m^4	$I_{b,cr}$, m^4	D, kN/m	h, m	C_F, kN/rad
1	1.85E-02	3.5E-03	10061	4	201220
2	1.85E-02	3.5E-03	10061	4	201220
3	1.04E-02	3.5E-03	17328	3	259920
4	1.04E-02	3.5E-03	17328	3	259920
5	5.34E-03	3.5E-03	15475	3	232122
6	5.34E-03	3.5E-03	15475	3	232122
7	3.65E-03	3.5E-03	14044	3	210667
8	3.65E-03	3.5E-03	14044	3	210667
9	1.49E-03	3.5E-03	9888	3	148327
10	1.49E-03	3.5E-03	9888	3	148327
11	4.73E-04	3.5E-03	4747	3	71212
12	4.73E-04	3.5E-03	4747	3	71212
13	4.73E-04	3.5E-03	4747	3	14242

Calculations of seismic forces including the torsional effect for each floor are presented in Tables 9.2-9.13.

Table 9.2. Seismic forces calculations including the torsional effect (Floor 2).

Floor #	Frame #	$F_{torsion}$, kN	F_{direct}, kN	F_{total}, kN
2	1	-2.9036	26.62	23.72
	2	-1.7421	26.62	24.88
	3	-0.5807	26.62	26.04
	4	0.5807	26.62	27.21
	5	1.7421	26.62	28.37
	6	2.9036	26.62	29.53

Table 9.3. Seismic forces calculations including the torsional effect (Floor 3).

Floor #	Frame #	$F_{torsion}$, kN	F_{direct}, kN	F_{total}, kN
3	1	-3.8856	35.63	31.74
	2	-2.3314	35.63	33.30
	3	-0.7771	35.63	34.85
	4	0.7771	35.63	36.41
	5	2.3314	35.63	37.96
	6	3.8856	35.63	39.52

Table 9.4. Seismic forces calculations including the torsional effect (Floor 4).

Floor #	Frame #	$F_{torsion}$, kN	F_{direct}, kN	F_{total}, kN
4	1	-5.4579	50.05	44.59
	2	-3.2747	50.05	46.77
	3	-1.0916	50.05	48.96

	4	1.0916	50.05	51.14
	5	3.2747	50.05	53.32
	6	5.4579	50.05	55.51

Table 9.5. Seismic forces calculations including the torsional effect (Floor 5).

Floor #	Frame #	$F_{torsion}$, kN	F_{direct}, kN	F_{total}, kN
5	1	-6.9909	64.10	57.11
	2	-4.1946	64.10	59.11
	3	-1.3982	64.10	62.71
	4	1.3982	64.10	65.50
	5	4.1946	64.10	68.30
	6	6.9909	64.10	71.10

Table 9.6. Seismic forces calculations including the torsional effect (Floor 6).

Floor #	Frame #	$F_{torsion}$, kN	F_{direct}, kN	F_{total}, kN
6	1	-8.7899	80.60	71.81
	2	-5.2739	80.60	75.33
	3	-1.7580	80.60	78.84
	4	1.7580	80.60	82.36
	5	5.2739	80.60	85.87
	6	8.7899	80.60	89.39

Table 9.7. Seismic forces calculations including the torsional effect (Floor 7).

Floor #	Frame #	$F_{torsion}$, kN	F_{direct}, kN	F_{total}, kN
7	1	-10.5794	97.01	86.43
	2	-6.3476	97.01	90.66
	3	-2.1159	97.01	94.89
	4	2.1159	97.01	99.13
	5	6.3476	97.01	103.36
	6	10.5794	97.01	107.59

Table 9.8. Seismic forces calculations including the torsional effect (Floor 8).

Floor #	Frame #	$F_{torsion}$, kN	F_{direct}, kN	F_{total}, kN
8	1	-12.5743	115.30	102.73
	2	-7.5446	115.30	107.76
	3	-2.5149	115.30	112.79
	4	2.5149	115.30	117.82
	5	7.5446	115.30	122.85
	6	12.5743	115.30	127.88

Table 9.9. Seismic forces calculations including the torsional effect (Floor 9).

Floor #	Frame #	$F_{torsion}$, kN	F_{direct}, kN	F_{total}, kN
9	1	-14.3721	131.79	117.42
	2	-8.6233	131.79	123.16
	3	-2.8744	131.79	128.91

	4	2.8744	131.79	134.66
	5	8.6233	131.79	140.41
	6	14.3721	131.79	146.16

Table 9.10. Seismic forces calculations including the torsional effect (Floor 10).

Floor #	Frame #	$F_{torsion}$, kN	F_{direct}, kN	F_{total}, kN
10	1	-16.5104	151.40	134.88
	2	-9.9062	151.40	141.49
	3	-3.3021	151.40	148.09
	4	3.3021	151.40	154.70
	5	9.9062	151.40	161.30
	6	16.5104	151.40	167.91

Table 9.11. Seismic forces calculations including the torsional effect (Floor 11).

Floor #	Frame #	$F_{torsion}$, kN	F_{direct}, kN	F_{total}, kN
11	1	-18.4351	169.04	150.61
	2	-11.0611	169.04	157.98
	3	-3.6870	169.04	165.36
	4	3.6870	169.04	172.73
	5	11.0611	169.04	180.11
	6	18.4351	169.04	187.48

Table 9.12. Seismic forces calculations including the torsional effect (Floor 12).

Floor #	Frame #	$F_{torsion}$, kN	F_{direct}, kN	F_{total}, kN
12	1	-20.6999	189.81	169.11
	2	-12.4199	189.81	177.39
	3	-4.1400	189.81	185.67
	4	4.1400	189.81	193.95
	5	12.4199	189.81	202.23
	6	20.6999	189.81	210.51

Table 9.13. Seismic forces calculations including the torsional effect (Floor 13 - Roof).

	Transverse				Longitudinal			
Floor	Frame	$F_{torsion}$, kN	F_{direct}, kN	F_{total}, kN	Frame	$F_{torsion}$, kN	F_{direct}, kN	F_{total}, kN
13	A	-8.3751	191.99	183.62	1	-41.1414	191.99	150.85
	B	8.3751	191.99	200.37	2	-24.6848	191.99	167.31
					3	24.6848	191.99	216.68
					4	41.1414	191.99	233.13

9.2 Appendix B

Calculations of wind forces including the torsional effect for each floor are presented in Tables 9.14-9.25 for case 2. For Case 4, all calculations are given in Tables 9.26-9.37.

Table 9.14. Calculation of wind forces on each frame including the torsional effect for Case 2 (Floor 2).

Floor #	Frame #	$F_{torsion}$, kN	F_{direct}, kN	F_{total}, kN
2	1	-1.2384	13.76	12.52
	2	-0.7430	13.76	13.02
	3	-0.2477	13.76	13.52
	4	0.2477	13.76	14.01
	5	0.7430	13.76	14.51
	6	1.2384	13.76	15.00

Table 9.15. Calculation of wind forces on each frame including the torsional effect for Case 2 (Floor 3).

Floor #	Frame #	$F_{torsion}$, kN	F_{direct}, kN	F_{total}, kN
3	1	-1.2981	12.34	11.05
	2	-0.7789	12.34	11.57
	3	-0.2596	12.34	12.08
	4	0.2596	12.34	12.60
	5	0.7789	12.34	13.12
	6	1.2981	12.34	13.64

Table 9.16. Calculation of wind forces on each frame including the torsional effect for Case 2 (Floor 4).

Floor #	Frame #	$F_{torsion}$, kN	F_{direct}, kN	F_{total}, kN
	1	-1.3471	12.77	11.42
	2	-0.8082	12.77	11.96

4	3	-0.2694	12.77	12.50
	4	0.2694	12.77	13.04
	5	0.8082	12.77	13.58
	6	1.3471	12.77	14.12

Table 9.17. Calculation of wind forces on each frame including the torsional effect for Case 2 (Floor 5).

Floor #	Frame #	$F_{torsion}$, kN	F_{direct}, kN	F_{total}, kN
5	1	-1.3890	13.14	11.75
	2	-0.8334	13.14	12.30
	3	-0.2778	13.14	12.86
	4	0.2778	13.14	13.41
	5	0.8334	13.14	13.97
	6	1.3890	13.14	14.53

Table 9.18. Calculation of wind forces on each frame including the torsional effect for Case 2 (Floor 6).

Floor #	Frame #	$F_{torsion}$, kN	F_{direct}, kN	F_{total}, kN
6	1	-1.4260	13.46	12.04
	2	-0.8556	13.46	12.61
	3	-0.2852	13.46	13.18
	4	0.2852	13.46	13.75
	5	0.8556	13.46	14.32

	6	1.4260	13.46	14.89

Table 9.19. Calculation of wind forces on each frame including the torsional effect for Case 2 (Floor 7).

Floor #	Frame #	$F_{torsion}$, kN	F_{direct}, kN	F_{total}, kN
7	1	-1.4592	13.76	12.30
	2	-0.8755	13.76	12.88
	3	-0.2918	13.76	13.47
	4	0.2918	13.76	14.05
	5	0.8755	13.76	14.64
	6	1.4592	13.76	15.22

Table 9.20. Calculation of wind forces on each frame including the torsional effect for Case 2 (Floor 8).

Floor #	Frame #	$F_{torsion}$, kN	F_{direct}, kN	F_{total}, kN
8	1	-1.4894	14.03	12.54
	2	-0.8936	14.03	13.14
	3	-0.2979	14.03	13.73
	4	0.2979	14.03	14.33
	5	0.8936	14.03	14.92
	6	1.4894	14.03	15.52

Table 9.21. Calculation of wind forces on each frame including the torsional effect for Case 2 (Floor 9).

Floor #	Frame #	$F_{torsion}$, kN	F_{direct}, kN	F_{total}, kN
9	1	-1.5172	14.28	12.76
	2	-0.9103	14.28	13.37
	3	-0.3034	14.28	13.98
	4	0.3034	14.28	14.58
	5	0.9103	14.28	15.19
	6	1.5172	14.28	15.80

Table 9.22. Calculation of wind forces on each frame including the torsional effect for Case 2 (Floor 10).

Floor #	Frame #	$F_{torsion}$, kN	F_{direct}, kN	F_{total}, kN
10	1	-1.5431	14.51	12.97
	2	-0.9258	14.51	13.59
	3	-0.3086	14.51	14.21
	4	0.3086	14.51	14.82
	5	0.9258	14.51	15.44
	6	1.5431	14.51	16.06

Table 9.23. Calculation of wind forces on each frame including the torsional effect for Case 2 (Floor 11).

Floor #	Frame #	$F_{torsion}$, kN	F_{direct}, kN	F_{total}, kN
	1	-1.5672	14.73	13.17
	2	-0.9403	14.73	13.79

11	3	-0.3134	14.73	14.42
	4	0.3134	14.73	15.05
	5	0.9403	14.73	15.67
	6	1.5672	14.73	16.30

Table 9.24. Calculation of wind forces on each frame including the torsional effect for Case 2 (Floor 12).

Floor #	Frame #	$F_{torsion}$, kN	F_{direct}, kN	F_{total}, kN
12	1	-1.5899	14.90	13.31
	2	-0.9540	14.90	13.95
	3	-0.3180	14.90	14.58
	4	0.3180	14.90	15.22
	5	0.9540	14.90	15.85
	6	1.5899	14.90	16.49

Table 9.25. Calculation of wind forces on each frame including the torsional effect for Case 2 (Floor 13 - Roof).

	Transverse				Longitudinal			
Floor	Frame	$F_{torsion}$, kN	F_{direct}, kN	F_{total}, kN	Frame	$F_{torsion}$, kN	F_{direct}, kN	F_{total}, kN
13	A	-0.6412	22.44	21.80	1	-3.2062	22.44	19.24
	B	0.6412	22.44	23.08	2	-1.9237	22.44	20.52
					3	1.9237	22.44	24.37

		4	3.2062	22.44	25.65

Table 9.26. Calculation of wind forces on each frame including the torsional effect for Case 4 (Floor 2).

Floor #	Frame #	$F_{torsion}$, kN	F_{direct}, kN	F_{total}, kN
2	1	-1.8593	10.33	8.47
	2	-1.1156	10.33	9.22
	3	-0.3719	10.33	9.96
	4	0.3719	10.33	10.70
	5	1.1156	10.33	11.45
	6	1.8593	10.33	12.19

Table 9.27. Calculation of wind forces on each frame including the torsional effect for Case 4 (Floor 3).

Floor #	Frame #	$F_{torsion}$, kN	F_{direct}, kN	F_{total}, kN
3	1	-2.5175	9.27	6.75
	2	-1.5105	9.27	7.76
	3	-0.5035	9.27	8.76
	4	0.5035	9.27	9.77
	5	1.5105	9.27	10.78
	6	2.5175	9.27	11.78

Table 9.28. Calculation of wind forces on each frame including the torsional effect for Case 4 (Floor 4).

Floor #	Frame #	$F_{torsion}$, kN	F_{direct}, kN	F_{total}, kN
4	1	-2.6125	9.58	6.97
	2	-1.5675	9.58	8.02
	3	-0.5225	9.58	9.06
	4	0.5225	9.58	10.11
	5	1.5675	9.58	11.15
	6	2.6125	9.58	12.20

Table 9.29. Calculation of wind forces on each frame including the torsional effect for Case 4 (Floor 5).

Floor #	Frame #	$F_{torsion}$, kN	F_{direct}, kN	F_{total}, kN
5	1	-2.4058	9.86	7.46
	2	-1.4435	9.86	8.42
	3	-0.4812	9.86	9.38
	4	0.4812	9.86	10.34
	5	1.4435	9.86	11.30
	6	2.4058	9.86	12.27

Table 9.30. Calculation of wind forces on each frame including the torsional effect for Case 4 (Floor 6).

Floor #	Frame #	$F_{torsion}$, kN	F_{direct}, kN	F_{total}, kN
	1	-2.4698	10.11	7.64
	2	-1.4819	10.11	8.63

6	3	-0.4940	10.11	9.61
	4	0.4940	10.11	10.60
	5	1.4819	10.11	11.59
	6	2.4698	10.11	12.58

Table 9.31. Calculation of wind forces on each frame including the torsional effect for Case 4 (Floor 7).

Floor #	Frame #	$F_{torsion}$, kN	F_{direct}, kN	F_{total}, kN
7	1	-2.2936	10.33	8.04
	2	-1.3762	10.33	8.95
	3	-0.4587	10.33	9.87
	4	0.4587	10.33	10.79
	5	1.3762	10.33	11.71
	6	2.2936	10.33	12.62

Table 9.32. Calculation of wind forces on each frame including the torsional effect for Case 4 (Floor 8).

Floor #	Frame #	$F_{torsion}$, kN	F_{direct}, kN	F_{total}, kN
8	1	-2.3411	10.53	8.19
	2	-1.4047	10.53	9.13
	3	-0.4682	10.53	10.06
	4	0.4682	10.53	11.00
	5	1.4047	10.53	11.94

	6	2.3411	10.53	12.87

Table 9.33. Calculation of wind forces on each frame including the torsional effect for Case 4 (Floor 9).

Floor #	Frame #	$F_{torsion}$, kN	F_{direct}, kN	F_{total}, kN
9	1	-1.6791	10.72	9.04
	2	-1.0075	10.72	9.71
	3	-0.3358	10.72	10.38
	4	0.3358	10.72	11.06
	5	1.0075	10.72	11.73
	6	1.6791	10.72	12.40

Table 9.34. Calculation of wind forces on each frame including the torsional effect for Case 4 (Floor 10).

Floor #	Frame #	$F_{torsion}$, kN	F_{direct}, kN	F_{total}, kN
10	1	-1.7077	10.90	9.19
	2	-1.0246	10.90	9.87
	3	-0.3415	10.90	10.55
	4	0.3415	10.90	11.24
	5	1.0246	10.90	11.92
	6	1.7077	10.90	12.60

Table 9.35. Calculation of wind forces on each frame including the torsional effect for Case 4 (Floor 11).

Floor #	Frame #	$F_{torsion}$, kN	F_{direct}, kN	F_{total}, kN
11	1	-0.8327	11.06	10.23
	2	-0.4996	11.06	10.23
	3	-0.1665	11.06	10.23
	4	0.1665	11.06	10.23
	5	0.4996	11.06	10.23
	6	0.8327	11.06	10.23

Table 9.36. Calculation of wind forces on each frame including the torsional effect for Case 4 (Floor 12).

Floor #	Frame #	$F_{torsion}$, kN	F_{direct}, kN	F_{total}, kN
12	1	-0.8448	11.19	10.34
	2	-0.5069	11.19	10.68
	3	-0.1690	11.19	11.02
	4	0.1690	11.19	11.35
	5	0.5069	11.19	11.69
	6	0.8448	11.19	12.03

Table 9.37. Calculation of wind forces on each frame including the torsional effect for Case 4 (Floor 13 - Roof).

	Transverse				Longitudinal			
Floor	Frame	$F_{torsion}$, kN	F_{direct}, kN	F_{total}, kN	Frame	$F_{torsion}$, kN	F_{direct}, kN	F_{total}, kN

13	A	-0.1703	16.85	16.68	1	-0.8517	16.85	16.00
	B	0.1703	16.85	17.02	2	-0.5110	16.85	16.34
					3	0.5110	16.85	17.36
					4	0.8517	16.85	17.70

9.3 Appendix C

Following figures show the lateral forces that were applied to the chosen first 2D and 3D frame, including wind loads assigned for Case 2, Case 3 and Case 4.

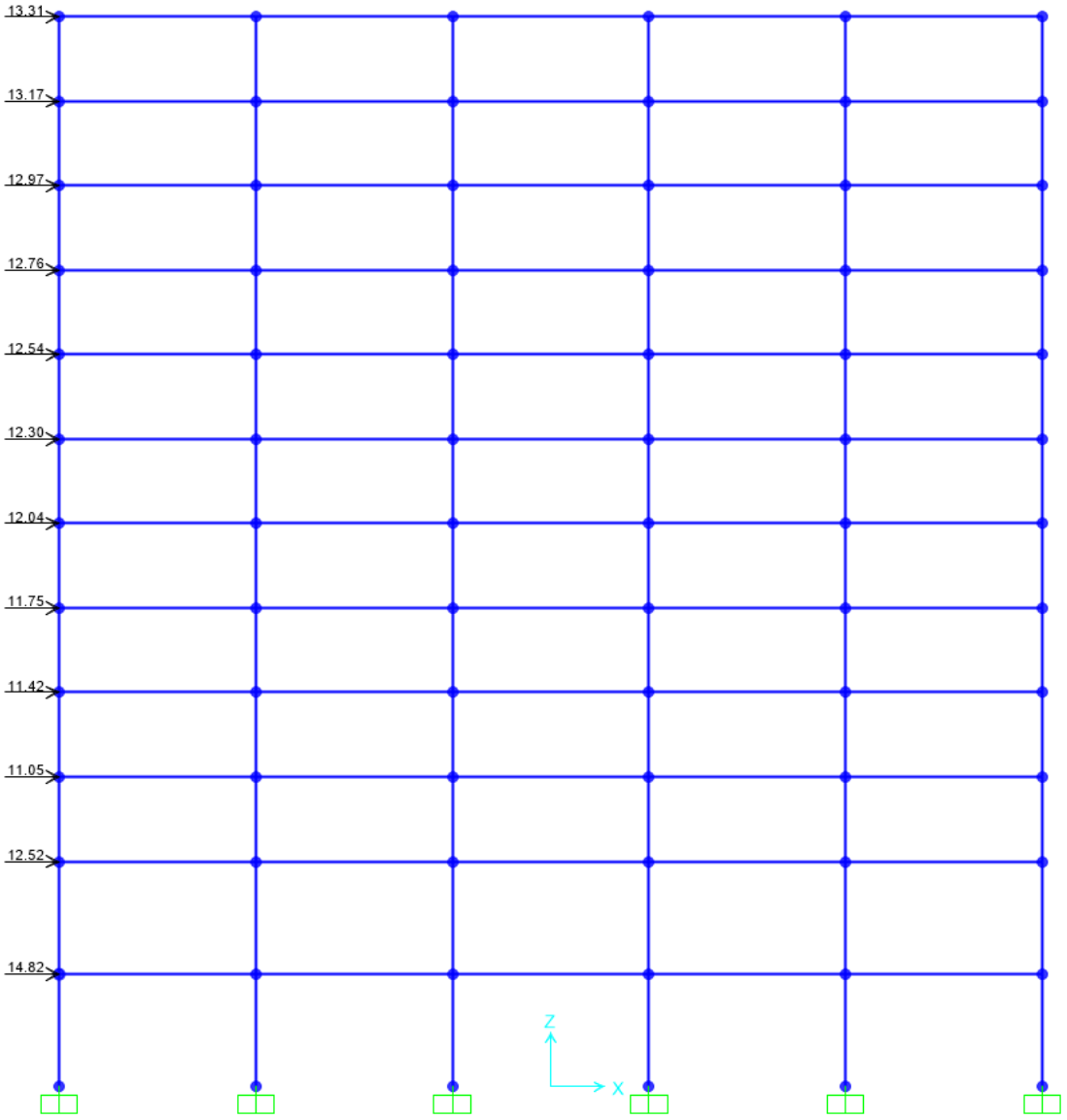

Figure 9.1. SAP2000: Assigned lateral forces for Case 2 wind loads on 2D frame.

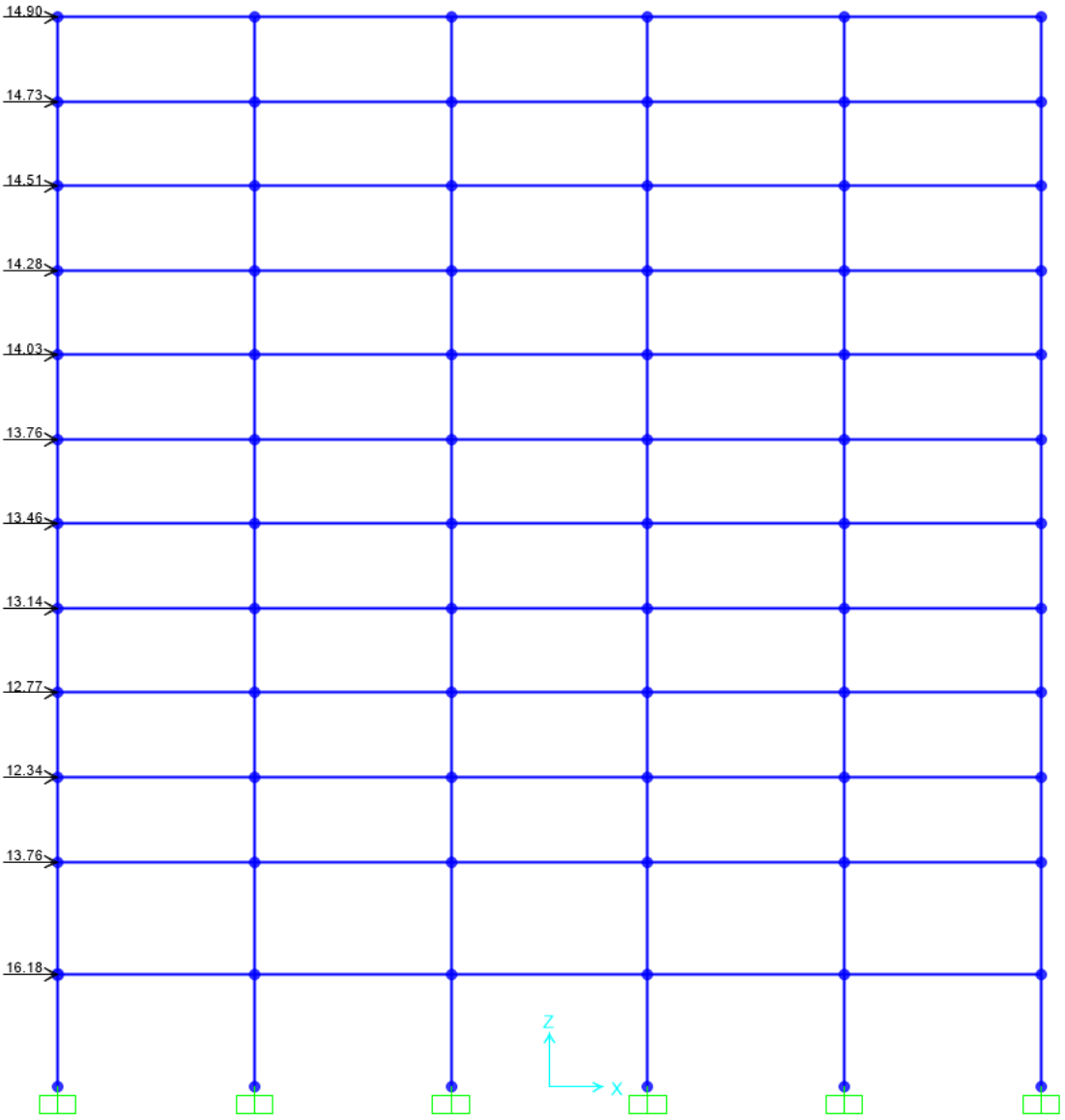

Figure 9.2. SAP2000: Assigned lateral forces for Case 3 wind loads on 2D frame.

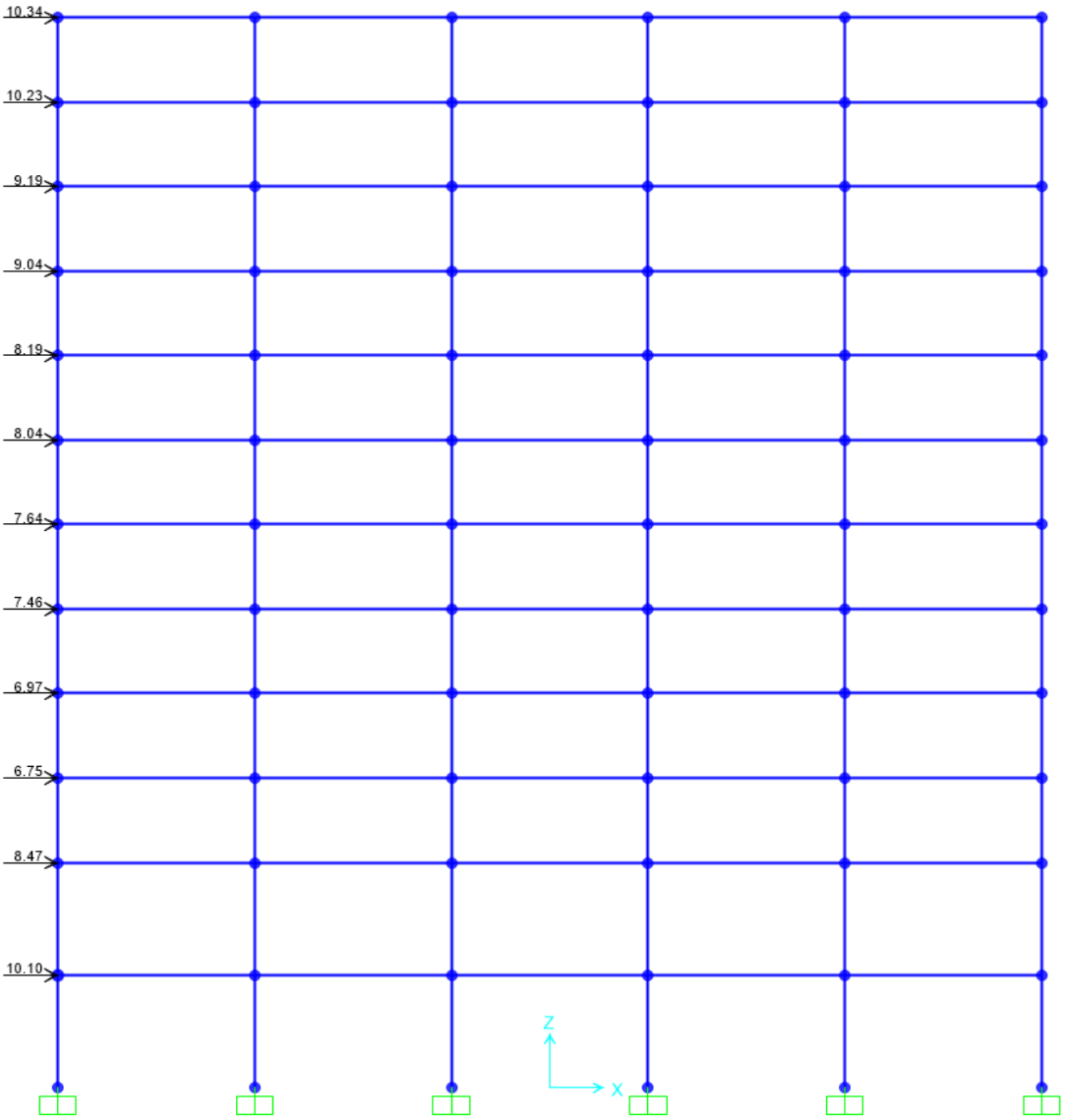

Figure 9.3. SAP2000: Assigned lateral forces for Case 4 wind loads on 2D frame.

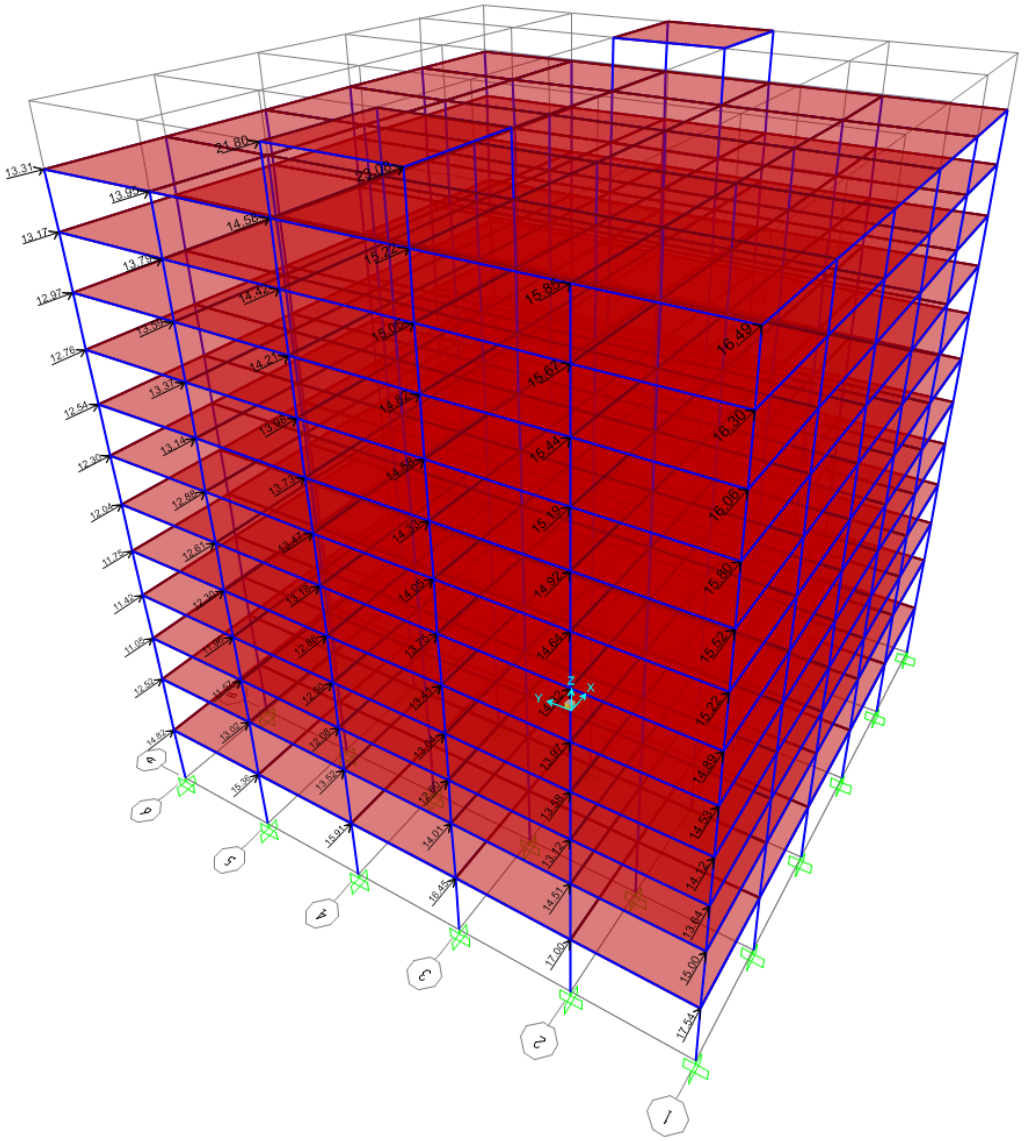

Figure 9.4. SAP2000: Assigned lateral forces for Case 2 wind loads on 3D frame.

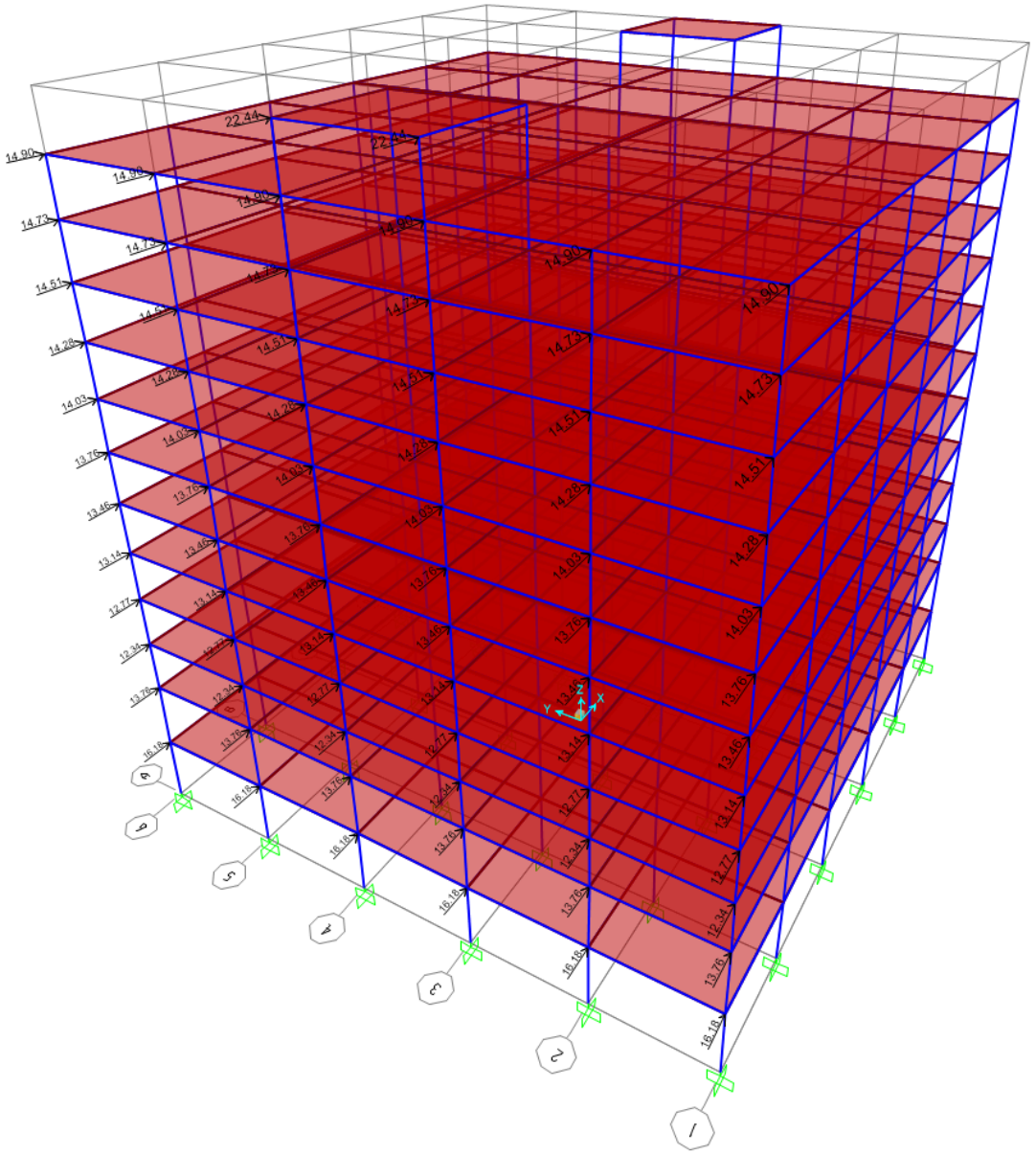

Figure 9.5. SAP2000: Assigned lateral forces for Case 3 wind loads on 3D frame.

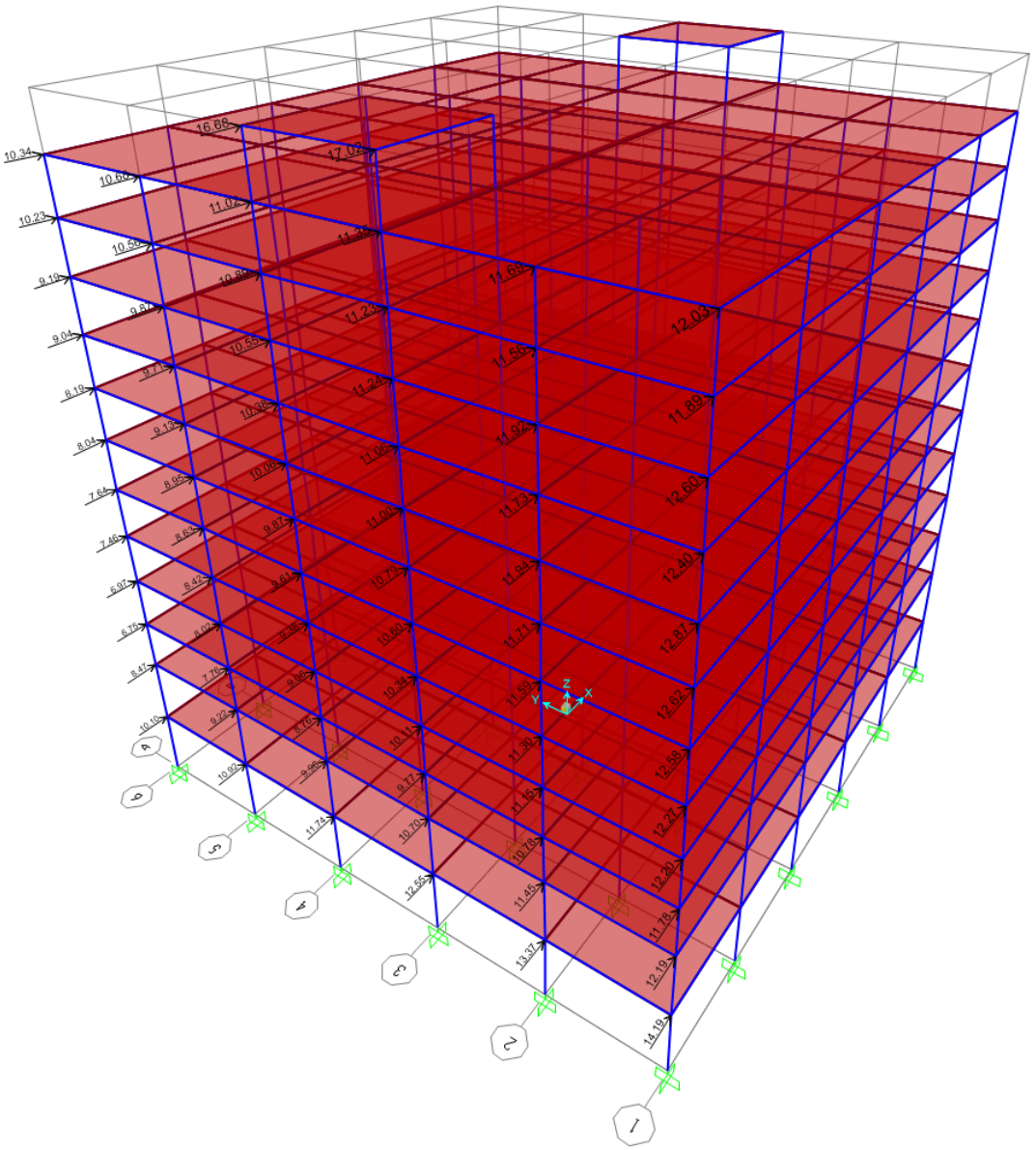

Figure 9.6. SAP2000: Assigned lateral forces for Case 4 wind loads on 3D frame.

9.4 Appendix D

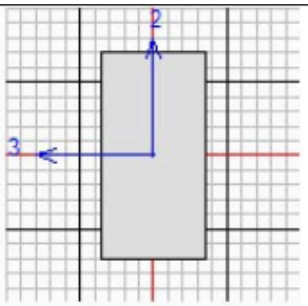

ACI 318-14 BEAM SECTION DESIGN Type:Sway Special Units: KN, m, C (Summary)

Element : 6	D=0.700	B=0.350	bf=0.350
Section ID : Major Beam	ds=0.000	dct=0.060	dcb=0.060
Combo ID : DCON8	E=29725410.0	fc=40000.000	Lt.Wt. Fac.=1.000
Station Loc : 0.000	L=7.000	fy=420000.000	fys=420000.000

Phi(Bending):	0.900
Phi(Shear):	0.750
Phi(Seis Shear):	0.600
Phi(Torsion):	0.750

Design Moments, M3

Positive Moment	Negative Moment	Special +Moment	Special -Moment
209.342	-418.684	209.342	-418.684

Flexural Reinforcement for Moment, M3

	Required Rebar	+Moment Rebar	-Moment Rebar	Minimum Rebar
Top (+2 Axis)	0.002	0.000	0.002	8.403E-04
Bottom (-2 Axis)	8.870E-04	8.870E-04	0.000	8.403E-04

Shear Reinforcement for Shear, V2

Rebar Av/s	Shear Vu	Shear phi*Vc	Shear phi*Vs	Shear Vp
0.001	242.622	0.000	242.622	122.170

Reinforcement for Torsion, T

Rebar At/s	Rebar Al	Torsion Tu	Critical Phi*Tcr	Area Ao	Perimeter Ph
0.000	0.000	0.666	45.050	0.136	1.744

Figure 9.7. Critical moment of the beam on the first floor.

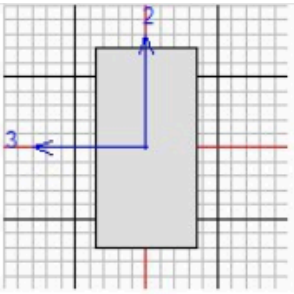

ACI 318-14 BEAM SECTION DESIGN Type:Sway Special Units: KN, m, C (Summary)

Element : 66	D=0.700	B=0.350	bf=0.350
Section ID : Major Beam	ds=0.000	dct=0.060	dcb=0.060
Combo ID : DCON8	E=29725410.0	fc=40000.000	Lt.Wt. Fac.=1.000
Station Loc : 0.000	L=7.000	fy=420000.000	fys=420000.000

Phi(Bending):	0.900
Phi(Shear):	0.750
Phi(Seis Shear):	0.600
Phi(Torsion):	0.750

Design Moments, M3

Positive Moment	Negative Moment	Special +Moment	Special -Moment
236.539	-473.077	236.539	-473.077

Flexural Reinforcement for Moment, M3

	Required Rebar	+Moment Rebar	-Moment Rebar	Minimum Rebar
Top (+2 Axis)	0.002	0.000	0.002	8.403E-04
Bottom (-2 Axis)	0.001	0.001	0.000	8.403E-04

Shear Reinforcement for Shear, V2

Rebar Av/s	Shear Vu	Shear phi*Vc	Shear phi*Vs	Shear Vp
0.001	258.886	0.000	258.886	136.402

Reinforcement for Torsion, T

Rebar At/s	Rebar Al	Torsion Tu	Critical Phi*Tcr	Area Ao	Perimeter Ph
0.000	0.000	0.766	44.909	0.136	1.744

Figure 9.8. Critical moment of the beam on the second floor.

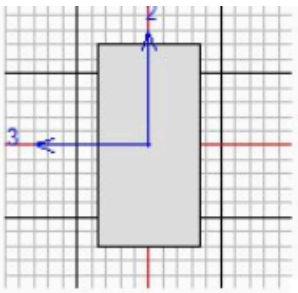

ACI 318-14 BEAM SECTION DESIGN Type:Sway Special Units: KN, m, C (Summary)

Element : 126	D=0.700	B=0.350	bf=0.350
Section ID : Major Beam	ds=0.000	dct=0.060	dcb=0.060
Combo ID : DCON8	E=29725410.0	fc=40000.000	Lt.Wt. Fac.=1.000
Station Loc : 0.000	L=7.000	fy=420000.000	fys=420000.000

Phi(Bending):	0.900
Phi(Shear):	0.750
Phi(Seis Shear):	0.600
Phi(Torsion):	0.750

Design Moments, M3

	Positive Moment	Negative Moment	Special +Moment	Special -Moment
	232.452	-464.905	232.452	-464.905

Flexural Reinforcement for Moment, M3

	Required Rebar	+Moment Rebar	-Moment Rebar	Minimum Rebar
Top (+2 Axis)	0.002	0.000	0.002	8.403E-04
Bottom (-2 Axis)	9.878E-04	9.878E-04	0.000	8.403E-04

Shear Reinforcement for Shear, V2

Rebar Av/s	Shear Vu	Shear phi*Vc	Shear phi*Vs	Shear Vp
0.001	256.933	0.000	256.933	132.988

Reinforcement for Torsion, T

Rebar At/s	Rebar Al	Torsion Tu	Critical Phi*Tcr	Area Ao	Perimeter Ph
0.000	0.000	0.708	44.829	0.136	1.744

Figure 9.9. Critical moment of the beam on the third floor.

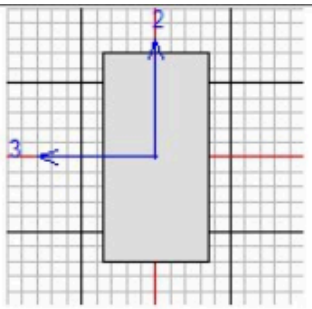

ACI 318-14 BEAM SECTION DESIGN Type:Sway Special Units: KN, m, C (Summary)

Element : 186	D=0.700	B=0.350	bf=0.350
Section ID : Major Beam	ds=0.000	dct=0.060	dcb=0.060
Combo ID : DCON8	E=29725410.0	fc=40000.000	Lt.Wt. Fac.=1.000
Station Loc : 0.000	L=7.000	fy=420000.000	fys=420000.000

Phi(Bending):	0.900
Phi(Shear):	0.750
Phi(Seis Shear):	0.600
Phi(Torsion):	0.750

Design Moments, M3

Positive Moment	Negative Moment	Special +Moment	Special -Moment
229.311	-458.622	229.311	-458.622

Flexural Reinforcement for Moment, M3

	Required Rebar	+Moment Rebar	-Moment Rebar	Minimum Rebar
Top (+2 Axis)	0.002	0.000	0.002	8.403E-04
Bottom (-2 Axis)	9.740E-04	9.740E-04	0.000	8.403E-04

Shear Reinforcement for Shear, V2

Rebar Av/s	Shear Vu	Shear phi*Vc	Shear phi*Vs	Shear Vp
0.001	255.113	0.000	255.113	130.334

Reinforcement for Torsion, T

Rebar At/s	Rebar Al	Torsion Tu	Critical Phi*Tcr	Area Ao	Perimeter Ph
0.000	0.000	0.621	44.707	0.136	1.744

Figure 9.10. Critical moment of the beam on the fourth floor.

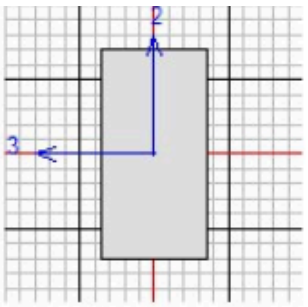

ACI 318-14 BEAM SECTION DESIGN Type:Sway Special Units: KN, m, C (Summary)

Element	: 246	D=0.700	B=0.350	bf=0.350
Section ID	: Major Beam	ds=0.000	dct=0.060	dcb=0.060
Combo ID	: DCON8	E=29725410.0	fc=40000.000	Lt.Wt. Fac.=1.000
Station Loc	: 0.000	L=7.000	fy=420000.000	fys=420000.000

Phi(Bending):	0.900
Phi(Shear):	0.750
Phi(Seis Shear):	0.600
Phi(Torsion):	0.750

Design Moments, M3

	Positive Moment	Negative Moment	Special +Moment	Special -Moment
	223.711	-447.423	223.711	-447.423

Flexural Reinforcement for Moment, M3

	Required Rebar	+Moment Rebar	-Moment Rebar	Minimum Rebar
Top (+2 Axis)	0.002	0.000	0.002	8.403E-04
Bottom (-2 Axis)	9.496E-04	9.496E-04	0.000	8.403E-04

Shear Reinforcement for Shear, V2

Rebar Av/s	Shear Vu	Shear phi*Vc	Shear phi*Vs	Shear Vp
0.001	252.048	0.000	252.048	126.674

Reinforcement for Torsion, T

Rebar At/s	Rebar Al	Torsion Tu	Critical Phi*Tcr	Area Ao	Perimeter Ph
0.000	0.000	0.484	44.667	0.136	1.744

Figure 9.11. Critical moment of the beam on the fifth floor.

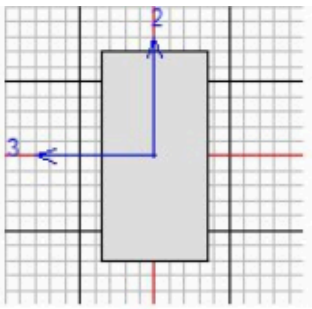

ACI 318-14 BEAM SECTION DESIGN Type:Sway Special Units: KN, m, C (Summary)

Element : 306	D=0.700	B=0.350	bf=0.350
Section ID : Major Beam	ds=0.000	dct=0.060	dcb=0.060
Combo ID : DCON8	E=29725410.0	fc=40000.000	Lt.Wt. Fac.=1.000
Station Loc : 0.000	L=7.000	fy=420000.000	fys=420000.000

Phi(Bending):	0.900
Phi(Shear):	0.750
Phi(Seis Shear):	0.600
Phi(Torsion):	0.750

Design Moments, M3

Positive Moment	Negative Moment	Special +Moment	Special -Moment
216.859	-433.717	216.859	-433.717

Flexural Reinforcement for Moment, M3

	Required Rebar	+Moment Rebar	-Moment Rebar	Minimum Rebar
Top (+2 Axis)	0.002	0.000	0.002	8.403E-04
Bottom (-2 Axis)	9.197E-04	9.197E-04	0.000	8.403E-04

Shear Reinforcement for Shear, V2

Rebar Av/s	Shear Vu	Shear phi*Vc	Shear phi*Vs	Shear Vp
3.720E-04	250.323	176.453	73.870	124.035

Reinforcement for Torsion, T

Rebar At/s	Rebar Al	Torsion Tu	Critical Phi*Tcr	Area Ao	Perimeter Ph
0.000	0.000	0.359	44.561	0.136	1.744

Figure 9.12. Critical moment of the beam on the sixth floor.

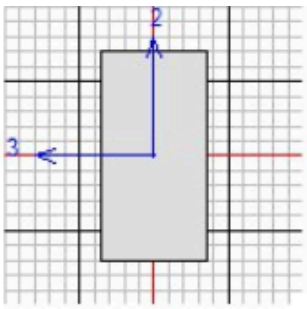

ACI 318-14 BEAM SECTION DESIGN Type:Sway Special Units: KN, m, C (Summary)

Element : 366	D=0.700	B=0.350	bf=0.350
Section ID : Major Beam	ds=0.000	dct=0.060	dcb=0.060
Combo ID : DCON8	E=29725410.0	fc=40000.000	Lt.Wt. Fac.=1.000
Station Loc : 0.000	L=7.000	fy=420000.000	fys=420000.000

Phi(Bending):	0.900
Phi(Shear):	0.750
Phi(Seis Shear):	0.600
Phi(Torsion):	0.750

Design Moments, M3

	Positive Moment	Negative Moment	Special +Moment	Special -Moment
	207.130	-414.259	207.130	-414.259

Flexural Reinforcement for Moment, M3

	Required Rebar	+Moment Rebar	-Moment Rebar	Minimum Rebar
Top (+2 Axis)	0.002	0.000	0.002	8.403E-04
Bottom (-2 Axis)	8.774E-04	8.774E-04	0.000	8.403E-04

Shear Reinforcement for Shear, V2

Rebar Av/s	Shear Vu	Shear phi*Vc	Shear phi*Vs	Shear Vp
3.573E-04	247.398	176.453	70.945	120.284

Reinforcement for Torsion, T

Rebar At/s	Rebar Al	Torsion Tu	Critical Phi*Tcr	Area Ao	Perimeter Ph
0.000	0.000	0.190	44.459	0.136	1.744

Figure 9.13. Critical moment of the beam on the seventh floor.

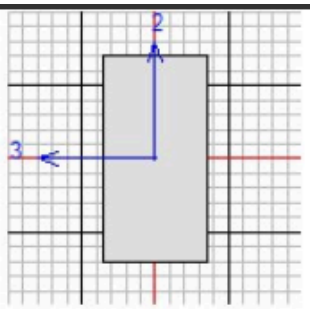

ACI 318-14 BEAM SECTION DESIGN Type:Sway Special Units: KN, m, C (Summary)

Element : 426	D=0.700	B=0.350	bf=0.350
Section ID : Major Beam	ds=0.000	dct=0.060	dcb=0.060
Combo ID : DCON8	E=29725410.0	fc=40000.000	Lt.Wt. Fac.=1.000
Station Loc : 0.000	L=7.000	fy=420000.000	fys=420000.000

Phi(Bending):	0.900
Phi(Shear):	0.750
Phi(Seis Shear):	0.600
Phi(Torsion):	0.750

Design Moments, M3

Positive Moment	Negative Moment	Special +Moment	Special -Moment
194.133	-388.267	194.133	-388.267

Flexural Reinforcement for Moment, M3

	Required Rebar	+Moment Rebar	-Moment Rebar	Minimum Rebar
Top (+2 Axis)	0.002	0.000	0.002	8.403E-04
Bottom (-2 Axis)	8.403E-04	8.211E-04	0.000	8.403E-04

Shear Reinforcement for Shear, V2

Rebar Av/s	Shear Vu	Shear phi*Vc	Shear phi*Vs	Shear Vp
3.260E-04	241.190	176.453	64.737	115.264

Reinforcement for Torsion, T

Rebar At/s	Rebar Al	Torsion Tu	Critical Phi*Tcr	Area Ao	Perimeter Ph
0.000	0.000	0.011	44.402	0.136	1.744

Figure 9.14. Critical moment of the beam on the eighth floor.

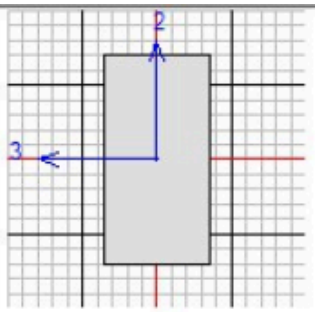

ACI 318-14 BEAM SECTION DESIGN Type:Sway Special Units: KN, m, C (Summary)

Element : 486	D=0.700	B=0.350	bf=0.350
Section ID : Major Beam	ds=0.000	dct=0.060	dcb=0.060
Combo ID : DCON8	E=29725410.0	fc=40000.000	Lt.Wt. Fac.=1.000
Station Loc : 0.000	L=7.000	fy=420000.000	fys=420000.000

Phi(Bending):	0.900
Phi(Shear):	0.750
Phi(Seis Shear):	0.600
Phi(Torsion):	0.750

Design Moments, M3

Positive Moment	Negative Moment	Special +Moment	Special -Moment
174.992	-349.983	174.992	-349.983

Flexural Reinforcement for Moment, M3

	Required Rebar	+Moment Rebar	-Moment Rebar	Minimum Rebar
Top (+2 Axis)	0.002	0.000	0.002	8.403E-04
Bottom (-2 Axis)	8.403E-04	7.384E-04	0.000	8.403E-04

Shear Reinforcement for Shear, V2

Rebar Av/s	Shear Vu	Shear phi*Vc	Shear phi*Vs	Shear Vp
2.747E-04	231.006	176.453	54.553	107.420

Reinforcement for Torsion, T

Rebar At/s	Rebar Al	Torsion Tu	Critical Phi*Tcr	Area Ao	Perimeter Ph
0.000	0.000	0.218	44.243	0.136	1.744

Figure 9.15. Critical moment of the beam on the ninth floor.

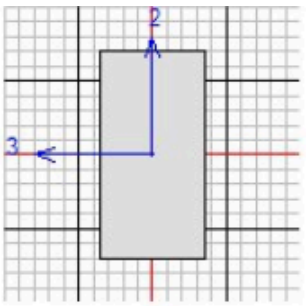

ACI 318-14 BEAM SECTION DESIGN Type:Sway Special Units: KN, m, C (Summary)

Element : 546	D=0.700	B=0.350	bf=0.350
Section ID : Major Beam	ds=0.000	dct=0.060	dcb=0.060
Combo ID : DCON8	E=29725410.0	fc=40000.000	Lt.Wt. Fac.=1.000
Station Loc : 0.000	L=7.000	fy=420000.000	fys=420000.000

Phi(Bending):	0.900
Phi(Shear):	0.750
Phi(Seis Shear):	0.600
Phi(Torsion):	0.750

Design Moments, M3

	Positive Moment	Negative Moment	Special +Moment	Special -Moment
	151.660	-303.320	151.660	-303.320

Flexural Reinforcement for Moment, M3

	Required Rebar	+Moment Rebar	-Moment Rebar	Minimum Rebar
Top (+2 Axis)	0.001	0.000	0.001	8.403E-04
Bottom (-2 Axis)	8.403E-04	6.381E-04	0.000	8.403E-04

Shear Reinforcement for Shear, V2

Rebar Av/s	Shear Vu	Shear phi*Vc	Shear phi*Vs	Shear Vp
1.964E-04	215.451	176.453	38.998	94.851

Reinforcement for Torsion, T

Rebar At/s	Rebar Al	Torsion Tu	Critical Phi*Tcr	Area Ao	Perimeter Ph
0.000	0.000	0.314	44.273	0.136	1.744

Figure 9.16. Critical moment of the beam on the tenth floor.

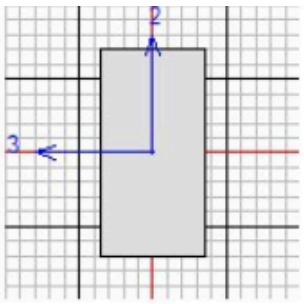

ACI 318-14 BEAM SECTION DESIGN Type:Sway Special Units: KN, m, C (Summary)

Element : 614	D=0.700	B=0.350	bf=0.350
Section ID : Major Beam	ds=0.000	dct=0.060	dcb=0.060
Combo ID : DCON8	E=29725410.0	fc=40000.000	Lt.Wt. Fac.=1.000
Station Loc : 0.000	L=7.000	fy=420000.000	fys=420000.000

Phi(Bending):	0.900
Phi(Shear):	0.750
Phi(Seis Shear):	0.600
Phi(Torsion):	0.750

Design Moments, M3

Positive Moment	Negative Moment	Special +Moment	Special -Moment
123.715	-247.429	123.715	-247.429

Flexural Reinforcement for Moment, M3

	Required Rebar	+Moment Rebar	-Moment Rebar	Minimum Rebar
Top (+2 Axis)	0.001	0.000	0.001	8.403E-04
Bottom (-2 Axis)	6.917E-04	5.188E-04	0.000	6.917E-04

Shear Reinforcement for Shear, V2

Rebar Av/s	Shear Vu	Shear phi*Vc	Shear phi*Vs	Shear Vp
1.230E-04	200.872	176.453	24.419	79.539

Reinforcement for Torsion, T

Rebar At/s	Rebar Al	Torsion Tu	Critical Phi*Tcr	Area Ao	Perimeter Ph
0.000	0.000	0.217	44.643	0.136	1.744

Figure 9.17. Critical moment of the beam on the eleventh floor.

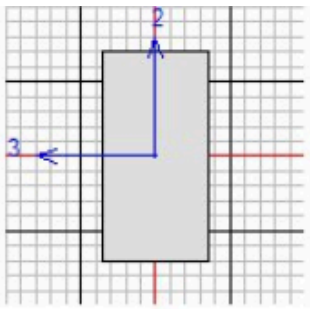

ACI 318-14 BEAM SECTION DESIGN Type:Sway Special Units: KN, m, C (Summary)

Element : 671	D=0.700	B=0.350	bf=0.350
Section ID : Major Beam	ds=0.000	dct=0.060	dcb=0.060
Combo ID : DCON7	E=29725410.0	fc=40000.000	Lt.Wt. Fac.=1.000
Station Loc : 7.000	L=7.000	fy=420000.000	fys=420000.000

Phi(Bending):	0.900
Phi(Shear):	0.750
Phi(Seis Shear):	0.600
Phi(Torsion):	0.750

Design Moments, M3

	Positive Moment	Negative Moment	Special +Moment	Special -Moment
	118.236	-236.473	118.236	-236.473

Flexural Reinforcement for Moment, M3

	Required Rebar	+Moment Rebar	-Moment Rebar	Minimum Rebar
Top (+2 Axis)	0.001	0.000	0.001	8.403E-04
Bottom (-2 Axis)	6.607E-04	4.955E-04	0.000	6.607E-04

Shear Reinforcement for Shear, V2

Rebar Av/s	Shear Vu	Shear phi*Vc	Shear phi*Vs	Shear Vp
3.649E-05	183.699	176.453	7.246	75.667

Reinforcement for Torsion, T

Rebar At/s	Rebar Al	Torsion Tu	Critical Phi*Tcr	Area Ao	Perimeter Ph
0.000	0.000	0.865	46.640	0.136	1.744

Figure 9.18. Critical moment of the beam on the twelfth floor.

9.5 Appendix E

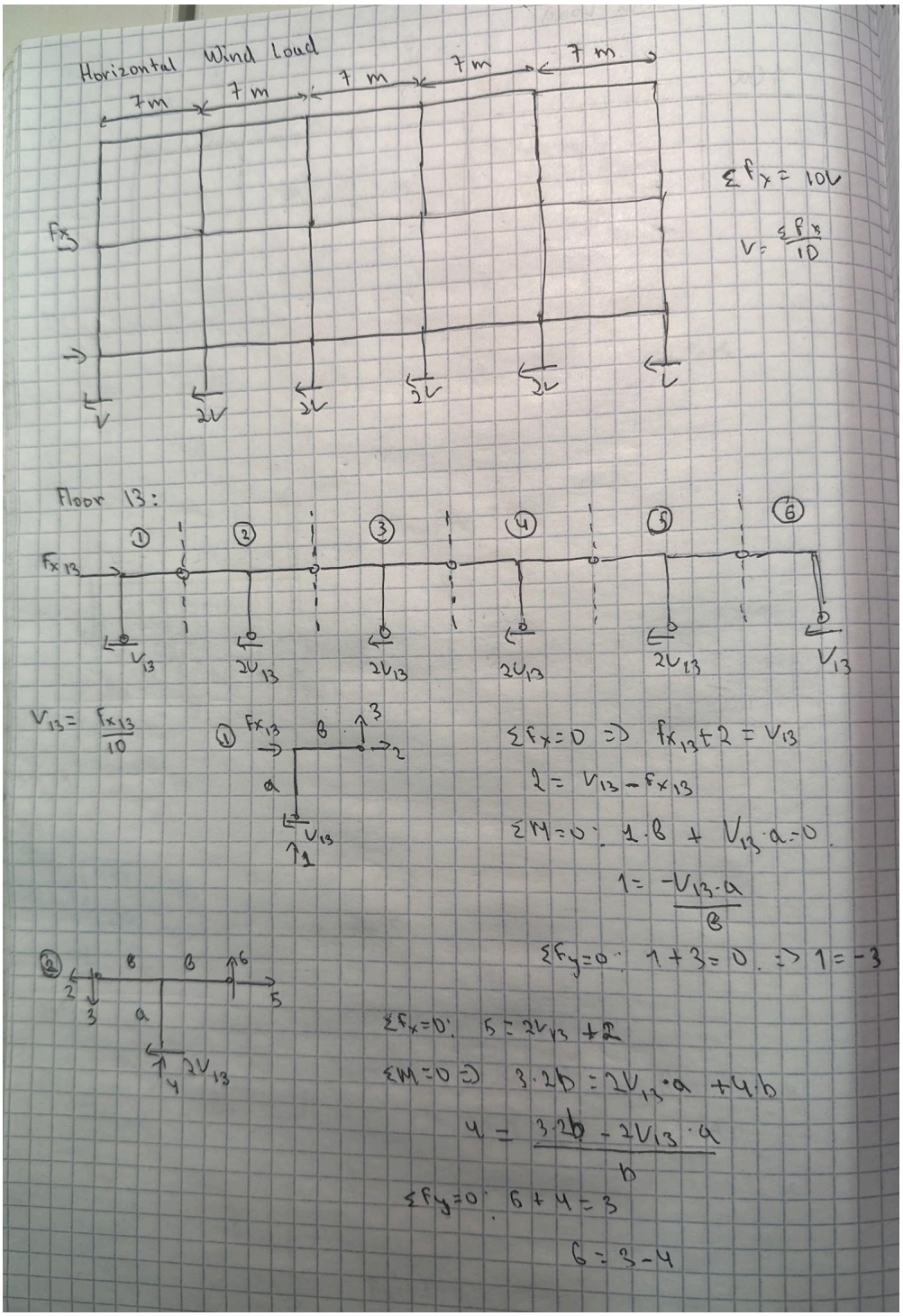

Figure 9.19. Hand calculation of internal forces under wind load - Part 1.

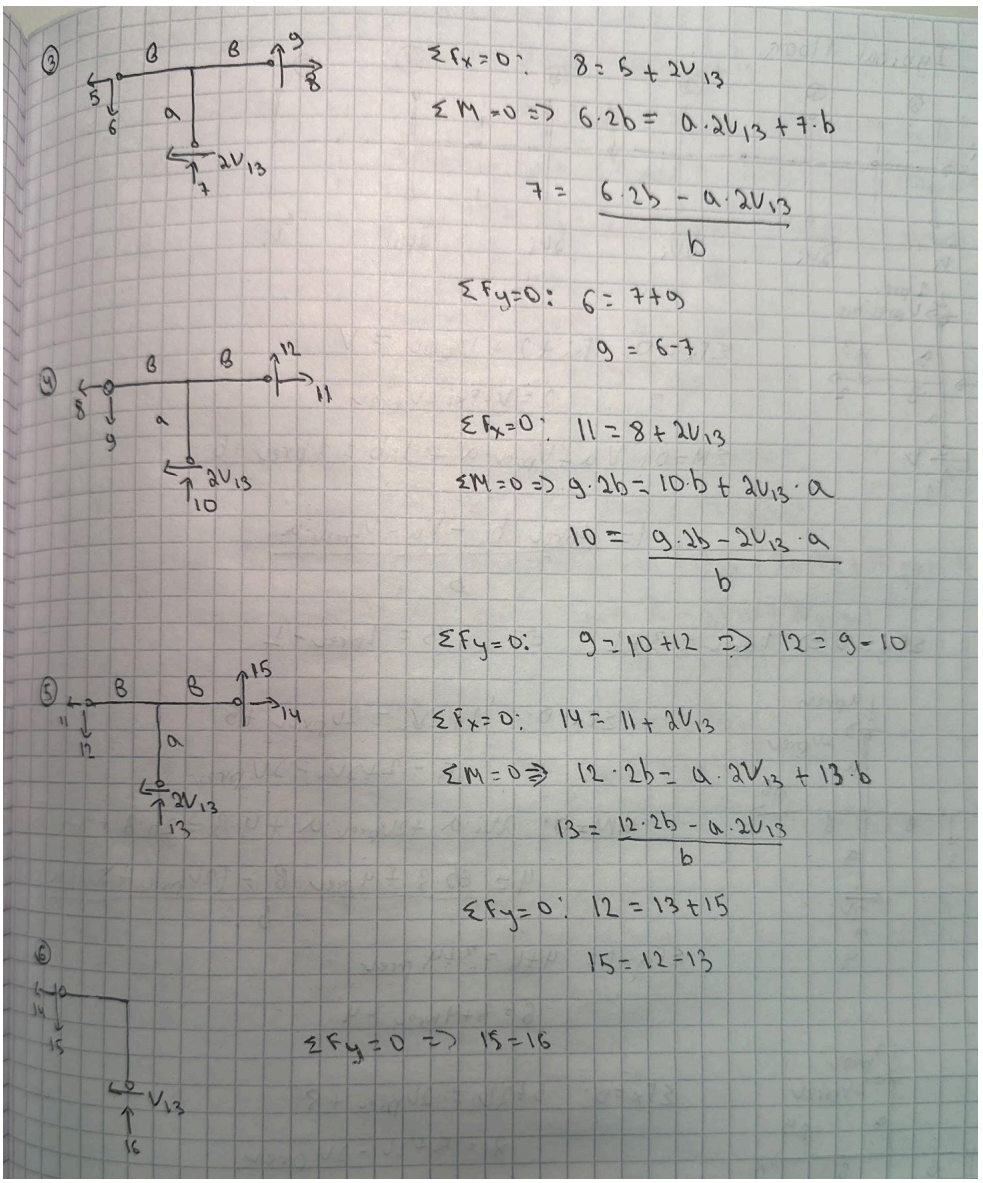

Figure 9.20. Hand calculation of internal forces under wind load - Part 2.

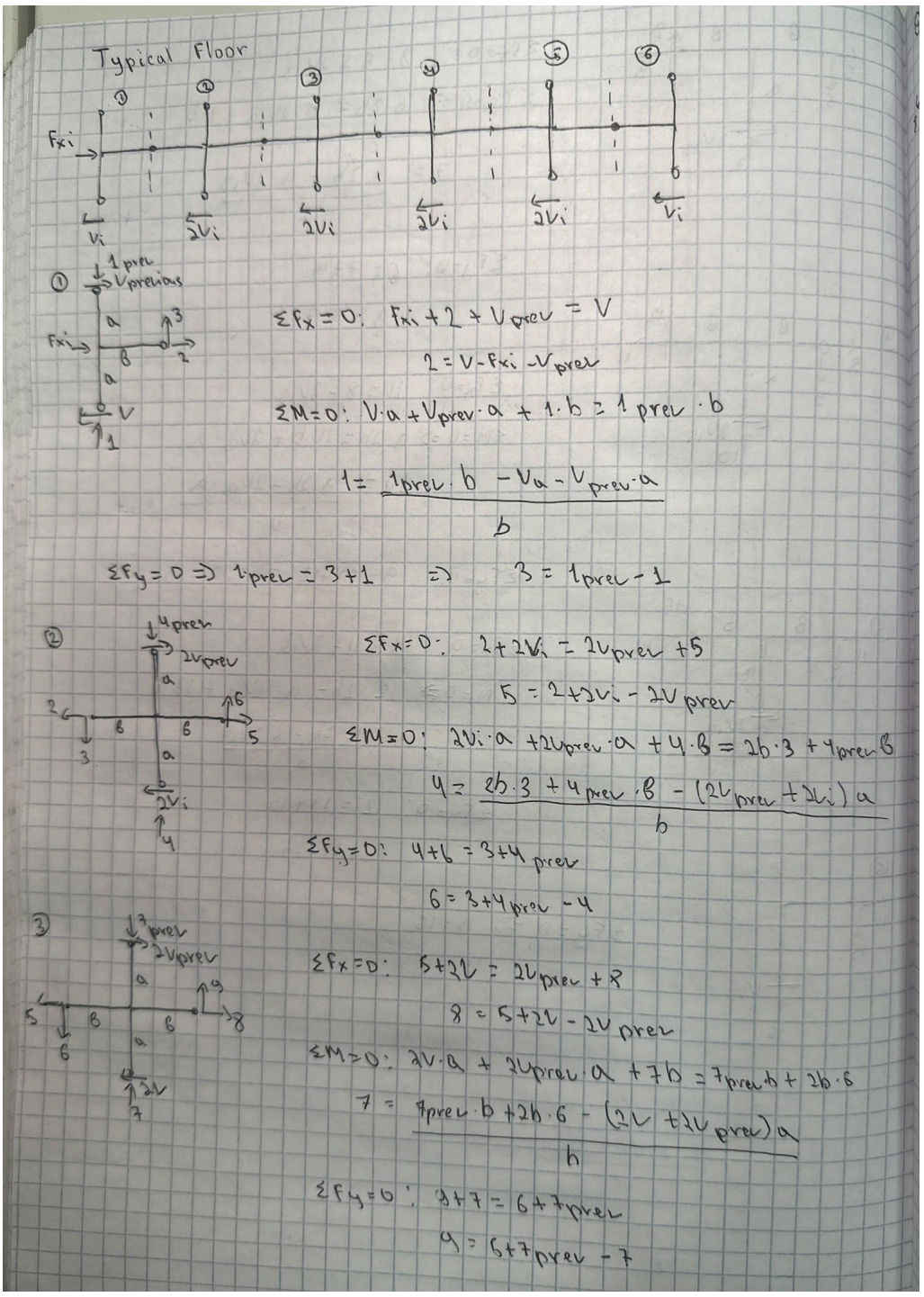

Figure 9.21. Hand calculation of internal forces under wind load - Part 3.

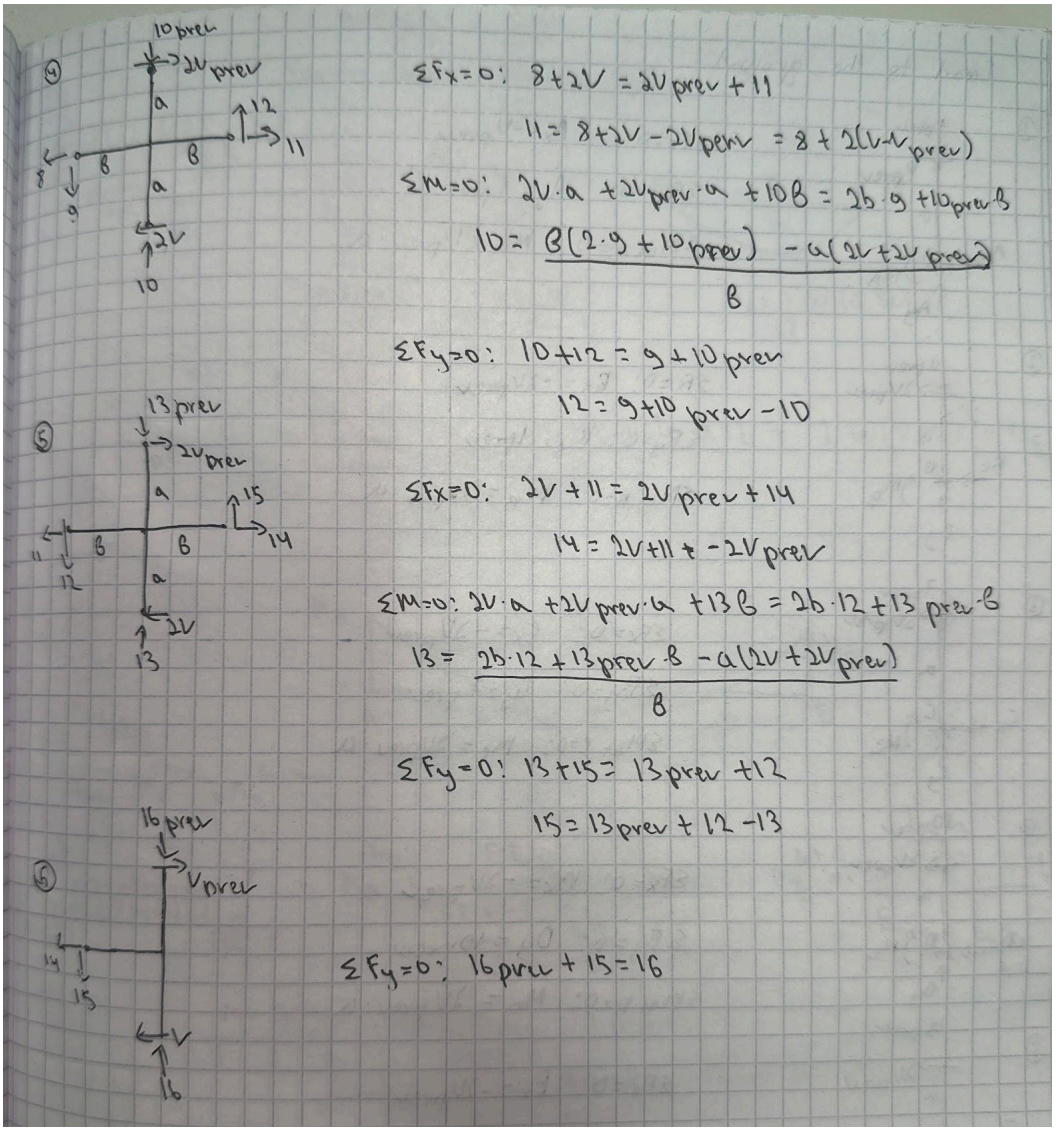

Figure 9.22. Hand calculation of internal forces under wind load - Part 4.